IL
NUOVO CIMENTO
ORGANO DELLA SOCIETÀ ITALIANA DI FISICA
SOTTO GLI AUSPICI DEL CONSIGLIO NAZIONALE DELLE RICERCHE

VOL. XX, N. 4 *Serie decima* 16 Maggio 1961

A Problem in Shock Waves.

R. S. MISHRA
Gorakhpur University

(ricevuto il 3 Novembre 1960)

Summary. — LANDAU and LIFSHITZ (1959) [1] have mentioned the following result: *If two (or more) successive shock waves take a gas from state* 1 *to state* 2 *and from there to state* 3, *the transition from state* 1 *to state* 3 *can not, in general, be effected by the passages of any one shock wave.* The object of this note is to obtain conditions for the transition from state 1 to state 3 to be effected by the passage of any one shock wave.

1. – Introduction.

Let us consider two successive oblique steady shock surfaces $S_{\alpha l}$ ($\alpha = 1, 2$). Let p_{rl}, ϱ_{rl}, u_{rl}^{i} and u_{rnl} ($r = 1, 2, 3$) (*) be the pressure, density, velocity components of a particle of the fluid and normal fluid velocity in the states 1, 2, 3 respectively at a point P. By state 1 we mean the region in front of S_{1l}, by state 2, the region behind S_{1l} or in front of S_{2l} and by state 3, the region behind S_{2l}. The strengths $V_{\alpha l}$ of the shock surfaces $S_{\alpha l}$ may be defined as (**)

$$V_{\alpha l} \stackrel{\text{def}}{=} -\frac{[u_{\alpha nl}]}{u_{\alpha l}}, \tag{1.1}$$

(1) L. D. LANDAU and E. M. LIFSHITZ: *Fluid Mechanics* (translated in English) (London, 1959).

(*) In this and in what follows Latin indices take the values 1, 2, 3 and Greek indices the values 1, 2.

(**) $V_{\alpha l}$ is generally defined as normal velocity strength, but for simplicity we have termed it only « strength ».

where [ ] denotes the difference of values of the quantity enclosed on two sides of the shock front; thus

$$[u_{\alpha n l}] = u_{\alpha+1\, n l} - u_{\alpha n l} .$$

The Rankine-Hugoniot jump conditions when the fluid passes a shock surface can be written as (*)

$$[u_{\alpha l}{}^{i}] = - V_{\alpha l} u_{\alpha n l} X_{\alpha l}{}^{i} , \tag{1.2a}$$

$$[\varrho_{\alpha l}] = \frac{V_{\alpha l}}{1 - V_{\alpha l}} \varrho_{\alpha l} , \tag{1.3a}$$

$$[p_{\alpha l}] = V_{\alpha l} \varrho_{\alpha l} u_{\alpha n l}^{2} , \tag{1.4}$$

where $X_{\alpha l}{}^{i}$ are components of the unit normal to the shock surface $S_{\alpha l}$.

By definition we have

$$u_{r n l} = u_{r l i} X_{\alpha l}{}^{i} . \tag{1.5}$$

The eq. (1.3*a*) is equivalent to

$$\varrho_{\alpha+1 l} = \frac{1}{1 - V_{\alpha l}} \varrho_{\alpha l} , \tag{1.3b}$$

from which we obtain that if $S_{\alpha l}$ is of positive strength, then

$$0 < V_{\alpha l} < 1 . \tag{1.6}$$

In consequence of (1.5) the eq. (1.2*a*) is equivalent to

$$u_{\alpha+1 n l} = (1 - V_{\alpha l}) u_{\alpha u l} . \tag{1.2b}$$

2. – Discussion of the problem.

We will now prove the following theorem.

THEOREM. *If two successive shock waves $S_{\alpha l}$ of positive strengths take a gas from state* 1 *to state* 2 *and from there to state* 3 *at a point P the necessary and sufficient condition that the transition from state* 1 *to state* 3 *be effected by the passage*

(*) In this and in what follows, the summation convention is not observed with respect to repeated indices behind the solidus.

of a single shock S, is that the three shock surfaces $S_{\alpha l}$ and S are tangential to one another at P.

PROOF. From (1.3) we have

$$\varrho_{2l} = \frac{1}{1 - V_{2l}} \varrho_{2l} = \frac{1}{(1 - V_{2l})(1 - V_{1l})} \varrho_{1l} . \tag{2.1}$$

If the transition is to be effected from state 1 to state 3 by the passage of a single shock surface S, then (2.1) must be of the form

$$\varrho_{3l} = \frac{1}{1 - V} \varrho_{1l} , \tag{2.2a}$$

where

$$0 < V < 1 . \tag{2.2b}$$

In consequence of (2.1) and (2.2a), we have

$$V_{1l} + V_{2l} - V_{1l} V_2 = V . \tag{2.3}$$

This equation is always satisfied because of the inequalities (1.6) and (2.2b).

Adding the two eq. (1.4) and using (1.2b) and (1.3b) we get,

$$p_{3l} - p_{1l} = \{V_{2l}(1 - V_{1l}) + V_{1l}\} \varrho_{1l} u_{1l}^2 \cos^2 \theta_{1l} , \tag{2.4a}$$

where $\begin{cases} \theta_{\alpha l} \\ \theta \end{cases}$ is the angle between a stream line in front and the normal to $\begin{cases} S_{\alpha l} \\ S \end{cases}$.

According to the requirement of the problem (2.4a) should be of the form

$$p_{3l} - p_{1l} = V \varrho_{1l} u_{1l}^2 \cos^2 \theta . \tag{2.4b}$$

Comparing the two eq. (2.4), we get

$$V_{1l} + V_{2l} - V_{1l} V_{2l} = \frac{V \cos^2 \theta}{\cos^2 \theta_{1l}} . \tag{2.5}$$

Using (2.3) in (2.5), we get

$$\theta = \theta_{1l} . \tag{2.6}$$

Adding the two eq. (1.2a) and using (1.2b), we get

$$u_{3l}^{\ i} - u_{1l}^{\ i} = - \{V_{1l} X_{1l}^{\ i} + V_{2l}(1 - V_{1l}) X_{2l}^{\ i}\} u_{1l} \cos \theta_{1l} . \tag{2.7a}$$

According to the requirement of the problem (2.7a) should be of the form

$$u_{3/}{}^{i} - u_{1/}{}^{i} = - V u_{1/} \cos\theta X^{i} . \tag{2.7b}$$

Comparing (2.7a, b) and using (2.6) we have

$$V_{1/} X_{1/}{}^{i} + V_{2/}(1 - V_{1/}) X_{2/}{}^{i} = V X^{i} , \tag{2.8}$$

whence we get

$$V_{1/}^{2} + V_{2/}^{2}(1 - V_{1/})^{2} + 2 V_{1/} V_{2/}(1 - V_{1/}) \cos\theta_{12/} = V^{2} , \tag{2.9}$$

where $\theta_{12/}$ is the angle between the normals to $S_{1/}$ and $S_{2/}$.

Using (2.3) in (2.9), we get

$$V_{1/} V_{2/}(1 - V_{1/})(\cos\theta_{12/} - 1) = 0 ,$$

or

$$\theta_{12/} = 0 , \tag{2.10}$$

in consequence of (1.6) and (2.2b).

Using (2.10) in (2.8) we get

$$X_{1/}{}^{i} = X_{2/}{}^{i} = X^{i} . \tag{2.11}$$

Hence we have the condition as the necessary one. The proof of the sufficiency of the condition is obvious. For, when (2.11) holds, then (2.6) and (2.10) also hold. Consequently (2.4a) can be put in the form (2.4b) and (2.7a) in the form (2.7b).

Note: The strength of the shock wave $S_{\alpha/}$ may also be defined as

$$P_{\alpha/} \overset{\text{def}}{=} \frac{[p_{\alpha/}]}{p_{\alpha/}} , \qquad \text{(pressure strength)}, \tag{2.12}$$

$$D_{\alpha/} \overset{\text{def}}{=} \frac{[\varrho_{\alpha/}]}{\varrho_{\alpha/}} , \qquad \text{(density strength)}. \tag{2.13}$$

In terms of pressure strength, the Rankine-Hugoniot jump conditions can be written as

$$[\varrho_{\alpha/}] = \frac{P_{\alpha/}}{(\varrho_{\alpha/}/p_{\alpha/}) u_{\alpha n/}^{2} - P_{\alpha/}} \varrho_{\alpha/} , \tag{2.14a}$$

$$[u_{\alpha/}{}^{i}] = - \frac{P_{\alpha/}}{(\varrho_{\alpha/}/p_{\alpha/}) u_{\alpha n/}} X^{i} , \tag{2.14b}$$

together with (2.12).

In terms of density strength, the Rankine-Hugoniot jump conditions can be written as

$$[u_{\alpha l}{}^{i}] = -\frac{D_{\alpha l}}{1 + D_{\alpha l}} u_{\alpha n l} X_{\alpha l}{}^{i}, \tag{2.15a}$$

$$[p_{\alpha l}] = \frac{D_{\alpha l}}{1 + D_{\alpha l}} \varrho_{\alpha l} u_{\alpha l}^{2}, \tag{2.15b}$$

together with (2.13).

The theorem in this section can also be proved either by using $P_{\alpha l}$ or by using $D_{\alpha l}$ in exactly the same way.

RIASSUNTO (*)

LANDAU e LIFSHITZ (1959) (1) hanno riferito il seguente risultato: *Se due (o più) onde d'urto successive portano un gas dallo stato 1 allo stato 2 e da questo allo stato* 3, *la transizione dallo stato 1 allo stato 3 non può essere prodotta, in generale, dal passaggio di un'onda d'urto qualunque*. Scopo di questa nota è di ottenere le condizioni in cui la transizione dallo stato 1 allo stato 3 sia prodotta dal passaggio di un'onda d'urto qualunque.

(*) *Traduzione a cura della Redazione.*

Electromagnetic Parameters of Matter and Conditions for Physical Realizability (*).

G. Gerosa

Istituto di Elettronica dell'Università - Roma

G. Latmiral and R. Vinciguerra

Istituto Universitario Navale - Napoli

(ricevuto il 10 Novembre 1960)

Summary. — 1) The conditions are examined which a complex function of real variable must satisfy in order that it may be considered as the frequency response of a linear system. The cases of the physical realizability and of the stability of the system are considered and use is made of the Hilbert transforms. 2) The relations existing between the real and the imaginary part of the e.m. parameters of matter are studied by means of the Hilbert transforms, also known as Kramers-Krönig equations. The case of imperfect dielectrics is particularly examined and a suitably modified form of K.-K. equations is presented. 3) The above considerations are extended to the anysotropic media; special reference is made to the susceptivity of magnetized ferrites. When losses are present, and the parameters of the tensor are consequently finite for any frequency, said parameters must comply with Kramers-Krönig equations. This is actually the case for the expressions which are generally used.

Introduction.

The subject of the present work has been dealt with in many papers (**) with different methods and symbologies. To introduce and justify some reasonings

(*) This paper was presented at the 46-th Meeting of the Italian Physical Society Naples, 29 Sept. 1960.

(**) Reference is made only to two recent papers, in which a more extended bibliography can, as well, be found: J. S. Toll: *Phys. Rev.*, **104**, 1760 (1956); B. S. Gourary: *Journ. Appl. Phys.*, **28**, 283 (1957).

and remarks not found in the bibliography it was considered not useless to re-examine the whole subject.

1. – Mathematical premises.

In order that a linear system be stable, *i.e.* that to any limited input correspond a limited output, the delayed part $\alpha(t)$ of the response to the unit impulse in $t = 0$ must be absolutely integrable.

This condition is necessary and sufficient.

The Fourier transform of $\alpha(t)$ is, in this case, the *frequency response*, $F(\omega) = f_1(\omega) + jf_2(\omega)$ of the system.

Moreover if we assume that the system is physically realizable, *i.e.* that the response $\alpha(t)$ to the unit impulse cannot precede its application [$\alpha(t) = 0$ for $t < 0$], the absolute convergence of the Fourier transform $F(\omega)$ implies that of the Laplace transform $F(p)$, where the real part of $p = r + j\omega$ is positive or zero.

$F(p)$, *transfer function* of the system, is then holomorphic in the right-hand complex half plane. Furthermore, if $\alpha(t)$ is assumed to be limited and consequently square integrable (its absolute integrability was already assumed), it follows that even $F(p)$ must be square integrable and that the Cauchy formula, which allows to compute $F(p)$ within a limited domain, can be applied even if we consider the $j\omega$ axis as the boundary of the domain.

When $r \to 0$, and the point p reaches the $j\omega$-axis, the Cauchy formula, if the real and the imaginary parts are separated, gives origin to the Hilbert transforms. These in turn become the Kramers-Krönig (K.-K.) relations when it is taken into account that $f_1(\omega)$ and $f_2(\omega)$, being the cosine and the sine transforms of $\alpha(t)$, must respectively be even and odd.

It is thus possible to prove that the K.-K. equations are a necessary condition for the physical realizability of a linear system; the condition is also sufficient provided that the significance of the Fourier integral is extended by introducing a mean convergence of it.

The two K.-K. equations can be compressed in a single complex one, also known as « *the dispersion relation* », which is widely used in Physics whenever an output function of time is a linear functional of an « input » function.

2. – Imperfect dielectrics.

In the study of the e.m. parameters of matter use is made of some functions, as *e.g.* the « equivalent dielectric constant » $F(p) = \varepsilon(p) + (\sigma(p)/p)$, which present poles on the $j\omega$-axis.

This can be caused by actual instability or (as in the case under examination) by the fact that these functions are mathematical operators which lose significance in said singular points, and are not true transfer functions (Laplace transforms of the impulsive response), *i.e.* real physical parameters.

It will be shown that even in these cases some integral relations can be deduced; these are, however, different from the K.-K. ones, which are valid only when no poles are present on the $j\omega$ axis.

« Original » Kramers-Krönig equations can be quickly deduced as follows.

If $F(p)$ is holomorphic in the right-hand complex half plane, even $F(p)/(p - j\omega_0)$ is such, except in $j\omega_0$. We integrate this function along the $j\omega$-axis, from which the $j\omega_0$-pole has been excluded by means of an half circle of infinitesimal radius. The contour is completed by an half circle of infinite radius, both of said half circles lying in the right-hand complex half plane, which is free from singularities.

Under the conditions pointed out in the Mathematical Premises, the last part of the contour integral vanishes and, since according to Cauchy's theorem, even its overall value must be zero, it follows that the integral along the $j\omega$-axis must equal the residue in $j\omega_0$, changed in sign and divided by 2.

Separating the real and the imaginary parts and taking into account the fact that f_1 is an even and f_2 an odd function, K.-K. equations are obtained (*):

$$f_1(\omega_0) = -\frac{2}{\pi}\int_0^\infty \frac{f_2(\omega)}{\omega^2 - \omega_0^2}\,\omega\,\mathrm{d}\omega; \tag{1}$$

$$f_2(\omega_0) = \frac{2}{\pi}\int_0^\infty \frac{f_1(\omega)}{\omega^2 - \omega_0^2}\,\omega_0\,\mathrm{d}\omega\,. \tag{2}$$

(*) The integrals have to be understood in the Cauchy sense whenever they do not have significance in the ordinary sense.

An alternative form of eq. (2) is the following (H. W. BODE: *Network Analysis*, p. 286 and p. 313):

$$f_2(\omega_0) = \frac{1}{\pi}\int_{-\infty}^{\infty} \frac{\mathrm{d}f_1(u)}{\mathrm{d}u}\,\ln \operatorname{ctgh}\,\frac{|u|}{2}\,\mathrm{d}u\,, \tag{2'}$$

where $u = \ln(\omega/\omega_0)$. As far as the logarithmic weighting function approaches the $\pi^2/2$ impulse in $u=0$ [Dirac's improper delta function $\delta(u)$ times $\pi^2/2$], the above relation approaches

$$f_2(\omega_0) \simeq \frac{\omega_0\pi}{2}\left|\frac{\mathrm{d}f_1(\omega)}{\mathrm{d}\omega}\right|_{\omega=\omega_0}. \tag{2''}$$

The immediate (real) response f_∞, when present, must be subtracted from f_1. As a matter of fact, both the real and the imaginary part of the frequency response $F(\omega)$, as they are the cosine and the sine transforms of $\alpha(t)$, must vanish when $\omega \to \infty$ (*).

When the $F(p)$ function has poles on the $j\omega$-axis, they must be encircled by means of a corresponding number of half circles and the integral relations which are obtained are no longer those by K.-K. F.i., in the above mentioned case of the « equivalent dielectric constant »:

$$F(\omega) = \varepsilon(\omega) - j\frac{\sigma(\omega)}{\omega} = \varepsilon_1(\omega) + j\varepsilon_2(\omega) - j\frac{\sigma_1(\omega) + j\sigma_2(\omega)}{\omega}, \tag{3}$$

the following integral relations are obtained, instead of (1) and (2):

$$\varepsilon_1(\omega_0) - \varepsilon_\infty + \frac{\sigma_2(\omega_0)}{\omega_0} = -\frac{2}{\pi}\int_0^\infty \frac{\varepsilon_2(\omega) - [\sigma_1(\omega) - \sigma_\infty]/\omega}{\omega^2 - \omega_0^2}\,\omega\,\mathrm{d}\omega, \tag{4}$$

$$\varepsilon_2(\omega_0) + \frac{\sigma(0) - \sigma_1(\omega_0)}{\omega_0} = \frac{2}{\pi}\int_0^\infty \frac{\varepsilon_1(\omega) - \varepsilon_\infty + \sigma_2(\omega)/\omega}{\omega^2 - \omega_0^2}\,\omega_0\,\mathrm{d}\omega. \tag{5}$$

These relations lose significance in the point $\omega_0 = 0$, where the dielectric and conductive phenomena are unrelated. If ε_∞, σ_∞, and $\sigma(0)$ are known ($\sigma(0)$ can be obtained by means of a d.c. measurement), expressions (4) and (5) allow to deduce the real part of the « equivalent dielectric constant » once the imaginary part is known and conversely.

The « original » K.-K. equations (1) and (2) hold even for imperfect dielectrics, *i.e.* when the conductivity $\sigma \neq 0$, only if, instead of the « equivalent dielectric constant », its square root, or its logarithm, are considered, or whatever function, which, by reducing below unity the order of the singularity, causes the corresponding residue to vanish.

Therefore, for the index of refraction $\sqrt{\varepsilon\mu}$, or for the intrinsic admittance $\sqrt{\varepsilon/\mu}$, K.-K. equations do always hold.

When K.-K. equations are valid, the behaviour of a linear system, stable and physically realizable, is completely determined when the real (f_1), or the imaginary (f_2), part of the frequency response F are known along the whole $j\omega$-axis; or when for some intervals f_1 and for the remaining f_2 are known;

(*) For $\omega \to 0$, $f_2 \to 0$ and $f_1 \to f_s$, where f_s is the static value of the frequency response. As for f_∞, it is the value which F takes for the highest frequencies at which the e.m. behaviour of matter can still be described by means of the macroscopic parameters ε, μ, σ.

briefly, if « half of the total information » is available. Besides, the « immediate response » f_∞, if present, must be determined.

If F presents poles on the $j\omega$-axis, relations of the modified type (4), (5) must be used and the residues in said poles must be known.

3. – Anisotropic media (magnetized ferrites).

We will now consider a more general case, in which the relation between the two physical quantities under examination is of tensor type.

Reference will be made to the Fourier transforms of the time-varying components of the magnetization $\boldsymbol{M}$ and the field $\boldsymbol{H}$ in a magnetized ferrite.

We have

$$\boldsymbol{M}(\omega) = \mu_0 \boldsymbol{X}(\omega) \cdot \boldsymbol{H}(\omega) , \tag{6}$$

where

$$\boldsymbol{X}(\omega) = \begin{vmatrix} X_{xx} & X_{xy} & X_{xz} \\ X_{yx} & X_{yy} & X_{yz} \\ X_{zx} & X_{zy} & X_{zz} \end{vmatrix} . \tag{7}$$

The $X_{ik} = X_{ik}^R + jX_{ik}^J$ are functions of ω.

We have considered the susceptivity tensor and not the permeability one so as to deal with quantities all of which vanish for $\omega \to \infty$.

Let

$$\boldsymbol{H}(t) = \boldsymbol{h}\, \delta(t) , \tag{8}$$

where $\boldsymbol{h}$ is an arbitrary constant vector and δ is the Dirac improper function. The Fourier transform of $\boldsymbol{H}(t)$ is then $\boldsymbol{H}(\omega) = \boldsymbol{h}$ and consequently

$$\boldsymbol{M}(\omega) = \mu_0 \boldsymbol{X}(\omega) \cdot \boldsymbol{h} . \tag{9}$$

Let us now consider the inverse Fourier transform

$$\boldsymbol{M}(t) = \frac{1}{2\pi} \int_{-\infty}^{+\infty} \boldsymbol{M}(\omega) \exp [j\omega t] \, \mathrm{d}\omega = \frac{\mu_0}{2\pi} \int_{-\infty}^{+\infty} \boldsymbol{X}(\omega) \cdot \boldsymbol{h} \exp [j\omega t] \, \mathrm{d}\omega . \tag{10}$$

Imposing that $\boldsymbol{M}(t)$ be real for any t and zero for $t < 0$ and taking advantage of the fact that $\boldsymbol{h}$ is an arbitrary vector (which can be assumed to be parallel to any one of the three axes) it results that for all components of

the susceptivity tensor the real and the imaginary part must respectively be even and odd functions of ω and that they must satisfy K.-K. relations:

$$X_{ik}^{R}(\omega_0) = -\frac{2}{\pi}\int_0^\infty \frac{X_{ik}^{J}(\omega)}{\omega^2 - \omega_0^2}\,\omega\,\mathrm{d}\omega, \tag{11}$$

$$X_{ik}^{J}(\omega_0) = \frac{2}{\pi}\int_0^\infty \frac{X_{ik}^{R}(\omega)}{\omega^2 - \omega_0^2}\,\omega_0\,\mathrm{d}\omega\,. \tag{12}$$

These relations are certainly satisfied if the X_{ik}, considered as functions of $p = r + j\omega$, are holomorphic functions in the $r \geqslant 0$ half plane.

We will now confine our attention to the case of saturated ferrite. If the static field is directed along the z-axis, we obtain for the susceptivity tensor the following form:

$$X = \begin{vmatrix} X_d & X_0 & 0 \\ -X_0 & X_d & 0 \\ 0 & 0 & 0 \end{vmatrix}, \tag{13}$$

where

$$X_d = \varrho\,\frac{1 + \alpha^2 + j\alpha\beta}{1 + \alpha^2 - \beta^2 + 2j\alpha\beta}, \tag{14}$$

$$X_0 = \varrho\,\frac{j\beta}{1 + \alpha^2 - \beta^2 + 2j\alpha\beta}, \tag{15}$$

and

$$\varrho = \frac{M_0}{\mu_0 H_0}; \tag{16}$$

$$\beta = \frac{\omega}{\omega_0}, \tag{17}$$

α is the attenuation factor caused by losses, M_0 the saturation magnetization, H_0 the static magnetic field and ω_0 the corresponding resonance angular frequency.

It is easy to verify that the real and imaginary parts of X_d and X_0 are respectively even and odd functions of β, *i.e.* of ω, and have the same poles.

Said poles are in the points

$$p = \omega_0(-\alpha \pm j)\,, \tag{18}$$

therefore, X_d and X_0 are holomorphic for $r \geqslant 0$ and comply consequently with K.-K. relations.

When $\alpha = 0$ (absence of losses), the poles reach the $j\omega$-axis and K.-K. relations are no longer satisfied. However, when losses are absent, the system is no more stable and, consequently, this result cannot be considered as unexpected.

As a conclusion, we can say that the susceptivity tensor of saturated ferrites, expressed in the generally used form (13)–(17), complies with K.-K. relations for physical realizability provided that losses are taken into account ($\alpha \neq 0$).

* * *

This Research has been sponsored by the European Office of the A.R.D.C., U.S.A.F., under Contract AF61(052)-36, and as a part of it.

RIASSUNTO

1) Si esaminano le condizioni cui deve soddisfare una funzione complessa di variabile reale perchè possa assumersi come risposta in frequenza di un sistema lineare, prendendo in considerazione i casi della realizzabilità fisica e della stabilità del sistema ed avvalendosi delle trasformate di Hilbert. 2) Si studiano le relazioni che legano parte reale e parte immaginaria dei parametri elettromagnetici della materia alla luce delle trasformate di Hilbert, note anche come equazioni di Kramers-Krönig, e si esaminano alcuni casi singolari, in particolare quello dei dielettrici imperfetti, per cui viene presentata una forma modificata delle equazioni di K.-K. 3) Si estendono le precedenti considerazioni alle sostanze anisotrope, con particolare riferimento alla suscettività delle ferriti magnetizzate. Nel caso in cui siano supposte presenti le perdite, ed i parametri del tensore risultino pertanto finiti per ogni frequenza, tali parametri debbono soddisfare le equazioni di K.-K. Ciò effettivamente accade per le espressioni generalmente usate.

IL NUOVO CIMENTO Vol. XX, N. 4 16 Maggio 1961

On the Nature of Radiation Damage due to Fast Neutron Bombardment in Ferromagnetic Materials: Very High Permeability Pure Iron and Nickel (*).

G. Biorci, A. Ferro (**) and G. Montalenti

Istituto Elettrotecnico Nazionale G. Ferraris
Centro Studi per l'Elettrofisica del C.N.R. - Torino

(ricevuto il 2 Gennaio 1961)

Summary. — The effects of fast neutron irradiation with doses of 10^{18} nvt on permeability, coercive force and approach to saturation of very high permeability pure iron and nickel were studied. No significant changes were noted on nickel (maximum permeability 5000). On iron (maximum permeability about 150000, H_c 2.5 A/m) coercive force increased by about 0.8 A/m, maximum permeability decreased by about 30%, and no change was noted in the curve of approach to saturation and hence in the anisotropy energy. After annealing the irradiated iron specimens at 100 °C, a further increase of coercive force was observed, and after annealing at 200 °C, on one of the specimens a loop with strong wasp-waisted form was noted. Finally most of the changes in magnetic properties due to irradiation were almost completely recovered below 250 °C. The possible theoretical interpretations of the results are discussed. The kinetics of the annealing leads to exclude that the effects are due to free iron interstitials and probably also to dislocations loops. Hence it shall be thought of some type of anisotropic point defects which interact with the magnetization vector and move with and activation energy of about 1.2 eV at temperatures of (100 ÷ 200) °C.

(*) The research reported in this document has been sponsored by the Air Force Office Scientific Research of the Air Research and Development Command, United States Air Force through its European Office, under Contract.

(**) Istituto Nazionale di Fisica Nucleare, Sezione di Torino.

1. – Introduction.

Several experiments have been recently carried out on radiation damage of different types of magnetic materials. In most cases the dose of neutrons used was of the order of 10^{18} nvt. Generally a deterioration of structure sensitive properties (permeability, coercive field) was observed, but no variations (except in some specific cases to be discussed later on) of the non structure sensitive properties were noted (saturation magnetization intensity, Curie point, anisotropy energy).

No significant variation of magnetic properties [1-3] was found on permanent magnets such as alnico, ferrites and steel.

Marked decrease of initial and maximum permeability (in some cases up to 90%) and of loop rectangularity, besides a noticeable increase of coercive field (in some cases 800%) were observed on high permeability iron-nickel alloys, while the variations observed on some other alloys, such as iron-silicon, iron-aluminum, iron-cobalt are very small [4-8].

Works on single crystals demonstrate furthermore that anisotropy energy variations are nought, excluding the case of Fe_3Al [9], where irradiation induces an order-disorder transformation.

On Fe-Ni alloys SCHINDLER and SALKOVITZ [10] have demonstrated the possibility of obtaining rectangular loops on a disordered permalloy (*i.e.* without orientation superstructures) by irradiation in a magnetic field. These exper-

[1] R. S. SERY, D. I. GORDON and R. H. LUNDSTEN: *Bull. Am. Phys. Soc.*, **4**, 137 (1959).

[2] D. I. GORDON, R. S. SERY and R. H. LUNDSTEN: Office of Naval Research 5 (Washington); *Materials Research in the Navy-Symposium* (Philadelphia, 1959), p. 253-292.

[3] FENNEL, HANCOCK and R. S. BARNES: AERE M/TN 48 (Atomic Energy Research Establishment, Harwell, 1958).

[4] R. S. SERY, R. E. FISHELL and D. I. GORDON: *Effects of Nuclear Radiation on Magnetic Properties of Core Materials.* Navord Rept. 4381 (16 Dec. 1956); and *Nucleonics*, **16**, 73 (1958).

[5] R. S. SERY, R. E. FISCHELL and D. I. GORDON: *Trans. Amer. Inst. Elec. Engrs.*, **77**, 453 (1957).

[6] D. I. GORDON and R. S. SERY: *International Conf. on Solid State Physics in Electronics*, Brussels, 1958 (London, 1960), p. 824.

[7] R. C. HALL, W. S. BYRNES and R. G. CRAWFORD: *Journ. Appl. Phys. Suppl.*, **30**, 288 S (1959).

[8] R. E. ALLEY jr.: *Journ. Appl. Phys. Suppl.*, **30**, 284 S (1959).

[9] R. C. HALL, W. S. BYRNES and R. G. CRAWFORD: *Journ. Appl. Phys.*, **30**, 1846 (1958).

[10] A. I. SCHINDLER, E. I. SALKOVITZ and G. S. ANSELL: *Journ. Appl. Phys. Suppl.*, **30**, 282 S (1959).

iments have been recently confirmed by other authors [11] who irradiated an iron-nickel alloy (Fe 50 % - Ni 50 %) in a magnetic field and measured the induced uniaxial anisotropy energy. The induced anisotropy energy obtained in this manner by irradiation with fast neutrons doses of the order of 10^{17} nvt is of the order of 10^4 erg/cm^3, while values only of the order of 10^3 erg/cm^3 are obtained in the same alloys with cooling in a magnetic field. The key [10-12] for interpretation of the modifications observed in the magnetic propreties of permalloys is given by the theory of NÉEL [13] and TANIGUCHI [14] on orientation superstructures. The main effect of irradiation is to allow low temperature diffusion processes which normally, in the same alloys, are possible only with treatments at about 500 °C.

ARONIN [15] irradiated a Ni_3Mn alloy with doses of 10^{20} nvt. A marked decrease of saturation magnetization intensity J_s was observed. This fact can be interpreted as an effect of disordering produced by irradiation in the ordered structure.

On various types of commercial ferrites [16-18] further to irradiation, a behaviour was observed similar to that noted with high permeability alloys. In some cases [17] a variation of J_s between 3 % and 15 % has been reported. Significant variations of high frequency properties have also been reported [18]; a conclusive interpretation would be at least premature as experiments were carried out on commercial samples. In many cases the nature of the effects is probably similar to the one of permalloys.

Only two experiments have been carried out on pure metals such as iron or nickel. The first one [19] by the authors of this work on iron having exceptional magnetic properties ($\mu_{max} = 150\,000$), indicated a marked reduction (15 % to 30 %) of maximum permeability and a noticeable increase (30 %) of coercive force. This proves that some defects are present after irradiation that could influence the structure sensitive magnetic properties.

The second one was carried out at Grenoble by MOSER, DAUTREPPE and

[11] J. PAULEVE and D. DAUTREPPE: *Compt. Rend. Acad. Sci.*, **250**, 3804 (1960).

[12] G. MONTALENTI: *Effect du Rayonnement Neutronique sur les Matériaux Magnétiques, Rendiconti S.I.F.*, XVIII Course (to be published).

[13] L. NÉEL: *Journ. Phys. et Rad.*, **15**, 225 (1954).

[14] S. TANIGUCHI: *Sc. Rep. Res. Inst. Tohoku Univ.*, A **7**, 269 (1955).

[15] L. R. ARONIN: *Journ. Appl. Phys.*, **25**, 344 (1954).

[16] E. I. SALKOVITZ, A. I. SCHINDLER, N. G. SAKIOTIS and G. S. ANSELL: *International Conf. on Solid State Physics in Electronics*, Brussels 1958 (London, 1960), p. 808.

[17] W. E. HENRY and E. I. SALKOVITZ: *Journ. Appl. Phys. Suppl.*, **30**, 278 S (1959).

[18] E. I. SAKIOTIS, E. I. SALKOVITZ and A. I. SCHINDLER: *International Conf. on Solid State Physics in Electronics*, Brussels, 1958 (London, 1960), p. 817.

[19] G. BIORCI, A. FERRO and G. MONTALENTI: *Journ. Appl. Phys.*, **31**, 2084 (1960).

BRISSONEAU ([20]). These authors, studying the diffusion viscosity on pure iron irradiated respectively at the temperature of liquid nitrogen and at room temperature, concluded that three types of defects are produced by irradiation: one type diffusing at a temperature between 80° and 100 °K with an activation energy of about 0.3 eV; the second diffusing with an energy of about 0.6 eV at about 200 °K; the third, which is only present after irradiation at room temperature, giving a viscosity effect with activation energy of about 1.2 eV at a temperature of about 370 °K. Neither the authors, as it will be seen later on, nor MOSER observed significant variations of magnetic properties in nickel. The importance of these experiments is to demonstrate that in iron, besides vacancies and interstitials, also defects of other types, that remain present at room temperature, are formed.

The purpose of this work is to report further experiments carried out on pure metals and discuss the possible interpretations of the facts observed.

In the present work new experiments were performed on high permeability iron, and the changes in magnetic properties were measured both in high and low fields. Specimens of nickel were also examined. The recovery of damage in iron with temperature was studied and the results obtained are discussed theoretically.

2. – Characteristics and preparation of specimens.

The previous experiments ([19]) and theoretical reasons suggested that the effects observable were very low and that valuable results could be obtained only on very high permeability pure metals.

The most suitable materials are therefore iron and nickel of good purity. Iron specimens of good purity and very high permeability have been prepared as in the preceding work ([19]) according to the technique of CIOFFI ([21,22]), *i.e.* by long annealing at 1480 °C in pure dry H_2. After this treatment permeabilities from 135000 to 190000 have been obtained. After heat treatment the carbon and nitrogen content of the specimens was controlled by internal friction techniques ([23]), and resulted lower than 0.0001 %. Therefore any aging effect due to these elements in the course of irradiation is prevented. The O_2 content was lower than 0.001 %; and S, determined by standard chemical methods, was lower than 0.003 %. The micrographs of the specimens resulted completely free from precipitates.

([20]) P. MOSER, D. DAUTREPPE and P. BRISSONEAU: *Compt. Rend. Acad. Sci.* (in the press).

([21]) P. P. CIOFFI: *Phys. Rev.*, **39**, 363 (1932); **45**, 742 (1934).

([22]) R. M. BOZORTH: *Ferromagnetism* (New York, 1950).

([23]) L. J. DIJKSTRA: *Philips Res. Rept.*, **2**, 357 (1947).

The nickel specimens were prepared according to a similar technique, by annealing at about 1300° in dry pure H_2 and very slow cooling. Notwithstanding the special attention given in the preparation of the specimens the maximum permeability obtainable in this case is however only 5000 and the coercive field about 20 A/m.

The specimens are in form of rings of the following dimensions: 35 mm o.d., 28 mm i.d. and 7 mm height. Rather thick specimens where chosen in order to avoid the effect of the free magnetic charges on the surface which lower permeability.

After heat treatment the windings on the specimens were carefully made with glass cloth insulated copper wire. After this the specimens were kept four days at 150 °C, or 12 hours at 200 °C. Thus, any aging effect in the specimen and the relaxation of any weak internal stress produced by the windings or caused by handling of the specimen occurred before irradiation. However, since no difference of permeability was observed before and after this treatment, it can be surely excluded that during irradiation any aging effect may be present.

Moreover a series of preliminary tests was performed in order to control the sensitivity of the specimens to strains, and special care was taken in handling the specimens in order to avoid any shock or stress on them. For irradiation the specimens were placed in an aluminum container. Irradiation was performed for all specimens in the Swimming Pool Reactor Melusine in Grenoble with an integrated neutron flux of $1.3 \cdot 10^{19}$ nvt and a corresponding fast neutron flux of about $1.3 \cdot 10^{18}$ nvt. The temperature of the specimens during irradiation was lower than 25 °C. After irradiation the specimens were left at room temperature for about one month in order to obtain a sufficiently low radioactivity level.

3. – Effects of irradiation on magnetic properties at high fields.

Determination of the curves of approach to saturation at high fields was performed on two of the iron specimens. Since the specimens were the same rings used for determining the magnetic properties at low fields, a special experimental set-up had to be used. To obtain the high fields requested the iron ring was placed on a copper bar in which a generator produced a very intense current (up to 15000 A). The specimen was kept at room temperature by means of intense water circulation around the specimen itself and in the conductors. Flux measurements were performed with a Norma fluxmeter, as the time constant of ballistic galvanometers is too low in relation to the time constant for current inversion in the generator. The values of the mag-

netic field were deduced from the measurements of the current and from the geometrical dimensions. A more complete description of the equipment used for measurements was given in another work [24]. Magnetic field measurements were reproducible up to 1%, and magnetic induction measurements up to ±1.5%. The maximum obtainable field was 150 000 A m. The experimental results obtained on one of the specimens are given in Fig. 1. For an induction above 1.5 Wb m^2 the curves of magnetization before and after irradiation practically coincide.

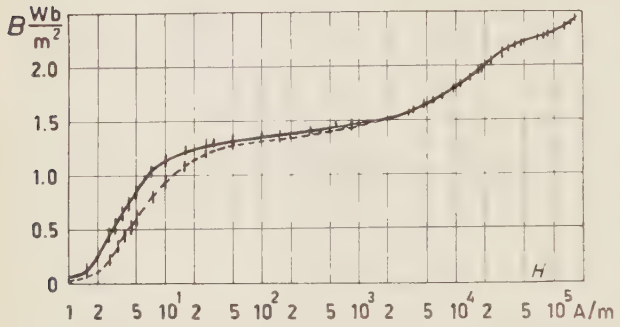

Fig. 1. – Magnetization curves up to 150 000 A m. High permeability iron, specimen 13 A. Irradiation dose: integrated flux: $1.3 \cdot 10^{19}$ nvt (fast flux, > 1 MeV, $1.3 \cdot 10^{18}$ nvt). Solid line: before irradiation, dotted line: after irradiation.

W. F. BROWN [25], SEEGER [26], VICENA [27] have studied the effect of dislocations and internal strains on approach to saturation. To observe the effects foreseen by BROWN, fields of the order of 10^6 A m are necessary and extremely precise measurements should be done. At the same time, to observe the effects of dislocations on approach to saturation studied by SEEGER, and considering that the effects of irradiation are quite low, it would be necessary to reach a precision of measurement of the magnetization intensity much higher than that obtainable with the equipment described above.

On the other hand, bearing in mind the theories of AKULOV [28], GANS [29], NÉEL [30] it can be deduced that the anisotropy energy did not markedly vary following irradiation. This is the only conclusion to be drawn from the measurements performed on the curve of approach to saturation before and after fast neutron irradiation on these materials.

[24] G. BIORCI, A. FERRO and G. MONTALENTI: *Effect of Neutron Bombardment on the Magnetic Properties of Iron and Nickel of Very High Permeability*. III. ARDC Contr. AF 61 (514) 1331 (February, 1960).

[25] W. F. BROWN: *Phys. Rev.*, **58**, 736 (1940).

[26] A. SEEGER: (Stuggart) to be published.

[27] F. VICENA: *Czecoslov. Journ. Phys.*, **5**, 4 (1955).

[28] N. S. AKULOV: *Zeits. Phys.*, **57**, 249 (1929); **69**, 822 (1931).

[29] R. GANS: *Ann. d. Phys.*, **15**, 28 (1932).

[30] L. NÉEL: *Journ. Phys. et Rad.*, **9**, 193 (1948).

4. – Effects of irradiation on magnetic properties at low fields.

The results obtained can be summarized as follows: *Nickel.* Notwithstanding the special attention given in performing the measurements, the values of the magnetization intensity were affected by a noticeable scattering, probably

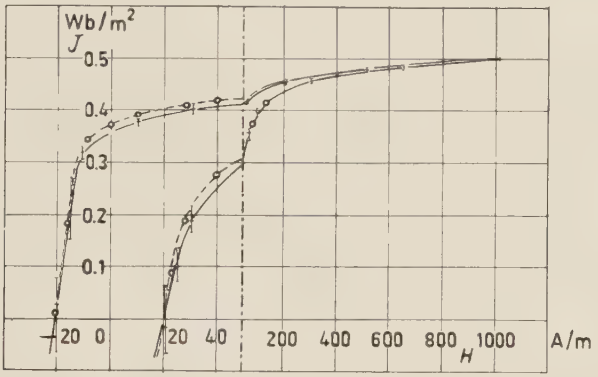

Fig. 2. – Hysteresis loop of pure annealed nickel before irradiation (solid line) and after irradiation (dotted line). Irradiation dose: integrated flux $1.24 \cdot 10^{19}$ nvt (fast flux, > 1 MeV, $1.2 \cdot 10^{18}$ nvt)

intrinsic of the material. The measurements were carried out with the specimen in a thermostatic liquid bath stabilized within 0.01 °C, performing demagnetization always in the same manner. In spite of this, the magnetization

TABLE I.

Irradiation dose: integrated flux $1.3 \cdot 10^{19}$ nvt, fast flux $1.3 \cdot 10^{18}$ nvt	Specimen T11A	Specimen T13A	Specimen T20A
Coercive force H_c before irradiation	2.4 A/m	2.3 A/m	2.4 A/m
H_c after irradiation	2.9 A/m	3.1 A/m	3.2 A/m
Variation of H_c	0.5 A/m	0.8 A/m	0.8 A/m
Maximum permeability before irradiation	145000	135000	190000
Maximum permeability after irradiation	118000	96000	152000
$\int_0^{J_s} H \, dJ$ (*)	11 J/m³	9.8 J/m³	10.3 J/m³

(*) The last item $\int_0^{J_s} H \, dJ$ indicates the value of the area between the magnetization curve before and after irradiation.

intensity values could be repeated only within about 5%. The magnetization curves observed after irradiation were still contained within this limit, Fig. 2. Hence no effect of irradiation on magnetic properties could be detected.

Iron. Experimental results are given in Fig. 3, 4, 5 and 8, 9, 10. They further confirm the results already published by the authors in a previous work [19]. The results obtained are summarized in Table I.

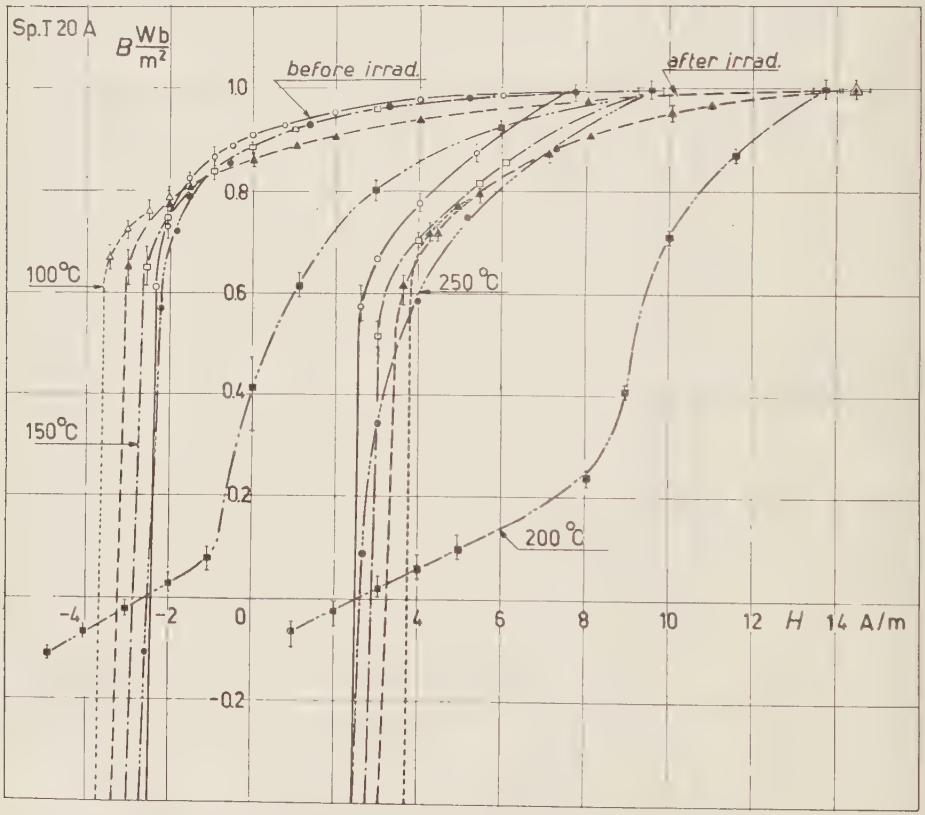

Fig 3. - Hysteresis loop before irradiation (full line), after irradiation (dotted line) and after different recovery stages (1 h at each temperature). Specimen T20A, high permeability iron. Irradiation dose: integrated flux $1.3 \cdot 10^{19}$ nvt (fast flux, >1 MeV, $1.3 \cdot 10^{18}$ nvt).

Substantially a marked decrease of maximum permeability (about 30%), a marked increase of coercive field about 0.6 A/m and no noticeable variation of the initial permeability were observed.

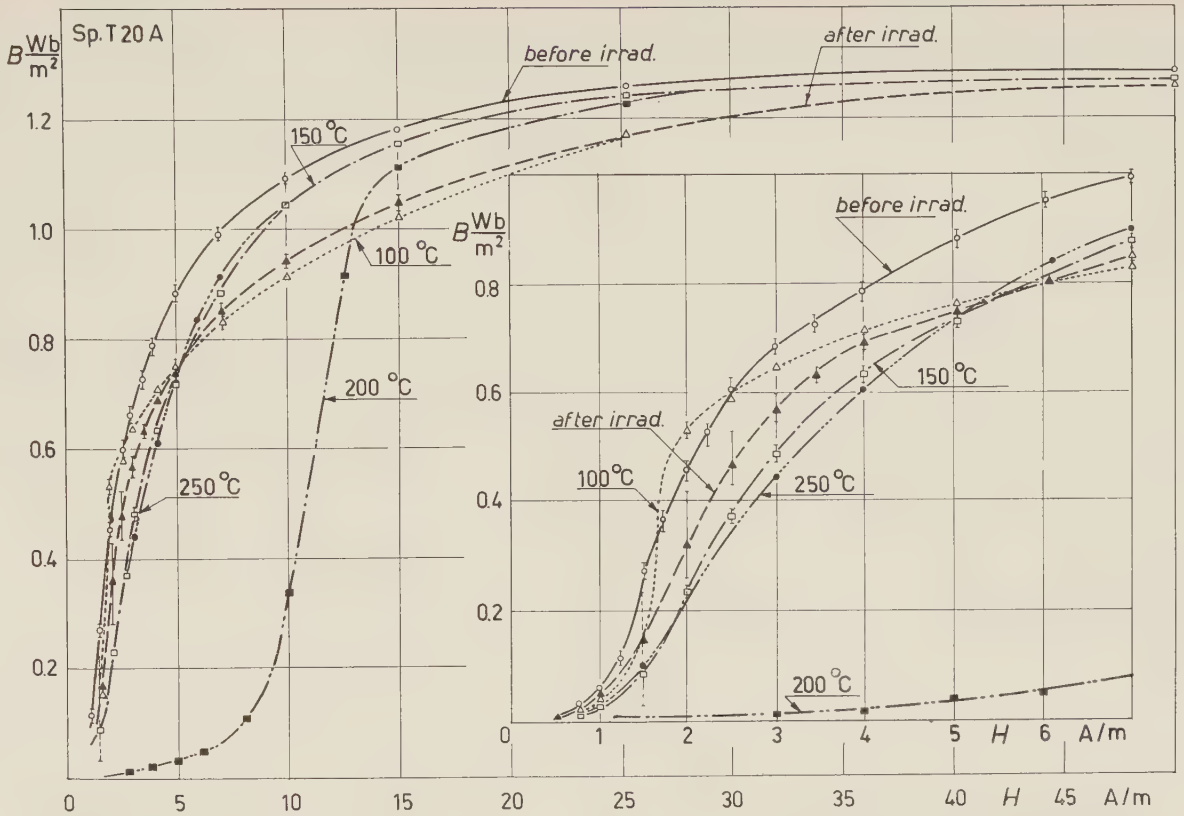

Fig. 4. – Specimen T20A (same as Fig. 3). Magnetization curves, before irradiation (full line), after irradiation (dotted line) and after the different recovery stages.

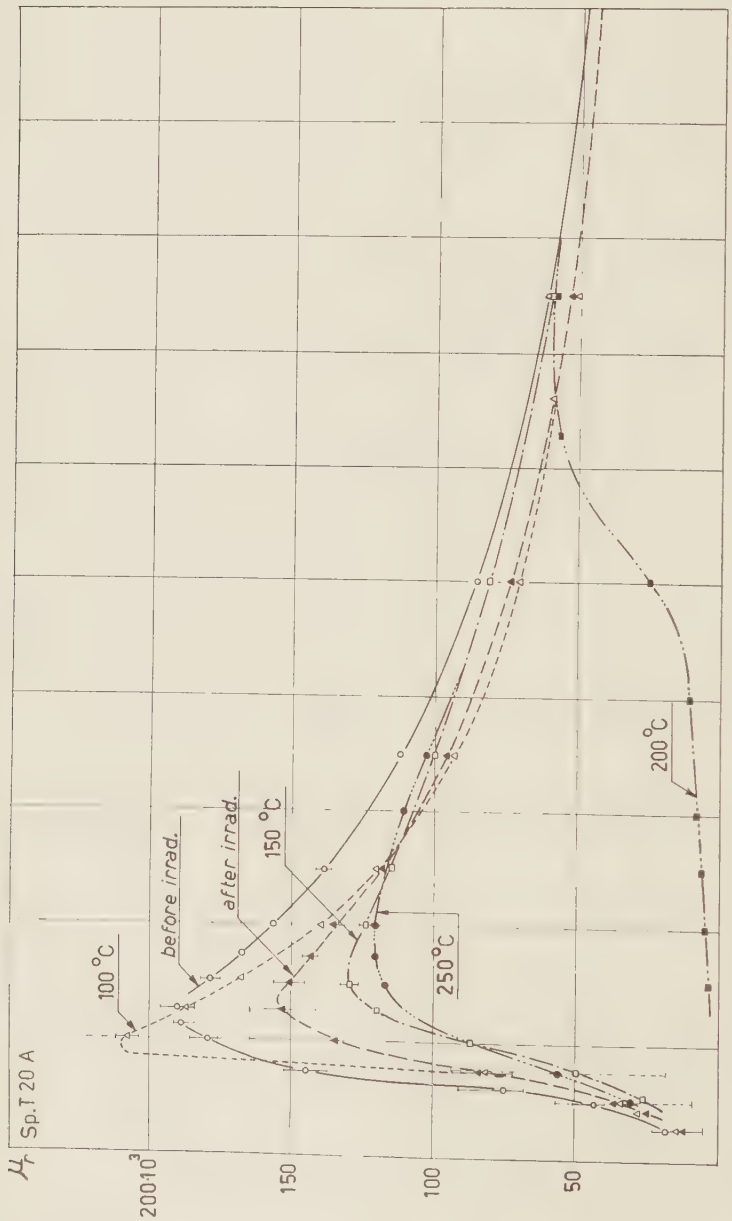

Fig. 5. — Specimen T20A (same as Fig. 3). Permeability curves before irradiation (full line), after irradiation (dotted line) and after the different recovery stages.

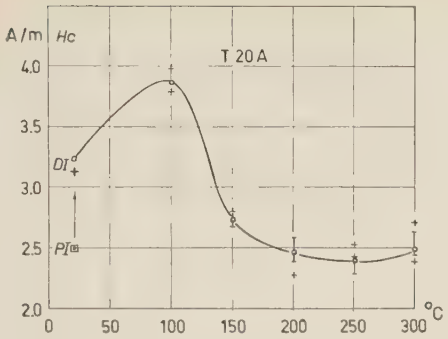

Fig. 6. – Specimen T20A (same as Fig. 3). Variation of the coercive field after irradiation as a function of the recovery temperature (1 h for each annealing step). Initial point (PI) before irradiation, (DI) one month after irradiation.

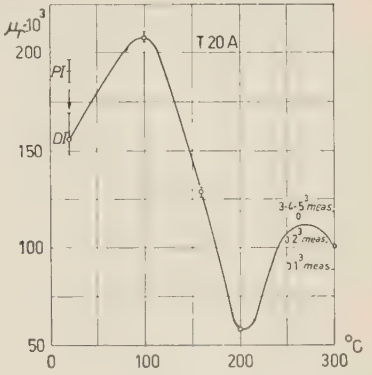

Fig. 7. – Specimen T20A (same as Fig. 6). Variation of permeability as a function of the recovery temperature.

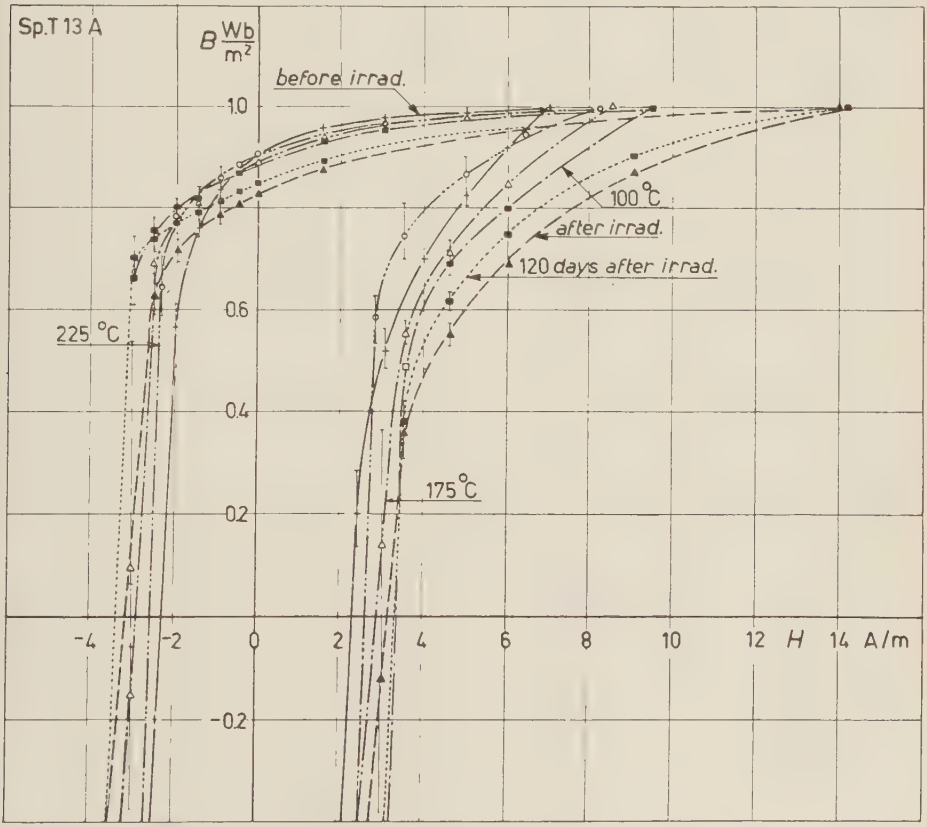

Fig. 8. – Hysteresis loop before irradiation (full line), after irradiation (dotted line, and after different recovery stages (1 h at each temperature). Specimen T13A, high permeability iron. Irradiation dose: integrated flux $1.3 \cdot 10^{19}$ nvt (fast flux, >1 MeV, $1.3 \cdot 10^{18}$ nvt).

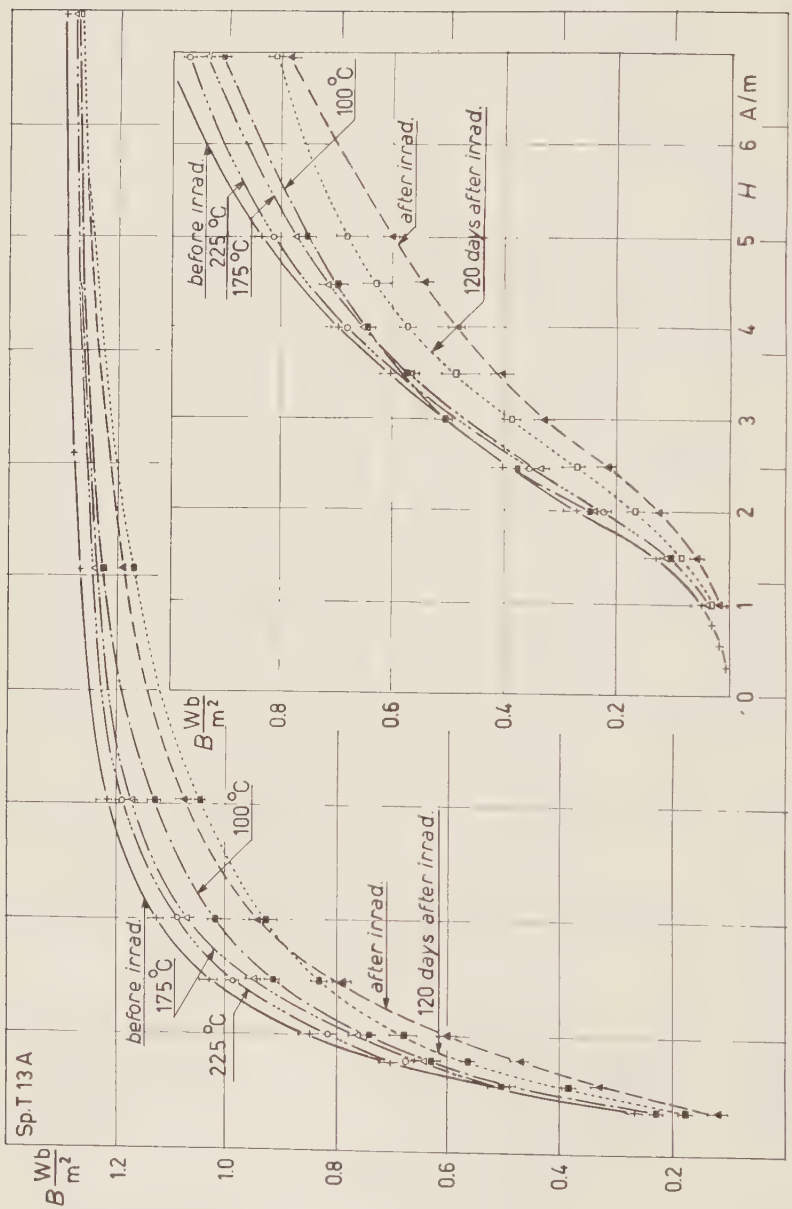

Fig. 9. Specimen T13A (same as Fig. 8). Magnetization curves, before irradiation (full line), after irradiation (dotted line) and after the different recovery stages.

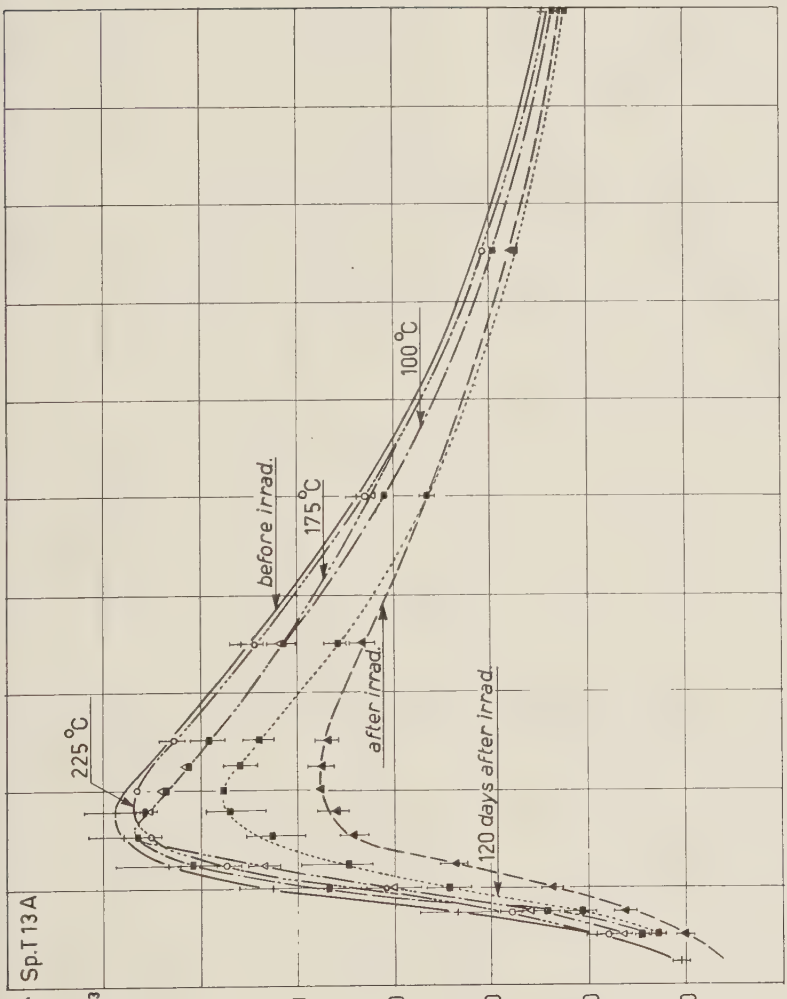

Fig. 10. — Specimen T13A (same as Fig. 8). Permeability curves before irradiation (full line), after irradiation (dotted line) and after the different recovery stages.

5. – Experiments on annealing the damage.

An important point for understanding the nature of the radiation damage observed is to study the annealing of the damage as a function of temperature. These experiments were performed on two iron rings by successively annealing the specimen up to 300 °C at steps of fifty degrees for one hour at each step. The changes in the magnetization curve and in the hysteresis loop were recorded at room temperature after each annealing step.

Ring 20 A. – On this specimen annealing was performed about one month after irradiation. Annealing times and temperatures are given in the figures. Coercive field increased markedly after annealing at 100 °C, then it decreased rapidly until at 150 °C it reached a value corresponding closely to what it had before irradiation, at least within the uncertainty of measurements (Fig. 6). Fig. 3, 4 and 5 list the different hysteresis loops, magnetization and permeability curves recorded. Of great interest is the hysteresis loop, recorded at room temperature, after annealing at 200 °C. A typical wasp-waisted loop is observed, in this case similar to what can be seen in iron due to the diffusion of interstitial carbon atoms, or to reordering of solute atom pairs in a ferromagnetic alloy. The characteristic knee of the cycle was found at a relatively high field: namely 8 A/m, Fig. 3. The changes in the magnetization curves, Fig. 4, also had a behaviour similar to the one of the coercive field. Maximum permeability in function of the annealing temperature is given in Fig. 7: a marked increase at 100 °C was observed. The subsequent cuve was similar to that of the coercive field. After annealing at 250 °C the magnetic properties again returned very close to those of the non irradiated material.

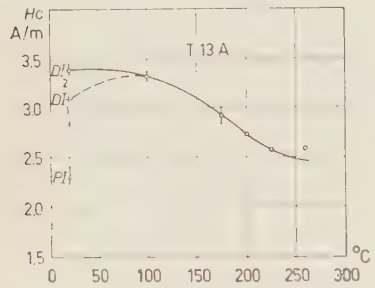

Fig. 11. – Specimen T13A (same as Fig. 8). Variation of the coercive field after irradiation as a function of the recovery temperature (1 h for each annealing step). Initial point (PI) before irradiation, (DI 1) one month after irradiation, (DI 2) five months after irradiation at room temperature.

Ring 13 A. – This specimen was annealed about five months after irradiation. Fig. 8 and 11 give the coercive field in function of the annealing temperature. It can be observed that five months at room temperature already produced a marked increase of coercive field and of maximum permeability similar to that of annealing at 100 °C. When annealing at 150 °C or at higher temperatures, the coercive field begins to decrease towards the values of the non irradiated material and at about 250 °C, within the dispersion of meas-

urements, reaches again the value it had before irradiation. On this specimen the wasp-waisted loop did not appear after annealing at 200 °C, Fig. 8 to 12. The reasons for this different behaviour as to specimen T 20A are not very clear. They could perhaps be related to a long stay at room temperature that could have altered the kinetics of formation and disappearance of the defects in the course of annealing, or to other reasons.

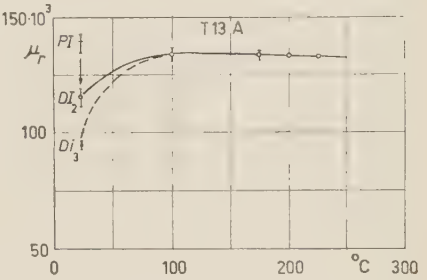

Fig. 12. – Specimen T13A (same as Fig. 11). Variation of permeability as a function of the recovery temperature.

The changes in the magnetization curve, Fig. 9, are analogous to the observed changes in coercive force: in this specimen no drop in the curve is observed in the region of 200 °C. After annealing at 225 °C the curve can be considered coincident, within the experimental errors, with the one relative to the non irradiated material.

6. – Interpretation of experimental results.

The facts prove that in iron, even at room temperature, after irradiation there remain some defects that can markedly influence magnetic properties. The most reasonable hypotheses explaining experimental facts are two, namely:

a) Internal strains are created, as an effect of irradiation which could be interpreted as dislocation rings interacting with Bloch walls. Observations of dislocation rings of a diameter of (100÷300) Å on irradiated materials have already been made for some materials. As far as we know, at least up to now, these rings have been observed only on copper ([31]) and aluminum ([32]).

b) At room temperature after irradiation there is a certain number of point defects having a definite anisotropy energy in relation to the magnetization vector. During irradiation, these defects, can distribute themselves according to the orientation of magnetization in every domain and produce effects of the same type as those ([33]) due to carbon in α-iron, or as those due to pairs of solute atoms in ferromagnetic alloys at high temperature ([13,34]). In iron, which is body-centred cubic, typical defects having a strong anisotropy

([31]) J. Silcox and P. B. Hirsch: *Phil. Mag.*, **4**, 1356 (1959).
([32]) R. E. Smallman and K. H. Westmacott: *Journ. Appl. Phys.*, **30**, 603 (1959).
([33]) L. Néel: *Journ. Phys. et Rad.*, **13**, 249 (1952).
([34]) L. Néel: *Journ. Appl. Phys. Suppl.*, **30**, 3 S (1959).

energy with respect to magnetization are interstitial atoms. However as will be seen later on, it is not very likely that free interstitial atoms can still be present for irradiations performed at room temperature. Other examples can be vacancy couples. Finally some other possibilities can be thought of: some interstitials strongly interacting with impurities or between themselves can survive; spikes and small clusters of point defects can be formed having a definite anisotropy with the magnetization vector. For a recent discussion on the possible type of the defects formed see for instance VINEYARD ([35]) and THOMPSON ([36]).

An attempt of quantitative evaluation of the hypotheses admitted can be given. To interpret the facts it seems better to consider the variations of coercive force and of the area between the curves of initial magnetization before and after irradiation. On the contrary, as known, there is no sufficiently precise theory for maximum permeability. It can only be said that a variation of this magnitude, if the others remain unchanged, is certainly due to defects of the same order of magnitude of the domains.

Hypothesis *a*). The average internal strains corresponding to the defects formed can very simply be deduced ([22,37]) from the observed changes in coercive force and in the area between the magnetization curves before and after irradiation. In the hypothesis that these internal strains correspond to an increase of the dislocation density due to irradiation also Vicena's ([27]) theory can be used.

However it must be observed that all these theories are essentially valid for strain distribution or dislocation loops with large path with respect to the domain wall thickness. On the contrary, from what is known from the literature and from the results of electron microscope observations ([31]) it must be thought that the dislocations eventually formed are small rings with dimensions of the order of 1/10 of the wall thickness, in iron 1000 Å. Also the spacing between the defects is very small with respect to the one usually considered in the theory of coercive field.

It is therefore probable that the calculations carried out following these theories have some serious limitations and can give underestimated results as the interaction with the walls decreases rapidly for defects with dimensions smaller than the walls themselves ([38]). The results of our calculations ([24])

([35]) G. VINEYARD: *The Dynamics of Radiation Damage, Rendiconti S.I.F.*, XVIII Course (to be published).

([36]) G. THOMPSON: *Radiation Damage in Body Centred Metals, Rendiconti S.I.F.*, XVIII Course (to be published).

([37]) C. KITTEL: *Rev. Mod. Phys.*, **21**, 541 (1949).

([38]) L. NÉEL: *Cahiers de Physique*, **12**, 1, (1942).

indicate values of internal strains as being of the order of 0.01 kg/mm² and a dislocation density as being of the order of 10^7 l/cm².

The dislocation density thus obtained is possibly underestimated by about two orders of magnitude for the reason suggested above. Keeping this point in mind, the value obtained is possibly not unreasonable in comparison with the electron microscope results on copper ([31]). On the other hand, the annealing experiments have demonstrated that at temperatures around 200 °C there is already a nearly complete recovery of magnetic characteristics to the values observed before irradiation. On the basis of what is known concerning the movement of dislocations in iron and from the electron microscope observation of HIRSCH ([31]) with annealing of irradiated Cu, it seems, at present, rather unlikely that dislocation rings can be eliminated at such low temperatures. We are therefore led to think that most of the effects observed are probably due to another cause.

Hypothesis *b*). As it is well known, in general the causes of the variations of coercive field are fluctuations of anisotropy energy existing in the material. In fact, in the magnetization process, the Bloch wall must overcome in its movement the forces corresponding to the anisotropy energy fluctuations. KERSTEN and later NÉEL ([39]) studied the problem in the specific case that the fluctuation of the wall energy is due to random internal strains existing in the material.

For the case of internal stresses we have ([37])

$$H_c = \pi \frac{\lambda\sigma}{J_s} \frac{d}{l}, \tag{1}$$

where H_c is the coercive field, λ the magnetostriction, σ the internal strains, J_s the saturation magnetization, d the wall thickness and l the path of the stress fluctuations. Let's now suppose that in each domain there is an induced anisotropy energy K_u. Let's consider a wall between two domains at 90°. It is obvious that the movement of the wall will be hindered by the induced anisotropy energy present. For the generalization of Kersten's formula it is sufficient to replace energy $\lambda\sigma$ with energy K_u and keep in account that the process only interest 90° walls. In this case the fluctuation of K_u will be of the order of the domain size, therefore

$$H_c = \frac{\pi}{p} \frac{K_u}{J_s} \frac{d}{l}, \tag{2}$$

([39]) L. NÉEL: *Ann. Univ. Grenoble*, **22**, 299 (1947).

where l/p represents the ratio between 90 and 180 walls. As an order of magnitude let's suppose that in iron $p = 10$. Moreover for iron $d = 0.1$ μm, $l = 10$ μm ([37]).

To apply (2) it will now be necessary to calculate the induced anisotropy energy K_u caused by the defects introduced by irradiation.

Unfortunately for iron irradiated at room temperature it is not possible at the present time to state any definite hypothesis on the form and size of the defects introduced and hence it is not possible to carry out any type of calculation.

In the case of iron there is, however, one case in which the calculation of the induced anisotropy energy K_u is possible: that is when it can be supposed that the defects present are a residual fraction of interstitial iron atoms. In this case in fact, for analogy with the case of carbon in iron ([33]), it is possible to reasonably estimate the order of magnitude of the effect, in relation to the concentration of interstitials present.

This case appears of some interest also because it may contribute to understand the possible mechanism with which point defects produced by irradiation can change the coercive force and the magnetization curves. The calculations are reported in detail in Appendix. Bearing in mind the results of WALKER ([10]) on resistivity of iron irradiated at low temperature with electrons, for irradiations at room temperature and fluxes of about 10^{18} nvt, the fraction of interstitials that remains present after irradiation is very small. Supposing that as an order of magnitude the remaining fraction is for example 1% of the Frenkel couples, calculated with the method suggested by SEITZ and KOHLER ([11-12]), eq. (2) given before gives values of coercive field about 100 times lower than those observed. On the other hand the subsequent measurements by MOSER ([20]) and co-workers prove that the defects formed by irradiation at room temperature cannot be free interstitials. In fact the defects responsible for the changes in magnetic properties at room temperature diffuse with an heat of activation of 1.2 eV a value too high for free interstitials. It can therefore be reasonably concluded that the defects present at room temperature after irradiation can not be free interstitials. The magnetic effects due to this type of defects are reasonably observable only with irradiation at a temperature of at least $-180°$. In iron irradiated with electrons at low temperature, as previously observed, WALKER ([40]) found that the first strong effects of recovery of resistivity are between 100 K and 200 °K. In accor-

([40]) R. WALKER: *Electron Induced Radiation Damage in Pure Metals. Rendiconti S.I.F.*, XVIII Course (to be published).

([41]) F. SEITZ and J. S. KOEHLER: *Displacement of Atoms During Irradiation, Solid State Physics*, vol. II (New York, 1956).

([42]) G. J. DIENES and G. H. VINEYARD: *Radiation Effects in Solids* (New York, 1957).

dance with this, irradiating specimens of iron at — 180 °C Moser and co-workers ([20]), have observed a very intense magnetic viscosity in the region of 100 °K, with an activation energy of 0.3 eV; this peak is probably due to free interstitials. According to the effects of magnetic viscosity which are observed at this temperature also an increase of coercive field should be observed in this region. It must therefore be imagined that probably some other point defects with a strong anisotropy energy with the magnetization vector should be formed for irradiation at room temperature and are responsible for the effects observed in this work. However the mechanism with which they can give rise to an increased coercive force is still very likely to be the same as that due to interstitials.

These defects can diffuse at a temperature of the order of (100÷200) °C with an activation energy, which from the measurements of Moser ([20]), is of the order of 1.2 eV. Defects of this type could perhaps be interstitials strongly interacting together in small clusters or couples of vacancies or other more complicated defects. As no more complete experimental data are available at present, it is however very difficult to draw more definite conclusions on this point.

7. – Conclusions.

Summarizing the results obtained the following conclusion can be drawn.

On nickel no change in magnetic properties is observed.

In iron, irradiation with fast neutrons at room temperature alters neither magnetization intensity nor anisotropy energy. Instead, on iron specimens of very high permeability and good purity, coercive field increase (about 1 A/m for 10^{18} nvt) and maximum permeability decreases (about 30 % for 10^{18} nvt).

Experiments on annealing have shown that almost complete recovery is obtained below 250 °C. At about 200 °C some of the defects produced by irradiation move, forming probably defects of other type and determining in this way intense modifications in the form of the loop which takes a typical wasp-waisted form. Unfortunately the conclusions to be drawn on the nature of these defects can not at present be definite. The calculations carried out demonstrated only that the effect cannot be due free interstitial iron atoms which certainly move at temperature much lower than room temperature, according also with Moser's results. In fact interstitials diffuse between 80 °K and 100 °K and therefore probably disappear almost completely at room temperature.

The hypothesis that the defects responsible for the changes in magnetic properties are dislocation rings is quantitatively consistent with the increases observed on the values of coercive field but seems in contradiction with the

results of annealing. In fact according to the present knowledge it seems improbable that dislocation rings in iron move below 250 °C. To draw more definite conclusions on the nature of the defects produced, other experiments would be necessary.

APPENDIX

A rough estimate of the induced anisotropy energy density due to a given concentration of iron interstitials can be obtained by comparison with the case of interstitial carbon in iron, considered in Néel theory ([33]). As known the interstitial carbon atoms occupy the octahedral positions $(\frac{1}{2}00)$ and give rise to a strong tetragonal strain in the lattice as in tetragonal martensite. The actual tetragonal strain observed in martensite by X-rays results close to the value deduced from the distortion produced by carbon atoms in the lattice in a simple model of rigid spheres.

The coupling energy between the magnetization vector and the interstitial atom be $E_0 \cos^2 \varphi$ where φ is the angle between the direction of magnetization and the axis of tetragonal simmetry of the occupied position. Knowing E_0 for interstitials non interacting between themselves, the maximum induced anisotropy energy density of the crystal is equal to ([33])

$$K = \frac{E_0^2 c}{3kT},$$

where c is the concentration of interstitials in atoms per cubic centimeter, k the Boltzmann constant and T the temperature at which the defects diffuse: is our case the temperature of irradiation.

In the case of interstitial carbon the experimental value of E_0 is about $6 \cdot 10^{-16}$ erg/atom.

Now it can reasonably be suggested that iron interstitials produced by irradiation very likely occupy the same positions and hence produce similar effects. Therefore the induced anisotropy energy K_u to be considered in eq. (2) of the text, to calculate the increase of coercive field, can be obtained in the identical way as in the case of carbon using eq. (3).

In this equation the only unknown value is E_0, *i.e.* the interaction energy of the iron interstitials with magnetization. This value can be estimated, as an order of magnitude, considering that in the case of interstitial carbon, one of the main terms of this energy is due to the magnetoelastic coupling ([43]). In fact for a carbon atom (diameter 1.60 Å) being h (0.38 Å) the height of the

([43]) G. BIORCI, A. FERRO and G. MONTALENTI: *Instability of the Bloch Walls due to Interstitial Atoms in a Ferromagnetic Lattice.* ARDC T. Note 1C Contr. A.F. 61 (514) 1331 (March, 1958).

interstice and a (2.86 Å) the lattice parameter, and using the following expression for E_0:

$$E_0 = \frac{3}{2}(C_{11} - C_{12})\lambda_{100}\left(\frac{d-h}{a}\right)^2 a^3, \tag{4}$$

where C_{11}, C_{12} are the elastic constants and λ_{100} the magnetostriction, a value of $3 \cdot 10^{-16}$ erg/atom is obtained against the experimental value of $6 \cdot 10^{-16}$ quoted above. This is due to the fact that also other contributions are present as already shown by DE VRIES [44] and others. However with this limitation the order of magnitude of E_0 for iron interstitial can be estimated. The atomic diameter for iron atoms is 2.48 Å and hence the tetragonal distortion due to one interstitial per atomic cell is about 0.7 against 0.4 for carbon. Hence E_0 should not be far from 10^{-15} erg/atom.

Using this value, if all the interstitials were still present at room temperature, from eq. (2) of the text and for $p = 10$, an increase of coercive force of about 1 A/m would be found. If the concentration of interstitials still present is only as suggested of 1% the value calculated previously is reduced accordingly.

[44] G. DE VRIES, D. W. VAN GEEST, R. GERSDORF and G. W. RATHENAU: *Physica*, **25**, 1131 (1959).

RIASSUNTO

Vengono studiati gli effetti dell'irradiazione con neutroni veloci (dose 10^{18} nvt) sulla permeabilità, campo coercitivo e approccio alla saturazione di ferro e nichel puri. Nessuna variazione significativa per effetto dell'irradiazione è stata osservata sul nichel (permeabilità massima 5000). Sul ferro (permeabilità massima intorno a 15000, campo coercitivo 2.5 A/m) il campo coercitivo cresce di circa 0.8 A/m, la permeabilità massima diminuisce di circa il 30% mentre non si osservano variazioni nella curva di approccio alla saturazione e quindi nel valore dell'energia di anisotropia. Con un rinvenimento dei provini di ferro a 100 °C si osserva un ulteriore aumento del campo coercitivo e dopo rinvenimento a 200 °C, per uno dei provini il ciclo assume in modo assai accentuato una caratteristica forma a vita di vespa. Per rinvenimenti a temperature poco superiori, 250 °C, la maggior parte delle variazioni delle proprietà magnetiche dovute all'irradiazione scompare. Si discutono le possibili interpretazioni teoriche dei risultati. Lo studio della cinetica della scomparsa del danno con il rinvenimento porta ad escludere che possa trattarsi di effetti dovuti a interstiziali liberi e probabilmente ad escludere che siano effetti dovuti alla formazione di anelli di dislocazioni. Si deve quindi pensare a formazione di qualche altro tipo di difetto con anisotropia di forma capace di interagire con il vettore magnetizzazione e di muoversi a temperature di (100 ÷ 200) °C con energia di attivazione di 1.2 eV.

Diffusione elastica di raggi γ di 1.25 MeV in piombo.

G. Manuzio e S. Vitale

Istituto di Fisica dell'Università - Genova
Istituto Nazionale di Fisica Nucleare - Sezione di Genova

(ricevuto il 5 Gennaio 1961)

Riassunto. — È stato misurato il grado di polarizzazione trasversale della radiazione di 1.25 MeV del ^{60}Co diffusa elasticamente su piombo a diversi angoli. Per un accurato confronto della situazione teorica con i risultati sperimentali occorrerebbero calcoli dettagliati del contributo degli elettroni dell'orbita L allo scattering Rayleigh.

Come è ben noto lo scattering elastico dei fotoni contro le particelle costituenti la materia può avvenire, prescindendo dai fenomeni di risonanza che non interessano il campo di indagine di questo lavoro, attraverso i seguenti tipi di interazioni:

1) scattering Thomson;
2) scattering Rayleigh;
3) scattering Delbrück [1].

Negli ultimi anni sono state condotte ricerche sia di carattere teorico, per calcolare il contributo di ciascuno di questi processi alla sezione d'urto totale, sia di carattere sperimentale, per verificare sperimentalmente la bontà di questi calcoli.

Si deve però osservare che al momento attuale può essere portata a fondo una teoria soddisfacente dello scattering Thomson che permette di descrivere compiutamente il processo soltanto ad energia abbastanza bassa da non interessare i gradi di libertà interni al nucleo.

[1] M. Delbrück: *Zeits. f. Phys.*, **84**, 144 (1933).

Per quanto riguarda invece lo scattering Rayleigh, le teorie finora elaborate si limitano a tener conto solo del contributo degli elettroni nell'orbita K, salvo una valutazione di massima del contributo degli elettroni L [2-6].

Infine per quanto si riferisce allo scattering Delbrück [7,8] calcoli completi della sezione d'urto esistono solo per angoli di scattering zero; per angoli diversi si hanno solo valutazioni dell'ampiezza della parte immaginaria dell'onda diffusa all'energia di 2.56 MeV.

In conclusione i risultati dei calcoli teorici finora eseguiti portano a concludere:

1) Ad energie attorno al MeV le sezioni d'urto ad angolo zero per i processi Thomson e Delbrück sono comparabili, mentre la sezione d'urto dello scattering Rayleigh, sempre ad angolo zero, è di tre ordini di grandezza maggiore di quella degli altri due processi.

2) Non si può tuttavia escludere la possibilità di un contributo dell'effetto Delbrück allo scattering ad angoli diversi da zero a causa della rapidissima discesa, con il crescere dell'angolo di scattering, della sezione d'urto differenziale per lo scattering Rayleigh+Thomson.

Sperimentalmente molti tentativi sono stati fatti per fare una verifica dei risultati teorici.

Negli ultimi anni sono state pubblicate varie misure riferentisi alla sezione d'urto totale per scattering elastico di raggi γ di energie comprese tra 0.1 e 2.56 MeV. I risultati più recenti sono quelli di BERNSTEIN e MANN [9], e nella bibliografia [10-14] abbiamo elencato gli altri più importanti autori di misure su questi effetti.

Le sezioni d'urto Rayleigh+Thomson, valutate usando per lo scattering Rayleigh i risultati di Brown e Mayers e tenendo quindi conto solo del contributo degli elettroni dell'orbita K, sono in accordo piuttosto soddisfacente con i risultati sperimentali ad energie inferiori ad 800 keV [9].

---

[2] W. FRANZ: *Zeits. f. Phys.*, **95**, 652 (1935).

[3] W. FRANZ: *Zeits. f. Phys.*, **98**, 314 (1936).

[4] G. E. BROWN, R. E. PEIERLS e J. B. WOODWARD: *Proc. Roy. Soc.*, A **227**, 51 (1955).

[5] S. BRENNER, G. E. BROWN e J. B. WOODWARD: *Proc. Roy. Soc.*, A **227**, 59 (1955).

[6] G. E. BROWN e D. F. MAYERS: *Proc. Roy. Soc.*, A **242**, 89 (1957).

[7] F. RÖHRLICH: *Phys. Rev.*, **108**, 169 (1957).

[8] P. KESSLER: *Journ. Phys. et Rad.*, **19**, 739 (1958).

[9] A. M. BERNSTEIN e A. K. MANN: *Phys. Rev.*, **110**, 805 (1958).

[10] A. K. MANN: *Phys. Rev.*, **101**, 4 (1956).

[11] P. EBERHARD, L. GOLDZAHL, E. HARA e J. MEY: *Journ. Phys. et Rad.*, **17**, 573 (1956).

[12] R. R. WILSON: *Phys. Rev.*, **80**, 720 (1953).

[13] S. MESSELT e A. STORRUSTE: *Proc. Phys. Soc.*, A **69**, 381 (1956).

[14] N. CINDRO e K. ILAKOVAC: *Nucl. Phys.*, **5**, 647 (1958).

A 1.33 MeV i punti sperimentali a grandi angoli sono tutti al di sopra della curva teorica.

A 2.56 MeV il disaccordo tra i risultati sperimentali e la curva teorica, ottenuta per extrapolazione dei dati di Brown e Mayers ad 1.33 MeV, è ulteriormente accresciuto ([9]).

In conclusione, i risultati sperimentali ad energie superiori al MeV non sembrano fornire una dimostrazione sufficiente della esattezza dei calcoli di Brown e Mayers, nè possiamo avere buone speranze che il perfezionamento di misure già eseguite (*) possa fornire nuovi risultati atti a decidere definitivamente sull'accordo o disaccordo tra le teorie di Brown e Mayers e l'esperienza.

Tuttavia deve essere tenuto presente che mentre i calcoli di Brown e Mayers forniscono le ampiezze di polarizzazione circolare dell'onda elettromagnetica diffusa, le esperienze finora condotte si limitano solo alle misure di sezione d'urto.

Infatti se A e B sono le ampiezze di polarizzazione dell'onda diffusa da un fascio non polarizzato, rispettivamente in senso orario e antiorario, la sezione d'urto è

$$\sigma = r_0^2\{|A|^2 + |B|^2\},$$

dove r_0 è il raggio classico dell'elettrone.

Si ha poi per la polarizzazione trasversale rispetto al piano di scattering

$$P_1 = \frac{2\,\mathrm{Re}\,(AB^*)}{|A|^2 + |B|^2}.$$

Poichè A e B sono quantità complesse, per determinarle completamente non è sufficiente misurare σ e P_1. Due ulteriori misure indipendenti sono necessarie ([17]). Esse possono essere:

1a) il grado di polarizzazione trasversale del fascio diffuso rispetto ad un piano a 45° con il piano di scattering, quando il fascio incidente è polarizzato circolarmente;

1b) il grado di polarizzazione circolare della radiazione diffusa usando un fascio incidente con polarizzazione trasversale in un piano a 45° con il piano di scattering: le misure 1a) e 1b) sono equivalenti e il valore P_2 previsto è dato da

$$P_2 = \frac{2\,\mathrm{Im}\,(AB^*)}{|A|^2 + |B|^2};$$

(*) Mentre questo lavoro era in corso sono state in realtà pubblicate due misure di polarizzazione ([15,16]).

([15]) B. S. Sood: *Proc. Roy. Soc.*, **247**, 375 (1958).

([16]) F. Fuschini, D. S. R. Murty e P. Veronesi: *Nuovo Cimento*, **15**, 847 (1960).

([17]) H. Böbel e G. Passatore: *Nuovo Cimento*, **15**, 979 (1960).

2*a*) il grado di polarizzazione circolare del fascio diffuso, quando il fascio incidente è polarizzato circolarmente;

2*b*) il grado di polarizzazione trasversale rispetto ad un piano a 45° con il piano di diffusione, quando il fascio incidente è polarizzato linearmente a 45° con il piano di scattering: anche 2*a*) e 2*b*) sono equivalenti e il valore previsto è

$$P_3 = \frac{|A|^2 - |B|^2}{|A|^2 + |B|^2}.$$

La misura di P_1, P_2, P_3 è equivalente dal punto di vista ottico all'analisi completa di un fascio di luce con prismi di Nicol (P_1), lamine a quarto d'onda (P_2) e lamine a mezz'onda (P_3).

È quindi sperabile di poter eseguire una nuova verifica della validità dei calcoli di Brown e Mayers attraverso misure dello stato di polarizzazione delle radiazioni diffuse elasticamente.

Si deve però notare che la determinazione delle tre grandezze P_1, P_2, e P_3 presenta difficoltà non indifferenti. In particolare per eseguire le misure delle quantità P_2 e P_3 si richiederebbero raggi γ polarizzati circolarmente; questi possono essere ottenuti con sufficiente intensità solo con l'uso della radiazione di bremsstrahlung da raggi β abbastanza energici, oppure di sorgenti con nuclei polarizzati.

In un caso o nell'altro sarebbero necessarie sorgenti radioattive di intensità così cospicua da rendere molto disagevoli le misure.

Operando con la radiazione di bremsstrahlung si dovrebbe superare l'ulteriore difficoltà dello spettro continuo. La misura di P_1 può invece essere affrontata con minori difficoltà poichè in questo caso occorre un fascio incidente non polarizzato.

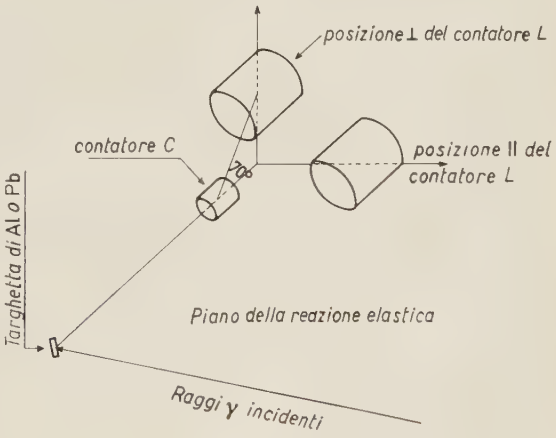

Fig. 1.

D'altra parte anche la conoscenza della sola P_1 può fornire una informazione indipendente da quella ottenuta attraverso la misura della sezione d'urto.

Scopo di questo lavoro è appunto la determinazione di P_1 relativa a raggi γ di 1.33 MeV diffusi elasticamente su piombo a diversi angoli.

La sorgente da noi impiegata era costituita da 1500 curie di ^{60}Co (un apparecchio di uso medico) e il fascio di raggi γ molto ben collimato prove-

niente da questa sorgente, veniva fatto incidere su targhette di Pb e di Al e l'energia e lo stato di polarizzazione dei fotoni diffusi erano analizzati con un polarimetro ad effetto Compton di tipo analogo a quello di Metzger e Deutch [18]. Quest'ultimo è costituito (Fig. 1) da un contatore A (NaI(Tl) 1×1 pollici) e da un contatore L (NaI(Tl) 2×2 pollici) disposto in modo da raccogliere la radiazione diffusa da A ad un angolo medio di $70° \pm 30°$. Gli impulsi forniti

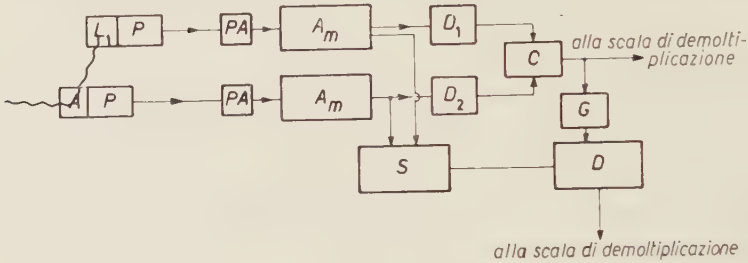

Fig. 2.

dai contatori A ed L sono selezionati dal circuito di Fig. 2 alle seguenti condizioni:

1) La somma delle perdite di energia dei raggi γ in L e A deve essere compresa tra 1.1 e 1.4 MeV (circuito di somma S e analizzatore a molti canali D), e ciò per garantire che il raggio γ abbia subito uno scattering elastico nelle targhette e sia stato diffuso correttamente da A in L. Infatti un raggio γ diffuso Compton nella targhetta, anche per l'angolo più piccolo usato, ha energia inferiore a 0.85 MeV. Il limite superiore, ad 1.4 MeV, elimina il fondo dovuto ai raggi cosmici.

2) Gli impulsi da L e da A devono essere coincidenti entro 10^{-7} s (coincidenza C e gate G) consentendo di ridurre le somme casuali a un numero trascurabile rispetto agli eventi fisici.

Oltre le condizioni 1) e 2) di per sè sufficienti a selezionare gli eventi di scattering che interessano questa misura, sono state imposte anche le condizioni supplementari:

a) L'altezza degli impulsi da A è più grande di quella corrispondente alla perdita di energia (~ 0.5 MeV) di un raggio γ di 1.1 MeV scatterato con il minimo angolo di scattering permesso dalla geometria (discriminatore D_2).

b) L'altezza degli impulsi da L corrisponde all'energia residua di un raggio γ scatterato all'angolo massimo permesso dalla geometria ($\simeq 0.3$ MeV; discriminatore D_2).

[18] M. Deutsch e F. Metzger: *Phys. Rev.*, **74**, 1542 (1948).

La condizione *a*) permette di non far pervenire a C i segnali dovuti a fotoni che hanno subito una interazione Compton nella targhetta oppure che, essendo stati diffusi elasticamente nella targhetta, hanno deviato in A di un angolo più piccolo di quello richiesto dalla geometria per essere analizzato.

La condizione *b*) impedisce l'accesso alla coincidenza alla maggior parte dei segnali dovuti a fotoni di fondo; naturalmente in questo modo vengono perduti anche dei fotoni non interamente assorbiti da L diminuendo in questo modo l'efficienza del polarimetro di circa il 10%.

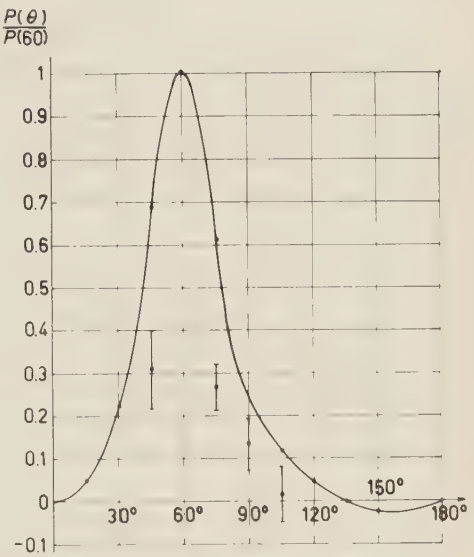

Fig. 3.

Le condizioni *a*) e *b*) consentono di ridurre gli impulsi spurii da C ad un valore dell'ordine del $(10 \div 15)\%$ delle coincidenze dovute ad eventi fisici.

Il funzionamento dell'insieme di contatori del circuito elettronico è stato saggiato disponendo una sorgente di ^{60}Co al posto della targhetta.

Dalle misure eseguite in queste condizioni è stato verificato che l'efficienza del dispositivo nella rivelazione di raggi γ è dell' 1% circa, in accordo con quella grossolanamente valutata. Da queste prove è stato ottenuto anche il potere analizzante del dispositivo rispetto alle applicazioni della condizione 1).

La Fig. 3 mostra lo spettro degli impulsi del discriminatore D quando la sorgente di ^{60}Co era al posto della targhetta.

Lo stato di polarizzazione dei fotoni diffusi elasticamente si può ottenere dalla quantità

$$A = \frac{N_\perp - N_\parallel}{N_\perp + N_\parallel},$$

normalmente chiamata asimmetria; in essa $N_\parallel$ è il numero degli eventi fisici (A, L) contati con il contatore L nel piano di scattering elastico e $N_\perp$ è l'analogo numero con L nel piano perpendicolare al piano di scattering elastico. Per determinare i valori di $N_\parallel$ e $N_\perp$ corretti per il fondo, venivano eseguiti gruppi successivi di quattro misure, alternando due misure con targhetta di diffusione di Pb a due misure con targhetta di Al. La targhetta di Al, avendo l'Al basso numero atomico, dà origine ad un numero trascurabile di eventi

elastici (che dipendono tutti da Z secondo potenze di almeno Z^2), mentre riproduce abbastanza bene la radiazione non elastica uscente dalla targhetta di Pb.

Se si sceglie, come in effetti è stato fatto, lo spessore della targhetta di Al in modo che l'intensità dei fotoni emessi coincida, attorno al picco Compton, con l'intensità dei fotoni emessi dalla targhetta di Pb nella stessa regione dello spettro di energia (entro l'1%), il numero di conteggi N_{Al} e N_{Al} eseguiti con la targhetta di Al fornisce la correzione per il fondo alle misure con la targhetta di Pb.

Gli eventi che contribuiscono a generare il fondo sono infatti, a parte eventi di probabilità trascurabile:

a) Coincidenze casuali pure originate da due fotoni indipendenti che interagiscono contemporaneamente in A e L. Le coincidenze casuali pure sono poche e il loro numero è sostanzialmente lo stesso per le targhette di Al e Pb. Così le differenze Pb — Al sono automaticamente corrette per coincidenze a caso, mentre il loro contributo all'errore statistico è praticamente inalterato. La misura di coincidenze casuali è stata fatta ritardando di circa 15 μs gli impulsi d'uno dei canali di ingresso della coincidenza veloce C.

b) Coincidenze di « impilamento » dovute ad un fotone che, diffuso per effetto Compton dalla targhetta, incide su A e viene diffuso in L, accompagnato casualmente da un altro fotone che interagisce contemporaneamente in A. Tali eventi possono dare sia in D_2 che in D_1 un segnale capace di arrivare a C e ciò perchè la soglia di D_1 deve essere regolata abbastanza bassa da non escludere gli eventi dovuti a fotoni elastici diffusi in A sotto gli angoli massimi consentiti dalla geometria. Il numero di queste coincidenze dette di impilamento è per piccoli angoli di scattering elastico molto più grande di quello delle coincidenze casuali pure, perchè in queste condizioni anche i fotoni diffusi per effetto Compton che incidono in A hanno una notevole energia (0.85 MeV a 45°) e sono in gran numero (la sezione d'urto differenziale per effetto Compton vale a 45° per il Pb $\simeq 1$ barn/sr contro una sezione d'urto elastica $\simeq 1$ mb/sr).

Infatti N_{Al}/N_{Pb}, che rappresenta il rapporto fra i conteggi spuri causati da fotoni Compton, ed il totale dei conteggi, è piccolo a grandi angoli ($\simeq 0.01$) mentre cresce progressivamente con il diminuire dell'angolo fino ad un valore di circa 0.3 per un angolo di 15° restando sempre il numero della coincidenza casuale pure dello stesso ordine di grandezza ($\simeq 0.01$, 0.02).

Si può dunque concludere, che una volta stabilita la condizione che l'intensità dei fotoni emessi dalla targhetta di Pb intorno al picco Compton sia uguale a quella emessa dalla targhetta di Al nelle stesse condizioni, il numero delle coincidenze spurie con targhetta di Pb risulterà uguale al numero delle coincidenze totali con targhetta di Al.

In definitiva la asimmetria di conteggio è data da

$$A = \frac{(N_{\perp \mathrm{Pb}} - N_{\perp \mathrm{Al}}) - (N_{\parallel \mathrm{Pb}} - N_{\parallel \mathrm{Al}})}{(N_{\perp \mathrm{Pb}} - N_{\perp \mathrm{Al}}) + (N_{\parallel \mathrm{Pb}} - N_{\parallel \mathrm{Al}})} .$$

Infine, poichè la disposizione del polarimetro poteva dar luogo a piccole asimmetrie strumentali dovute, per esempio, ad un cattivo allineamento dell'asse del polarimetro, si sono eseguite misure di asimmetria strumentale sostituendo alla targhetta di Pb una sorgente di ^{60}Co. Tale asimmetria è sempre risultata inferiore all'1%; in ogni modo i dati sono stati corretti per questo effetto strumentale. Nota l'asimmetria di conteggio A, corretta nei modi ora detti, si può ottenere la polarizzazione P da

$$P = AR , \tag{1}$$

dove R è la quantità

$$R = \left\langle \frac{\sigma_0(\varphi)}{2\sigma_1(\varphi)} \right\rangle_{\text{media}} ,$$

e $\sigma_0(\varphi)$ e $\sigma_1(\varphi)$ sono le parti della sezione d'urto per scattering Compton rispettivamente insensibile e sensibile alla polarizzazione del fotone incidente; la media è fatta sugli angoli permessi dalla geometria del polarimetro. Per la nostra geometria la valutazione numerica di R ha dato

$$R = 3.4$$

con una incertezza di $\simeq 0.1$.

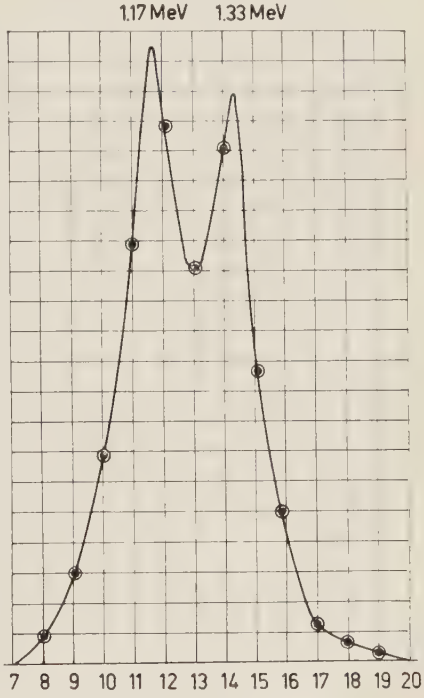

Fig. 4.

I risultati ottenuti dalle misure sono riportati nella Tabella I. Nel grafico di Fig. 4 è riportato il rapporto sperimentale $P(\theta)/P(60°)$, e questo è confrontato con l'andamento della curva teorica ottenuta tenendo conto dello scattering Thomson e dello scattering Rayleigh sugli elettroni K secondo i calcoli di Brown e Mayers. L'uso del rapporto è opportuno perchè in tal modo nel confronto fra teoria e esperienza ci si può svincolare dagli eventuali errori introdotti dal fattore moltiplicativo R della (1).

I punti sperimentali sembrano indicare una curva più stretta di quella

calcolata, con differenza massima tra le due curve a 45°. Tale differenza potrebbe essere attribuita alla eventualità di una incompleta discriminazione del fondo dalla radiazione elastica a piccoli angoli, in modo che un fondo depolarizzante si sovrapponesse al conteggio dei fotoni elastici riducendo la polarizzazione totale. Per eliminare questo sospetto abbiamo calcolato in base alle nostre intensità le sezioni d'urto per il processo di scattering elastico.

TABELLA I. – *Grado di polarizzazione.*

Angolo	Calcolato (B.M.) (%)	Misurato ($P=AR$) (ns. risultati) (%)	Misurato ($P=AR$) (risultati di altri) (%)
45°	— 68.3	— 32.4 ±8.5	—
60°	— 99.1	— 100.1 ±5.8	—
75°	— 60.8	— 27 ±4.6	—
90°	— 24.5	— 13.5 ±5.6	— 6.3±5 (SOOD) ([15])
105°	— 11.7	— 1.36±6.3	—
57°	—	—	— 100 (FUSCHINI, *et.al.*) comun. privata ([16])

La tabella riporta i risultati ottenuti fino ad ora nelle misure di polarizzazione a 1.25 MeV confrontati con le previsioni teoriche secondo i calcoli di Brown e Mayers.

I risultati, riportati in Tabella II, sono naturalmente affetti da incertezze dovute all'autoassorbimento della targhetta, che nel nostro caso non è sottile e al fatto che non è nota con adeguata precisione l'efficienza del polarimetro.

TABELLA II. – *Sezione d'urto.*

	Nostri risultati	Risultati di BERNSTEIN e MANN ([9])
	in unità di 10^{-28} cm^2	
45°	11.3±2	16 ±4
60°	5.7±1.4	4.5±0.5
75°	1.6±0.3	2.2±0.2
90°	1.5±0.3	1.6±0.2
105°	1.3±0.25	1.2±0.2

Nella tabella sono confrontate le misure di sezione d'urto da noi ottenute per lo scattering elastico con le misure di Bernstein e Mann ([9]).

Se si tiene conto però che queste correzioni si riducono solo a fattori moltiplicativi se ne deduce che, salvo una eventuale normalizzazione, i nostri dati possono essere paragonati con quelli già ottenuti da altri autori.

Poichè il risultato di questo paragone è, come mostrano le due ultime righe della Tabella I, pienamente rassicurante, possiamo escludere che a piccoli angoli fosse presente un fondo di intensità apprezzabile sfuggito alle nostre correzioni.

Abbiamo quindi pensato alla presenza eventuale di qualche altro contributo al processo di scattering elastico, oltre i due considerati.

Questo potrebbe essere:

a) Un contributo ulteriore dello scattering Rayleigh sugli elettroni L.

b) Un contributo dell'effetto Delbrück.

A questo proposito dobbiamo osservare che i calcoli con il fattore di forma per il contributo degli elettroni L non sono sufficienti per la valutazione della polarizzazione e calcoli più raffinati al momento attuale non esistono.

Tuttavia ampiezze dell'ordine di grandezza di questo fattore di forma potrebbero rendere conto del disaccordo, quando interferissero in maniera opportuna.

Al contrario, per quanto riguarda l'effetto Delbrück, l'interferenza di ragionevoli parti immaginarie dell'ampiezza di scattering Delbrück con le ampiezze Rayleigh + Thompson lascia praticamente invariata la polarizzazione del fascio diffuso.

Per fare queste valutazioni ci siamo serviti dei risultati dei calcoli di KESSLER ([17]). Resta aperta la possibilità di un notevole contributo della parte reale dell'ampiezza di scattering Delbrück.

Questo sarebbe però in contrasto con le previsioni teoriche che prevedono una parte reale delle ampiezze di scattering minore della parte immaginaria.

* * *

Desideriamo ringraziare vivamente il prof. ETTORE PANCINI per l'attenzione che ha prestato al nostro lavoro e per i consigli e i suggerimenti che ci ha dato.

I nostri ringraziamenti vanno pure al prof. BORSELLINO per alcune utili discussioni e al dr. BÖBEL per l'aiuto che ci ha dato nella preparazione dell'esperienza e per successive utili discussioni.

SUMMARY

The degree of transverse polarization of the radiation from a source of ^{60}Co, elastically scattered by a lead target, has been measured at various angles. Experimental results are shown in Table I: a comparison has been made between these and the theoretical predictions for the contribution of the Thomson and Rayleigh effects. Amplitudes calculated for K electrons by BROWN and MAYERS ([6]) have been used. For an accurate test of the theoretical situation by means of the experimental results, refined calculations of L-shell contribution to Rayleigh scattering are needed.

Meson Production in Nucleus-Nucleus Collisions (*).

G. Alexander (**), J. Avidan, A. Avni (**) and G. Yekutieli

Department of Physics, The Weizmann Institute of Science - Rehovoth

(ricevuto il 12 Gennaio 1961)

Summary. — Nucleus-nucleus collisions at cosmic ray energies are described in terms of nucleon-nucleon collisions. The average multiplicity for different types of reactions is predicted and compared with experimental observation.

1. – Introduction.

Since the discovery of Heavy Primaries (H.P.) in the Cosmic Radiation (C.R.) by Freier *et al.* [1] the nuclear interaction of C.R. nuclei in photographic emulsion was studied by various authors [2]. These studies revealed the main features of nucleus-nucleus reactions.

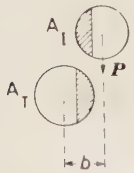

Fig. 1. A nucleus-nucleus collision.

A nucleus-nucleus collision is schematically described in Fig. 1. The incident nucleus A_I moves with very high momentum $\boldsymbol{P}$, and hits the target nucleus A_T, with an impact parameter b. The reaction starts with violent collisions between nucleons in the overlapping volumes of both the incident and

(*) This work has been sponsored in part by the Air Force Cambridge Research Center, Geophysics Research Directorate of the Air Research and Development Command, United States Air Force, through its European Office.

(**) Also from the I.A.E.C. Laboratories, Rehovoth.

(1) P. Freier, P. E. Lofgren, E. P. Ney, F. Oppenheimer, H. L. Bradt and B. Peters: *Phys. Rev.*, **74**, 213 (1948).

(2) Some of these papers are reviewed and referred to by B. Peters: *Prog. Compt. Rend. Phys.*, **1**, 193 (1952) and S. F. Singer: *Prog. Compt. Rend. Phys.*, **4**, 203 (1958).

target nuclei (shaded areas in Fig. 1). In these collisions many mesons are produced. At very high energies the secondary nucleons and mesons are highly collimated in the forward direction and further secondary collisions are confined mostly to the overlapping volumes. The energetic mesons and nucleons so formed make the jet of shower particles observed in photographic emulsion. Relatively little energy is transferred to the non-directly hit parts of both the incident and target nuclei. These parts of the nuclei are excited and consequently the nucleus is reduced in size or even completely disintegrated by the ejection of low energy nucleons, α-particles, and heavier fragments. The nuclear fragments of the non-colliding part of the incident nucleus emerge, after the reaction, with practically the same momentum per nucleon as the incident one. In the photographic emulsion they show up as a very collimated beam of tracks moving in the direction of the incident H.P. The nuclear fragments of the target, on the other hand, are mainly low energy nucleons and α-particles, that make the heavy prongs of the star associated with the nucleon-nucleon collision. At lower incident energies secondary collisions are not confined any more to the overlapping volumes, and some mesons and secondary fast nucleons are produced around the boundaries of the directly hit sections of the two nuclei.

In reality, even at high enough energies a nucleus-nucleus collision is a complicated process involving interactions between many particles. The schematic model described above, may serve only as an aid to analyse nucleus-nucleus reactions. This model was already used in a previous paper ([3]), for calculating the reaction cross-section in nucleus-nucleus collisions. In this paper the geometrical model is used to analyse particle production in nucleon-nucleon collisions. We make the assumption that the number of mesons produced in nucleus-nucleus collisions is proportional to the average number of incident nucleons, N_I, that participate in primary collision. With this assumption several features of nucleon-nucleon collisions, like charge multiplicity, are predicted and compared to experimental data, in Sections **3** and **4**. The fragmentation of the incident nucleus is discussed in Section **5** and evidence for the movement of the target nucleus is given in Section **6**.

The experimental data used for comparison in this paper are obtained from the works of Fowler *et al.* ([4]), Rajopadhye and Waddington ([5]), Cester *et al.* ([6]) and Lohrmann *et al.* ([7]) and from new material presently measured.

([3]) G. Alexander and G. Yekutieli: *Nuovo Cimento*, **19**, 103 (1961). Hereafter will be called paper I.

([4]) P. H. Fowler, R. R. Hillier and C. J. Waddington: *Phil. Mag.*, **2**, 293 (1957).

([5]) V. Y. Rajopadhye: *Phil. Mag.*, **3**, 19 (1958).

([6]) R. Cester, H. Benedetti, C. M. Garelli, B. Quassiati, L. Tallone and M. Vigone: *Nuovo Cimento*, **7**, 371 (1958).

([7]) E. Lohrmann and M. W. Teucher: *Phys. Rev.*, **115**, 636 (1959); and P. L. Jain, E. Lohrmann and M. W. Teucher: *Phys. Rev.*, **115**, 643 (1959).

2. – Experimental.

A G-5 emulsion block of dimensions $(20 \cdot 30 \cdot 0.06)$ cm^3 that has been exposed to cosmic radiation in Texas at a height of about 80000 feet was scanned for heavy primary interactions. The heavy nuclei tracks were picked up at about 5 mm from the top edge of the block and then followed until they interacted or left the stack. Tracks having a dip angle of $< 30°$ or that interacted at a distance of less than 1 cm from the edge were disregarded. In this way 177 interactions have been obtained.

δ-ray calibration points have been obtained by a few cases where a complete splitting has occured. These calibration points were used together with the knowledge of the ionization change with energy to determine the charge of the interacting particles and the fragments of $Z > 2$ that emerged from them. In this way the charge Z of the incident heavy primaries was determined to one charge unit. All secondary tracks were subject to a dip and projected angle measurements, out of which the true angle has been computed. Black tracks were followed to rest and other secondary particles were subject to ionization measurements by grain counting. Tracks having an ionization value $3.5 < I/I\,\mathrm{min} < 4.5$ were followed until their identity as a proton or an α-particle has been obtained.

The energy of the heavy primaries was estimated by three different methods. 1) Whenever two or more α-particles emerged from the interaction in the forward cone the KAPLON *et al.* ([8]) method of estimating the incident energy by the opening angle of the α-particles was used. 2) In cases of low energy primaries, less than 1.5 GeV per nucleon, the ionization of α-particles and protons, believed to be fragments of the incident nucleus, was measured. The energies based on these ionization measurements agree well with the energies found by the KAPLON *et al.* method. The energies estimated according to these two methods are compared in Table I. 3) The incident energy of the more energetic events $E \cdot 1.5$ GeV per nucleon was estimated by the angular distribution of the shower particles according to CASTAGNOLI *et al.* ([9]). The 177 interactions analysed are divided into two groups according to their incident energy. All events induced by primaries with kinetic energy $E \cdot 1.5$ per nucleon are included in the higher group, while all other events induced by primaries of lower energy are included in the lower group. In each energy group the events are grouped according to the charge Z of the incident heavy primary. The Light, Medium and Heavy groups con-

([8]) M. F. KAPLON, B. PETERS, H. L. REYNOLDS and P. O. RITSON: *Phys. Rev.*, **85**, 295 (1952).

([9]) C. CASTAGNOLI, G. CORTINI, C. FRANZINETTI, A. MANFREDINI and D. MORENO: *Nuovo Cimento*, **10**, 1539 (1953).

Table I. – *Incident energy estimation according to Kaplon-Peters method* (E_{KP}) *and the ionization method* (E_{ion}).

Event no.	E_{KP} (GeV)	E_{ion} (GeV)	E_{KP}/E_{ion}
1	0.2	0.9	0.22
2	5.5	1.0	5.5
3	1.1	1.3	0.84
4	0.8	0.8	1.00
5	1.75	1.1	1.59
6	1.00	1.1	0.91
7	0.28	0.5	0.56
8	0.45	0.55	0.82
9	0.50	0.70	0.71
10	0.37	0.75	0.49
11	0.85	1.0	0.85
12	0.20	0.4	0.5
13	0.70	1.0	0.7
13	0.47	1.0	0.47
15	0.25	1.0	0.25

tained primaries with $3 \leqslant Z \leqslant 5$; $6 \leqslant Z \leqslant 9$ and $Z \geqslant 10$ respectively. The 177 events grouped according to their incident energy and primary charge are listed in Table II. The relatively low number of events in the light group is due to scanning bias for low charge H.P.

3. – Meson production in nucleus-nucleus collisions.

Meson production in nucleus-nucleus collisions is described in terms of nucleon-nucleon interactions. Following paper I, the target and the incident nuclei are described as clusters of A_T and A_I nucleons, with density distributions ϱ_T and ϱ_A similar to their respective charge distributions ([10]).

In the following we deal mainly with reactions induced by heavy C.R. particles in photographic emulsion. The incident heavy C.R. particles consist mostly of Li, Be, B, C, N, O nuclei and some less abundant heavier elements. The target nuclei in emulsion, on the other hand, are C, N, O and Br and Ag. Hence in the majority of the reactions the incident particle is lighter than the target. Therefore we shall analyse a nucleus-nucleus reaction in terms of the average number of incident nucleons $N_{IT}(b)$ that participate in this reaction. $N_{IT}(b)$ is a function of the impact parameter b, in a given nucleus-nucleus

([10]) For details of the density distribution used see Table I of ref. ([3]), paper I

TABLE II. – *Characteristics of heavy primary stars in emulsions.* (N_h = number of heavy prongs, N_α = number of relativistic α-particles, N_l = number of secondaries with $I < 3.51_{\min}$ N_s = number of secondaries with $I < 1.41_{\min}$.)

$E < 1.5$ GeV

Primary	Fragments	N_h	N_α	N_l	N_s	Primary	Fragments	N_h	N_α	N_l	N_s
Be		1	2	—	—	F	Be	4	1	3	2
Be		5	—	4	4	F	N	—	1	4	1
B		3	2	3	3	F	B	2	1	3	3
B		3	—	7	7	F	Li	6	2	6	3
B		10	—	7	1	F	Be	6	—	9	8
B		9	2	4	1	F		13	—	32	9
B		1	1	4	3	F		7	—	6	6
C	Li	8	—	5	1	F		26	1	23	4
C	B	4	—	—	—	F	N	—	1	1	1
C		3	—	11	5	F		3	—	13	3
C	Be	6	—	2	—	Ne	O	1	1	1	—
C		8	3	4	1	Ne	Li	—	2	1	1
C		14	—	9	5	Ne		7	—	11	9
C		10	—	14	7	Ne		11	—	13	10
C		3	—	9	6	Na		13	1	4	2
C		12	—	8	5	Na		—	3	6	6
C		10	—	17	11	Na		2	3	10	9
C		16	—	14	1	Na		17	2	17	5
C	Be	1	1	1	1	Na		18	—	23	9
C		1	2	6	1	Na	Li	4	2	10	2
N	Li	14	—	8	7	Mg	C	10	3	2	1
N		—	2	3	1	Mg	B, Be	2	1	1	—
N		3	2	7	6	Mg	F	—	1	1	1
N		16	—	9	6	Mg	C	—	1	5	2
N		—	1	9	6	Mg		23	—	54	16
N		21	—	48	19	Mg		21	—	31	11
N		11	—	14	8	Mg	C	3	2	6	4
N		—	1	7	7	Mg	O	12	—	5	1
N		5	3	1	1	Al	N, Li	—	1	2	2
N		33	—	24	7	Al		2	2	25	15
N		3	2	5	3	Al	Be	23	—	24	5
N		32	—	16	3	Si		28	—	18	5
O		13	1	5	—	P	Li	20	—	16	—
O	N	11		3	1	P		15	—	24	9
O	Li	1	—	4	1	S	B	27	—	15	4
O		10	—	4	2	A	B	10	2	19	1
O		4	2	7	6						
O		2	—	10	9						
O		—	3	5	2						
O		4	—	10	4						

TABLE II. (*Continued*) $E \geqslant 1.5$ GeV

Primary	Fragments	N_h	N_α	N_l	N_s	Primary	Fragments	N_h	N_α	N_l	N_s
Li		1	1	1	1	F	N	—	1	1	
B	Li	5	—	7	3	F	Be	6	—	7	7
B		16	—	39	18	F	F	2		3	3
B		7	1	30	26	F		10	—	19	16
B		3	2	5	2	F	Be	2	2	8	6
Be	Li	2	1	3	1	F		6	—	36	25
C		1	—	11	2	F		32	—	34	11
C		18	2	13	2	F	B	—	2		
C	Be	3	—	6	4	F		18	1	36	16
C		8	2	5	2	Ne		1	3	1	1
C	C	3	—	2	—	Ne	N	7	1	2	
C		14	—	29	14	Ne		20	—	48	26
C		3	12	10	—	Ne		16	—	23	14
C		27	—	25	7	Ne		15	—	39	19
C		2	—	27	19	Ne	Li	4	2	10	6
C		14	—	21	7	Ne	O	—	1		
C		5	2	12	10	Ne		5	1	12	7
C		—	3	—	—	Na	C, Li	3	1	3	3
C		2	2	2	1	Na		16	1	42	21
C		20	—	122	91	Na		1	3	16	11
C		21	—	18	9	Na	Li	23	1	21	9
C	Be	2	1	1	—	Na	Be	15	—	15	5
C	C	3	—	5	2	Mg		23	1	25	17
N		26	—	15	6	Mg	Be	2	2	5	3
N		6	1	11	1	Mg		24	1	30	17
N		1	2	9	7	Al	F	3	2	7	2
N		4	—	15	6	Al	Ne	—	1	2	—
N		5	1	18	18	Al		—	5	2	—
N		1	—	21	18	Al	O	5	2	7	5
N		15	2	19	5	Al	B	—	3	4	4
N		30	—	28	13	Al		14	1	20	13
N		34	—	49	26	Si		22	1	20	13
N	L	1	—	7	6	Si		—	2	7	5
O		4	—	17	7	Si		5	3	17	12
O		5	2	4	2	Si		23	2	35	11
O	Be	4	—	6	3	P	Li	1	3	8	7
O		—	3	1	1	P	Mg	—	1	9	6
O	O	4	—	1	—	P	B	7	1	10	9
O		22	—	27	5	Cl	C	14	1	26	13
O		1	—	35	32	A		16	—	55	25
O		15	1	13	9	Cl		10	1	118	85
O		26	—	23	8	Cl		19	1	41	8
O		6	1	42	20	K	Be	—	4	16	15
O	Li	22	19	13	—	K	P, Li	5	—	13	—
O		12	—	27	13	Ca	Al	1	1	11	8

collision (I-T),

$$N_{IT}(b) = \iiint \varrho_I(x - b, y, z)\{1 - \exp[-\sigma n_T(x, y)]\}\,\mathrm{d}x\,\mathrm{d}y\,\mathrm{d}z\,. \tag{3.1}$$

where $\sigma n_T(x, y) = \sigma \int_{-\infty}^{\infty} \varrho_T(x, y, z)\,\mathrm{d}z$ is the average number of collisions made by a nucleon, with a reaction cross-section σ, moving along the z-direction. The z integration in (3.1) is extended from $-\infty$ to $+\infty$, while the (x, y) integration is above the overlapping area, of the incident and target nucleus, with impact parameter b (see Fig. 1).

Using the density distribution function $\varrho(r)$ as given in I ([3]), and $\sigma = 30$ mb, $N_{IT}(b)$ was integrated numerically for a number of incident-target pairs. An example of this integration for a carbon nucleus is shown in Fig. 2. For each

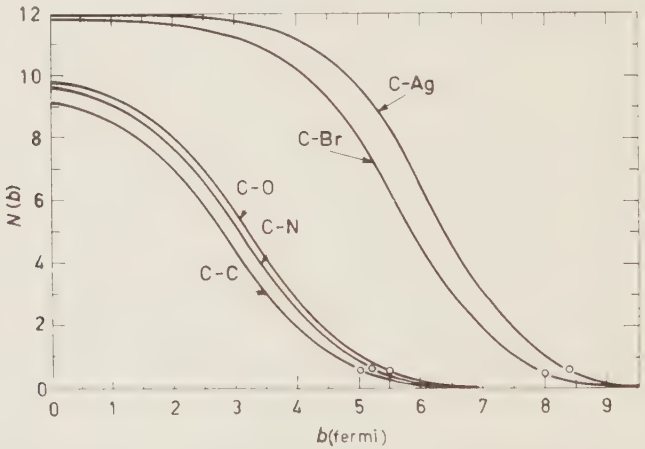

Fig. 2. – Average number of colliding incident nucleons $N(b)$ as a function of impact parameter, b, in collisions of carbon nuclei in emulsion.

nucleus-nucleus reaction (I-T) an effective impact parameter $b_{\mathrm{ef}} = \sqrt{\sigma_{IT}/\pi}$ is defined with the help of its reaction cross-section as calculated in paper I. The corresponding effective impact parameters are shown, by circles, on Fig. 2. The average number of incident nucleons $N_{IT}(b_{\mathrm{ef}})$ corresponding to them are just below unity, as expected. This allows us to approximate σ_{IT} by $\pi b_{IT}^2 (\bar{N} = 1)$. The average number of incident nucleons that made primary collisions, per nuclear reaction induced by an I incident nucleus in emulsion is

$$N_I = \sigma_I \sum y_T \int_0^{\infty} N_{IT}(b) 2\pi b\,\mathrm{d}b\,, \tag{3.2}$$

where σ_I is the reaction cross-section of an I nucleus in emulsion, and g_T is the density of the T target nucleus in emulsion. The summation is over the different nuclei in photographic emulsion with the exclusion of hydrogen. Using the reaction cross-sections σ_I's, of paper I, the average number of colliding incident nucleons, N_I, per nuclear reaction induced by an I nucleus in emulsion was calculated. The results are given in Table III. The observed numer of shower particles ($I \leqslant 1.4\ I_{\min}$) per star with $N_h > 1$, for Li, Be and B stars as quoted in Table III were measured by the Bristol ([4,5]) and Turin ([6])

TABLE III. – *Multiplicity N_s versus number of interacting incident nucleons N_I in nucleus-nucleus collisions.*

Incident nucleus	N_I	N_s	N_s/N_I
Li	3.50	6.5 ± 1.1	1.85 ± .31
Be	4.26	6.7 ± 1.1	1.57 ± .26
B	5.02	9.1 ± .9	1.81 ± .18
C	5.26	11.8 ± .9	2.22 ± .18
N	5.70	9.3 ± .9	1.63 ± .18
O	6.27	11.4 ± 1.2	1.82 ± .20

groups, while our present results for $E \geqslant 1.5$ GeV per nucleon are also incorporated in the multiplicities of the C N O stars.

It appears from Table III that the charge multiplicity N_s, is proportional to the average number of incident nucleons per nucleus-nucleus collision N_I, the average proportionality factor for light and medium primaries with $E \geqslant 1.5$ GeV per nucleon in emulsion is $N_s/N_I = 1.81$.

The observation of LOHRMANN *et al.* ([7]) and the results of this paper are used to estimate the average multiplicity for incident primaries with $E \geqslant 7$ and $E < 1.5$ GeV per nucleon, respectively. The average charge multiplicities for these two cases are given for three groups of heavy primaries: 1) Light particles: $L =$ Li, Be, and B. 2) Medium particles: $M =$ C, N, O and heavy particles, $H =$ all nuclei heavier than F.

The average charged multiplicities N_s for these groups together with those

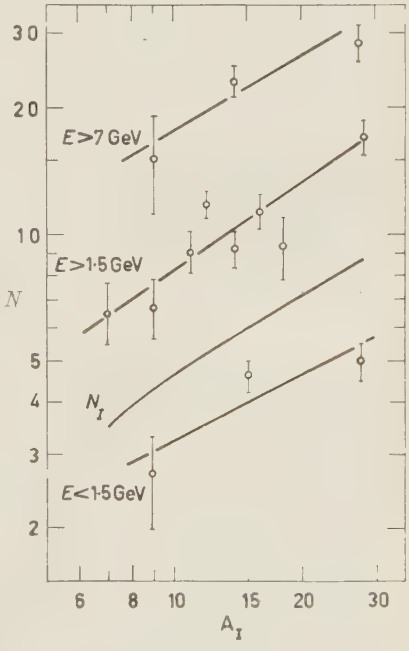

Fig. 3. – Multiplicity, N, in nucleus-nucleus collisions, as a function of incident nucleus size, A_I.

of Table I are plotted on Fig. 3. It appears from Fig. 3 that proportionality $N_s \propto N_I$ holds well for primaries with $E \geq 1.5$ GeV per nucleon and for the other two groups. The average ratios N_s/N_I for nuclear events of heavy primaries in emulsions, are compared in Table IV with the average charged multiplicities N_s of protons of the same energy. The multiplicities of the proton stars were taken from CAMERINI *et al.* [11] and using a C.R. spectrum of $E^{-2}\mathrm{d}E$.

TABLE IV. – *Observed multiplicities in stars induced by heavy primaries and protons in emulsion.*

Energy per nucleon GeV	Average multiplicity per incident nucleon	
	H.P. stars N_I/N_s	C.R. proton stars
$E < 1.5$ GeV $\bar{E} = 0.65$	$1.50 \pm .30$	0.2 ± 0.1
$E > 1.5$ GeV	$1.81 \pm .10$	1.52 ± 0.6
$E > 7$ GeV	$3.70 \pm .50$	$3.90 + 0.7$

The results summarized in Table IV may be interpreted as follows. Some of the shower particles in H.P. stars are relativistic protons originating from the incident nucleus. At low energies when few mesons are produced these protons make the majority of shower particles in H.P. stars, and this is why the relative multiplicity in these stars is higher than in proton stars of the same energy per nucleon. On the other hand, the observation that at higher energies the multiplicity of proton induced stars is equal (or even higher) to that of H.P. stars, indicates that a single proton in a nucleon-nucleus collision produces more mesons than a single nucleon in a nucleus-nucleus collision.

4. – Integral multiplicity spectrum.

The integral multiplicity spectra in nuclear collisions induced by light and medium C.R. particles are deduced from the observations of Bristol [4,5], Turin [6] and Chicago [7]. By comparing the observed integral spectrum of shower particles to that of the colliding incident nucleons, one may examine the effectiveness of individual nucleons to produce shower particles.

The probability per unit length of emulsion that the average number of

[11] U. CAMERINI, J. H. DAVIES, C. FRANZINETTI, W. O. LOCK, D. H. PERKINS and G. YEKUTIELI: *Phil. Mag.*, **7**, 1261 (1951).

colliding nucleons of an incident nucleus I, exceed N_I, is

$$P_I(\geqslant N) = \sum g_T \pi b_{IT}^2(N) \,, \tag{4.1}$$

where $b_{IT}(N)$ is the impact parameter in a I-T collision corresponding to an average number of $N_{IT}(b)$ colliding nucleons, and g_T is the density of the T target nucleus in emulsion. For a mixed group of primaries (light or medium) the probability for the same event is

$$P(\geqslant N) = \sum_{I,T} h_I g_I \pi b_{IT}^2(N) \,, \tag{4.2}$$

where h_I is the relative intensity of individual primaries in the group. The normalized probability per nucleus-nucleus interaction is $\tilde{P}(\geqslant N) = P(\geqslant N)/P(\geqslant 1)$;

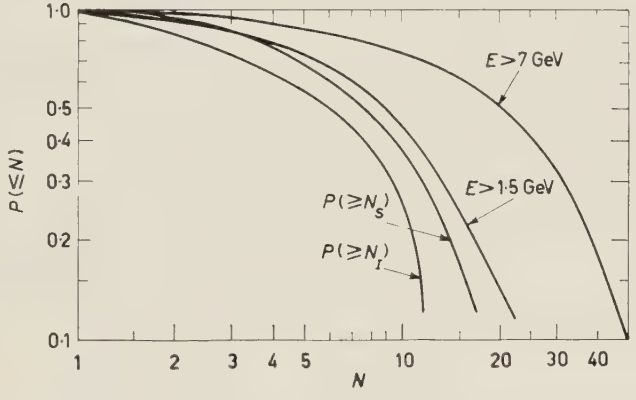

Fig. 4. – Integral multiplicity spectra for light incident nuclei.

where the reaction mean free path in emulsion is approximated by $1/P(\geqslant 1)$. The integral colliding nucleons spectra $\tilde{P}(\geqslant N)$ for light and medium C.R. primaries are plotted in Fig. 4 and 5. On the same Fig. 4 and 5 the observed

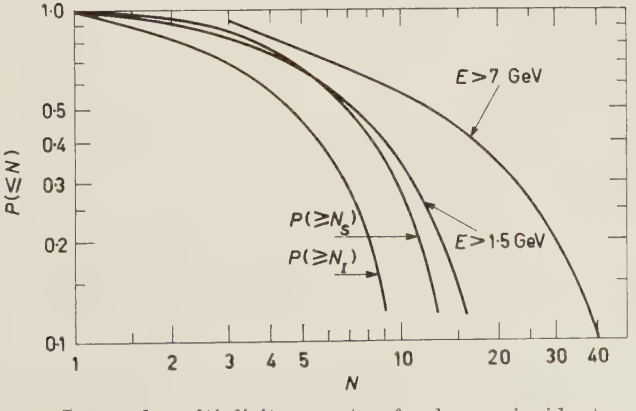

Fig. 5. – Integral multiplicity spectra for heavy incident nuclei.

integral spectra of shower particles for primaries with $E \geqslant 1.5$ GeV per nucleon and for $E \geqslant 7.0$ GeV per nucleon as observed by the Bristol, Turin and Chicago groups are also given. If the observed multiplicity was proportional to the average number of colliding nucleons, their respective integral spectra were represented by parallel curves on Fig. 4 and 5. However, because there are large fluctuations in the number of charged particles produced per nucleon-nucleon collision, the observed integral spectra are shifted towards higher multiplicities. The fluctuations in the number of shower particles are due to *a*) fluctuations in the number of mesons and relativistic nucleons (neutral and charged) formed in each collision and *b*) fluctuations in the number of charged particles. An attempt was made to account for the charge fluctuations for collision with $E \geqslant 1.5$ GeV per nucleon. In this case, on the basis of the results reported in the last section and with the help of a charge balance calculation, we estimate that, on the average 1.8 charged shower particles and 1.2 similar neutral particles are formed by each colliding nucleon. With these parameters the integral spectrum of shower particles $F(\geqslant N_s)$ was calculated from the integral spectrum of colliding nucleons $\tilde{P}(\geqslant N)$. The calculated spectra for light and medium primaries are shown on Fig. 4 and 5. The calculated spectra for $E \geqslant 1.5$ GeV seem to approach the observed one in the right directions. Moreover we believe that the introduction of the fluctuations in the number of mesons and relativistic nucleons formed per colliding nucleon, will improve the calculated integral spectra of shower particles.

5. – Fragmentation versus multiplicity.

Both fragmentation and multiplicity depend strongly on the impact parameter in nucleus-nucleus collisions. The larger the impact parameter b, the larger is the part of the incident nucleus that does not participate in the reaction, and so on the average more fragments are ejected and less shower particles are produced, and vice versa.

Let us estimate the effective size of the non-colliding part of the incident nucleus by the charge Z_f of α-particles and heavy fragments ejected from the reaction. We shall tentatively assume that for close collisions $0 \leqslant b \leqslant b_1$, the non-colliding part of the incident nucleus is so small that on the average not a single α-particle is ejected ($Z_1 < 1$). Next for $b_1 < b \leqslant b_2$, on the average only a single α-particle is ejected ($Z_2 = 2$); for $b < b \leqslant b_2$ a Li or Be fragment or two α-particles are ejected: $2 < Z_3 \leqslant 4$; and so on. Following this convention, the probability for the emission of fragments with effective charge Z_k is equal to the probability of nucleus-nucleus collision with $b_k < b \leqslant b_{k+1}$, *i.e.*

$$P(Z_k) = \frac{\pi b_{k+1}^2 - \pi b_k^2}{\pi b^2 (N = 1)}, \tag{5.1}$$

where $b(N=1)$ is the impact parameter for a single collision and $\pi b^2(N=1)$ stands for the cross-section for nucleus-nucleus reaction.

The relative frequency $P(Z_k)$ of stars with different effective fragment charge Z_k, as observed by the Bristol ([4,5]), Turin ([6]) and Rehovoth groups, in stars induced by light and medium primaries with $E \sim 1.5$ GeV are summarized in Table V. The impact parameters b_{k+1} and b_k corresponding to the observed $P(Z_k)$ are calculated by (5.1) and are given in Table V, together with the average number of colliding nucleons $N_I(b)$ of (3.2). Next the expected multiplicity N_s is calculated on the assumption that 1.81 shower particles are formed per each colliding nucleon, and compared in Table V to the observed multiplicity N_s of the corresponding stars. The expected multiplicity ranges $N_s - N_{s'}$ estimated in this way are found to be in good agreement with the observed multiplicity $\bar{N}_s$. Finally, the average number of incident nucleons that did not participate in the collision, $A - N_I(b)$, are also given. It is remarkable that the average number of non-colliding incident nucleons agrees with twice the effective fragment charge Z_k of the corresponding group of stars in Table V.

TABLE V. – *Effective fragment Z vs. average multiplicity in light and medium stars.*

	Light group			Medium group			
Z_k	$Z_1 \leqslant 1$	$Z_2 = 2$	$2 < Z_3$	$Z_1 \leqslant 1$	$Z_2 = 2$	$2 < Z_3 \leqslant 4$	$4 < Z_4$
$P(Z_k)$	0.53	0.30	0.18	0.42	0.20	0.18	0.20
$b_k - b_{k+1}$	0 ÷ 4.7	4.7 ÷ 6.8	6.8 ÷ 8.5	0 ÷ 4.4	4.7 ÷ 5.4	5.4 ÷ 6.8	6.8 ÷ 9.0
$N_{I-\mathrm{cm}}(b)$	8.2 ÷ 4.9	4.9 ÷ 1.4	1.4 ÷ 0.1	12.2 ÷ 8.0	8.0 ÷ 5.5	5.5 ÷ 2.3	2.3 ÷ 0.1
N_s exp.	14.9 ÷ 8.9	8.9 ÷ 2.5	2.5 ÷ 0.2	22.1 ÷ 14.5	14.5 ÷ 9.9	9.9 ÷ 4.2	4.2 ÷ 0.2
N_s obs.	10.6	6.45	2.5	17.6	9.7	6.0	1.82
$A - N_I(b)$	0 ÷ 3.3	3.3 ÷ 6.6	6.6 ÷ 8.1	0 ÷ 4.2	4.2 ÷ 6.7	6.7 ÷ 9.9	9.9 ÷ 12.1

6. – Recoil of the target nucleus.

Some idea on the motion of the non-directly hit part of the target nucleus can be obtained from the angular distribution of black prongs associated with heavy primary stars in emulsion. The angular distributions of black prongs ($I_b \geqslant 6\, I_{\min}$) for two groups of stars *i.e.* induced by heavy primaries with *a*) $E < 1.5$ and *b*) $E \geqslant 1.5$ GeV per nucleon are given in Fig. 6 and 7 respectively. The angular distributions of small stars, ($N_h \leqslant 7$) are shown by broken lines on both Fig. 6 and 7. Black prongs of large stars ($N_h > 7$) are due mainly to low energy protons and α-particles resulting from the evaporation of excited heavy (Br and Ag) target nuclei. Let us assume that the excited heavy target

nuclei associated with large stars are moving with an effective velocity β_c, and that the low energy protons and α-particles are ejected from it isotropically and with an average velocity β_0. In this case the effective velocity β_c of the excited target nuclei can be estimated from the median angle $\theta_{\frac{1}{2}}$ of the black prongs: $\gamma_c \cot\theta_{\frac{1}{2}} = \beta_c\beta_0$. Now for a very slow moving system $\gamma_c = 1$ and $\beta_c = \beta_0 \cot\theta_{\frac{1}{2}}$.

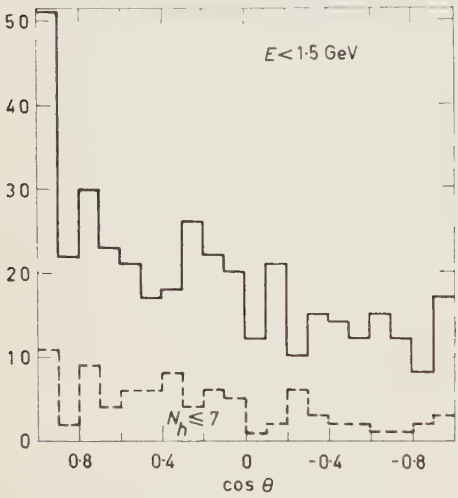

Fig. 6. – Angular distribution of black prongs; $E < 1.5$ GeV per nucleon.

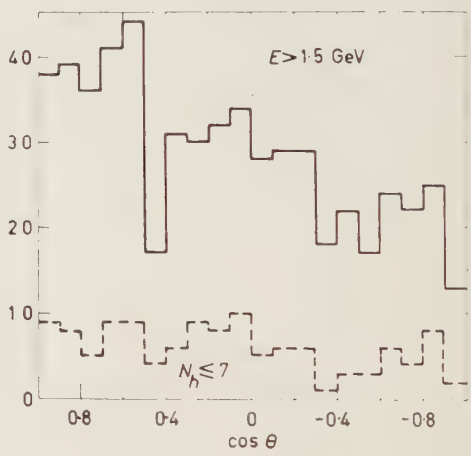

Fig. 7. – Angular distribution of black prongs; $E \geq 1.5$ GeV per nucleon.

The median angles of black prongs associated with different groups of stars are summarized in Table VI. The effective excited target velocity β_c, is estimated for $\beta_0 = 0.16$, which is the velocity of a typical evaporated proton.

TABLE VI. *Median angles $\theta_{\frac{1}{2}}$ of black prongs.*

Energy group	Star size	$\theta_{\frac{1}{2}}$	β_c
$E > 1.5$ GeV	all stars	85°	0.029
	$N_h > 7$	86°	0.029
$E < 1.5$ GeV	all stars	75°	0.043
$E = 0.69$ GeV	$N_h > 7$	77°	0.036
	$N_h \leq 7$	69°	0.060

It appears from Table VI that the excited target nuclei (Br and Ag) associated with large stars, recoil as a result of the nucleus-nucleus collision and move slowly with $\beta_c \approx 0.03$. It is worth-while noting that the excited target

nuclei of the lower primary energy group ($E < 1.5$ GeV) seem to move faster than those of the higher energy group.

Qualitative comparison of the above results to those observed for stars induced by cosmic ray protons of the same energy per nucleon ([12]) show that the excited target nuclei induced by heavy primaries are accelerated more than those induced by proton primaries.

7. – Conclusions.

Nucleus-nucleus collisions at high energies can be described by a simple geometrical model (see Fig. 1) as a reaction, in two stages:

a) Violent head-on collisions between incident and target nucleons in the overlapping volumes of the two colliding nuclei, in which many mesons and relativistic nucleons are formed, and make the jet of shower particles of the H.P. stars in photographic emulsion. The average number of shower particles so produced is proportional to the average number of colliding incident nucleons. Moreover the multiplicity per colliding incident nucleon is in agreement with that induced by primary protons of the same energy.

b) Nuclear excitation of the non-directly hit parts of both incident and target nuclei. This excitation causes in most cases the complete disintegration of the incident nucleus into nucleons, α-particles, and heavier fragments. We were able to demonstrate a correlation between the effective size of the non-interacting part of the incident nucleus and the star multiplicity, and to predict the average multiplicity of stars as a function of their total fragment charge. The analysis of the angular distribution of protons and α-particles (black prongs) associated with large stars ($N_h > 7$) indicate a slight movement, $\beta \approx 0.03$ of the excited heavy (Br ang Ag) target nuclei.

* * *

We would like to thank Prof. Houtermans and the Bern C.R. group for their kind co-operation, and the loan of the Texas stack of emulsion for this experiment; and to Messrs. A. Levy and U. Karshon who did most of the numerical calculations.

([12]) U. Camerini, O. W. Lock and D. H. Perkins: *Prog. Compt. Rend. Phys.* **1**, 3 (1952).

RIASSUNTO (*)

Descriviamo, in termini di collisioni nucleone-nucleone, le collisioni nucleo-nucleo alle energie dei raggi cosmici. Prediciamo la molteplicità media per differenti tipi di reazioni e la confrontiamo con le osservazioni sperimentali.

(*) *Traduzione a cura della Redazione.*

High-Energy Interactions of a Heavy Primary in Emulsion.

G. Biczó, G. Bozóki, E. Fenyves and E. Gombosi

Central Research Institute of Physics - Budapest
Roland Eötvös University - Budapest

(ricevuto il 23 Gennaio 1961)

Summary. — Two successive high-energy interactions of a heavy primary cosmic ray particle in emulsion were analysed. The differential angular distribution of shower particles generated does not show any significant deviation from the distribution predicted by the hydrodynamical theory (4).

Two successive high-energy collisions of a heavy primary cosmic ray particle were found in plates of the I stack irradiated in the Po-Valley Expedition, 1955. The first interaction is of the type $2+15Z_{\mathrm{I}}$ and the second one $16+115Z_{\mathrm{II}}$ using the Bristol notation of jets (1). The values of Z_{I} and Z_{II} were estimated from the δ-ray density of tracks (2) as $Z_{\mathrm{I}} \approx 17$ and $Z_{\mathrm{II}} \approx 12$. The energy of the heavy primary was estimated from the angular distribution of secondary particles created assuming that the interaction of a heavy primary particle with a nucleus is a superposition of simultaneous nucleon-nucleon collisions in a common center-of-mass system (c.m.s.). The value of γ_c corresponding to this c.m.s. was estimated for both interactions using the method of Castagnoli *et al.* (3) as

$$\gamma_{c,\mathrm{I}} = 27 \pm 7\,, \qquad \gamma_{c,\mathrm{II}} = 10.3 \pm 1.0\,, \tag{1}$$

(1) R. R. Daniel, J. H. Davies, J. H. Mulvey and D. H. Perkins: *Phil. Mag.*, **43**, 753 (1952).

(2) A. D. Dainton, P. H. Fowler and D. W. Kent: *Phil. Mag.*, **43**, 729 (1952).

(3) C. Castagnoli, G. Certini, C. Franzinetti, A. Manfredini and A. Moreno: *Nuovo Cimento*, **10**, 1539 (1953).

where $\gamma_{c,\mathrm{I}}$ and $\gamma_{c,\mathrm{II}}$ correspond to the first and second interaction, respectively (Table I).

TABLE I. – *Interactions of the heavy primary particle.*

Interaction	γ_c
$(2 \pm 15)\, Z_{\mathrm{I}}$	27 ± 7
$(16 \pm 115)\, Z_{\mathrm{II}}$	10.3 ± 1.0

The two values of γ_c are not significantly different and from their weighted mean the energy of the heavy primary particle can be estimated as about $2 \cdot 10^{11}$ eV/nucleon (*).

Two secondary interactions of charged shower particles generated in the second interaction of the heavy primary and a secondary interaction of a neutral particle were found. The values of γ_c of these interactions, estimated in the same way as those of the primary interactions, and the transverse momenta of generating particles are collected in Table II. The transverse momentum of the neutral particle was calculated by assuming that it is a neutron generated in the second interaction of the heavy primary particle.

TABLE II. – *Secondary interactions.*

Interaction	γ_c	$p_\perp$ (GeV/c)
(6+2) p	(≈ 4)	(≈ 2.4)
(14+1) p	—	—
(7+7) n	3.3 ± 1.2	0.26 ± 0.10

The differential angular distributions of shower particles generated in both interactions of the heavy primary particle are plotted in Fig. 1 and 2. The great number of shower particles generated in the second interaction ($16 \pm 115 Z_{\mathrm{II}}$) makes possible to compare their angular distribution with that predicted by the hydrodynamical theory for nucleus-nucleus collisions [4] which is given in the form

$$f(\lambda)\,\mathrm{d}\lambda = c \cdot \exp\left(-\frac{\lambda}{2L}\right)\mathrm{d}\lambda\,, \tag{2}$$

(*) The same energy per nucleon would be obtained, if the interaction were assumed to be a central collision of two nuclei having equal masses.

[4] G. A. MILEKHIN: *Žurn. Éksp. Teor. Fiz.*, **35**, 1185 (1958).

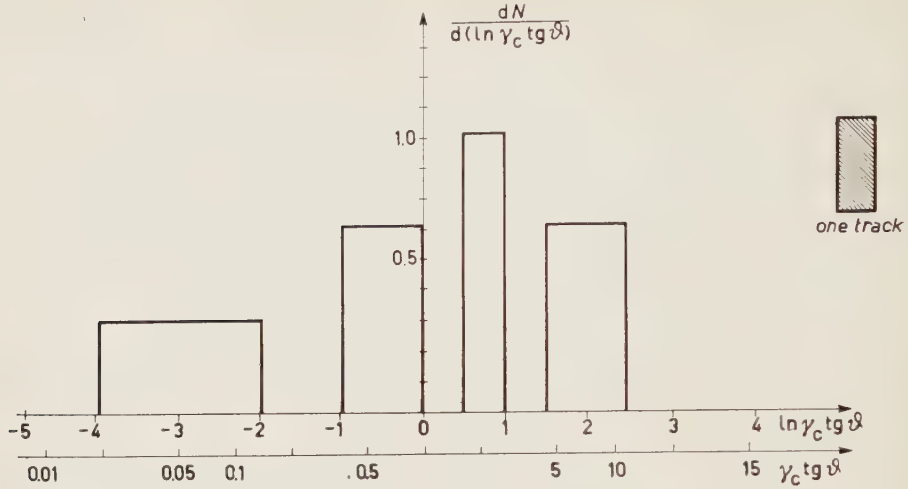

Fig. 1. – Differential angular distribution of shower particles generated in the $(2+15)Z_{\mathrm{I}}$ interaction.

where c is the constant of normalization.

(3) $$\lambda = -\ln(\gamma_c \operatorname{tg}\vartheta),$$

(4) $$L = 0.56 \ln 2\gamma_c^2 + 1.6\left(1 + \ln\frac{2}{l+l'}\right),$$

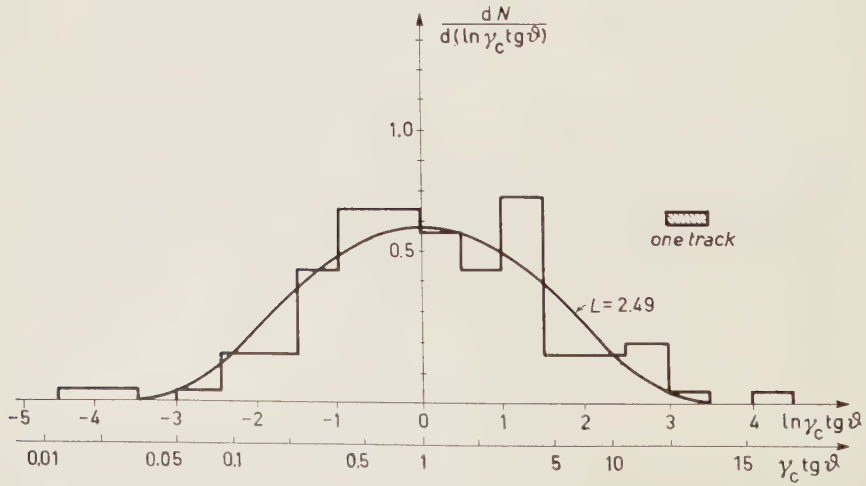

Fig. 2. – Differential angular distribution of shower particles generated in the $(16+115)Z_{\mathrm{II}}$ interaction. The smooth curve shows the distribution predicted by the hydrodynamical theory [4] for a nucleus-nucleus collision with $\gamma_c \approx 10$, $l \approx 4.6$ and $l' \approx 2.9$ (see text).

and l is the length of the « tunnel » of the hit emulsion nucleus and l' the length of the « tunnel » of the incident particle. Assuming $l \approx 4.6$ (average length of the tunnel of heavy emulsion nuclei (and $l' \approx 2.9$) average length of the « tunnel » of a nucleus having charge $Z \approx 12$, there is no significant difference between the experimental and theoretical distributions.

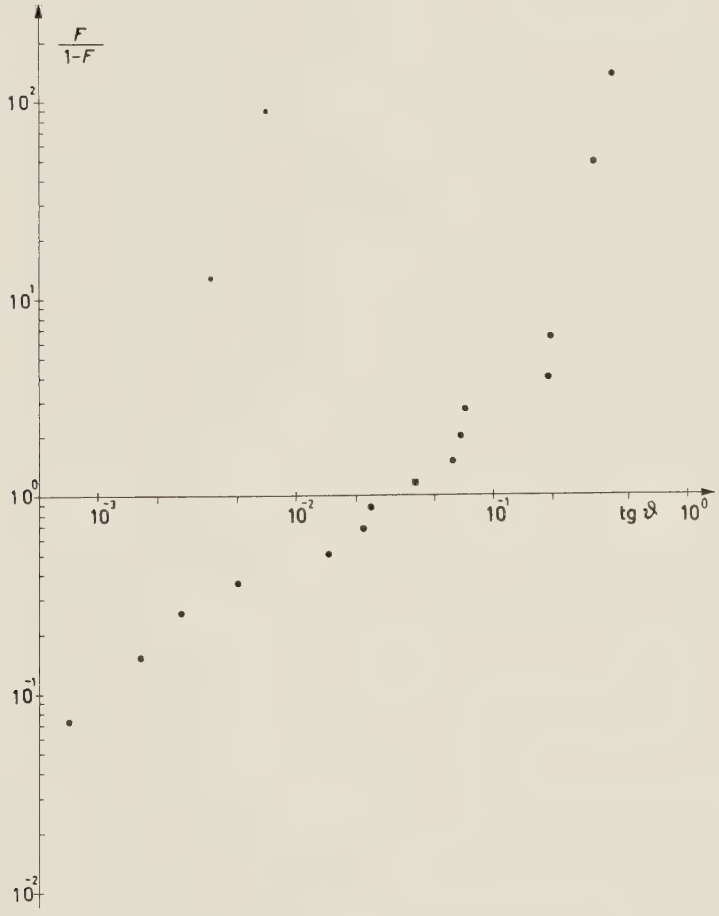

Fig. 3. – Duller-Walker plot of the shower particles generated in the $(2 \pm 15)Z_I$ interaction.

The Duller-Walker $F/(1-F)$ plot (5) of the integral angular distributions (Fig. 3 and 4) as well as the differential angular distributions (Fig. 1 and 2)

(5) N. M. Duller and V. D. Walker: *Phys. Rev.*, **93**, 215 (1954).

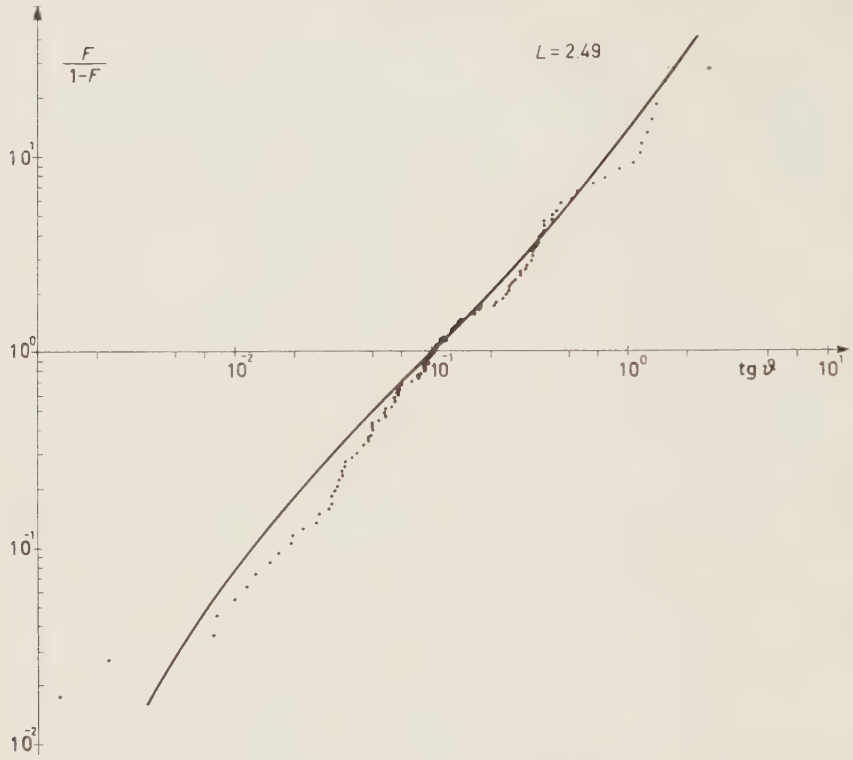

Fig. 4. – Duller-Walker plot of the shower particles generated in the $(16 \div 115) Z_{\mathrm{II}}$ interaction.

do not show any pronounced double-maximum structure, as expected for the comparatively low γ_c value.

* * *

The authors are indebted to Prof. L. JÁNOSSY for valuable discussions, to Prof. M. DANYSZ who has kindly provided the emulsion plates for the present investigation, and to Dr. PERNEGR and Dr. SEDLAK for having sent us the data measured on the first interaction of the heavy primary in their plates in Prague.

RIASSUNTO (*)

Abbiamo analizzato in emulsione due sucessive interazioni di alta energia di una particella pesante dei raggi cosmici primari. La distribuzione angolare differenziale delle particelle dello sciame non presenta alcuna significativa deviazione dalla distribuzione predetta dalla teoria idrodinamica [4].

(*) *Traduzione a cura della Redazione.*

IL NUOVO CIMENTO Vol. XX, N. 4 16 Maggio 1961

Dynamic Behaviour of Polymethyl Methacrylate between 60 and 300 °K.

P. G. Bordoni

Istituto di Fisica Matematica dell'Università - Pisa

M. Nuovo and L. Verdini

Istituto Nazionale di Ultracustica - Roma

(ricevuto il 30 Gennaio 1961)

Summary. — The resonant frequency and the coefficient of energy dissipation have been measured as a function of temperature in the interval (60÷3 ( ) °K for several specimens of polymethyl methacrylate of the plasticized and unplasticized type. The specimens have the shape of circular plates, and the measurements have been made for flexural vibrations in the frequency range (6÷40) kHz, with a strain amplitude smaller than 10^{-7}. A thermally activated relaxation effect gives rise to a peak in the dissipation temperature curve. For the above frequency range the temperature of the peak is about 110 °K. At the same temperature a slight inflexion is observed in the frequency-temperature curve in accordance with the theory of linear dynamic deformations. The relaxation effect, which is probably due to the rearrangement of side chains, is superposed to another cause of energy dissipation which cannot be explained by means of the above theory in its present state, as the corresponding dissipation coefficient increases not only with temperature but also with frequency. The frequency-temperature curve exhibits a *knee* near 230 °K. This temperature is apparently independent of the vibration frequency, and the knee seems to be due to a second order transition.

1. – Introduction.

A large amount of experimental work concerning high polymers has been carried out during the last years by measuring the elastic coefficient and the

energy dissipation by means of vibration methods [1-11] (*). However the exper-

[1] M. BACCAREDDA, P. G. BORDONI, E. BUTTA and A. CHARLESBY: *La Chimica e l'Industria*, **28**, 561 (1956).

[2] L. VERDINI: *Nuovo Cimento*, **5**, 648 (1957).

[3] M. BACCAREDDA and E. BUTTA: *La Chimica e l'Industria*, **40**, 6 (1958).

[4] M. BACCAREDDA, E. BUTTA and R. CAPUTO: *La Chimica e l'Industria*, **40**, 356 (1958).

[5] M. BACCAREDDA and E. BUTTA: *La Chimica e l'Industria*, **40**, 732 (1958).

[6] M. BACCAREDDA and E. BUTTA: *La Chimica e l'Industria*, **40**, 983 (1958).

[7] E. BUTTA: *Proprietà meccaniche dinamiche e punti di transizione dei politereftalati*, in « Pubbl. Istit. Chim. Ind. e Appl. dell'Università di Pisa ». Ottobre 1958.

[8] E. BUTTA: *Annali di Chimica*, **48**, 802 (1958).

[9] M. BACCAREDDA and E. BUTTA: *Journ. Pol. Sci.*, **31**, 189 (1958).

[10] G. NATTA, M. BACCAREDDA and E. BUTTA: *La Chimica e l'Industria*, **41**, 737 (1959).

[11] M. BACCAREDDA and E. BUTTA: *Annali di Chimica*, **49**, 559 (1959).

[12] M. BACCAREDDA, P. G. BORDONI and E. BUTTA: *Mechanical relaxation in partially crystalline high polymers*, in *Proc. of the Third International Congress of Acoustics*, Stuttgart (September 1959), in press.

[13] M. BACCAREDDA and E. BUTTA: *Dynamic mechanical properties of polytrifluorochloroethylene*, in *Symposium über Makromolekule*, Wiesbaden (October 1959), to be published.

[14] I. G. MIKHAILOW: *Dokl. Akad. Nauk SSSR*, **59**, 1555 (1948).

[15] D. S. HUGHES, W. L. PANDROM and R. L. MIMS: *Phys. Rev.*, **73**, 1552 (1949).

[16] G. G. PARFITT: *Nature*, **164**, 489 (1949).

[17] T. F. PROTZMANN: *Journ. Appl. Phys.*, **20**, 627 (1949).

[18] E. FUKADA: *Journ. Phys. Soc. Japan*, **6**, 254 (1951); **9**, 786 (1954).

[19] N. F. OTPUSHCHENNIKOV: *Žurn. Èksp. Teor. Fiz.*, **22**, 436 (1952).

[20] J. L. MELCHIOR and A. A. PETRAUSKAS: *Ind. Eng. Chem.*, **44**, 716 (1952).

[21] K. SCHMIEDER and K. WOLF: *Kolloid Zeits.*, **127**, 65 (1952); **34**, 149 (1953).

[22] S. IWAYANAGI and T. HIDESHIMA: *Journ. Phys. Soc. Japan*, **8**, 365; 368 (1953).

[23] K. DEUTSCH, E. A. HOFF and W. REDDISH: *Journ. Pol. Sci.*, **13**, 565 (1954).

[24] S. V. SUBRAHMANYAM: *Journ. Chem. Phys.*, **22**, 1562 (1954).

[25] IR. J. HEIJBOER, P. DEKKING and A. J. STAVERMAN: *Proc. of the Second International Congress of Rheology* (1953) (London, 1954), p. 123.

[26] E. JENCKELS and K. H. MILLERS: *Zeits. Naturfor.*, **9a**, 440 (1954).

[27] M. KRISHNAMURTI and G. SIVARAMA SASTRI: *Nature*, **174**, 132 (1954).

[28] P. HATFIELD: *Nature*, **174**, 1186 (1954); *Journ. Chem. Phys.*, **22**, 1133 (1954).

[29] E. A. HOFF, D. W. ROBINSON and A. H. WILLBOURN: *Journ. Pol. Sci.*, **18**, 161 (1955).

[30] N. F. OTPUSHCHENNIKOV: *Žurn. Èksp. Teor. Fiz.*, **28**, 371 (1955).

[31] S. IWAYANAGI: *Journ. Sci. Res. Inst.* (*Tokyo*), **49**, 13; 23 (1955).

[32] G. W. BECKER: *Kolloid. Zeits.*, **140**, 1 (1955).

[33] B. MAXWELL: *Journ. Pol. Sci.*, **20**, 551 (1956).

[34] R. N. WORK: *Journ. Appl. Phys.*, **27**, 69 (1956).

[35] IR. J. HEIJBOER: *Kolloid. Zeits.*, **148**, 36 (1956).

[36] H. THURN and K. WOLF: *Kolloid. Zeits.*, **148**, 16 (1956).

[37] J. D. FERRY and R. F. LANDEL: *Kolloid. Zeits.*, **148**, 1 (1956).

[38] K. YAMAMOTO and Y. WADA: *Journ. Phys. Soc. Japan*, **12**, 374 (1957).

[39] A. E. WOODWARD and J. A. SAUER: *Adv. in Pol. Sci.*, **1**, 114 (1958).

[40] K. M. SINNOT: *Journ. Pol. Sci.*, **35**, 273 (1959).

[41] IR. J. HEIJBOER: *Kolloid. Zeits.*, **171**, 7 (1960).

(*) The papers [1-13] deal with dynamic measurements of elastic coefficients and energy dissipation on polymers by means of the frequency modulation technique. The papers [14-41] refer on the dynamic behaviour of PMMA in general.

imental evidence which is presently available is still incomplete as in many cases these measurements were made for some special purpose, such as the determination of the second order transition points, and not with the aim of making a systematic investigation on the elastic and anelastic behaviour of polymers. For this reason the experimenters have generally neglected to measure at the same time *both* the parameters which characterize the dynamic behaviour (energy dissipation and one of the elastic coefficients) as functions of *both* the variables (temperature and frequency) upon which the dynamic behaviour depends.

It may be added that usually no information is given on the strain amplitude at which the measurements were made. As a consequence it is impossible to separate the truly linear effects from the amplitude-dependent ones, and this confusion may be responsible for some of the contradictions which are found in the experimental results obtained by different investigators (*).

The final purpose of dynamic investigations on polymers is that of giving a structural interpretation of the experimental data relating them to the motions of the main- or of the side-chains. However these data do not lend themselves directly to such an interpretation unless they are previously analyzed in the light of the theory of dynamic deformations, and unless some sort of stress-strain relationship is derived from the experimental curves which give the energy dissipation and the elastic coefficients as a function of frequency or as a function of temperature. The improper use of the theory and of some basic physical concepts, like those of *transition* and *dispersion*, has proved a source of confusion. For instance it has been suggested that the dissipation maxima which occur at temperatures increasing with frequency are due to a *transition*. Now from the physical standpoint it is obvious that a

---

(*) An instance of these contradictions is afforded by the relation between the vibration frequency and the temperature T_g of the so-called second order transition from the *glassy* to the *rubber-like* state, which is observed in the temperature interval between 55 °C and 75 °C. According to Protzmann ([17]) the temperature *decreases* with increasing frequency; Melchior and Petrauskas ([20]) observed no such dependence; this result agrees with the dilatometric measurements of Robinson and Baldwin (see paper ([20])) and with the dynamic measurements of Subrahmanyam ([24]) and with those of Krishnamurti and Sastri ([27]). On the other hand Deutsch, Hoff and Reddish ([23]) have found that the modulus-temperature curve is displaced towards the higher temperatures when the frequency increases. However these measurements were made with a quasi-static technique and the strain was probably much larger than in truly dynamic measurements. This could account for the different result, but the AA. clearly state that the measurements were made in the linear range. A faint frequency-dependence of T is shown by the three-dimensional diagrams of Maxwell ([33]) Further information on this point may be found in the papers of Verdini ([2]) and of Work ([34]). Some measurements of T for frequencies in the kilohertz range have also been made by Baccaredda and Butta ([3,8]).

transition whose temperature depends upon frequency is meaningless if the frequency is that of the experiment, as this would imply that the transition is *caused* by the measurement itself. On the other hand, if the word is used with the meaning of « frequency of some kind of vibration », the idea of a transition temperature which depends upon frequency is not self-consistent, as a wide spectrum of vibration frequencies is always present in solids owing to the thermal agitation. In fact the observed dissipation peaks whose temperature depends upon frequency are due to thermally activated relaxation effects: the difference is not a simple matter of terminology, as these effects are *not* associated with a characteristic *temperature*, but with a characteristic *time* and with a characteristic *activation energy*.

The concept of dispersion ([33,39,40]), that is of a frequency-dependence of the phase velocity of the elastic waves, has been employed in a less improper way in connection with the partial relaxation effects of the type considered by ZENER ([42]) which are analogous to the dielectric relaxation investigated by DEBYE ([43]). However the dispersion may be a very evident effect for electromagnetic waves but the same is not true for the elastic vibrations. In the common case of thermally activated effects, when the elastic coefficients are measured as a function of temperature, the changes in velocity due to the dispersion are generally masked by the larger changes due to the thermal dilatation and may be detected with some difficulty. Moreover the dispersion of elastic waves is not *typical* of the partial relaxation effects being also present, and much more evident, in the case of a total relaxation which corresponds to a different physical process. Hence it is more convenient to focus the attention not on the dispersion but on the energy dissipation. When this is done, no confusion is possible: the dissipation *peaks* characterize the *partial* or Zener relaxation, whilst a *gradual increase* of the dissipation with the temperature or with the vibration period is typical of a *total* relaxation process.

The above remarks have directed the present investigation which concerns the dynamic behaviour of polymethyl methacrylate in the temperature interval between 60 °K and 300 °K. The elastic coefficient associated with the flexural vibrations of plates, which is very near to the Young's modulus, and the corresponding energy dissipation have been measured at different frequencies in the range between 6 and 40 kHz, with strain amplitudes smaller than 10^{-7}. No amplitude-dependence of the parameters measured has been observed.

The linear theory of dynamic deformations has been employed to analyse the experimental data. In its present state this theory considers two types

---

([42]) C. ZENER: *Elasticity and Anelasticity of Metals* (Chicago, 1948), p. 41.

([43]) For the dielectric relaxation see for instance C. KITTEL: *Solid State Physics* (New York, 1953), p. 107, or paper ([23]).

of effects: *partial* relaxation and *total* relaxation (*); each type may be associated either with a single characteristic time or with a time-spectrum ([42,44]).

No partial relaxation with a single time has been observed as it could be expected, this type of effect being associated with *atomic* processes, such as the motion of interstitials in a regular lattice. The only partial relaxation peak which has been found, at temperatures somewhat above 100 °K, is associated with a wide spectrum. The analogy with the results obtained by other experimenters on different polymers of the same series ([29,40]) and the values of the main parameters of the effect (activation energy, characteristic time, spectrum width, total relaxation strength) indicate that it is probably due to some motion of the lateral chains. A large *background* dissipation, due to different causes, masks in part the relaxation peak. This is probably the reason why the effect has not been observed until now.

The background dissipation increases with the temperature according to an exponential law: this would indicate the presence of a thermally activated total relaxation with a single characteristic time or with a very narrow spectrum ([44]). However the frequency dependence of this part of the dissipation is not that predicted by theory for total relaxation, and a more satisfactory mathematical analysis of the experimental results is needed before any structural interpretation is proposed.

A *knee* has been observed in the modulus- or frequency-temperature curves at about 230 °K. This knee is similar to the other one corresponding to the transition from the *glassy* to the *rubber-like* state at higher temperatures ([2,3,17,20,23,24,27,34]). No frequency-dependence of the temperature of the knee has been noticed in the whole frequency range investigated. This would indicate the existence of a second order transition, which cannot be explained by means of an operational stress-strain relation, but is due to an *instability* effect produced by an increase of temperature, according to the qualitative explanations which have been suggested for similar transitions ([2,3]).

2. – Experimental technique.

The apparatus which was originally designed by one of us ([45]) to make dynamic measurements on metals in a wide range of temperatures and fre-

(*) It may be shown that no other physically significant types of relaxation effects exist when the differential operator which gives the simbolic stress-strain relationship is the ratio of two polynomes of the first order.

([44]) P. G. Bordoni: *Suppl. Nuovo Cimento*, **7**, 144 (1950); *Colloque International sur les Ultrasons dans les Gaz et les Liquides*, publié par la Koninklijke Vlaamse Akademie voor Wetenschappen, Letteren en Schone Kunsten van België, Bruxelles (Juni 1951), p. 164.

([45]) P. G. Bordoni: *Nuovo Cimento*, **4**, 177 (1947); *Ric. Scient.*, **18**, 103 (1948).

quencies, and which has been successively improved ([46-49]), has also been found useful in investigating the mechanical behaviour of polymers.

The operation is based on the measurement of the resonant frequencies and of the coefficient of energy dissipation Q^{-1} for a vibrating specimen of the polymer. The driving force is supplied by the electrostatic attraction between the specimen and a small electrode parallel to the vibrating surface and very near to it. The same electrode, connected to a high frequency resonant circuit, is employed to measure the amplitude of the vibrations. A detailed description of the vibration detector and of the subsidiary electrical equipment has been given in previous papers ([45-49]). The surface of the polymer is made electrically conducting by a metal coating; a thin and uniform metallic layer (thickness $\simeq 1.5 \cdot 10^{-2}$ mm) is obtained for instance by spraying the « Silver Print » no. 21-2 of the General Cement Mfg. Co.

A technique of this type has been employed by BACCAREDDA and coworkers ([1-13]) for the measurement of the elastic coefficients and of the energy dissipation in connection with the second order transition points and with the radiation damage in a large number of high polymers. In these investigations the specimens had the shape of cylindrical rods vibrating on their lowest extensional modes. During the measurement the rods were directly supported by the electrode itself, being insulated from it by a thin sheet of mica or cellophane, and the surrounding gas was at atmospheric pressure. As it has been shown ([46]) the additional dissipation due to the mechanical contact between the specimen and the electrode is small, whilst the influence of the surrounding air is somewhat larger (*). The total additional dissipation for a polymer rod vibrating with a frequency of the order of 10 kHz may correspond to a Q^{-1} of the order of $10^{-3} \div 10^{-4}$. In many cases the internal energy dissipation of polymers is much larger than this value, and the additional dissipation due to the contact with the electrode and to the surrounding air may be neglected.

This is not the case with the present measurements, as the value of Q^{-1} due to the internal dissipation in PMMA is smaller than 10^{-3} at the lowest temperatures which have been attained. The measurements have been made in an evacuated container, in which the pressure of the gas was of the order of a few microns Hg, and therefore the influence of the gas was negligible.

The specimens employed have the shape of circular plates vibrating on their lowest flexural symmetrical modes, with nodal circles and no nodal dia-

---

([46]) P. G. BORDONI and M. NUOVO: *Acustica*, **4**, 184 (1954); *Ric. Scient.*, **24**, 560 (1954).

([47]) P. G. BORDONI and M. NUOVO: *Acustica*, **7**, 1 (1957); *Ric. Scient.*, **27**, 695 (1958).

([48]) P. G. BORDONI, M. NUOVO and L. VERDINI: *Nuovo Cimento*, **14**, 273 (1959).

([49]) M. NUOVO: *Mesures dynamiques de constantes élastiques et anélastiques*, in *Nuovo Cimento* (to be published).

(*) For a metal rod the total additional dissipation corresponds to $Q^{-1} \simeq 20 \cdot 10^{-5}$ at 760 mm Hg, and $\simeq 2 \cdot 10^{-5}$ at 10^{-1} mm Hg, if the frequency of vibration is $\geqslant 10$ kHz.

meters. One of the main advantages of plates over specimens with other shapes is the larger vibration amplitude which is obtained for a given frequency and a given vibromotive force ([48]). It may be added that it is quite easy to support a circular plate without perturbing its vibrations by means of three pins located in small holes on a nodal circle ([48]) as it is shown in Fig. 1. Two of these pins are made out of copper and constantan wires and are employed as a thermocouple to measure the temperature of the plate; the experiment shows that the measurements made with this kind of « *broken* » thermocouple give the *actual* temperature of the plate within $\pm$ 0.2 °K, being not appreciably affected by the rate of temperature changes, or by the nature of the metal coating ([48]).

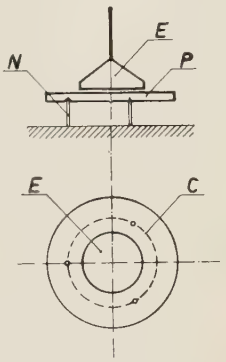

Fig. 1. – Vibrating plate *P*, supported by the three pins *N*; *C*, nodal circle; *E*, electrode.

Another advantage of the use of vibrating plates is that it is easy to keep them parallel to an electrode which does not touch the specimen (Fig. 1) even when the temperature is varied in a wide range and the supporting device is exposed to accidental vibrations.

The rate of the temperature changes of the specimen is easily controlled by varying the pressure inside the container. During the cooling or heating process, the exchange gas filling the container (helium or nitrogen) is kept at a pressure of about 1 mm Hg in order to increase the heat exchanges with the plate. The pressure is reduced to about 10^{-3} mm Hg during the measurements, not only to reduce the additional dissipation, as it has been already explained, but also to reduce the heat exchanges and to make the temperature variations of the specimen very slow in comparison with the time required by the measure of the resonant frequency and of the energy dissipation. In this way a whole run from room temperature down to the boiling point of nitrogen (77 °K) does not require more than five hours. A slow refrigeration of the specimen and of its container is obtained by adding small amounts of liquid nitrogen into the cylindrical Dewar flask at regular time intervals, and keeping a temperature difference of about 20 °K between the plate and the container. Measurements are also made while the plate is heating up; to this purpose an electrical heater is applied to the metal container.

Temperatures below 77 °K are reached by pumping the liquid nitrogen contained in the Dewar flask by means of a high speed rotary pump.

The resonant frequency is measured by means of a quartz-controlled electronic counter (Hewlett Packard, type 521 CR). The accuracy of the measurement is generally limited by the sharpness of the mechanical resonance of the specimen, being not better than the larger of the following values: a few units $10^{-1} \cdot Q^{-1}$ or a few units 10^{-5}.

The coefficient of energy dissipation Q^{-1} is directly measured from the width of the resonance curve. In this case the accuracy is limited by the measurement of the maximum amplitude at the resonance and of the two side measurements at $1/\sqrt{2}$ of the maximum amplitude. The average error affecting Q^{-1} is of the order of 10^{-2} of its value.

3. – Experimental results.

The circular plates have been machined out from sheets of « Perspex » produced by the Imperial Chemical Industries, both of the *plasticized* and *unplasti-*

TABLE I. – *Characteristics of the specimens.*

	Specimen	Mechanical and thermal treatments	Size		No. of nodal circles	Frequency at 293 °K (kHz)	Q^{-1} at 293 °K
			diameter (mm)	thickness (mm)			
Plasticized	1	(*a*) Machined from a sheet of the same thickness (*b*) Silver coated	36.0	4.01	1	11.04	$2100 \cdot 10^{-5}$
					2	39.22	2300
		(*c*) Reduced in diameter (*d*) Silver coated	25.0	4.01	1	21.18	2100
	2	(*a*) Machined from a sheet of the same thickness (*b*) Silver coated	25.0	1.16	1	7.250	2630
Unplasticized	3	(*a*) Machined from a sheet of the same thickness (*b*) Silver coated	36.0	2.00	1	5.900	2660
		(*c*) Heated at 50 °C for 4 h, in vacuum			1	5.930	2600
	4	(*a*) Machined from a sheet of the same thickness (*b*) Silver coated	25.0	0.91	1	5.530	2680
	5	(*a*) Machined from a sheet of the same thickness (*b*) Permanently strained in a hydraulic press (*c*) Reduced in diameter (*d*) Silver coated	24.9	0.91	1	5.950	2680

cized type, without changing the original thickness of the sheets. The characteristics of the specimens are listed in Table I, together with the thermal and mechanical treatments undergone by the material. In the same Table are also given the values of the resonant frequencies and the corresponding dissipation coefficients measured at room temperature.

The resonant frequencies and the dissipation coefficients have been measured in the temperature range between 60 °K and 300 °K. A typical dissipation-temperature curve (Fig. 2, specimen no. 1 (*b*), lowest mode) shows

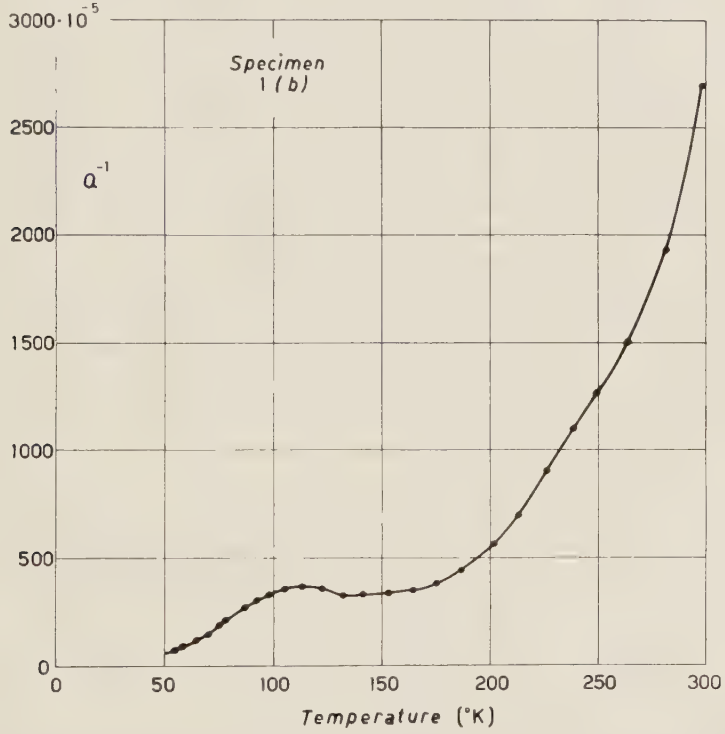

Fig. 2. – Dissipation-temperature curve for the specimen no. 1 after the treatment (*b*) (see Table I); fundamental vibration mode with one nodal circle; resonant frequency at the temperature of the peak: 12.88 kHz.

a gradual increase of the dissipation coefficient with temperature in addition to a small peak at a temperature of about 110 °K. When the vibration frequency of the same specimen is increased by repeating the measurements on the second vibration mode, the general behaviour of the dissipation-temperature curve is essentially unchanged, but the temperature of the superposed peak is higher (Fig. 3). If the values of Q^{-1} are plotted in a logarithmic scale

against T^{-1}, one finds that the gradual increase of dissipation in the high temperature range (200 ° ÷ 300 °K) follows an exponential law of the type

$$Q^{-1}(T) = Q_0^{-1} \exp\left[-\frac{H}{kT}\right], \tag{1}$$

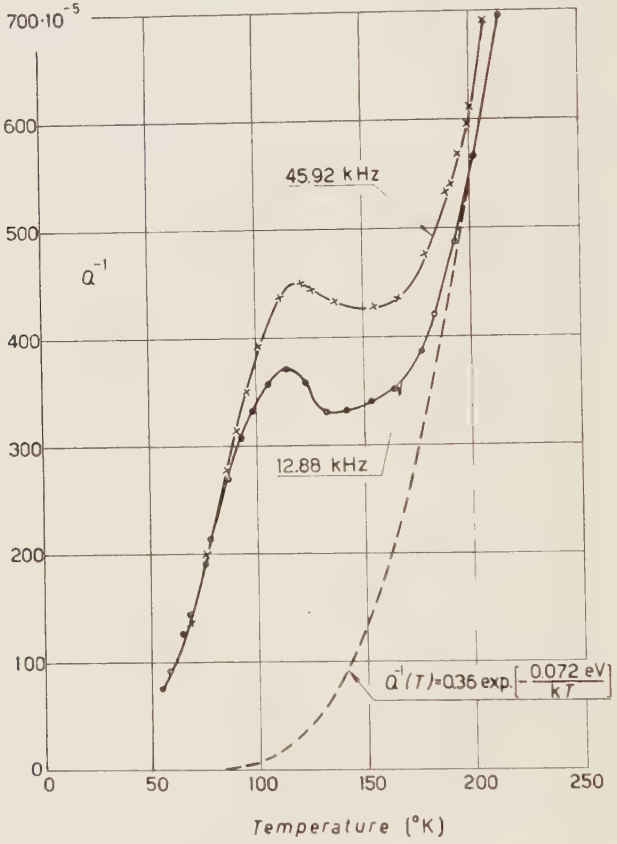

Fig. 3. Solid lines: frequency-dependence of the temperature of the dissipation peak for the specimen no. 1 after the treatment (*b*) (see Table I); dotted line: extrapolated values of the exponential part of the dissipation curve. The resonant frequencies correspond to the temperature of the peak.

where Q_0^{-1} is the limiting value of the dissipation coefficient for very high temperatures; H is the activation energy of the process which gives rise to this part of the energy dissipation; k is the Boltzmann's constant ($8.617 \cdot 10^{-5}$ eV °K^{-1}) and T is the absolute temperature. In the case of Fig. 3 the same value of the activation energy $H = 0.072$ eV (1660 cal mole^{-1}) is found for the high temperature part of the two experimental curves.

The dissipation peak may be separated from the exponential part of the curve by subtracting from the experimental data the values computed by means of eq. (1), and taking for H and Q_0^{-1} the values given in Table II.

TABLE II. – *Fundamental parameters of the exponential part of the dissipation-temperature curve.*

Specimen	Last treatment	Frequency at 293 °K (kHz)	H (eV)	Q_0^{-1}	Q^{-1} at 200 °K
3	(*b*)	5.900	0.070	$34 \cdot 10^{-2}$	$575 \cdot 10^{-5}$
2	(*b*)	7.250	0.076	51	625
1	(*b*)	11.04	0.072	36	550
	(*d*)	21.18	0.075	40	520
	(*b*)	39.22	0.072	40	610

When this is done (Fig. 4) the frequency dependence of the temperature T_m of the peak is quite evident. The same diagram shows the dissipation peak

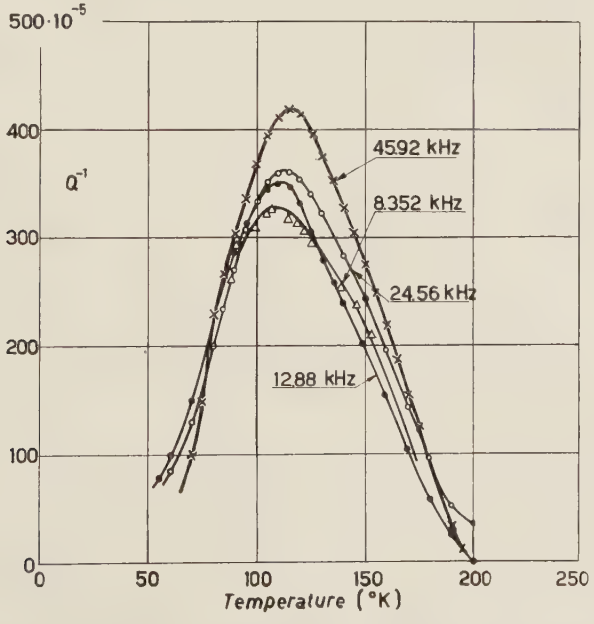

Fig. 4. – Dissipation peak for the specimens no. 1 after the treatments (*b*, and (*d*), and no. 2 after the treatment (*b*) (see Table I); the resonant frequencies correspond to the temperature of the peak.

which has been measured in specimen no. 1 after a reduction of its diameter from 36 mm to 25 mm (Table I).

The same results have been obtained for the plate no. 2 which is made out from a plasticized material, like plate no. 1 (Fig. 4 triangles, and Fig. 5). The value of the activation energy ($H = 0.076$ eV) is very near to the value found for the specimen no. 1, and the same happens with the limiting value of the dissipation coefficient (Table II).

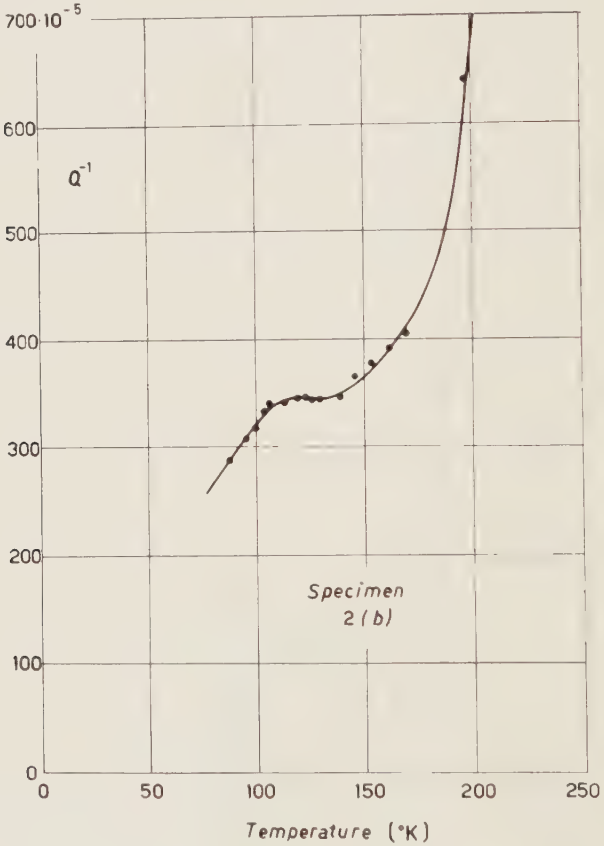

Fig. 5. – Dissipation-temperature curve for the specimen no. 2 after the treatment (*b*) (see Table I); fundamental vibration mode with one nodal circle; resonant frequency at the temperature of the peak: 8.352 kHz.

The height of the low temperature peak and its temperature T_m are both lower than the values found for plate no. 1 (Fig. 4). This agrees with the fact that the fundamental frequency of the specimen no. 2 is lower than the cor-

responding frequency of the latter, and Fig. 4 shows that both the height of the peak and the temperature T_m increase with frequency.

In the *unplasticized* material (specimens no. 3, 4 and 5) the peak is less evident, being reduced to a small « bump » (Fig. 6), while the exponential part of the dissipation is essentially unchanged (Table II).

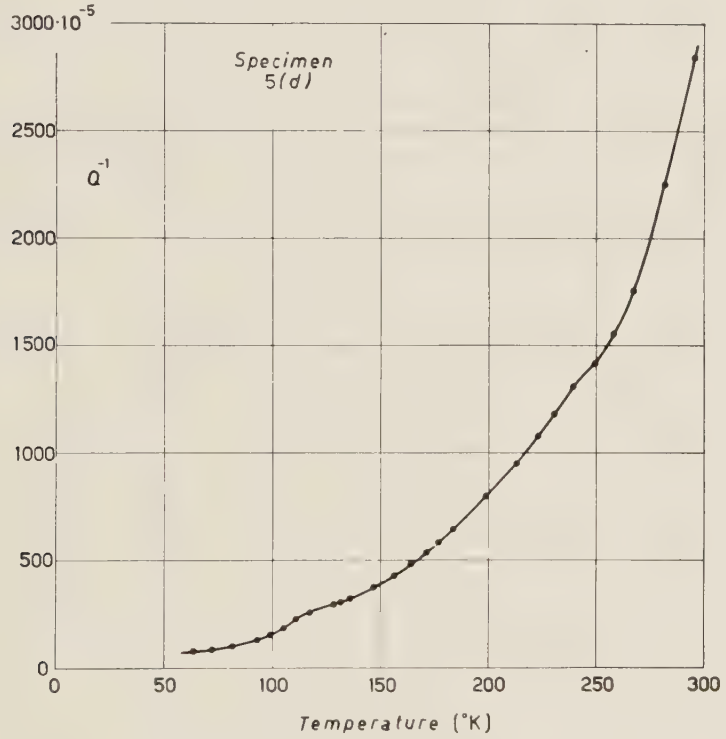

Fig. 6. – Dissipation-temperature curve for the specimen no. 5 after the treatment (*d*) (see Table I); fundamental vibration mode with one nodal circle; resonant frequency at the temperature of the peak: 6.985 kHz.

The influence of thermal and mechanical treatments upon the low temperature peak has been investigated in plate no. 3 which was kept for 4 hours, at 50 °C in an evacuated container, and on plate no. 5 which has been compressed until its diameter has been permanently increased of about 6 %. Both treatments have produced no appreciable change in the dissipation-temperature curve.

The most evident feature of the frequency-temperature curves is the change

of the slope which is observed at about 230 °K (Fig. 7, 8) and which looks like the second-order transition found at about 335 °K ([2,3,17,20,23,24,27,34]).

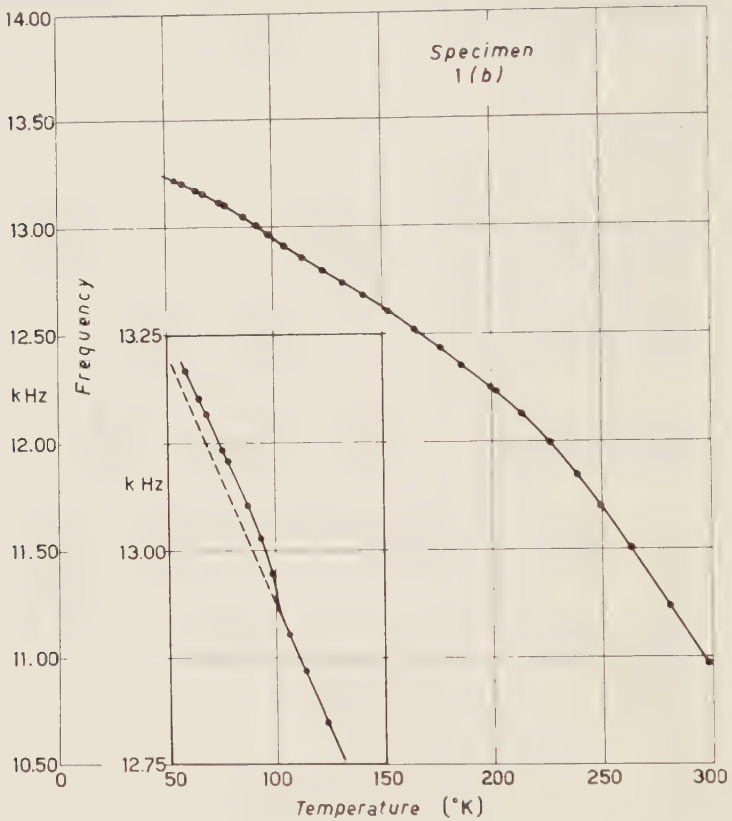

Fig. 7. – Frequency-temperature curve for the specimen no. 1 after the treatment (*d*) (see Table I); fundamental vibration mode with one nodal circle. The enlarged part of the diagram shows the inflexion corresponding to the dissipation peak of Fig. 2, 3 and 4.

In the temperature interval in which the low temperature dissipation peak is observed, an inflexion is superposed to the gradual variation of the frequency with temperature, as it is clearly shown by the enlarged part of the diagram in Fig. 7. This inflexion is hardly noticeable for the plates which have a small dissipation peak (specimens no. 3, 4 and 5, see for instance Fig. 8) whilst the change of slope at 230 °K has about the same value in all the experimental curves and does not seem to be affected by the frequency of measurement.

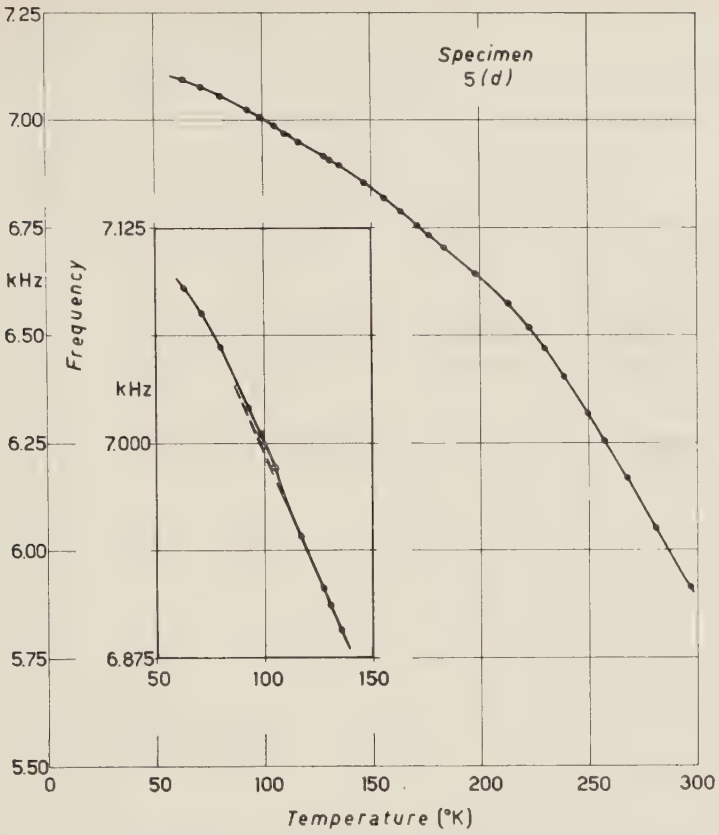

Fig. 8. – Frequency-temperature curve for the specimen no. 5 after the treatment (*d*) (see Table I); fundamental vibration mode with one nodal circle. A slight inflexion is shown in the enlarged part of the diagram.

4. – Discussion.

4·1. *Exponential increase of energy dissipation with temperature.* – The exponential increase of the dissipation coefficient Q^{-1} with T could be ascribed to a thermally activated *total relaxation* effect, of the type which has been illustrated in a previous paper ([44a]). As it has been shown, the relation between the stress $\sigma(t)$ and the strain $\varepsilon(t)$ for an effect of this type is given by

$$\sigma(t) = M_U \frac{\tau p}{1 + \tau p} \varepsilon(t) , \tag{2}$$

where M_U is the *unrelaxed* modulus; τ a characteristic time and p is the symbol of partial derivation with respect to time, $p = \partial/\partial t$.

When the stress and the strain are both sinusoidal functions of time, that is

$$\sigma(t) = \Sigma \exp[j\omega t]\,; \qquad \varepsilon(t) = E \exp[j\omega t]\,, \tag{3}$$

the complex ratio between the amplitudes of stress and strain is given by

$$\frac{\Sigma}{E} = \boldsymbol{M} = M_U \left[\frac{\omega^2\tau^2}{1+\omega^2\tau^2} + j\,\frac{\omega\tau}{1+\omega^2\tau^2}\right]. \tag{4}$$

The dissipation coefficient is given with a good approximation by the ratio of the coefficients of the imaginary and of the real part of $\boldsymbol{M}$ in eq. (4)

$$Q^{-1} = \frac{\mathscr{P}\mathscr{I}[\boldsymbol{M}]}{\mathscr{P}\mathscr{R}[\boldsymbol{M}]} = \frac{1}{\omega\tau}\,. \tag{5}$$

If the characteristic time τ is related to the temperature by an Arrhenius equation

$$\tau = \tau_0 \exp\left[\frac{H}{kT}\right], \tag{6}$$

where τ_0 is the limiting value of the characteristic time for very high temperatures and H is the activation energy, the temperature dependence of Q^{-1} is represented by

$$Q^{-1}(T) = (\omega\tau_0)^{-1} \exp\left[-\frac{H}{kT}\right], \tag{7}$$

in complete agreement with the experimental results, provided the values given in Table II for H and Q_0^{-1} are substituted in (7) to the activation energy and to the product $(\omega\tau_0)^{-1}$ respectively.

The eq. (5) and (7) show that for measurements made at a constant temperature the dissipation coefficient must be inversely proportional to the vibration frequency, and that the same must happen to the limiting value Q_0^{-1}. The inspection of Table II shows that this is not the case; a set of comparable measurements, like those made at different frequencies on the plate no. 1 after the treatment (*b*) and (*d*), exhibit a slight *increase* of Q_0^{-1} with the frequency, instead of a linear *decrease*. The disagreement between the experiment and the theory of total relaxation cannot be eliminated by assuming that the causes of energy dissipation interact between them. As it has been shown (*) in this case the relation between Q_0^{-1} and $1/\omega\tau$ is not linear. However in the pres-

(*) C. CRUSSARD: private communication.

ent case a *negative exponent* would be required for $1/\omega\tau$ to account for the observed dependence of Q_0^{-1} upon the frequency, and this would correspond to a *negative* activation energy, which seems to be devoid of physical significance.

In previous measurements made by PARFITT [16] on polymethyl methacrylate of the unplasticized type, prepared like the present specimens by the Imperial Chemical Industries, a slight *decrease* of the room temperature dissipation was found when the frequency was increased. The exponent of $1/\omega\tau$ in this case would be positive and about 0.14. It must however be observed that the comparison of the dissipation values measured at different frequencies at room temperature is not very significant, as above the room temperature a peak is observed in the dissipation curve between 290 °K and 370 °K [2,23,29,33,35,39]. The dissipation at room temperature is then due to the sum of the « exponential » part and of the dissipation associated with the maximum, and its variations with frequency are rather intricate.

A comparison between dissipation measurements made at frequencies between 0.66 and 10 MHz at room temperature has been made by OTPUSHCHENNIKOV [30], which found that Q^{-1} at room temperature is *proportional* to $\sqrt{\omega}$. A similar *increase* of dissipation with frequency has been found in the same frequency range by MELCHIOR and PETRAUSKAS [20]. However, this increase may be due in part to a diffraction effect, owing to the short wave lengths employed in these measurements.

It may be concluded that the present experimental evidence is not sufficient to individuate the law which relates the exponential part of the dissipation to the frequency of measurements. In any case this law is certainly not a linear relation between Q_0^{-1} and $1/\omega\tau$ as required by the eq. (5) and (7). There is also some evidence that the exponent of $1/\omega$ must be negative. In this case the theory of relaxation must be discarded, as it requires that Q_0^{-1} depends in the same way upon ω and τ, and this would give rise to a *negative* activation energy in the case considered.

When Q_0^{-1} increases slightly with frequency, as in the present measurements, (Table II) while the temperature dependence of the same parameter is given by eq. (1), this means that the temperature is effective in controlling *not* a characteristic time of the effect, but the *total amount* of the anelastic strain. If we assume that this strain is associated with the increase of free space between molecules [8] and with the motion of the side chains, each elementary process associated with a given side chain in a given environment may be pictured as a sudden release of the chain itself, taking place at a temperature which depends essentially on the environment conditions. The time required by the motion of the chain can be considered as almost independent of temperature owing to the character of the process; hence the dissipation coefficient is almost independent of frequency at a fixed temperature. The probability

of finding a released or active side chain increases exponentially in a given temperature interval, and this corresponds to a temperature dependence of the dissipation coefficient of the type of eq. (1).

4·2. *Relaxation effect at low temperature.* – The most important experimental result is the existence of a dissipation peak and of a corresponding inflexion in the frequency-temperature curve. Their simultaneous presence is characteristic of a thermally activated *partial relaxation effect* of the Zener type [42-44] associated with the following stress-strain relation

$$\sigma(t) = M_R \frac{1 + \tau_\sigma p}{1 + \tau_\varepsilon p} \varepsilon(t) , \tag{8}$$

where M_R is the *relaxed* modulus; τ_σ, τ_ε are two characteristic times and $p = \partial/\partial t$.

When stress and strain are both sinusoidal functions of time of the type described by eq. (3), the complex ratio between the amplitudes of stress and strain is given by

$$\frac{\Sigma}{E} = \boldsymbol{M} = M_R \frac{1 + j\omega\tau_\sigma}{1 + j\omega\tau_\varepsilon} . \tag{9}$$

The dissipation coefficient is obtained with a good approximation as in the case of a total relaxation considered above, by computing the ratio of the coefficients of the imaginary and of the real part of $\boldsymbol{M}$ in eq. (9)

$$Q^{-1} = \frac{\Delta M}{M} \frac{\omega\tau}{1 + \omega^2\tau^2} = S \frac{\omega\tau}{1 + \omega^2\tau^2} , \tag{10}$$

where τ, M, ΔM and the relaxation strenght or *modulus defect* S are related to the parameters M_R, τ_σ, τ_ε of eq. (8) and (9) by the following equations

$$\begin{cases} M = \sqrt{M_U M_R} , & M_U = M_R \dfrac{\tau_\sigma}{\tau_\varepsilon} \\ \Delta M = M_U - M_R , & \\ S = \dfrac{\Delta M}{M} , & \tau = \sqrt{\tau_\sigma \tau_\varepsilon} . \end{cases} \tag{11}$$

When the characteristic time depends upon the temperature according to an Arrhenius equation of the type (6), the relation between Q^{-1} and T becomes

$$Q^{-1}(T) = Q_m^{-1} \operatorname{sech} \left[\overline{W} k^{-1} (T_m^{-1} - T^{-1}) \right] , \tag{12}$$

where the activation energy has been denoted by $\overline{W}$ to avoid any confusion with the analogous quantity denoted by H and considered in the previous discussion on the exponential increase of the dissipation with temperature.

Eq. (12) shows the existence of a peak in the dissipation-temperature curve, in agreement with the experimental results. The temperature T_m of the peak is obtained from the condition $\omega\tau = 1$ which corresponds to the maximum dissipation according to eq. (10). Making use of the Arrhenius equation and of this condition, the value of T_m is given by

$$(13) \qquad T_m^{-1} = -\frac{k}{\overline{W}} \ln (2\pi f_m \overline{\tau}_0) ,$$

as in every case it is: $2\pi f_m \overline{\tau}_0 < 1$. According to (13) the temperature of the peak increases with the logarithm of the vibration frequency. When the experimental values of $k \ln f_m$ are plotted against T_m^{-1} the experimental points fall on a straight line (Fig. 9) whose slope gives the activation energy $\overline{W}$, while the limiting value of the characteristic time $\overline{\tau}_0$ may be computed from the intercept of the same line with the frequency axis.

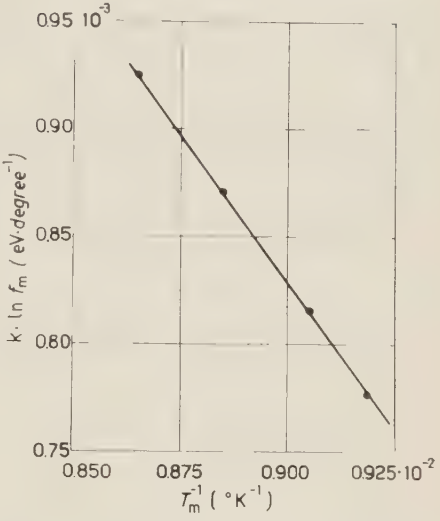

Fig. 9. – Relation between the frequency f_m and the temperature T_m of the dissipation peak for the specimens no. 1 after the treatments (*b*) and (*d*), and no. 2 after the treatment (*b*) (see Tables I and III).

TABLE III. – *Frequency, temperature and height of the dissipation peak.*

Specimen	f_m (Hz)	$k \ln f_m$ (eV · °K^{-1})	T_m (°K)	T_m^{-1} (°K^{-1})	Q_m^{-1} (*)
2 (*b*)	$8.352 \cdot 10^3$	$0.7779 \cdot 10^{-3}$	108.7	$0.918 \cdot 10^{-2}$	$327 \cdot 10^{-5}$
1 (*b*)	12.88	0.8155	110.5	0.905	350
1 (*d*)	24.56	0.8710	113.0	0.885	363
1 (*b*)	45.92	0.9248	115.5	0.865	420

(*) The values of Q_m^{-1} have been computed subtracting from the experimental data the exponential part of the dissipation curve.

The values of f_m, T_m and the corresponding dissipation Q_m^{-1} are listed in Table III. The values of the activation energy and of the limiting time computed from Fig. 9 are

$$(14) \qquad \begin{cases} \overline{W} = (0.273 \pm 0.004)\ \text{eV}\ , \\ \overline{\tau}_0 = 4.3 \cdot 10^{-18}\ \text{s}\ . \end{cases}$$

It may be observed that the value of $\overline{\tau}_0$ is smaller than the period of the highest mechanical vibrations which can propagate through a lattice, according to the Brillouin theory ([50]). The difficulty is only apparent as it must be remembered that $\overline{\tau}_0$ is a limit in the mathematical sense of the characteristic time for very high temperatures. When the value of $\overline{\tau}_0$ is computed for the highest temperatures that the PMMA can stand without changing its structure, the values found are of the order of 10^{-13} s, which are consistent with the present theories for the vibrations of solids.

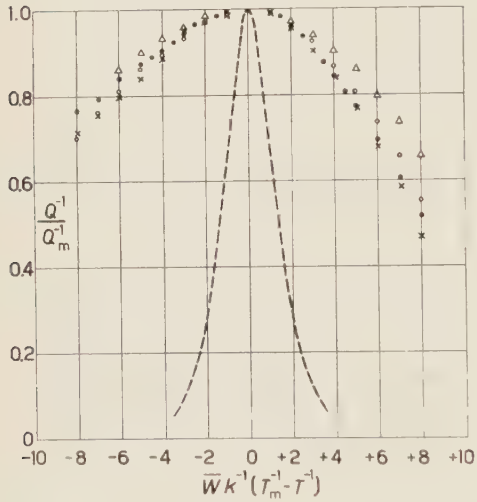

Fig. 10. – Normalized values Q^{-1}/Q_m^{-1} of the dissipation coefficient as a function of the *universal* variable $\overline{W}k^{-1}(T_m^{-1} - T^{-1})$; ●, specimen no. 1 (*b*), 12.88 kHz; ○, specimen no. 1 (*d*), 24.56 kHz; ×, specimen no. 1 (*b*), 45.92 kHz; △, specimen no. 2 (*b*), 8.352 kHz; dotted line, Zener's dissipation curve for a single relaxation time.

As it has been shown elsewhere ([48,51]) when the experimental values of the ratio Q^{-1}/Q_m^{-1} are plotted against the *universal* variable $\overline{W} \cdot k^{-1}(T_m^{-1} - T^{-1})$, the experimental points (*) must fall on the same curve, which does not depend upon the frequency of the measurements and whose equation is given by (12). When this is done (Fig. 10) the experimental curves are much broader than the theoretical curve (12). This result shows that the relaxation

([50]) L. BRILLOUIN: *Wave Propagation in Periodic Structures* (New York, 1946).

([51]) P. G. BORDONI: *Theory of relaxation effects with a continuous spectrum*, in *Proc. of the Third International Congress of Acoustics* (Stuttgart, Sept. 1959; in press); *Sur le calcul des spectres des effects de relaxation activés thermiquement*, in *Colloque sur le frottement intérieur* (Saint Germain en Laye, Oct. 1960).

(*) Of course in this case the values of Q^{-1} and Q_m^{-1} are those related to the effect; these are computed subtracting the exponential part of the dissipation from the measured values, as it is done in Fig. 4 and in Table III.

effect is not associated with a single characteristic time as it is assumed in the simple Zener theory outlined above, but with a whole spectrum of characteristic times. The value (14) computed above for $\bar{\tau}_0$ is the center of the spectrum ([48,51]).

As it has been shown ([51]), no detailed information about the spectrum can be derived from attenuation measurements, owing to their limited resolving power with respect to the spectral lines. The attempts which have been made to *compute* the relaxation spectrum of polyisobutilene ([52,53]) don't rest on a safe mathematical basis, as the same computation method applied to the Zener's curve (12) gives a relaxation spectrum with *negative* components instead of a single relaxation time. Moreover the absolute value of these components *increases* with *increasing approximation*. However some information about the width of the spectrum can be obtained by making use of the Fuoss-Kirkwood theory ([48,54]). According to this theory the single characteristic time τ is substituted by a continuous distribution of relaxation times, whose density with respect to $\ln \tau$ is given by a symmetrical bell-shaped curve. The corresponding dissipation-temperature curve is given by

$$Q^{-1}(T) = Q_m^{-1} \operatorname{sech} [\gamma \overline{W} k^{-1}(T_m^{-1} - T^{-1})] . \tag{15}$$

Eq. (15) differs from the Zener eq. (12) owing to the factor γ which multiplies the independent variable and characterizes the width of the spectrum. For $\gamma = 1$ the spectrum reduces to a single relaxation time (eq. (12)); for $\gamma = 0$ a white-noise spectrum is obtained. The width of the spectrum may be evaluated, as it is done in the theory of elecrical filters, by considering the ratio of the times τ_2 and τ_1 which correspond to a density of $1/\sqrt{2}$ times the maximum density.

The values of the parameter γ obtained from the experimental data and the corresponding logarithmic spectrum width $\ln \tau_2/\tau_1$ are listed in Table IV.

TABLE IV. – *Logarithmic spectrum width according to the Fuoss-Kirkwood approximation.*

Specimen	f_m (kHz)	γ	$\ln (\tau_2/\tau_1)$	τ_2/τ_1
2 (*b*)	8.352	0.113	15.36	$47.0 \cdot 10^5$
1 (*b*)	12.88	0.117	14.30	16.3
1 (*d*)	24.56	0.120	14.26	15.7
1 (*b*)	45.92	0.126	13.54	7.6

([52]) C. ROESLER and W. A. TWYMAN: *Proc. Phys. Soc.*, **68**, 97 (1955).
([53]) F. SCHWARZL: *Kolloid. Zeits.*, **148**, 47 (1956).
([54]) R. M. FUOSS and J. G. KIRKWOOD: *Journ. Chem. Phys.*, **63**, 385 (1941).

The existence of the low-temperature relaxation effect in PMMA was not noticed in the measurements made by BACCAREDDA *et al.* as the temperatures were not low enough ([1,3,8]); the same happens with the work of HEJBOER ([35,41]). In a series of measurements made on different polymers of the methacrylic and cloroacrylic series HOFF *et al.* ([29]) found a relaxation effect in the terms of the series having long and flexible side chains, like the *n*-propyl, *n*-butyl and *sec*-butyl ester polymers, of both series. For a vibration frequency of about 500 Hz the temperature of the peaks is near 120 °K and their activation energies are between 0.15 and 0.25 eV. From their experimental results the authors concluded that no process of this type is apparent in the methyl ester polymers. The process was pictured as a molecular rearrangement in a *limited length* of the side chains. This hypothesis is consistent with the low energy of activation and with the absence of a process of the same order of magnitude in either the methyl or the ethyl esters.

It must be observed that the peaks found by the previous authors are very high, the value of Q_m^{-1} being about $6 \cdot 10^{-2}$, that is more than ten times larger than the peaks of Fig. 4.

In a later experimental work SINNOT ([40]) found a relaxation peak in polyethyl methacrylate, at a temperature of about 40 °K for a vibration frequency of 8 Hz. The activation energy was not measured; the height of the peak is of the order of $1000 \cdot 10^{-5}$ that is much higher than the peaks of Fig. 4. In polymethyl methacrylate for the same vibration frequency no peak was found in the whole temperature range between 4.2 and 100 °K. The peak in the ethyl ester polymer was ascribed to a rearrangement of the side chains, and its absence in the PMMA was explained either by the smallness of the effect, or by a very low value of the temperature of the maximum, which according to the author could fall below 4.2 °K.

The extrapolation of the present measurements shows that the first explanation is probably correct. From the value of $\bar{\tau}_0$ and $\overline{W}$, the temperature T_m for a vibration frequency of 8 Hz is about 88 °K, that is well within the range of Sinnot's measurements. However Fig. 4 shows that the height of the peak decreases with the temperature of the maximum, that is with the vibration frequency. When the logarithm of Q_m^{-1} is plotted against T_m^{-1} the experimental values fall on a straight line (Fig. 11). The value of Q_m^{-1} computed according to this graph for the temperature of 88 °K corresponding to the vibration frequency of 8 Hz, is smaller than the dissipation coefficient measured at this temperature by SINNOT, which is about $160 \cdot 10^{-5}$. This may explain why the peak has not been observed by this author.

The above remarks show that the low temperature peak found in PMMA may be due to a rearrangement of the side chains notwithstanding their limited lenght. This assumption is supported by the agreement between the values of the activation energies and of the limiting times of the peak with

those observed by HOFF *et al.* ([29]). The smallness of Q_m^{-1} for PMMA in comparison with the peaks of *n*-propyl and *n*-butyl ester polymers is consistent with the fact that the rearrangement of a short chain gives rise to little addi-

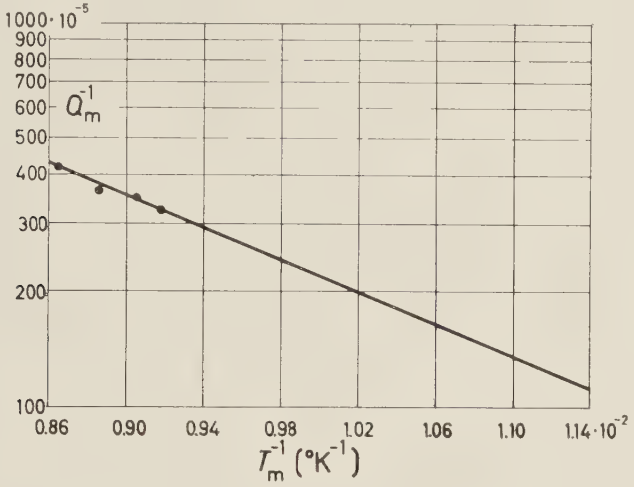

Fig. 11. – Dependence of the height of the dissipation peak upon the value of T_m^{-1}; specimens no. 1 after the treatments (*b*) and (*d*), and no. 2 after the treatment (*b*) (see Table I and Fig. 4).

tional space available to neighbouring chains. On the other hand it must be remembered that the peak is much higher in the plasticized (Fig. 2, 5) than in the unplasticized material (Fig. 6). Hence a more or less direct influence of the plasticizer must be taken into account in the structural model for the relaxation effect (*).

It must be observed that the presence of a peak in the dissipation-temperature curve does not correspond to a *transition* in the polymer as it has been suggested ([23,29,33,39]). It is clear from the eq. (10), (12) and (13) that the temperature T_m of the peak has not an *intrinsic meaning* as it is the case with a *transition temperature*, but depends upon the frequency of measurement.

(*) In a more recent paper SINNOT (*Journ. Pol. Sci.*, **42**, 3 (1960)) announces that, in some measurements to be published, a loss peak has been found in PMMA at 100 °K for a vibration frequency of about 1 Hz. This peak has been attributed to the motion of the main chain methyl groups. A similar explanation could also be given for the peaks observed in the present measurements; however the temperature and the frequency of the Sinnot's peak are not in agreement with the values of $\overline{W}$ and $\overline{\tau}_0$ given by (14). According to these values, the temperature of the peak for a vibration frequency of 1 Hz is about 83 °K.

The theory of the thermally activated relaxation effects with a continuous spectrum, which is summarized in eq. (8)–(15) does not account for all the experimental results, as it does not predict the observed dependence of Q_m^{-1} upon temperature. To the hypothesis of an exponential relation between τ and T^{-1} it is then necessary to add another hypothesis concerning a dependence of the same type of the total relaxation strength $S = \Delta M/M$ upon T^{-1}.

$$S = S_0 \exp\left[-\frac{A}{kT}\right]. \tag{16}$$

In fact, in the case of a single relaxation time, eq. (10) shows that the relaxation strenght equals $2Q_m^{-1}$. When the latter value is substituted to S, eq. (16) represents the observed dependence of the dissipation peak upon temperature. The same happens for a relaxation spectrum of the Fuoss-Kirkwood type, the relation between S and Q_m^{-1} being in this case [48,53]

$$S = \frac{2}{\gamma} Q_m^{-1}. \tag{17}$$

In other words the experimental results point out that a temperature variation has a double effect: it changes not only the characteristic time of the relaxation effect but also the total number of elementary processes involved in the effect. It is remarkable that the activation energy associated with the dependence of Q_m^{-1} upon T^{-1} and computed from Fig. 11 has the value

$$A = 0.037 \text{ eV}, \tag{18}$$

which is very near to one half of the energy H of the exponential increase of dissipation (Table II).

4·3. *Dependence of frequency upon temperature.* – The variation of the slope of the frequency-temperature curves which is observed near 230°K (Fig. 7 and 8) is similar to the second order transition from the *glassy* to the *rubber-like* state which is found in an higher temperature range [1-3,8,17,20,23,24,27,28,34]. The lower transition has not been noticed by the above experimenters either because their temperature range was too narrow or their measurements of frequency were not accurate enough.

The use of the term *transition* seems to be appropriate in the present case as no frequency dependence has been detected for the slope change. This change may be roughly evaluted approximating the frequency-temperature curve by two straight lines on the two sides of the transition temperature, and comparing the « *relative slopes* » of these two lines, that is the value of the

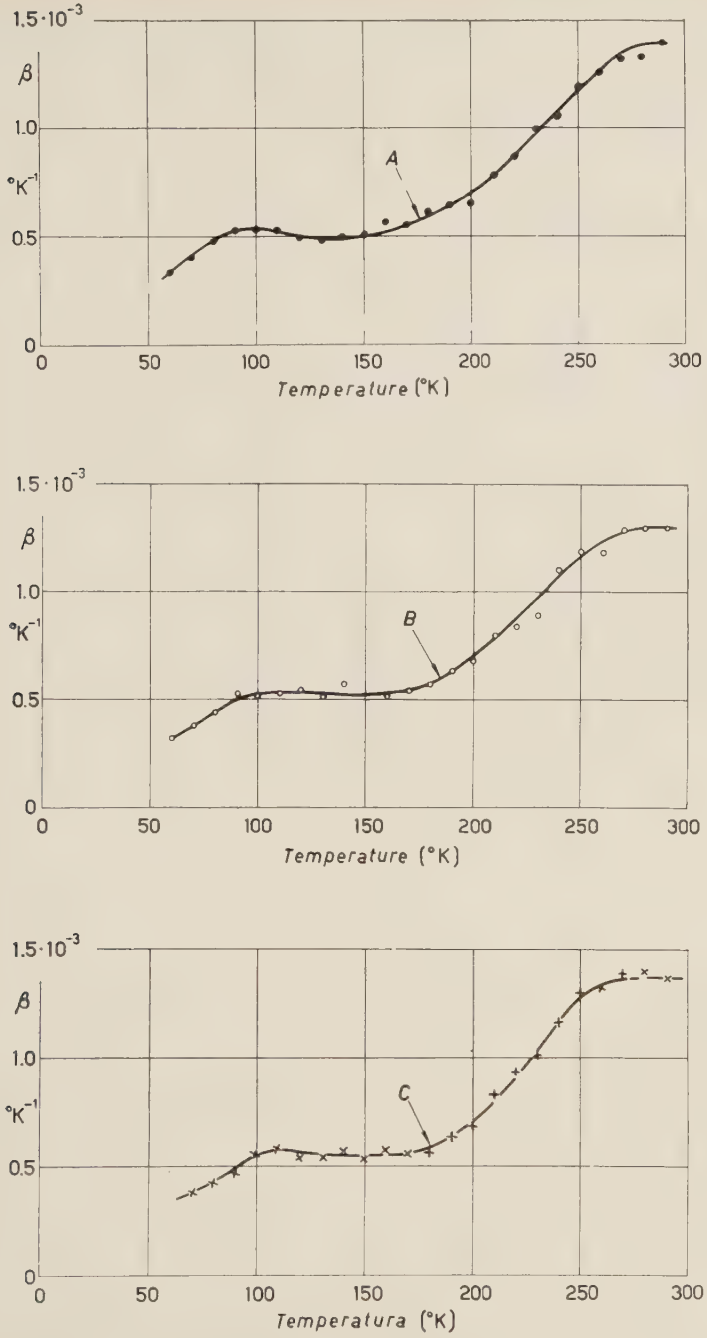

Fig. 12. – Temperature dependence of $\beta = -(\partial \ln f)/\partial T$ for the specimen no. 1 after the treatments (*b*) and (*d*) (see Table I); vibration frequencies at room temperature: curve *A*, 11.04 kHz; *B*, 21.18 kHz; *C*, 39.22 kHz.

logarithmic derivative of frequency with respect to temperature $\beta = -\partial \ln f / \partial T$. The following data show that the slope change of the curve at 230 °K is smaller than the corresponding change from the *glassy* to the *rubber-like* state transition in the same material ([3,8]).

Transition at 230 °K	*Transition at* 337 °K
$10^3 \cdot \beta$	$10^3 \cdot \beta$
$0.58 \rightarrow 1.35$	$1.50 \rightarrow 6.46$

This difference between the two transitions may explain why no appreciable change in the exponential part of the dissipation is found for the low-temperature transition (Fig. 2, 6) whilst for the glass-rubber transition BUTTA ([8]) found a large change in the activation energy associated with the exponential part of the dissipation. A value of 0.066 eV was found below the transition temperature T_g in agreement with the data of Table II for the same temperature range. Above T_g the same author found an energy of 0.284 eV. It may be added that for the low temperature transition a small bump is noticed in the dissipation-temperature curves (Fig. 2 and 6) near 230 °K. However this deviation from the exponential law is too small to make possible a determination of its dependence upon frequency and may eventually mask a slight change in the characteristic exponent of the dissipation.

Some additional light is thrown on the 230 °K transition by the curves of Fig. 12 which show the temperature dependence of β for three different vibration frequencies of the same plate (specimen no. 1, after the treatment (*b*) and (*d*)). The « *knee* » of the frequency-temperature curve is not very sharp, and a whole *transition region* exists, between 190 °K and 260 °K, in which β is a linear function of the temperature. Within the limits of the accuracy of the measurements and of the computation of β the temperature interval of this region is the same for the three vibration frequencies.

At temperatures below 150 °K a small peak is found in the β-temperature curve, which corresponds to the inflexion of the frequency-temperature curve shown in detail in the enlarged part of the diagrams of Fig. 7 and 8 and is related to the partial relaxation effect according to eq. (9), (10) and (17).

5. – Conclusions.

The dynamic behaviour of polymethyl methacrylate for flexural vibrations in the frequency range from 6 to 40 Hkz, in the temperature interval (60 ÷ 300) K and for strain amplitudes smaller than 10^{-7}, is characterized by a partial relaxation effect superposed to a gradual increase of the energy dis-

sipation with temperature, and by a *knee* in the frequency-temperature curve at about 230 °K.

The temperature dependence of the relaxation effect is somewhat more general than that which has been considered hitherto. In addition to the exponential relationship between the relaxation time and the temperature, which is characteristic of the thermally activated effects, a dependence of the same type has been found between the relaxation strength and the temperature. The analogy with the relaxation effects found in the *n*-propyl and *n*-butyl ester polymers shows that the peak of PMMA may be due to a rearrangement of the side chains.

The gradual increase of dissipation with temperature follows an exponential law, but does not seem to be due to a *total relaxation effect*, as the dissipation *increases* slightly with the vibration frequency. In this case the temperature seems to be effective in controlling not the characteristic *time*, but the *number* of the elementary processes which give rise to the anelastic strain and to the energy dissipation.

The knee in the frequency-temperature curve corresponds to a temperature interval in which the coefficient $\beta = -\partial \ln f/\partial T$ is a linear function of the temperature. No frequency dependence of this interval has been detected; this would indicate the existence of a second order transition at about 300 °K. If this is the case, a corresponding knee must be found in the curves which give the length of the specimen as a function of temperature.

RIASSUNTO

La frequenza di risonanza ed il coefficiente di dissipazione Q^{-1} dell'energia elastica sono stati misurati su alcune piastre circolari di polimetilmetacrilato, sia del tipo plastificato, sia prive di plastificante. Le misure sono state effettuate in funzione della temperatura nell'intervallo (60 ÷ 300) °K, per frequenze comprese tra 6 e 40 kHz, mediante vibrazioni flessionali e con coefficienti di deformazione non superiori a 10^{-7}. Un effetto di rilassamento attivato termicamente produce un massimo nella curva dissipazione-temperatura a circa 110 °K, e nello stesso tempo dà luogo ad una leggera inflessione della curva frequenza-temperatura, come è previsto dalla teoria delle deformazioni lineari dinamiche. Questo effetto è probabilmente dovuto ad un riassestamento delle catene laterali. Esso si sovrappone ad un'altra causa di dissipazione dell'energia elastica, la quale non rientra tra quelle considerate attualmente dalla teoria delle deformazioni dinamiche, in quanto produce una dissipazione che aumenta sia con la temperatura, sia, in misura minore, con la frequenza. Ad una temperatura di circa 230 °K la curva frequenza-temperatura forma un *gomito* che sembra dovuto ad una transizione di seconda specie poichè la sua temperatura appare indipendente dalla frequenza di misura.

On the Physical Interpretation of Complex Poles of the S-Matrix – II.

H. M. Nussenzveig

Centro Brasileiro de Pesquisas Físicas - Rio de Janeiro

(ricevuto il 21 Febbraio 1961)

Summary. — The initial-value problem for a Schrödinger particle interacting with a partially transparent sphere (δ-function potential) is solved by an extension of the method described in Part I [1]. The general solution is expanded in terms of the propagators of transient modes. The relation between this expansion and the stationary-state expansion for an impenetrable sphere is discussed. Two special cases are considered: the decay of a wave packet initially confined within the sphere and the scattering of a wave packet by the sphere in the case of a sharp resonance. In the decay problem, the domain of validity of the exponential law and the deviations from this law are investigated. In the resonance scattering problem, the behaviour of the solution in the internal and external regions as a function of the width of the excitation is discussed. The concept of time delay at resonance is analysed.

1. – Introduction.

In the first part of this paper [1] (hereafter referred to as I), the connection between the transient behaviour of a system and the poles of the associated S-matrix was investigated by means of some examples. It was shown in these examples that the general solution of the initial-value problem can be expanded in terms of propagators of transient modes, which are associated with the poles of the S-matrix. This eliminates the difficulties that occur in the usual treatment by the method of complex eigenvalues.

[1] G. Beck and H. M. Nussenzveig: *Nuovo Cimento*, **16**, 416 (1960).

The examples treated in I had some restrictive features in common. They gave rise only to short-lived transient modes, whereas the case of long-lived modes is of greater physical importance. Furthermore, in each example, the S-matrix had only a finite number of poles for given angular momentum. In order to extend the treatment to the interaction of non-relativistic particles with an arbitrary potential of finite range, it is necessary to overcome this limitation, since the S-matrix then has an infinite number of poles for each value of the angular momentum ([2]).

In the present work, the treatment will be extended to an example which does not suffer from either of the above limitations. We shall consider the initial-value problem for a Schrödinger particle interacting with a partially transparent sphere. The transparency of the sphere can be adjusted to obtain transient modes of arbitrarily long lifetimes. In the limiting case of an impenetrable sphere, the modes go over into the stationary states of a particle in a spherical box with impenetrable walls.

By suitably specializing the initial conditions, one can describe either the decay of a wave packet initially confined within the sphere or the scattering of a wave packet by the sphere. A different treatment of the decay problem for the same model has been given by PETZOLD ([3]).

The transient-mode expansion for an infinite number of poles is obtained by means of a Mittag-Leffler expansion. Such an expansion has been employed in electric circuit theory ([4]), and it has been shown that it can be applied to an arbitrary potential of finite range in stationary scattering theory ([5,6]). In this way, the treatment given in I can be extended to the interaction of Schrödinger particles with an arbitrary potential of finite range. It has been found more instructive, however, to consider in detail an explicit example such as the present one.

In Section **2**, the general solution of the initial-value problem for s-waves and its expansion in transient modes will be derived. The relation between the transient-mode expansion and the stationary-state expansion for an impenetrable sphere will be investigated. It will be shown that the transient-mode expansion behaves like the stationary-state expansion for large times, but it gives a better description of the early stages of propagation within the sphere.

In Section **3**, the solution will be specialized to the case of decay. The asymptotic form of the decay law and the domain of validity of the exponential law will be discussed.

([2]) T. REGGE: *Nuovo Cimento*, **8**, 671 (1958).
([3]) J. PETZOLD: *Zeits. Phys.*, **155**, 422 (1959).
([4]) B. GROSS: *Suppl. Nuovo Cimento*, **3**, 235 (1956).
([5]) J. HUMBLET: *Mém. in-8° Soc. Roy. Sci. Liège*, **12**, n. 4 (1952).
([6]) V. I. SERDOBOLSKII: *Sov. Phys. J.E.T.P.*, **9** (36), 1354 (1959).

In Section 4, the resonance scattering problem will be considered. The behaviour of the solution in the internal and external regions and its dependence on the width of the excitation will be examined. The relation between the results and the concept of time delay at resonance will be discussed.

2. – General solution of the initial-value problem.

2·1. *The propagators.* – We shall be concerned with the initial-value problem for the s-wave Schrödinger equation (in units $\hbar = m = 1$) associated with the central potential $V(r) = \frac{1}{2}(A/a)\,\delta(r-a)$ $(A > 0)$, which describes a penetrable sphere of radius a. In the above units, A is a dimensionless parameter, which measures the opacity of the sphere.

We denote by indices 1 and 2 the interior and the exterior of the sphere, respectively, and introduce corresponding radial functions $\varphi_j(r, t) = r\psi_j(r, t)$ $(j = 1, 2)$. The problem is then equivalent to the solution of the free-particle Schrödinger equations

$$\left(\frac{\partial^2}{\partial r^2} + 2i\,\frac{\partial}{\partial t}\right)\varphi_j(r, t) = 0\,, \tag{1}$$

subject to the boundary conditions

$$\varphi_1(0, t) = 0\,, \tag{2}$$

$$\varphi_1(a, t) = \varphi_2(a, t)\,, \tag{3}$$

$$\frac{\partial\varphi_2}{\partial r}(a, t) - \frac{\partial\varphi_1}{\partial r}(a, t) = \frac{A}{a}\,\varphi_2(a, t)\,, \tag{4}$$

and the initial conditions

$$\varphi_j(r, 0) = f_j(r)\,. \tag{5}$$

We want to express the general solution in terms of propagators:

$$\varphi_j(r, t) = \int_0^a G_{j1}(r, \varrho, t)\, f_1(\varrho)\,\mathrm{d}\varrho + \int_a^\infty G_{j2}(r, \varrho, t) f_2(\varrho)\,\mathrm{d}\varrho\,. \tag{6}$$

For this purpose, in accordance with the method employed in I, we write down the general solutions of (1)

$$\varphi_j(r, t) = \int_{-\infty}^{\infty} U(\varrho, t)\,\chi_j(r - \varrho)\,\mathrm{d}\varrho\,, \tag{7}$$

where

$$U(r, t) = \exp[-i\pi/4](2\pi t)^{-\frac{1}{2}} \exp[ir^2/2t] . \tag{8}$$

The initial conditions give $\chi_1(\varrho) = f_1(\varrho)$ $(0 \leqslant \varrho \leqslant a)$; $\chi_2(\varrho) = f_2(\varrho)$ $(\varrho \geqslant a)$, and (2) implies $\chi_1(-\varrho) = -\chi_1(\varrho)$, so that the unknown functions in (7) are $\chi_1(a+\varrho)$ and $\chi_2(a-\varrho)$ for $\varrho > 0$. They are determined by conditions (3) and (4), which can be solved by the Laplace transformation method (cf. I).

Let $X_1(p)$, $X_2(p)$, $F_1(p)$ and $F_2(p)$ denote the Laplace transforms of $\chi_1(a+\varrho)$, $\chi_2(a-\varrho)$, $H(a-\varrho)f_1(a-\varrho)$ and $f_2(a+\varrho)$, respectively, where $H(t)$ is Heaviside's step function. The Laplace transforms of (3) and (4) become

$$[1 - \exp(-2ap)]X_1(p) - X_2(p) = -[F_1(p) - \exp(-2ap)F_1(-p)] + F_2(p) ,$$

$$p[1 + \exp(-2ap)]X_1(p) + \left(p + \frac{A}{a}\right) X_2(p) =$$

$$= p[F_1(p) - \exp(-2ap)F_1(-p)] + \left(p - \frac{A}{a}\right) F_2(p) .$$

Solving these equations for X_1 and X_2, applying the inverse Laplace transformation and substituting the results in (7), we are led to the following expressions for the propagators defined in (6):

$$G_{11}(r, \varrho, t) = G_1(x, t) - G_1(y, t) , \tag{9}$$

where

$$x = |r - \varrho| , \qquad y = r + \varrho , \tag{10}$$

$$G_1(x, t) = U(x,t) + \int_0^\infty [U(2a + x + \xi, t) + U(2a - x + \xi, t)] R_{11}(\xi)\, d\xi ; \tag{11}$$

$$G_{12}(r, \varrho, t) = G(x, t) - G(y, t) = G_{21}(\varrho, r, t) , \tag{12}$$

where

$$G(x, t) = \int_0^\infty U(x + \xi, t) R_{12}(\xi)\, d\xi ; \tag{13}$$

$$G_{22}(r, \varrho, t) = U(x, t) + \int_0^\infty U(y - 2a + \xi, t) R_{22}(\xi)\, d\xi . \tag{14}$$

The functions $R_{jk}(\xi)$ are given by ($\mathscr{L}^{-1}$ denotes the inverse Laplace trans-

form)

$$R_{11}(\xi) = A\,\mathscr{L}^{-1}[Q(2ap)]\,, \tag{15}$$

$$R_{12}(\xi) = 2a\,\mathscr{L}^{-1}[pQ(2ap)]\,, \tag{16}$$

$$R_{22}(\xi) = \mathscr{L}^{-1}\{[(A-2ap)\exp[-2ap]-A]Q(2ap)\} = \\ = -\mathscr{L}^{-1}\{\exp[-2ap]\,S(ip)\}\,, \tag{17}$$

where

$$Q(z) = (A + z - A\exp[-z])^{-1}\,, \tag{18}$$

and

$$S(k) = -Q(-2ika)/Q(2ika) \tag{19}$$

is the S-function (diagonal element of the S-matrix) for s-waves.

2·2. *The poles of the S-matrix.* – The poles of the functions of p appearing in (15) to (17) are related by the transformation $p = -ik$ with the poles of $S(k)$ in the k-plane. The latter are roots of the equation

$$A - 2i\beta - A\exp[2i\beta] = 0\,, \tag{20}$$

where $\beta = ka$. Methods for locating the roots of complex transcendental equations of this type have been given elsewhere (7). Here we shall be interested only in some limiting cases.

For each value of A, there exists an infinite number of poles, all of which are simple and are located in the lower half of the k-plane. The pole distribution is symmetrical with respect to the imaginary axis, so that it suffices to consider the lower right quadrant. There is one pole β_n in each strip $(n-1)\pi < \mathrm{Re}\,\beta < n\pi$ $(n = 1, 2, 3, \ldots)$. When A approaches zero (free particles), β_n approaches $(n - \frac{1}{2})\pi - i\infty$. When A increases, β_n moves upwards and away from the imaginary axis, and $\beta_n \to n\pi$ when $A \to \infty$. In this limiting case, therefore, we get the eigenvalues associated with a particle in a spherical box with impenetrable walls, as ought to be expected.

For given A, the asymptotic behaviour of the pole distribution for large n is given by (7)

$$\beta_n \approx (n - \tfrac{1}{4})\pi - \tfrac{1}{2}i\log[(2n - \tfrac{1}{2})\pi/A] \qquad (n\pi \gg A). \tag{21}$$

We shall be interested mainly in the case $A \gg 1$, in which the lowest-order poles are very close to their limiting values on the real axis. They are then

(7) H. M. NUSSENZVEIG: *Nucl. Phys.*, **11**, 499 (1959).

given by

$$\beta_n = n\pi[1 - (A+1)^{-1}] - i(n\pi/A)^2 + O[(n\pi/A)^3] \qquad (n\pi \ll A). \tag{22}$$

The « lifetime » of the transient mode associated with (22) is

$$\tau_n = \tfrac{1}{2}(n\pi)^{-3}A^2a^2 \,. \tag{23}$$

These long-lived transient modes can be interpreted in terms of multiple-reflection interference effects similar to those which occur in the Fabry-Pérot interferometer. In particular, we have $\tau_n = 2a(v_n\Theta_n)^{-1}$, where v_n is the velocity within the sphere and Θ_n is the transmissivity of the potential.

2·3. *The transient-mode expansion.* – In order to derive the transient-mode expansion of the propagators, we need the Mittag-Leffler expansion of the expressions within brackets in (15) to (17). The Mittag-Leffler expansions associated with R_{11} and R_{12} are derived in the Appendix. If we define

$$b_0 = \tfrac{1}{2}(A/a)(A+1)^{-1}\,; \quad b_n = \tfrac{1}{2}(A/a)(A+1-2i\beta_n)^{-1} \quad (n = \pm 1, \pm 2, ...,); \tag{24}$$

$$c_n = -2i\beta_n b_n/A = -i(\beta_n/a)(A+1-2i\beta_n)^{-1} \qquad (n = \pm 1, \pm 2, ...,), \tag{25}$$

where $\beta_{-n} = -\beta_n^*$, it follows from (15), (16), (A.7) and (A.8) that

$$R_{11}(\xi) = b_0 + \sum b_n \exp[-ik_n\xi] \,, \tag{26}$$

$$R_{12}(\xi) = \tfrac{1}{2}\,\delta(\xi) + \sum c_n \exp[-ik_n\xi] \,, \tag{27}$$

where the terms n and $-n$ must always be taken together in the summations.

Instead of deriving a similar expansion for R_{22}, it is more convenient to express it in terms of R_{12}. It follows from (16) and (17) that

$$R_{22}(\xi) = -\delta(\xi) + R_{12}(\xi) - H(\xi - 2a)\,R_{12}(\xi - 2a) \,. \tag{28}$$

Substituting (26) to (28) into (11), (13) and (14), we find

$$G_1(x,t) = U(x,t) + b_0[M(2a+x,\,0,\,t) + M(2a-x,\,0,\,t)] + \\ + \sum b_n[M(2a+x,\,k_n,\,t) + M(2a-x,\,k_n,\,t)] \,, \tag{29}$$

$$G(x,t) = \tfrac{1}{2}U(x,t) + \sum c_n M(x,k_n,t) \,, \tag{30}$$

$$G_{22}(r,\varrho,t) = U(x,t) - \tfrac{1}{2}[U(y-2a,\,t) + U(y,t)] + \\ + \sum c_n[M(y-2a,\,k_n,\,t) - M(y,\,k_n,\,t)] \,, \tag{31}$$

where

$$M(x, k, t) = \int_{-\infty}^{\infty} H(\xi - x) \exp[ik(x - \xi)]\, U(\xi, t)\, d\xi \tag{32}$$

is the Schrödinger propagator of a transient mode, which was introduced in I. The transient-mode expansion of the propagators is contained in (9), (12) and (29) to (31).

The physical interpretation of $M(x, k, t)$ was discussed in I. It was also shown there that, if A and B denote the regions of the complex plane *above* and *below* the second bisector, respectively, and if

$$w = (2t)^{-\frac{1}{2}}(x - kt)\,, \tag{33}$$

the following asymptotic expansions are valid:

$$M(x, k, t) = M_A(x, k, t) = it(x - kt)^{-1} U(x, t)[1 - \tfrac{1}{2}iw^{-2} - \ldots + (-\tfrac{1}{2}i)^n (2n-1)!!\, w^{-2n} + R_n(w)] \qquad \text{if } w \in A, \tag{34}$$

$$M(x, k, t) = M_B(x, k, t) = \exp[i(kx - Et)] + M_A(x, k, t) \qquad \text{if } w \in B, \tag{35}$$

where $(2n-1)!! = 1 \cdot 3 \cdot 5 \ldots (2n-1)$, $E = \frac{1}{2}k^2$, and

$$|R_n(w)| \leqslant \pi^{\frac{1}{2}} 2^{-n-1} (2n+1)!!\, |w|^{-2n-1} \qquad (n = 0, 1, 2, \ldots). \tag{36}$$

2·4. *The limiting case of an impenetrable sphere.* – Before applying the general solution to the special cases of decay and of resonance scattering, it is instructive to consider the limiting case of an impenetrable sphere. In this limit ($A \to \infty$), (15) becomes

$$R_{11}(\xi) = \mathscr{L}^{-1}\{[1 - \exp[-2ap]]^{-1}\} = \tfrac{1}{2}\,\delta(\xi) + \tfrac{1}{2}a^{-1}[1 + \sum \exp[-ik_n\xi]]\,, \tag{37}$$

where $k_n = n\pi/a$. Substituting this in (11), we get

$$G_1(x, t) = U(x, t) + \tfrac{1}{2}[U(2a + x, t) + U(2a - x, t)] + \tfrac{1}{2}a^{-1}[M(2a + x, 0, t) + M(2a - x, 0, t)] + \tfrac{1}{2}a^{-1} \sum [M(2a + x, k_n, t) + M(2a - x, k_n, t)]\,. \tag{38}$$

It is also possible to expand G_{11} in terms of the stationary states of the

particle within the impenetrable sphere:

$$G_{11}(r, \varrho, t) = 2a^{-1} \sum_{n=1}^{\infty} \sin(k_n r) \sin(k_n \varrho) \exp[-\tfrac{1}{2} i k_n^2 t] .$$

This can be rewritten in the form (9), with (*)

$$G_1(x, t) - \tfrac{1}{2} a^{-1} + a^{-1} \sum_{n=1}^{\infty} \cos(k_n x) \exp[-\tfrac{1}{2} i k_n^2 t] = \frac{1}{2a} \theta\left(\frac{x}{2a} \middle| -\frac{\pi t}{2a^2}\right), \tag{39}$$

where $\theta(x|\tau)$ is the Jacobi θ-function ([8]). If we apply Jacobi's transformation formula ([8])

$$\theta(x|\tau) = (\tau/i)^{-\frac{1}{2}} \exp[-\pi i x^2/\tau] \theta\left(\frac{x}{\tau} \middle| -\frac{1}{\tau}\right), \tag{40}$$

eq. (39) becomes

$$G_1(x, t) = U(x, t) + \sum_{n=1}^{\infty} [U(2na - x, t) + U(2na + x, t)] . \tag{41}$$

Eq. (38), (39) and (41) give three different representations of the same propagator. In the theory of heat conduction, the transformation (40) is employed to transform a series which converges rapidly for large τ (large times) into a series which converges rapidly for small τ (small times) ([8]). A similar result is valid here. The characteristic time interval is $T = 4a^2/\pi$, the period of the ground state.

For $t \gg T$, the contributions from large values of n in the stationary-state expansion (39) oscillate very rapidly, and tend to cancel one another by destructive interference. Thus, the main contribution arises from the lowest values of n. On the other hand, for $t \ll T$, a large number of terms will contribute, so that the convergence becomes very slow.

The expansion (41), when replaced in (9), corresponds to the result which is found by applying the method of images: there is an infinite series of images, corresponding to the successive reflections at $r = 0$ and $r = a$. This series is rapidly convergent for $t \ll T$, on account of the rapid oscillation of the terms with large n. For very short times, the propagator does not differ very much from the free-particle propagator, as ought to be expected. However, for $t \gg T$, the series (41) does not converge well.

(*) The constant term in (39) is arbitrary; the choice was dictated by reasons of convenience.

([8]) A. SOMMERFELD: *Partial Differential Equations in Physics* (New York, 1949), p. 72.

It can be easily shown, with the help of (34) and (35), that the transient-mode expansion (38) behaves like the stationary-state expansion for $t \gg T$, whereas, for $t \ll T$, it is dominated by the free-particle propagator. *Thus, the transient-mode expansion combines the advantages of the stationary-state expansion with those of the expansion by the method of images: it converges well both for small and for large times.* Furthermore, unlike the others, it can still be applied when A has a finite value.

Since each term in the transient-mode expansion approaches the corresponding term in the stationary-state expansion for large t, it is clear that the expansion coefficient will give the probability amplitude associated with the level in question. Thus, in the limiting case of an impenetrable sphere, the transient-mode expansion is closely related with the stationary-state expansion.

3. – The decay problem.

3·1. *Behaviour of the propagators.* – In order to describe the decay of a particle which is initially confined within the sphere, it suffices to specialize the initial conditions (5), by requiring that $f_2(\varrho) = 0$. The behaviour of the solution in regions 1 and 2 is then determined by the propagators G_{11} and G_{21}, respectively.

Let us consider the behaviour of G_{11} as a function of time. We shall be interested only in times much larger than the « period » associated with the lowest transient mode, *i.e.* $t \gg a^2$. Under these conditions, $|w_n| \gg 1$ for all the functions $M(2a \pm x, k_n, t)$ in (29), where w_n is the parameter defined in (33). We can therefore employ the expansions (34) and (35). Denoting by $\sum_A$ the sum over all poles located above the second bisector, we get

$$(42) \qquad G_1(x,t) = U(x,t) + \sum_A b_n \exp[i(k_n x - E_n t)] + \{b_0 M(2a+x,\ 0,\ t) +$$

$$+ it\, U(2a+x,\ t) \sum b_n [(2a+x-k_n t)^{-1} - it(2a+x-k_n t)^{-3} -$$

$$- 3t^2(2a+x-k_n t)^{-5}] + (x \leftrightarrow -x)\} + a^{-1} O[(a^2/t)^3],$$

where the last term in the expression within curly brackets denotes antisymmetrization of the expression with respect to x.

The sum of each of the series that appear within the curly brackets can be explicitly computed by employing the Mittag-Leffler expansions given in the Appendix. For instance, according to (24) and (A.8),

$$\sum b_n(\xi - k_n t)^{-1} = -\tfrac{1}{2} A \{[a(A+1)\xi]^{-1} + 2it^{-1} Q(-2ia\xi/t)\},$$

and the sums of the remaining series follow by repeated differentiation with respect to ξ. The results can then be expanded in powers of $a\xi/t$. Making similar expansions for the other terms of (42), and substituting the results in (9), we finally get, for $t \gg a^2$,

$$(43)\quad G_{11}(r,\varrho,t) = 2a^{-1}\sum_{A}[1-(A+1-2i\beta_n)^{-1}]\sin(k_n\varrho)\sin(k_n r)\exp[-iE_n t] - \\ - (2/\pi)^{\frac{1}{2}}\exp[i\pi/4](A+1)^{-2}\varrho r t^{-\frac{3}{2}} + 2(2/\pi)^{\frac{1}{2}}\exp[-i\pi/4]A(A+1)^{-3}\cdot \\ \cdot\left\{[A-2-\tfrac{1}{3}(1+\tfrac{1}{2}i)(2A-1)A(A+1)^{-1}]a^2 + \tfrac{1}{8}A^{-1}(A+1)(r^2+\varrho^2)\right\}\cdot \\ \cdot\varrho r t^{-\frac{5}{2}} + a^{-1}O[(a^2/t)^3]\,.$$

Each term of the series appearing in (43) decays exponentially (the lifetime of the n-th term is given by (23)). For $t\to\infty$, G_{11} is dominated by the term in $t^{-\frac{3}{2}}$. The same term has been found in reference [3]. The asymptotic decay law is therefore in general (*) an inverse third power law. This agrees with the discussion given in I.

Eq. (43) enables us to obtain the decay law corresponding to a given excitation, for all times $t \gg a^2$. A specific example will be given below.

The propagator G_{21} may be treated in a similar way. Each transient mode $k_n = k_n' - i\varkappa_n$ $(k_n \in A)$ in (30) gives rise to an exponential wave train with a diffuse wave front at $r \approx (k_n' - \varkappa_n)t$, ahead of which the amplitude decreases rapidly (cf. the general discussion in I). Behind the wave front associated with the lowest mode, all the wave trains overlap. For points far behind this wave front $(r \ll k_1' t)$ and times $t \gg a^2$, we find

$$(44)\quad G_{21}(r,\varrho,t) = -2i\sum_{A} c_n \sin(k_n\varrho)\exp[i(k_n r - E_n t)] + \\ + (A+1)^{-1}\left\{1+\frac{i}{3}A(A+1)^{-1}[3A(A+1)^{-1}-2](a^2/t)\right\}[U(r-\varrho,t)-U(r+\varrho,t)] - \\ - iA(A+1)^{-2}(a/t)[(r-\varrho)U(r-\varrho,t)-(r+\varrho)U(r+\varrho,t)] + (aA)^{-1}O[(a^2/t)^2]\,.$$

In the derivation of this result, we have made use of (30), (34), (35) and the Mittag-Leffler expansion (A.7).

The terms of the series that appear in (43) and (44) correspond to the « complex-energy wave functions » which are employed in the method of complex eigenvalues. Each term $\sin(k_n r)$ in (43) corresponds to a term $T_n \exp[ik_n r]$ in (44), where T_n is the « transmission coefficient », given by

$$(45)\qquad T_n = -\beta_n \exp[-2i\beta_n]/A\,.$$

(*) An exception occurs if $f_1(\varrho)$ is chosen orthogonal to ϱ over the interval $(0, a)$.

For $t \gg r^2$, (44) becomes

$$(46) \qquad G_{21}(r, \varrho, t) = -2i \sum_A c_n \sin(k_n \varrho) \exp[i(k_n r - E_n t)] - \\ - (2/\pi)^{\frac{1}{2}} \exp[i\pi/4](A+1)^{-1}[r - A(A+1)^{-1}a]\varrho t^{-\frac{3}{2}} + \ldots$$

and the last term predominates for $t \to \infty$. This term has also been given in reference (3).

3·2. *The decay law.* – In order to investigate the domain of validity of the exponential decay law under the most favourable conditions, let us consider the decay of a long-lived mode, *e.g.* the lowest mode for $A \gg 1$. To concentrate the excitation as much as possible on this mode, we shall choose the initial (unnormalized) wave function (*) $f_1(\varrho) = \sin(k_1 \varrho)$, which corresponds to a « complex resonance ».

Employing (43) and (22), this leads to

$$(47) \qquad \varphi_1(r, t) = [1 - i\pi A^{-2} + O(A^{-3})] \sin(k_1 r) \exp[-iE_1 t] + \\ + \pi^{-\frac{3}{2}} A^{-1}[2^{\frac{1}{2}} \exp[i\pi/4] A^{-1} + \tfrac{4}{3} i(a^2/t)][1 + O(A^{-1})] r a^2 t^{-\frac{3}{2}} + \Delta\varphi_1(r, t) \quad (\text{for } t \gg a^2),$$

where

$$(48) \qquad \Delta\varphi_1(r, t) = \sum_{n=2}^{\infty} [1 - (A + 1 - 2i\beta_n)^{-1}][(\beta_n - \beta_1)^{-1} \sin(\beta_n - \beta_1) - \\ - (\beta_n + \beta_1)^{-1} \sin(\beta_n + \beta_1)] \sin(k_n r) \exp[-iE_n t] + O[(a^2/t)^3] .$$

It follows from (21) and (22) that only modes with $n\pi \ll A$ give an appreciable contribution to (48), so that we may write

$$(49) \qquad \Delta\varphi_1(r, t) \approx 2i\pi A^{-2} \sum_{n=2}^{\bar{n}} (-)^n (n/n+1) \sin(n\pi r/a) \cdot \\ \cdot \exp[-\tfrac{1}{2} i(n\pi/a)^2 t - \tfrac{1}{2} n^3 t/\tau_1] + O[(a^2/t)^3] ,$$

where $\bar{n}$ is such that the contribution from $n \geq \bar{n}$ is negligible ($\bar{n}\pi \ll A$) and τ_1 is the lifetime of the mode $n = 1$, which is given by (23).

According to (47) and (49), there are only very small corrections to the exponential law for $a^2 \ll t \leqslant \tau_1$. For $t \geqslant \tau_1$, the main correction arises from

(*) The choice $f_1(\varrho) = \sin(\pi\varrho/a)$ would lead to amplitudes of the order A^{-1} (instead of A^{-2}) for the higher modes.

the term in $t^{-\frac{3}{2}}$, so that

$$\varphi_1(r,t) \approx \sin(\pi r/a)\exp\left[-\tfrac{1}{2}i(\pi/a)^2 t - \tfrac{1}{2}t/\tau_1\right] - \\ - 2^{\frac{1}{2}}\pi^{-\frac{3}{2}}\exp\left[i\pi/4\right]A^{-2}a^2 r t^{-\frac{3}{2}} \qquad (t \gtrsim \tau_1). \tag{50}$$

The probability that the particle is still confined within the sphere after a time t gives the decay law:

$$P(t) = \left[\int_0^a |f_1(r)|^2\,\mathrm{d}r\right]^{-1}\int_0^a |\varphi_1(r,t)|^2\,\mathrm{d}r\,. \tag{51}$$

According to (50), we get

$$P(t) \simeq \exp\left[-t/\tau_1\right] - (2/\pi)^{\frac{5}{2}}A^{-2}\cos\left(\frac{1}{2}\pi^2 a^{-2}t + \frac{\pi}{4}\right)\exp\left[-\tfrac{1}{2}t/\tau_1\right](a^2/t)^{\frac{3}{2}} + \\ + \tfrac{4}{3}\pi^{-3}A^{-4}(a^2/t)^3\,, \qquad (t \gtrsim \tau_1)\,. \tag{52}$$

The deviations from the exponential law will become important when the first term of (52) becomes of the same order of magnitude as the last one, *i.e.* $\exp[t/\tau_1] \approx (t/\tau_1)^3 A^{10}$, which gives

$$t/\tau_1 \approx 10\log A + 3\log\log A\,. \tag{53}$$

Thus, the t^{-3} law predominates only after the probability that the particle still has not decayed becomes smaller than A^{-10}. This is extremely small for all values of A which correspond to even moderately long-lived modes. In this case, therefore, it seems to be extremely difficult to detect deviations from the exponential law, in the present model. A similar conclusion has been reached by PETZOLD ([3]).

According to KRYLOV and FOCK ([9]), the decay law is entirely determined by the energy spectrum of the initial state. This follows from their definition of the decay law as the probability of finding the system in the initial state at time t, namely, $|(\psi(\boldsymbol{r},t),\psi(\boldsymbol{r},0))|^2$, where $\psi(\boldsymbol{r},t)$ is the normalized wave function. It must be pointed out, however, that this definition, although it would lead to essentially the same results as (51) in the case of (50), becomes inadequate in other cases. For instance, it would imply a definite « decay law » even for a wave packet confined within an impenetrable sphere. The

([9]) N. S. KRYLOV and V. A. FOCK: *Žurn. Èksp. Teor. Fiz.*, **17**, 93 (1947). Cf. also L. A. KHALFIN: *Sov. Phys. J. E. T. P.*, **6**, 1053 (1958), and J. PETZOLD: *Zeits. Phys.*, **157**, 122 (1959).

definition (51) does not suffer from this disadvantage. In the case of non-zero angular momentum, however, due to the presence of the centrifugal barrier, the definition of the decay law requires further consideration.

4. – The resonance scattering problem.

4·1. *Solution in the internal region.* – The general solution derived in Section 2 can also be applied to describe the scattering of an arbitrary initial wave packet by the sphere. In this case, $f_1(\varrho) = 0$ in (6), so that the behaviour of the solution in regions 1 and 2 is determined by the propagators G_{12} and G_{22}, respectively.

We shall consider only the case of a sharp resonance. In order to investigate the effect of the excitation conditions, we shall take an initial wave packet depending on two variable parameters, which correspond to its mean momentum and its width in momentum space. A convenient choice for this purpose is (*)

$$f_2(\varrho) = \exp\left[-ik_0(\varrho - a)\right], \tag{54}$$

where $k_0 = k_0' - i\varkappa_0$ is a complex parameter with negative imaginary part ($\varkappa_0 > 0$).

For definiteness, we shall associate the resonance with the lowest transient mode. Thus, it will be assumed throughout that $|(k_0 - k_1)/k_1| \ll 1$ and $A \gg 1$. For $k_0 = k_1$, we have a « complex resonance ».

Substituting (54) in (6), and taking into account (12) and (30), we find

$$\varphi_1(r, t) = F(r, t) - F(-r, t), \tag{55}$$

where

$$F(r, t) = \tfrac{1}{2}\int_a^\infty U(\varrho - r, t) \exp\left[-ik_0(\varrho - a)\right] \mathrm{d}\varrho + \\ + \sum c_n \int_a^\infty M(\varrho - r, k_n, t) \exp\left[-ik_0(\varrho - a)\right] \mathrm{d}\varrho . \tag{56}$$

(*) For the sake of simplicity, the initial instant is taken to coincide with the time at which the incident wave front impinges on the surface. It would amount to the same to take the initial position of the wave front at any reasonable distance from the sphere (for not too large distances, the spread of the wave packet on its way to the surface can be neglected).

It follows from (32) that

$$(57)\qquad \int_a^\infty U(\varrho - r, t) \exp\left[-ik_0(\varrho - a)\right] \mathrm{d}\varrho = M(a - r, k_0, t)\,,$$

$$(58)\qquad \int_a^\infty M(\varrho - r, k_n, t) \exp\left[-ik_0(\varrho - a)\right] \mathrm{d}\varrho =$$

$$= i(k_0 - k_n)^{-1}\left[M(a - r, k_0, t) - M(a - r, k_n, t)\right], \qquad \text{if } k_0 \neq k_n\,,$$

$$= itU(a - r, t) - (a - r - k_n t)\, M(a - r, k_n, t)\,, \qquad \text{if } k_0 = k_n\,.$$

The last term of (58) appears only at the complex resonance ($k_0 = k_1$). Excluding this case, for the moment, (56) becomes

$$59)\qquad F(r, t) = -2i\beta_0 Q(-2i\beta_0)\, M(a - r,\, k_0,\, t) -$$

$$- i \sum c_n (k_0 - k_n)^{-1} M(a - r,\, k_n,\, t)\,,$$

where $\beta_0 = k_0 a$, and (A.7) has been employed to compute the coefficient of the first term.

Let us investigate the behaviour of (55) for times much larger than the « period » of the lowest mode ($t \gg a^2$). Under these circumstances, the asymptotic expansions (34) and (35) can be employed in (59). The resulting series can be summed with the help of the Appendix, and the results can be expanded in powers of a^2/t (cf. the similar treatment of G_{11} in Section 3·1). Grouping together the first term of (59) and the resonance term ($n = 1$) in the series, and expanding them in powers of $k - k_1$, we finally get

$$(60)\qquad \varphi_1(r, t) = -2i\beta_1 \exp\left[i\beta_1\right](A + 1 - 2i\beta_1)^{-1}\left\{\sin(k_1 r)\, g(k_0, t) +\right.$$

$$\left. + \beta_1^{-1}\left[k_1 r \cos(k_1 r) + \sin(k_1 r)\right] \exp\left[-iE_0 t\right]\right\} + 2i \sum_A{}' \beta_n \exp\left[i\beta_n\right](\beta_0 - \beta_n)^{-1} \cdot$$

$$\cdot (A + 1 - 2i\beta_n)^{-1} \sin(k_n r) \exp\left[-iE_n t\right] + (2/\pi)^{\frac{1}{2}} \exp\left[i\pi/4\right]\beta_1^{-2} \cdot$$

$$\cdot (1 + i\beta_1)(A + 1)^{-1} a^2 r t^{-\frac{3}{2}} + \ldots \qquad (t \gg a^2)\,,$$

where the accent in the summation sign indicates the exclusion of $n = 1$, and

$$(61)\qquad g(k_0, t) = (\beta_0 - \beta_1)^{-1}\left\{\exp\left[-iE_0 t\right] - \exp\left[-iE_1 t\right]\right\} \qquad (k_0 \neq k_1).$$

At the complex resonance, according to (58), (60) is still valid, with

$$(62)\qquad g(k_1, t) = \lim_{k_0 \to k_1} g(k_0, t) = -i(k_1 t/a) \exp\left[-iE_1 t\right].$$

According to (60), the amplitudes of the non-resonant modes are at most of the order of the corresponding transmission coefficients (45), and decrease as they get further away from the resonant mode, on account of the factor $(\beta_0 - \beta_n)^{-1}$. The effect of the resonance is contained in the « amplitude gain factor » $|g(k_0, t)|$, which measures the increase in the amplitude of the mode $n = 1$ due to the resonance.

At the complex resonance, (62) gives

$$|g(k_1, t)| \approx \tfrac{1}{2}(A/\pi)^2 (t/\tau_1) \exp[-\tfrac{1}{2}t/\tau_1] . \tag{63}$$

Thus, the amplitude increases linearly with the time, to begin with, and attains its maximum value $|g|_{max} = e^{-1}(A/\pi)^2$ after a rise time $t = 2\tau_1$; thereafter, it decreases, with a decay time which is also of the order of $2\tau_1$.

Outside of the complex resonance, we have to consider the effect of the displacement of the center of the exciting line (54) and the effect of its width variation. These two effects can be considered separately.

If only the center of the exciting line is shifted, its width remaining the same, we find, as ought to be expected, that this gives rise to « beats » with the difference frequency, and the maximum gain decreases in proportion with the distance from exact resonance.

It is more interesting to consider the effect of the width variation. Let the center of the exciting line be kept at its resonance value, while the width is changed; then, (61) gives

$$|g(k_0, t)| \approx (A/\pi)^2 \left(1 - \frac{\tau_1}{\tau_0}\right)^{-1} \left\{\exp[-\tfrac{1}{2}t/\tau_0] - \exp[-\tfrac{1}{2}t/\tau_1]\right\} , \tag{64}$$

where τ_0 is the « lifetime » associated with the exciting line.

It follows from (64) that, in the case of excitation by a narrow line ($\tau_0 \gg \tau_1$), the rise time and the maximum gain are of the same order as at the complex resonance, whereas the decay time is of the order of $2\tau_0$. On the other hand, for excitation by a broad line ($\tau_0 \ll \tau_1$), the decay time is of the same order as at the complex resonance, but both the rise time and the maximum gain are reduced by a factor of the order of τ_0/τ_1.

The above results can be summed up as follows: *the rise (decay) time is the shorter (longer) of τ_0 and τ_1; the maximum amplitude gain is of the order of $(A/\pi)^2$ times the fraction of the width of the excitation that falls upon the width of the resonant mode.*

4·2. *Solution in the external region.* – It follows from (54), (6), (31), (56), (57) and (59) that

$$\varphi_2(r, t) = \varphi_{2H}(r, t) + \varphi_{2R}(r, t) , \tag{65}$$

where

$$\varphi_{2H}(r, t) = M(a-r, k_0, t) - M(r-a, k_0, t) , \tag{66}$$

$$\varphi_{2R}(r, t) = F(2a-r, t) - F(-r, t) = -2i\beta_0 Q(-2i\beta_0)[M(r-a, k_0, t) - \\ - M(r+a, k_0, t)] - i\sum c_n(k_0-k_n)^{-1}[M(r-a, k_n, t) - M(r+a, k_n, t)] . \tag{67}$$

This corresponds to a decomposition of φ_2 into a « hard-sphere term » φ_{2H} which is identical to the solution for an impenetrable sphere, and a « resonance term » φ_{2R}.

We shall consider only the case of an excitation centered at the resonance momentum but of variable width, *i.e.* $k_0 = k_1' - i\varkappa_0$, where $k_1 = k_1' - i\varkappa_1$. We want to find the shape of the scattered wave at a time t larger than the lifetime $\tau_1 = \frac{1}{2}(k_1'\varkappa_1)^{-1}$, but still much smaller than the « spreading time » $t_s = \\ = \mathrm{Min}(\varkappa_1^{-2}, \varkappa_0^{-2})$, so that the effect of the spreading of the wave packet will be very small. According to (23), this means that (*)

$$A^2 \ll t/a^2 \ll A^4 . \tag{68}$$

The wave front associated with the scattered wave is located at $r-a \approx k_1' t$. Around this wave front, according to the general discussion given in I, there is a domain of width $(2t)^{\frac{1}{2}}$, where « diffraction in time » effects play an important role. We shall consider only the behaviour of the wave function far behind this region, so that

$$\zeta = k_1' t - r \gg t^{\frac{1}{2}} . \tag{69}$$

This allows us to employ the asymptotic expansions (34) and (35), restricting (34) to its first term. Thus, (66) becomes

$$\varphi_{2H}(r, t) = -2i \sin[k_0(r-a)] \exp[-iE_0 t] - \\ - 2it(r-a)[(r-a)^2 - k_0^2 t^2]^{-1} U(r-a, t) + \dots , \tag{70}$$

and (67), with the help of (A.7) and expansion in powers of $k_0 - k_1$, gives

$$\varphi_{2R}(r, t) = f(r, t) + 2i\pi A^{-1} \exp[i(k_0 r - E_0 t)] + \\ + 2i \sum_A{}' \beta_n \sin\beta_n(\beta_0 - \beta_n)^{-1}(A + 1 - 2i\beta_n)^{-1} \exp[i(k_n r - E_n t)] + \\ + 2a(r-a)(r-a-k_0 t)^{-1} Q[-2ia(r-a)/t] U(r-a, t) - \\ - 2a(r+a)(r+a-k_0 t)^{-1} Q[-2ia(r+a)/t] U(r+a, t) + \dots , \tag{71}$$

(*) Notice that $t \ll \varkappa_0^{-2}$ also implies a restriction on the width of the incident wave packet, namely, $\varkappa_0 a \ll (\varkappa_1 a)^{\frac{1}{2}} \approx \pi/A$. We restrict our consideration to wave packets satisfying this condition.

where the accent in the summation sign indicates the exclusion of $n = 1$, and

$$(72) \qquad f(r, t) = 2\varkappa_1(\varkappa_0 - \varkappa_1)^{-1}\left\{\exp[-\varkappa_0\zeta] - \exp[-\varkappa_1\zeta]\right\}\exp[i(k_1'r - \tfrac{1}{2}k_1'^2 t)] .$$

According to (45), $\sin\beta_n = T_n \exp[i\beta_n]$, so that the amplitude of each non-resonant mode in (71) differs from the corresponding amplitude in (60) only by the transmission factor, and is of order A^{-2} for $n\pi \ll A$. Under the assumptions (68) and (69), it can be shown that the dominant term in (71) is $f(r, t)$ (the remaining terms give only small corrections).

Since $f(r, t)$ is the transmitted wave corresponding to the first term of (60), its spatial behaviour is just the transmitted counterpart of the time behaviour within the sphere. The amplitude of the resonance term at a distance ζ behind the wave front corresponds to the amplitude of the resonant mode within the sphere at a time $t = \zeta/k_1'$.

The total outgoing wave, under the above conditions, is given by

$$(73) \qquad \varphi_{2,\,\mathrm{out}}(r, t) \approx \left\{2\varkappa_1(\varkappa_0 - \varkappa_1)^{-1}[\exp[-\varkappa_0\zeta] - \exp[-\varkappa_1\zeta]] + \right.$$
$$\left. + \exp[-\varkappa_0\zeta]\right\}\exp[i(k_1'r - \tfrac{1}{2}k_1'^2 t)] ,$$

where the last term in the curly brackets represents the contribution from hard-sphere scattering.

This result has a simple interpretation in terms of the expansion in stationary scattering states,

$$(74) \qquad \varphi_2 = \varphi_{2,\,\mathrm{in}} + \varphi_{2,\,\mathrm{out}} = -\frac{1}{2\pi i}\int_{-\infty}^{+\infty}\exp[-ik(r-a) - \tfrac{1}{2}ik^2 t]\,\frac{\mathrm{d}k}{(k - k_0)} +$$
$$+ \frac{1}{2\pi i}\int_{-\infty}^{+\infty} S_a(k)\exp[ik(r-a) - \tfrac{1}{2}ik^2 t]\,\frac{\mathrm{d}k}{(k - k_0)} ,$$

where $S_a(k) = \exp[2ika]\,S(k)$, and $S(k)$ is given by (19). It can readily be shown that (73) corresponds to the result which is obtained by taking the *one-level approximation* [10]

$$(75) \qquad S_a(k) = (k - k_1^*)(k - k_1)^{-1} .$$

Thus, under the above conditions, only the immediate neighbourhood of the resonant level gives an appreciable contribution to the integral.

The hard-sphere term in (73) always interferes destructively with the res-

[10] A. M. Lane and R. G. Thomas: *Rev. Mod. Phys.*, **30**, 257, 321 (1958).

onance term. The resulting « absorption dip » in the surface-reflected wave represents the part of the incident wave packet which penetrates within the scatterer to build up the resonant mode.

The absolute values of the factor within curly brackets in (73) and its component terms are plotted as a function of ζ in Fig. 1, in the following cases:

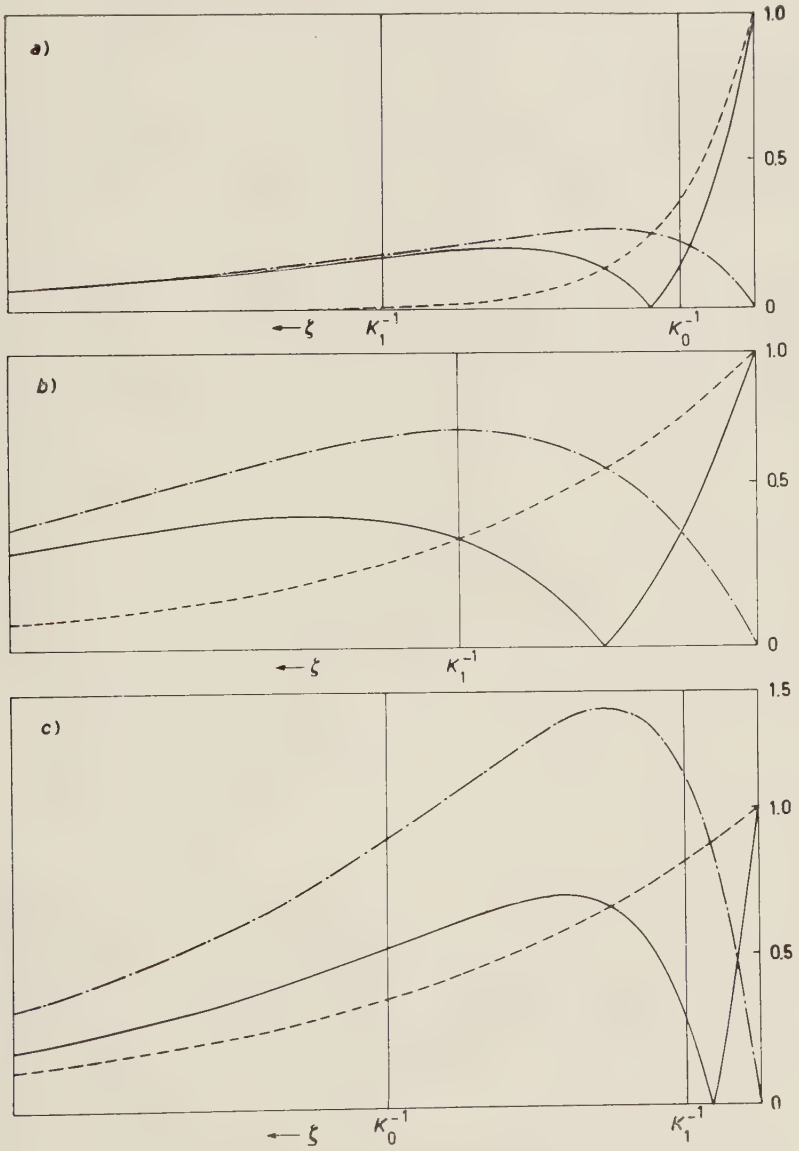

Fig. 1. – Profiles of the hard-sphere term (– – –), the resonance term (—·—·—) and the total outgoing wave (———) as a function of the distance ζ behind the wave front. *a*) $\varkappa_0 = 5\varkappa_1$ (broad line); *b*) $\varkappa_0 = \varkappa_1$ (complex resonance); *c*) $\varkappa_0 = \varkappa_1/5$ (narrow line).

a) broad line ($\varkappa_0 \gg \varkappa_1$); *b*) complex resonance ($\varkappa_0 = \varkappa_1$); *c*) narrow line ($\varkappa_0 \ll \varkappa_1$). The amplitude of the resonance term also represents the behaviour of the resonant mode within the sphere as a function of time.

The curves in Fig. 1 represent probability amplitudes. The corresponding probability distributions can be obtained by squaring them. In all cases, the total outgoing wave consists of a peak due to direct reflection at the surface, followed by a tail which represents the effect of resonance scattering.

4·3. *The time delay.* – According to EISENBUD [11], the energy derivative of the scattering phase shift represents the time delay suffered by the incident wave packet in the scattering process. The retardation suffered by the center of the outgoing wave packet is given by $-2\,\mathrm{d}\eta/\mathrm{d}k$, where $\eta(k)$ is the phase shift.

According to WIGNER [12], this result leads to a simple physical interpretation of the energy dependence of η. At energies for which the incident particle hardly enters the scatterer, the « retardation » will be close to $-2a$ (a being the radius of the scatterer), whereas it will assume large positive values close to resonances, where the incident particle is captured and retained for some time by the scatterer.

In the case of a sharp resonance, where the one-level approximation (75) can be applied, the retardation at resonance is given by $-2/\varkappa_1$, where $\varkappa_1$ is the width of the level in wave-number units. This corresponds to a time delay of twice the lifetime associated with the level. If $\varkappa_0$ is the width of the incident wave packet, it is assumed in this case that $\varkappa_0 \ll \varkappa_1$, so that the variation of $\mathrm{d}\eta/\mathrm{d}k$ over the width $\varkappa_0$ can be neglected.

According to (73) and Fig. 1(*c*), the results which have been found in the present example in the case of a narrow line ($\varkappa_0 \ll \varkappa_1$) are not in agreement with Eisenbud's expression. The « retardation » of the outgoing wave front is $\approx -2a$, and the shape of the outgoing wave packet differs from that of the incident wave, so that a description in terms of a retardation of the center of the wave packet is not appropriate.

The reason for this discrepancy is that the momentum distribution of the incident wave packet (cf. (74)) does not fulfil one of the conditions which are required for the validity of Eisenbud's expression. This condition is that the momentum distribution should go to zero sufficiently rapidly outside of its width $\varkappa_0$. An example is provided by a Gaussian wave packet of width $\varkappa_0$ (*). In this case, the strong surface reflection which was found above disappears, because the internal region is excited adiabatically. The initial excitation

[11] L. EISENBUD: Princeton dissertation, unpublished (1948).

[12] E. P. WIGNER: *Phys. Rev.*, **98**, 145 (1955).

(*) The author wishes to thank Professor E. P. WIGNER for drawing his attention to this point.

within the scatterer does not vanish, but it can be made arbitrarily small by taking the initial position of the center of the wave packet sufficiently far from the scatterer. The outgoing wave packet is also of Gaussian shape, and the retardation of its center is given by Eisenbud's expression.

It should be emphasized, however, that the retardation, under these conditions, is a very small effect. A retardation $\Delta = 2/\varkappa_1$ produces a decrease in the probability density at the unretarded position of the center of the Gaussian wave packet by an amount $1 - \exp[-\varkappa_0^2\Delta^2] \approx 4(\varkappa_0/\varkappa_1)^2$, which is very small for $\varkappa_0 \ll \varkappa_1$.

In order to render the retardation effect more conspicuous, one can try to associate it with a sharper signal. However, this necessarily involves a violation of the requirements for the validity of Eisenbud's expression, as we have seen in the case of an initial wave packet having a sharp front. If one takes an incident wave packet of width $\varkappa_0 \gg \varkappa_1$, so that the corresponding uncertainty in position is much smaller than the retardation in question, Eisenbud's expression cannot be applied, because $d\eta/dk$ varies greatly over the width $\varkappa_0$. As shown in Fig. 1(*a*), the outgoing wave packet then has a tail of small amplitude ($\sim \varkappa_1/\varkappa_0$), which decays with the lifetime of the level, *i.e.* much more slowly than the incident wave. This can also be called a time delay, but it is again a small effect.

* * *

The author is indebted to Professor S. A. Wouthuysen for suggesting the example treated in this paper. He wishes to thank Professor N. G. Van Kampen and Professor G. Beck for valuable discussions, and Professor L. Van Hove for the hospitality of the Institute for Theoretical Physics, Utrecht, where part of this work was done. A fellowship of the National Research Council of Brazil is gratefully acknowledged.

Appendix

The Mittag-Leffler expansions.

We want to find the Mittag-Leffler expansions of $Q(z)$ and of $zQ(z)$, where $Q(z)$ is defined by (18). Let z_n ($n = 1, 2, \ldots$) be the poles of $zQ(z)$ in the lower left quadrant of the z-plane. The poles in the upper left quadrant are $z_{-n} = z_n^*$. The residue at z_n is

$$r_n = z_n(A + 1 + z_n)^{-1}, \tag{A.1}$$

and, according to (21),

$$z_n \approx -\log[(2n - \tfrac{1}{2})\pi/A] - i(2n - \tfrac{1}{2})\pi, \qquad (n\pi \gg A). \tag{A.2}$$

The Mittag-Leffler expansion of $zQ(z)$ can be obtained by applying Cauchy's

method ([13]). For this purpose, consider a sequence of squares C_n with corners at the points $(2n + \frac{1}{2})(\pm 1 \pm i)\pi$. It is easily shown that $zQ(z)$ is bounded on this system of contours taken as a whole. It follows that

$$zQ(z) = \frac{1}{A+1} + \sum r_n \left(\frac{1}{z - z_n} + \frac{1}{z_n} \right), \tag{A.3}$$

where the terms n and $-n$ must be taken together in the summation. According to (A.1) and (A.2), each of the series within brackets is absolutely convergent, so that we may write

$$\frac{1}{A+1} + \sum \frac{r_n}{z_n} = C = zQ(z) - \sum \frac{r_n}{z - z_n}. \tag{A.4}$$

To determine the constant C, add to (A.4) the same equation with z replaced by $-z$. This gives

$$C = \tfrac{1}{2}[zQ(z) - zQ(-z)] - \sum \frac{r_n z_n}{(z^2 - z_n^2)}. \tag{A.5}$$

According to (A.1) and (A.2), the series in (A.5) converges uniformly on the real axis as a whole (which is not true for the series in (A.4)). Therefore, it does not contribute in the limit $z \to \pm\infty$, and we find

$$C = \tfrac{1}{2} \lim_{z \to \pm\infty} [zQ(z) - zQ(-z)] = \tfrac{1}{2}, \tag{A.6}$$

so that the Mittag-Leffler expansion finally becomes

$$zQ(z) = \frac{1}{2} + \sum \frac{r_n}{z - z_n}. \tag{A.7}$$

Dividing both members of (A.3) by z, we obtain the Mittag-Leffler expansion of $Q(z)$:

$$Q(z) = \frac{1}{(A+1)z} + \sum \frac{r_n}{z_n(z - z_n)}. \tag{A.8}$$

([13]) E. C. Titchmarsh: *The Theory of Functions*, 2nd ed. (Oxford, 1939), p. 110.

RIASSUNTO (*)

Il problema del valore iniziale per una particella di Schrödinger, che interagisce con una sfera parzialmente trasparente (potenziale della funzione μ), viene risolto con una estensione del metodo descritto nella prima parte ([1]). La soluzione generale viene sviluppata in termini dei propagatori dello stato stazionario per una sfera impenetrabile. Vengono presi in considerazione due casi speciali: il decadimento di un pacchetto d'onde inizialmente confinato entro la sfera e lo scattering di un pacchetto d'onde sulla sfera nel caso di una risonanza netta. Nel problema del decadimento, vengono esaminati il campo di validità della legge esponenziale e le deviazioni da questa legge. Nel problema dello scattering della risonanza, viene discusso il comportamento della soluzione nelle regioni interna ed esterna in funzione dell'ampiezza dell'eccitazione. Si analizza il concetto del ritardo alla risonanza.

(*) *Traduzione a cura della Redazione.*

Three-Body Final States from K^- Capture in Helium and Deuterium (*).

M. M. Block

Department of Physics, Duke University - Durham, N. C.

(ricevuto il 23 Febbraio 1961)

Summary. — Impulse-model calculations have been made for interactions at rest of K^--mesons in ^4He and D. With the assumptions of non-interacting emergent particles, momentum spectra have been calculated for the reactions:

$$K^- + {}^4He \to \Lambda^0 + \pi^- + {}^3He$$

$$\to \Sigma^\pm + \pi^\mp + {}^3H$$

and

$$K^- + D \to \Lambda^0 + \pi^- + p$$

$$\to \Sigma^\pm + \pi^\mp + n\,.$$

1. – Introduction.

The analysis of the three-body final state reactions

(1) $$K^- + {}^4He \to \Lambda^0 + \pi^- + {}^3He$$

(2) $$\to \Sigma^- + \pi^+ + {}^3H$$

(3) $$\to \Sigma^+ + \pi^- + {}^3H$$

resulting from the at-rest capture of negative kaons in helium is of particular interest because of the recent results obtained by the Helium Bubble Chamber Collaboration Group [1], indicating the dominant role these processes played.

(*) This work was supported by a joint ONR-AEC Contract.

(1) Helium Bubble Chamber Collaboration Group: *Proc. of the Annual Intern. Conference on High Energy Physics at Rochester* (1960), p. 426.

In this communication, we will compute the momentum spectra for the emergent particles (both pions and ^{3}He(^{3}H)) using an impulse model and neglecting final state interactions. The general treatment will include, as a particular case, the corresponding reactions in deuterium,

$$K^- + D \to \Lambda^0 + \pi^- + p \tag{4}$$

$$\to \Sigma^- + \pi^+ + n \tag{5}$$

$$\to \Sigma^+ + \pi^- + n\,. \tag{6}$$

It will be assumed that the K^- is absorbed on a single nucleon, *e.g.*, a neutron in ^{4}He for reaction (1), and that the elementary reaction $K + N \to Y - \pi$ occurs from an *s*-state. All final-state interactions between the three emergent products will be neglected. Further, we take the K^- as pseudoscalar ([2]), and assume that the Σ and the Λ have the same parity.

The K^- is assumed to be absorbed from an *s*-state Bohr orbit ([3]). We evaluate the Bohr orbit wave function at the origin, since the nuclear extension is small compared to the orbit radius. The appropriate transition operator for the elementary reaction is scalar (taken as constant), which we denote as a.

The initial wave function is

$$\Psi_i = \Psi_{\text{Bohr}}(0)\Psi_{^4\text{He}}(Y, 2, 3, 4)\,,$$

where nucleon Y is the one that captures the K^- and transforms to the Y-π. Since our purpose is to compute spectral distributions, and $\Psi_{\text{Bohr}}(0)$ is a pure number, we need not consider it further. A gaussian wave function was taken for $\Psi_{^4\text{He}}(Y, 2, 3, 4)$, the internal wave function of the α-particle. It was adjusted so that the nucleon density distribution is the same as the charge density distribution measured by Hofstadter ([4]) and collaborators in electron scattering experiments. In particular, we use ([5])

$$\Psi_{^4\text{He}}(Y, 2, 3, 4) = N_4 \exp\left[-\left(\tfrac{1}{2}\beta \sum r_{ij}^2\right)\right]\,,$$

where N_4 is a normalization constant, and the parameter β is given by $\beta = 9/(32\,R_4^2)$, where R_4, the r.m.s. radius of ^{4}He (after making allowance for

([2]) M. M. Block, E. B. Brucker, I. S. Hughes, T. Kikuchi, C. M. Meltzer, F. Anderson, A. Pevsner, E. Harth, J. Leitner and H. Cohn: *Phys. Rev. Lett.*, **3**, 291 (1959); Helium Bubble Chamber Collaboration Group: *Proc. of the Annual Intern. Conference on High Energy Physics at Rochester* (1960), p. 419.

([3]) T. B. Day and G. A. Snow: *Phys. Rev. Lett.*, **5**, 112 (1960); T. B. Day: *Nuovo Cimento*, **18**, 381 (1960).

([4]) R. Hofstadter: *Rev. Mod. Phys.*, **28**, 214 (1956).

([5]) Units are chosen such that $\hbar = c = 1$.

the finite proton size) is (1.44 ± 0.07) fermi ([4,6]). This wave function can be factored to give

$$\Psi_{^4\mathrm{He}}(\Upsilon, 2, 3, 4) = \Psi(\varrho)\Psi'_{^3\mathrm{He}}(2, 3, 4) ,$$

where we define $\boldsymbol{\rho} = \boldsymbol{r}_\Upsilon - \boldsymbol{r}_{^3\mathrm{He}}$, where $\boldsymbol{r}_{^3\mathrm{He}}$ is the center of mass of nucleons 2, 3 and 4, *i.e.*, $\Psi_{^3\mathrm{He}}$ is the internal wave function of the virtual ^{3}He(^{3}H) in the ^{4}He nucleus. $\Psi(\varrho)$ and $\Psi'_{^3\mathrm{He}}$ are chosen so that they are individually normalized.

If the momenta of the three emerging particles ^{3}He(^{3}H), π and Υ are given by $\boldsymbol{p}$, $\boldsymbol{q}$ and $\boldsymbol{s}$, respectively, then the final state wave function (unnormalized) for *non-interacting* particles is

$$\Psi_f = \Psi_{^3\mathrm{He}}(2, 3, 4) \exp\left[i(\boldsymbol{p}\cdot\boldsymbol{r}_{^3\mathrm{He}} + \boldsymbol{q}\cdot\boldsymbol{r}_\pi + \boldsymbol{s}\cdot\boldsymbol{r}_\Upsilon)\right) ,$$

where $\Psi_{^3\mathrm{He}}(2, 3, 4)$ is the internal (normalized) wave function of the emergent ^{3}He(^{3}H). After noting that $\boldsymbol{p} + \boldsymbol{q} + \boldsymbol{s} = 0$, and that the impulse approximation requires $\boldsymbol{r}_\pi = \boldsymbol{r}_\Upsilon$, the final wave function can be rewritten more simply as

$$\Psi_f = \Psi_{^3\mathrm{He}}(2, 3, 4) \exp\left[-i\boldsymbol{p}\cdot\boldsymbol{\rho}\right] ,$$

where we recall that $\boldsymbol{\rho} = \boldsymbol{r}_\Upsilon - \boldsymbol{r}_{^3\mathrm{He}}$. The transition matrix element,

$$M = \int \Psi_i a \Psi_f \, \mathrm{d}\tau ,$$

factors into two terms and is given by

$$M = b \int \Psi_{^3\mathrm{He}}(2, 3, 4)\Psi'_{^3\mathrm{He}}(2, 3, 4) \, \mathrm{d}\boldsymbol{r}_2 \, \mathrm{d}\boldsymbol{r}_3 \, \mathrm{d}\boldsymbol{r}_4 \int \Psi(\varrho) \exp\left[-i\boldsymbol{p}\cdot\boldsymbol{\rho}\right] \mathrm{d}\boldsymbol{\rho} , \tag{7}$$

where the constant b is given by $a\Psi_{\mathrm{Bohr}}(0)$.

The first term is readily recognized as the overlap integral of the real emergent ^{3}He(^{3}H) with the virtual ^{3}He(^{3}H) core of the ^{4}He. The square of this is the probability that in a reaction in which a Υ and π are produced, the three recoiling nucleons emerge as a bound ^{3}He(^{3}H). The last term is the Fourier transform of $\Psi(\varrho)$, the portion of the ground state α-particle wave function which describes the relative motion of a single nucleon with respect to a ^{3}He(^{3}H)-like core.

Let us further assume that the ground state of ^{3}He(^{3}H) can be represented by a gaussian wave function

$$\Psi_{^3\mathrm{He}} = N_3 \exp\left[-\frac{\gamma}{2}\right] \sum r_i^2 ,$$

([6]) R. H. Dalitz and B. W. Downs: *Phys. Rev.*, **111**, 967 (1958).

where N_3 is a normalization factor and $\gamma = 1/(3R_3^2)$, where R_3 is the r.m.s. radius of ^{3}He(^{3}H), corrected for the finite proton size. It can be readily shown that P_{III}, the probability for the emission of a ^{3}He(^{3}H), is given by

$$P_{III} = \left(\frac{12\sqrt{2R_3R_4}}{8R_4^2 + 9R_3^2}\right)^6, \tag{8}$$

where (8) is a pure number depending only on our choice of nuclear radii, and is thus independent of the reaction dynamics. If we use in (8) the value $R_3 = 1.38$ fermi, the radius deduced by DALITZ and DOWNS [6] from examination of the ^{3}He(^{3}H) Coulomb energy differences, we obtain $P_{III} = 1.00$, which is obviously an upper limit; it is a numerical accident that depends solely upon the chosen nuclear radii R_3 and R_4. The recent helium bubble chamber results [2] indicate an observed value for $P_{III} \sim 0.6$. This could be explained in various ways—a poor radius assignment for R_3, or, just as likely, that strong final state interactions between the ^{3}He(^{3}H) and the Y and/or the π broke up *produced* ^{3}He(^{3}H), an effect completely neglected in the above calculations.

It is clear from an inspection of (7) that the only dynamical variable that the matrix element depends upon is $|\boldsymbol{p}|$, and thus we may write it as $M(p)$.

2. – Momentum spectrum of ^{3}He(^{3}H).

The transition probability R for reactions (1)–(3) can be written, ignoring constant factors, as

$$R = |M(p)|^2 \frac{\mathrm{d}\boldsymbol{q}\,\mathrm{d}\boldsymbol{p}}{\mathrm{d}E}. \tag{9}$$

Using energy conservation, where we treat the pion relativistically and the others in the *non-relativistic* limit, we obtain

$$R = 4\pi m_Y |M(p)|^2 pq\,\mathrm{d}q\,\mathrm{d}p, \tag{10}$$

where m_Y is the hyperon mass. Introducing k as the *relative* momentum of the Y-π system, *i.e.*, $\boldsymbol{k} = \boldsymbol{q} - \boldsymbol{s}$, and integrating over q to obtain the momentum spectrum $P(p)$, we find apart from normalization, that

$$P(p)\,\mathrm{d}p = |M(p)|^2 p^2 k\,\mathrm{d}p. \tag{11}$$

The quantity $k = |\boldsymbol{k}|$ is deducible from p by energy and momentum conservation. We see that if k were constant, the spectrum in p would be given simply by the Fourier transform. It is the additional factor k which establishes

overall energy and momentum conservation in reaction (1)–(3), since as $p \to p_{max}$, $k \to 0$. Also, we note that the only factor that depends on the kinematical details (such as whether a Λ or Σ is formed) is the quantity k. However, k is slowly varying over the region of interest in which the term $p^2 |M(p)|^2$ is large, so that only the high energy tail of the spectrum is influenced by the behaviour of k. This is the justification for the conclusion that the predicted ^{3}He spectrum from (1) and the ^{3}H spectra from (2) and (3) are almost identical.

The generalization of (7) to the deuterium reaction (4)–(6), is clear. The first overlap, *i.e.*, of a nucleon in the deuterium with the emergent nucleon, is obviously unity. Thus, $M(p)$ is the Fourier transform of the ground state deuteron wave function. In (11), p is now the recoil nucleon momentum and k again is the magnitude of the relative Y-π momentum. As before, the spectra $P(p)$ for (4)–(6) are expected to be almost identical, with only small differences in the high momentum tails.

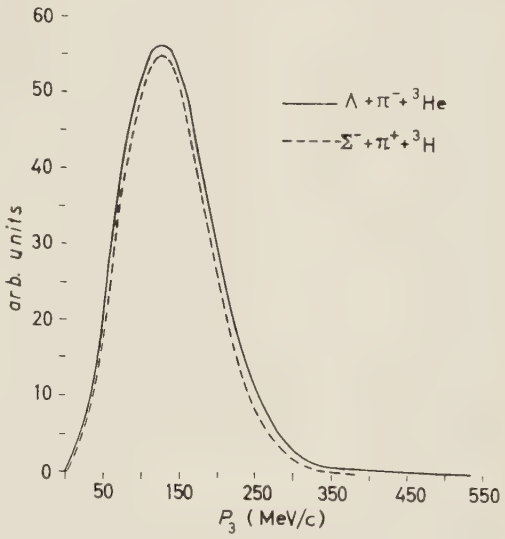

Fig. 1. – ^{3}He and ^{3}H momentum spectra from the reactions $K^- + {}^4He \to \Lambda^0 + \pi^- + {}^3He$ and $K^- + {}^4He \to \Sigma^- + \pi^+ + {}^3H$ respectively. The solid curve is the ^{3}He spectrum and the dotted curve is the ^{3}H spectrum.

Fig. 1 shows the ^{3}He spectrum from reaction (1) and the ^{3}H spectrum from (2). The appropriate $M(p)$ is given by

$$M(p) \propto N(\beta) \int \exp\left(-\frac{3}{2}\beta\varrho^2 + i\boldsymbol{p}\cdot\boldsymbol{\varrho}\right) \mathrm{d}\boldsymbol{\varrho} = N(\beta) \exp\left\{-\frac{p^2}{6\beta^2}\right\}, \tag{12}$$

where $N(\beta)$, the normalization factor, is given by $(3\beta/\pi)^{\frac{3}{4}}$.

Shown in Fig. 2 is $P(p)$ for reaction (4) in deuterium. We have employed the Hulthén wave function,

$$\Psi = (N/\varrho)(\exp[-\alpha\varrho] - \exp[-\delta\varrho]),$$

with

$$\alpha = (M\varepsilon)^{\frac{1}{2}}, \qquad \delta = 6.2\alpha, \qquad N = \left[\frac{\alpha}{2\pi(1-\alpha\varrho_t)}\right]^{\frac{1}{2}},$$

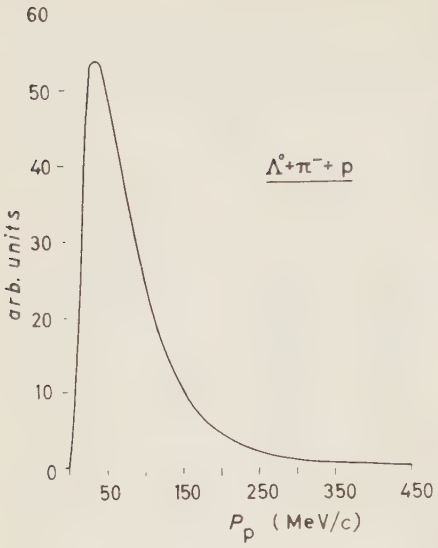

where ϱ_t, the triplet effective range, is given by $\varrho_t = 1.7 \cdot 10^{-13}$ cm, M is the nucleon mass and ε is the deuteron binding energy. Thus, $M(p)$, apart from numerical factors, is given by

$$M(p) = \left\{ \frac{1}{\alpha^2 + p^2} - \frac{1}{\delta^2 + p^2} \right\}^2 . \tag{13}$$

Fig. 2. – Proton momentum distribution from the reaction $K^- + D \to \Lambda^0 + \pi^- + p$.

3. – Pion momentum distribution.

To find the probability distribution $G(q)$ for the momentum of the emergent pion, we need only to integrate (10) over p first. For ^{4}He, we obtain, apart from normalization,

$$G(q)\,\mathrm{d}q = q \left\{ \sinh\left(\frac{2}{3\beta} \frac{M_{\mathrm{III}}}{M} q K \right) \right\} \exp\left\{ -\frac{1}{3\beta} \left(\frac{M_{\mathrm{III}}}{M} q \right)^2 - \frac{1}{3\beta} K^2 \right\} \mathrm{d}q \, . \tag{14}$$

K is the relative momentum of the Y-^{3}He(^{3}H) system, and is given by

$$K \left| 2\mu \left(Q \quad E_\pi \quad \frac{q^2}{2M} \right) \right|^{\frac{1}{2}} , \tag{15}$$

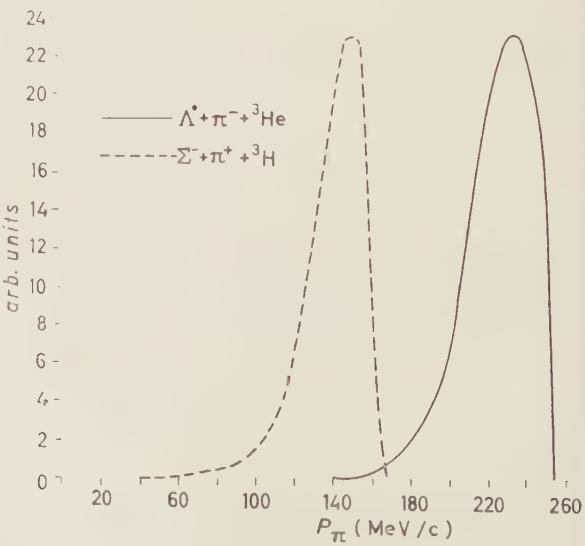

Fig. 3. – Pion momentum spectra from the reactions $K^- + {}^4\mathrm{He} \to \Lambda^0 + \pi^- + {}^3\mathrm{He}$ (solid) and $K^- + {}^4\mathrm{He} \to \Sigma^- + \pi^+ + {}^3\mathrm{H}$ (dashed).

where $Q = M_{^4\mathrm{He}} + m_{\mathrm{K}} - M_{\mathrm{Y}} - M_{\mathrm{III}}$, $1/\mu = (1/M_{\mathrm{Y}}) + (1/M_{\mathrm{III}})$, $M = M_{\mathrm{Y}} + M_{\mathrm{III}}$, $E_\pi = (q^2 + m_\pi^2)^{\frac{1}{2}}$, and $M_{^4\mathrm{He}}$, m_{K}, M_{Y}, M_{III}, and m_π are the rest masses of ^{4}He, K^-, hyperon, ^{3}He(^{3}H) and pion, respectively. Fig. 3 shows the pion momentum distributions $G(q)$ from reactions (1) and (2), using (14). Because of the rest mass differences between Σ^- and Σ^-, the corresponding spectrum for Σ^+ is of the same shape but shifted about 8 MeV/c toward lower momenta. These spectra are quite narrow, and are peaked near the maximum possible pion momentum. This is in accord with our *a priori* expectation for an impulse model, in which, loosely speaking, we expect that the line spectrum from the 2-body elementary interaction $\mathrm{K}^- + \mathcal{N} \to \mathrm{Y} + \pi$ is shifted slightly and broadened by the internal momentum distribution of the capturing nucleon. Shown in Fig. 4 is the pion spectrum $G(q)$ computed for the deuterium reaction (4). We find (7)

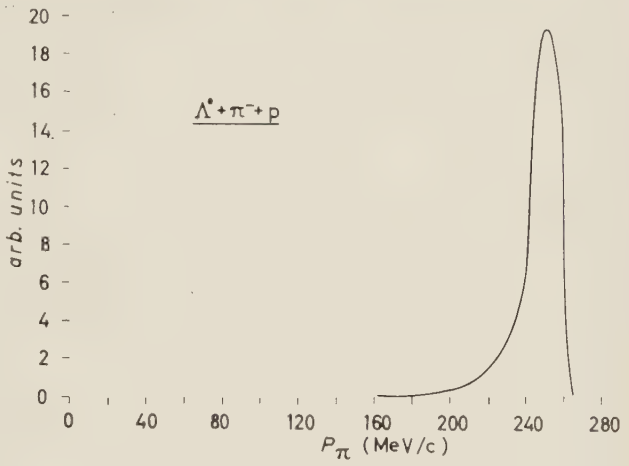

Fig. 4. – Pion momentum spectrum from the reaction $\mathrm{K}^- + \mathrm{d} \to \Lambda^0 + \pi^- + \mathrm{p}$.

$$(16) \qquad G(q)\,\mathrm{d}q = 2q \left\{ \left| \frac{1}{\alpha^2 + p^2} + \frac{1}{\delta^2 + p^2} + \frac{2}{\delta^2 - \alpha^2} \ln \left(\frac{\beta^2 + p^2}{\alpha^2 + p^2} \right) \right|_{p_{\min}}^{p_{\max}} \right\} \mathrm{d}q \,,$$

where $p_{\min}^{\max} = (M_{\mathcal{N}}/(M_{\mathcal{N}} + M_{\mathrm{Y}}))q \pm K$, where K is obtained from q, just as for the ^{4}He case (see eq. (15)), by the replacements $M_{^4\mathrm{He}} \to M_{\mathrm{D}}$, $M_{\mathrm{III}} \to M_{\mathcal{N}}$, where M_{D} and $M_{\mathcal{N}}$ are the rest masses of the deuteron and nucleon, respectively. The spectral differences between helium and deuterium reflect both the binding energy differences (the different Q's in the appropriate reactions) as well as the differences in internal momentum distributions.

(7) This result is similar to that deduced by A. Fujii and R. E. Marshak: *Nuovo Cimento*, **8**, 643 (1958).

4. – Angular distribution.

It is of interest to compute the angular distribution of the pion from reactions (1)–(3) in the rest frame of the Y-π system, relative to its motion. This is most simply done by introducing the co-ordinates $\boldsymbol{k}$ and $\boldsymbol{p}$, where θ is the angle between $\boldsymbol{k}$ and $-\boldsymbol{p}$. Thus, (9) becomes

$$R = 4\pi |M(p)|^2 \frac{p^2 \mathrm{d}p \; k^2 \mathrm{d}k \, \mathrm{d}(\cos\theta)}{\mathrm{d}E} . \tag{17}$$

In the non-relativistic limit,

$$k = \left[2\mu \left(Q' - \frac{q^2}{2m} \right)^{\frac{1}{2}} \right], \tag{18}$$

where $Q' = M_{^3\mathrm{He}} + m_{\mathrm{K}} - M_{\mathrm{Y}} - M_{\mathrm{III}} - m_\pi$, $1/\mu = (1/M_{\mathrm{Y}}) + (1/m_\pi)$, $1/m = (1/M_{\mathrm{III}}) + (1/M)$, and $M = M_{\mathrm{Y}} + m_\pi$, respectively. Since $\mathrm{d}E = \mathrm{d}Q'$, we obtain

$$R = 4\pi\mu |M(p)|^2 p^2 k \, \mathrm{d}p \, \mathrm{d}(\cos\theta). \tag{19}$$

If we were to integrate (19) over $\cos\theta$, we would obtain the same spectrum as in (11). However, if we integrate first over p, replacing k from (18), we immediately see, since p and θ are independent of each other, that the resulting angular distribution is isotropic. A similar conclusion is reached for the deuterium reactions.

5. – Conclusion.

Both the pion and recoil nucleon (nucleus) spectra, as well as the angular distributions, for K^- absorption in deuterium and helium have been calculated in the impulse model limit. It must be emphasized that these are the spectra expected in the *absence* of any final state interactions, *i.e.*, they are the equivalent « phase-space » for the absorption of a K^- meson in deuterium or helium. Any marked departure from these predicted distributions would be indicative of either a breakdown of our model (which is a reasonable one for the process) or of the importance of strong interactions among the emergent particles (a more likely cause). A comparison, therefore, of these results with experiment would shed light on these as yet unknown interactions.

* * *

The author would like to thank Dr. R. Gessaroli for many helpful discussions, Dr. G. Snow for illuminating advice, and Mr. J. Kopelman for aiding in numerical computation.

RIASSUNTO

Usando l'« impulse-model », si sono calcolati spettri di impulso nel caso di interazioni di K^- a riposo in ^4He e D, facendo l'ipotesi di particelle non interagenti nello stato finale. I calcoli si riferiscono in particolare alle reazioni

$$K^- + {}^4He \to \Lambda^0 + \pi^- + {}^3He$$
$$\to \Sigma^\pm + \pi^\mp + {}^3H$$

e

$$K^- + D \to \Lambda^0 + \pi^- + p$$
$$\to \Sigma^\pm + \pi^\mp + n\,.$$

IL NUOVO CIMENTO Vol. XX, N. 4 16 Maggio 1961

K^- Absorption in ^4He.

I. – The Hyperon-Pion Resonance (*).

Helium Chamber Collaboration Group

M. M. Block, E. B. Brucker, R. Gessaroli (**), T. Kikuchi, A. Kovacs and C. M. Meltzer

Duke University - Durham, N. C.

R. Kraemer, M. Nussbaum, A. Pevsner, P. Schlein and R. Strand

Johns Hopkins University - Baltimore, Md.

H. O. Cohn

Oak Ridge National Laboratory - Oak Ridge, Tenn.

E. M. Harth and J. Leitner

Syracuse University - Syracuse, N. Y.

L. Lendinara, L. Monari and G. Puppi

Istituto di Fisica dell'Università - Bologna

(ricevuto il 23 Febbraio 1961)

Summary. — Results are given on a hyperon-pion resonance. This resonance has been investigated in the absorption of K^--mesons in ^4He. The experiment was performed, using the Duke Helium Bubble Chamber. We give tentative assignments of spin, parity and level width of the Y^* state.

(*) Supported in part by ONR, AEC, OSR and NSF.

(**) On leave of absence from Istituto di Fisica, Bologna, Italy.

1. – Introduction.

The existence of a hyperon-pion resonance has recently been discovered [1], in the reaction $K^- + p \to Y^* + \pi$, where Y^* denotes the isobar representing the resonant state. In detail they observed that the isobar had a mass of ~ 1380 MeV, with a full width at half-maximum of ~ 65 MeV, and that it could decay via the scheme $Y^* \to \Lambda + \pi$, indicating that it had an isotopic spin $T_{Y^*} = 1$. The purpose of this communication is to present preliminary evidence confirming the existence of the isobar and to assign tentative spin and parity values to this level.

2. – Experiment.

The Duke Helium Bubble Chamber [2] $(20 \times 12.5 \times 10)$ cm^3, located in a uniform magnetic field of 14 kG, was exposed to a slow K^- beam from the Bevatron. In this communication, we have restricted our consideration to only those events corresponding to *at-rest* absorption of kaons.

Because of experimental conditions of recognition, measurability, etc., we have selected for detailed analysis the following reactions:

$$(1) \qquad K^- + {}^4He \to \Lambda^0 + \pi^- + {}^3He$$

$$(2) \qquad \to \Sigma^+ + \pi^- + {}^3H$$

$$(3) \qquad \to \Sigma^- + \pi^+ + {}^3H\,.$$

The above reactions are sufficiently overdetermined kinematically so that they may be unambiguously separated from the large number of permissible reactions in ^4He. The kinematically optimized results are used in this work.

We can produce Λ's in ^4He either « directly » or « indirectly » [3]. The term « direct » production implies that the Λ was produced in the elementary interaction $K + \mathcal{N} \to \Lambda + \pi$. The term « indirect » production is taken to mean the two-step process, wherein a Σ was produced which « converted » into a Λ via

(1) M. Alston, L. W. Alvarez, P. Eberhard, M. L. Good, W. Graziano, H. K. Ticho and S. G. Wojcicki: *Phys. Rev. Lett.*, **5**, 520 (1960).

(2) M. M. Block, W. M. Fairbank, E. M. Harth, T. Kikuchi, C. M. Meltzer and J. Leitner: *CERN Proc. Intern. Conference on High Energy Accelerators and Instrumentation* (1959), p. 461.

(3) Helium Bubble Chamber Collaboration Group: *Proc. of the Annual Intern. Conference on High Energy Physics at Rochester* (1960), p. 423.

a collision with a second nucleon in the ^{4}He, *i.e.*, the chain of reactions

$$\text{(4)} \qquad K + \mathcal{N}_1 \to \Sigma + \pi$$

$$\text{(5)} \qquad \Sigma + \mathcal{N}_2 \to \Lambda + \mathcal{N} .$$

The 75 MeV mass difference between the Σ and Λ causes a kinetic energy ~ 40 MeV to be imparted to the recoiling nucleon in (5), thus rupturing a bound 3-nucleon system. Therefore, neglecting *virtual* reactions, the presence of the weakly-bound ^{3}He in (1) allows us to conclude that the Λ was produced « directly ».

Reactions (1)–(3) can be produced either by a « phase-space »-impulse ([4]) type of interactions, similar to $K + \mathcal{N} \to \Lambda + \pi$, where the ^{3}He(^{3}H) plays a spectator role, or by the decay of the isobar Y* from the reactions

$$\text{(1')} \qquad K^- + {}^4\text{He} \to Y^{*-} + {}^3\text{He} , \qquad Y^{*-} \to \Lambda^0 + \pi^-$$

$$\text{(2')} \qquad \to Y^{*0} + {}^3\text{H} , \qquad Y^{*0} \to \Sigma^+ + \pi^-$$

$$\text{(3')} \qquad \to Y^{*0} + {}^3\text{H} , \qquad Y^{*0} \to \Sigma^- + \pi^+ .$$

From charge independence, we require both that the rate of (2') be that of (3'), and that the isobar Y^{*-} be produced twice as often as Y^{*0}. Reactions (1')–(3') correspond to particular decay channels of the Y*. The complete set of possibilities allowed for a $T = 1$ isobar by the conservation laws, including charge independence, are

$$Y^{*-} \to \begin{cases} \Lambda^0 + \pi \\ \Sigma^0 + \pi^- \\ \Sigma^- + \pi^0 \end{cases} \qquad Y^{*0} \to \begin{cases} \Lambda^0 - \pi^0 \\ \Sigma^+ + \pi^- \\ \Sigma^- + \pi^+ \end{cases}$$

The larger available phase-space due to the Λ being 75 MeV lighter than the Σ, increases the transition rate for $Y \to \Lambda + \pi$ over $Y \to \Sigma + \pi$ by approximately 60%. Thus, even in the absence of dynamical factors, we expect the yield of Σ's from (2') and (3') to be considerably less than Λ's from (1'). Thus, it is reasonable that of the observed reactions (1) could be rich in Y* yield, whereas (2) and (3) might be predominantly due to the impulse model type of interaction. Indeed, we note immediately that not more than $\sim 50\%$ of (2) could *possibly* be due to isobar formation, since the observed yield of (2) to (3) is $\sim 2:1$, whereas the formation via an isobar requires a 1:1 ratio.

([4]) M. M. BLOCK: *Nuovo Cimento*, **20**, 715 (1961).

3. – Momentum distribution of ³He and ³H.

If T is the sum of the kinetic energies of the $\Lambda(\Sigma)$ and pion in the $\Lambda(\Sigma)$-π rest frame, and p is the ³He(³H) laboratory momentum, then

$$T = \{(E^* - E)^2 - p^2\}^{\frac{1}{2}} - (m + \mu)\,, \tag{4}$$

where $E^* = m_1 + m_2$, $E = (p^2 + M^2)^{\frac{1}{2}}$, and m_1, m_2, M, m and μ are the rest masses of the K^-, ⁴He, ³He(³H), hyperon and pion respectively. Thus, the momentum of the recoiling ³He(³H) in (1), (2) and (3) is a measure of the relative energy in the $\Lambda(\Sigma)$-π.

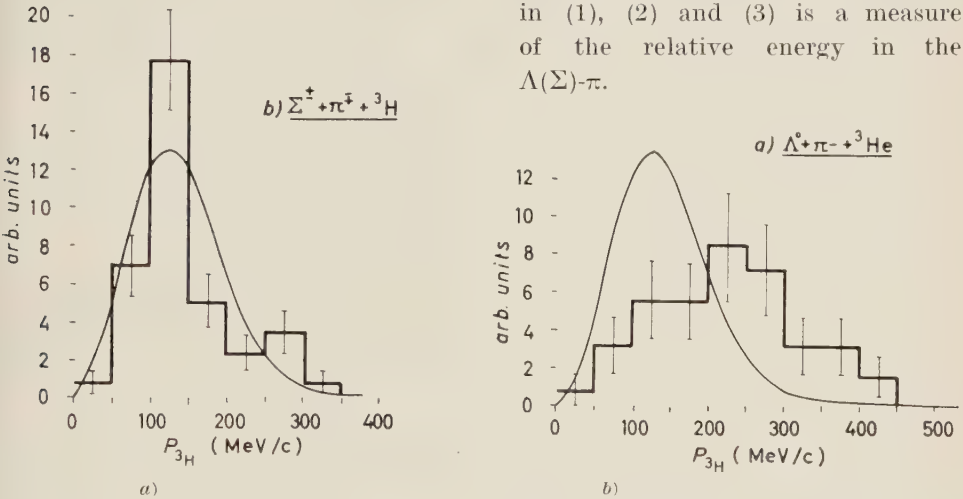

a) b)

Fig. 1. – *a*) Momentum spectrum of ³He from the reaction $K^- + {}^4He \to \Lambda^0 + \pi^- + {}^3He$. The theoretical curve, normalized to experimental, is an impulse-model calculation. *b*) Momentum spectrum of ³H from the sum of the reactions $K^- + {}^4He \to \Sigma^\pm + \pi^\mp + {}^3H$. The theoretical curve, normalized to experimental, is an impulse-model calculation. Note that the two histograms have been normalized to the same area.

In Fig. 1*a* and 1*b* we have plotted the momentum distributions of the ³He from reaction (1) and the ³H from the *sum* of (2) and (3). Both histograms are normalized to the same area. Also shown in Fig. 1*a* and 1*b* are the theoretical predictions (⁴) for the ³He spectrum (⁵) of (1), and ³H spectrum of (2) and (3), respectively, using an impulse-model calculation normalized to the experimental area. The theoretical assumption of *non-interacting* final state particles makes

(⁵) It is shown in reference (⁴) that the ³H spectrum from (2) or (3) is almost identical to the ³He spectrum of (1), except in the high momentum tail. The difference is negligible for our purpose.

the impulse-model predictions the equivalent of « phase-space » distributions for comparison with experiment. There are 96 events in the ^{3}H spectra and 50 in the ^{3}He spectrum. We note that there is substantial agreement between the « phase-space » theory and experiment for the ^{3}H's from (2) and (3), whereas the ^{3}He momentum distribution shows a marked departure, far outside experimental limits. It should be noted that since the ^{3}He momentum is obtained from range measurements, the average momentum uncertainty is ~ 7 MeV/c for the region $200 \leqslant p \leqslant 500$ MeV/c. The observed peak near 250 MeV/c is just what is expected if a Y* of mass 1380 MeV were formed. In order to examine these results in a more appropriate reference frame, we have replotted the ^{3}He distribution in terms of T, the internal kinetic energy of Λ-π system. These results are shown in Fig. 2 as the solid histogram. We

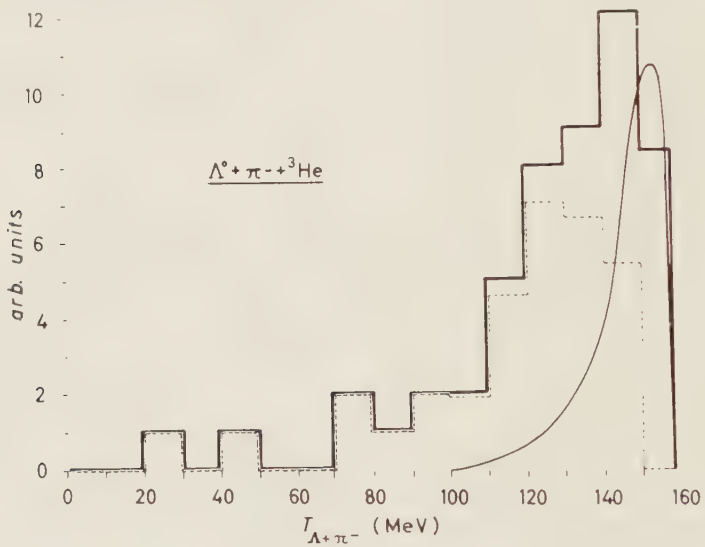

Fig. 2. – The distribution of T, the sum of the kinetic energies of the Λ and π in the Λ-π rest frame, from the reaction $K^- + {}^4He \to \Lambda^0 + \pi^- + {}^3He$. The solid histogram represents all 50 events. The dashed curve is the isobar contribution. The « phase-space » distribution (normalized to the interval $150 \div 158$) has been subtracted off and the *remainder* plotted as the dashed curve.

have attempted to estimate an upper-limit for the equivalent « phase-space » contribution in the following manner. The area of the last energy interval ($(150 \div 158)$ MeV) in the histogram was made equal to the area under the appropriate theoretical curve for the same energy interval. This yields a « phase-space » contribution of $\sim 35\,\%$. The dotted histogram is the remainder after subtraction of the theoretical spectrum. These remaining events have the shape we would expect if an isobar Y* were formed. If we accept the isobar

interpretation, we obtain a Y^* mass of 1385 MeV and a full width ~ 35 MeV not in disagreement with the hydrogen chamber results [1]. Since our average energy resolution is ~ 3 MeV, we conclude that the *natural* level width is comparable with the observed width. We can further conclude that a majority of reaction (1) proceeds via isobar formation. We have pointed out earlier that the number of Y^*'s channels (2) and (3) is expected to be much smaller than in (1), even in the absence of dynamical factors, such as a possible Σ-Λ parity difference, etc. An examination of Fig. 1*b* shows the difficulty of detecting any Y^{*0} decays from reactions (2) and (3). A reasonable upper limit for Y^{*0} contributions to this spectrum is $\sim 20\,\%$.

4. – Pion momentum spectra.

In order to check on the internal consistency of the isobar assumption, we have examined the pion spectra from (1), (2), and (3).

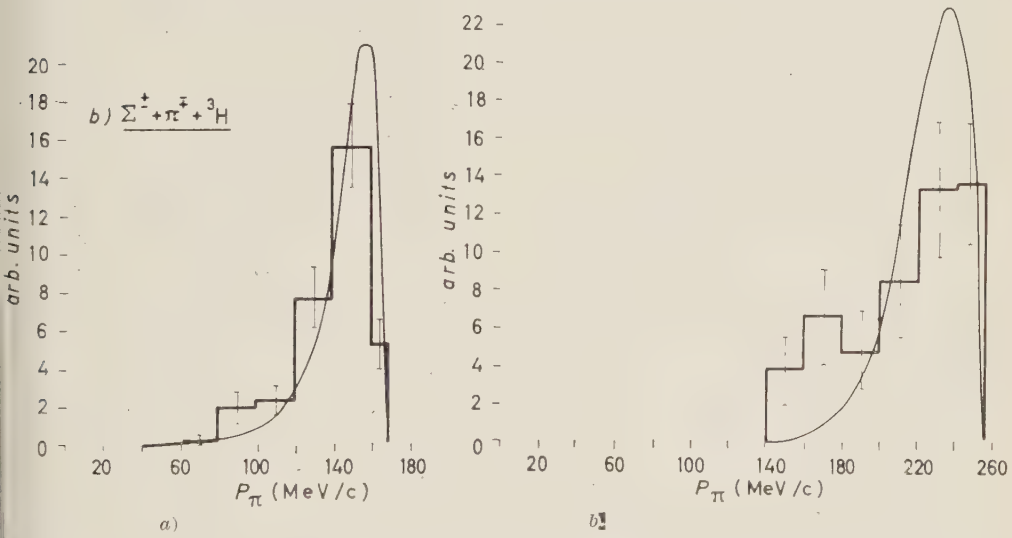

Fig. 3. – *a*) Pion momentum spectrum from the reaction $K^-+{}^4He \to \Lambda^0+\pi^-+{}^3He$. The theoretical curve, normalized to experimental, is an impulse-model calculation. *b*) Pion momentum spectrum from the sum of the reactions $K^-+{}^4He \to \Sigma^{\pm}+\pi^{\mp}+{}^3H$. The theoretical curve, normalized to experimental, is an impulse-model calculation.

The pion momentum distribution from (1) is shown in Fig. 3*a* and that from the sum of (2) and (3) is plotted in Fig. 3*b*. Also shown for comparison are the impulse model spectra [1,6], normalized to the total area of the histo-

[6] J. LEITNER and S. LICHTMAN: *Nuovo Cimento*, **15**, 719 (1960).

gram. We see that the Σ events are more or less in agreement with equivalent « phase-space » whereas the pion distribution from the Λ events is considerably broader than the predicted spectrum. This experimental result is in qualitative agreement with the model consisting of a superposition of two basic types of interactions, impulse plus isobar. The impulse peak is narrow (spread only by internal motion of the nucleons in ^{4}He) and located near the maximum possible momentum (corresponding to the elementary reaction $K^- + N \to \Lambda + \pi$), whereas the pion spectra from (1′) is expected to be broad and centered at a considerably lower pion momentum (~ 200 MeV/c), due to the energy absorbed by the recoiling Y* and ^{3}He.

5. – Spin of Y*.

Day and Snow (7) have indicated that the Stark effect causes predominantly s-state absorption of K^--mesons in ^{4}He. The simplicity of s-state absorption, and the zero spin of ^{4}He allow us to make a direct spin determination of the Y*. In the absorption reaction $K^- + {}^4\mathrm{He} \to Y^* + {}^3\mathrm{He}$, the total angular momentum J equals zero. Picking our axis of quantization as the direction of the Y*, we note that angular momentum conservation requires that the magnetic quantum number m_{s_Y} be $\pm \frac{1}{2}$, independent of the spin S_Y of the Y*. Therefore, for $S_Y = \frac{3}{2}$, we have an *aligned state* present, and the decay angular distribution can be simply shown to be $1 + 3\cos^2\theta^*$. Whereas if $S_Y = \frac{1}{2}$, each possible magnetic quantum state is equally populated, and the corresponding angular distribution is isotropic. In the above, θ^* is the angle (in the rest frame of the Y*) that the Λ makes with respect to the Y* direction.

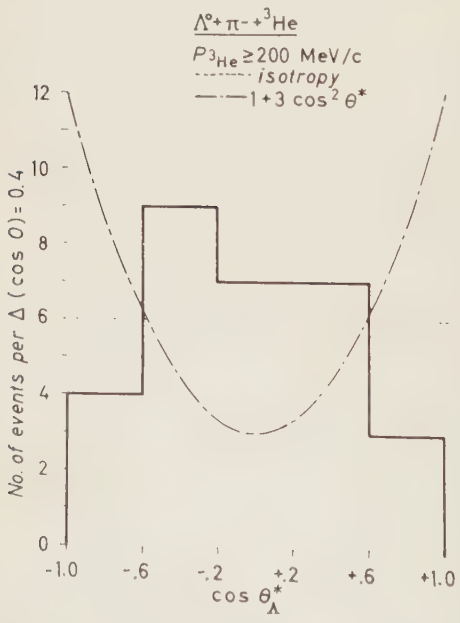

Fig. 4. – Angular distribution of the Λ in the rest frame of the Λ-π system, for the 30 cases with $p_{^3\mathrm{He}} \geq 200$ MeV/c, in the reaction $K^- + {}^4\mathrm{He} \to \Lambda^0 + \pi^- + {}^3\mathrm{He}$. The expected angular distributions for $S_Y = \frac{1}{2}$ and $\frac{3}{2}$, respectively, *i.e.*, isotropy and $1 + 3\cos^2\theta^*$ are given normalized to the experimental data.

(7) T. B. Day and G. A. Snow: *Phys. Rev. Lett.*, **5**, 112 (1960); T. B. Day: *Nuovo Cimento*, **18**, 321 (1960).

In order to assure ourselves that the cases of reaction (1) which we examine to determine S_Y are indeed due to Y* formation, *i.e.*, reaction (1′), we have limited this analysis to those events having a ^3He momentum ≥ 200 MeV/c, a momentum beyond which the equivalent « phase-space » contribution has effectively « died off ». The appropriate angular distributions for the 30 cases satisfying this momentum restriction have been plotted in Fig. 4. It is observed that the data are compatible with isotropy, whereas, $1+3\cos^2\theta^*$ is a rather poor fit. Before it is concluded that $J=\frac{1}{2}$, we must take into account effects over and above the obvious one that our sample is small. The Y* travels a mean distance ([8]) of ~ 1 fermi before decaying, and thus the decay products Λ and π may be within the nuclear force range of the ^3He. Hence, final state Λ-^3He forces could seriously distort the expected angular distributions. However, this type of effect would most likely cause an *angular asymmetry* about 90°. In Fig. 5 a scatter diagram of θ^* *vs.* p for *all* (50) events from (1) is plotted. The lack of symmetry about 90° for $p \lesssim 200$ MeV/c is probably a reflection of the strong final state interactions between the Λ and the ^3He (virtual hyperfragment) which prefers low relative Λ-^3He energies, *i.e.*, the Λ and ^3He going off together in the same direction. However, the data for $p \geq 200$ MeV/c—the Y* region—seem to be free of this defect and thus, more confidence can be lent to the spin determination. A χ^2 fit to the data of Fig. 4 gives a $\chi^2 = 4.0$ for isotropy, with an expected χ^2 of 4 ± 2, whereas $1+3\cos^2\theta$ yields $\chi^2 = 17.2$. The data obviously strongly favor isotropy and hence $S_Y = \frac{1}{2}$.

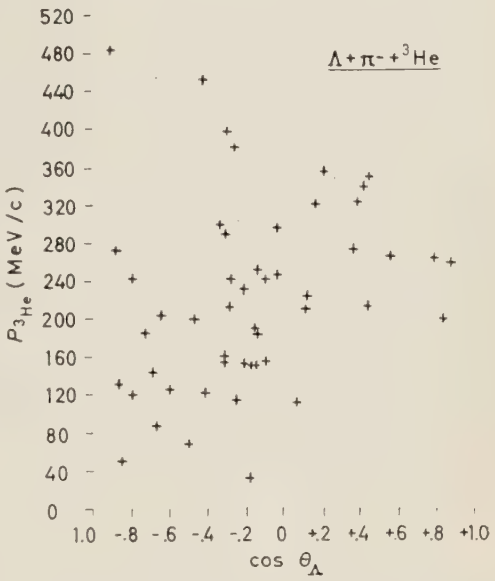

Fig. 5. – Scatter diagram of $\cos\theta^*$ *vs.* $p_{^3He}$ for all events from the reaction $K^- + {}^4He \to \Lambda^0 + \pi^- + {}^3He$

([8]) Estimated from a lifetime computed from the uncertainty principle.

6. – Y* parity.

If we accept the preliminary spin determination $S_Y = \frac{1}{2}$, and further accept our tentative parity assignment of the K^- as pseudoscalar ([9]), then we can make an argument on the Y* parity. Let l be the orbital angular momentum of the Λ relative to the π^-, *i.e.*, the internal orbital angular momentum of the Y*, and let L be the orbital angular momentum of the Y* relative to the ^{3}He. We note that for a pseudoscalar K and $S_Y = \frac{1}{2}$, only two combinations are possible, either $l = 0$, $L = 0$ or $l = 1$, $L = 1$. The later combination, corresponding to a spin-flip of the absorbing nucleon, would be expected to be inhibited relative to the former by the angular momentum barrier. Since our yield of Y* is rather large ($\sim 65\%$) the assignment $l = 1$, $L = 1$ seems unlikely. Moreover, in the spirit of the impulse model, if the elementary virtual reaction $K + \mathcal{N} \to Y^*$ were dominant, the Y* would be expected to have $S_Y = \frac{1}{2}$, $l = 0$ for s-state absorption. Although the above arguments are weak, we suggest that the most natural Y* assignment is spin $\frac{1}{2}$, odd parity.

* * *

We gratefully acknowledge the assistance, co-operation and whole-hearted support of the Lawrence Radiation Laboratory staff, and in particular, Dr. E. McMillan, Dr. E. Lofgren and the Bevatron staff, in making this experiment possible. One of us (M. M. B). wishes to thank the John Simon Guggenheim Memorial Foundation for a fellowship during the early stages of this research.

([9]) M. M. Block, E. B. Brucker, I. S. Hughes, T. Kikuchi, C. M. Meltzer, F. Anderson, A. Pevsner, E. M. Harth, J. Leitner and H. O. Cohn: *Phys. Rev. Lett.*, **3**, 291 (1959); Helium Bubble Chamber Collaboration Group: *Proc. of the Annual Intern. Conference on High Energy Physics at Rochester* (1960), p. 419.

RIASSUNTO

In questa comunicazione sono presentati risultati su una risonanza pione-iperone. Questa risonanza è stata studiata nel caso di assorbimento di mesoni K^- in ^{4}He e l'esperimento è stato fatto usando la Duke Helium Bubble Chamber. Si è anche tentato di assegnare spin, parità e larghezza a questo stato isobarico.

IL NUOVO CIMENTO Vol. XX, N. 4 16 Maggio 1961

Unitarity and the Mandelstam Representation - II.

R. W. Lardner

St. John's College - Cambridge

(ricevuto il 25 Febbraio 1961)

Summary. — An earlier investigation into the analyticity of the three-particle unitarity contribution to a scattering absorptive part is discussed more completely. The general term is shown to reduce to the same form as the three-particle term.

1. – Introduction.

The hope is often expressed that the use of the unitarity condition in addition to those axioms used in deriving analytic properties of S-matrix elements should produce yet more powerful results. It is the purpose of this paper to investigate to what extent this is true for the scattering amplitude. In order to establish some support for this view, we examine the structure of the many-particle intermediate state terms in the unitarity equation by postulating some property of the relevant production amplitudes and discussing the effect of this on the scattering amplitude. The behaviour we postulate is in the fact that the general production amplitude satisfies a single dispersion relation in a momentum transfer. This, of course, is not a rigorously established property; furthermore, since the completion of this work, it has been shown to be violated by the simplest single loop perturbation theory diagram [1]. However, it is instructive to see exactly what does fol-

[1] P. V. Landshoff and S. B. Treiman: Cambridge preprint; L. F. Cook and J. Tarski: Princeton preprint, to appear shortly.

low from so extensive an assumption, and to some extent disillusioning in the amount of manipulation needed to obtain any result at all from it.

In a previous paper ([2]) the three-particle term was examined under these assumptions, and it was found that they were sufficient to enable the behaviour on z (the cosine of the total scattering angle) to be isolated. The singularities in z were found and it was shown that if certain cuts associated with the function were drawn suitably, the singularities could be limited to lying in a neighbourhood of the real axis. There were in this paper a number of unsupported statements needing justification; this is carried out in Section 2 and 3 in which is given a full discussion of the argument sketched in I. Apart from the obvious advantage of having a proof rather than an indication, these sections contain a list of all the possible configurations of singularities and cuts needed to obtain analyticity in the whole cut z-plane, and bring to light one of the problems created by this investigation: that it is necessary on occasions to partition off the whole physical z-region by cuts from the rest of the z-plane, making nonsense of the requirement that the physical function should be the boundary value of an analytic function.

This difficulty stems from two features of the problem. Firstly, as is evident from I, the function obtained by performing the two integrations has infinities in the physical region. Secondly the function as defined by unitarity for any particular physical value of z is not necessarily the continuation of the function defined for all other physical z. Both of these undesirable properties we know are not possessed by the actual scattering absorptive part, and so must be removed by later integrations. So also must the ambiguity we find at this stage as to which branch of the function to continue into the complex plane, and where to draw the cuts between different continuations. It is plausible that properties obtained from any particular continuation are, by virtue of the later integrations, independent of that continuation.

In view of all this, it seems likely that a more promising approach would be to assume double-variable properties of the initial production amplitudes. Since the inception of this work, such properties have been obtained ([3]) from causality and mass-spectrum conditions, making their use here realistic.

In the final section we show that it is possible to choose a set of invariants in such a way as to reduce the general unitarity term to the same form as the three-particle term as far as the first four integrations are concerned. This is shown for all except the five-particle term; for this it is established that there can only be a very limited analyticity region on the basis of our single-variable assumptions. This makes the use of double-variable properties even more imperative.

([2]) R. W. LARDNER: *Nuovo Cimento*, **19**, 77 (1961), (referred to as I).
([3]) R. ASCOLI: *Nuovo Cimento*, **18**, 754 (1960).

2. – Summary of previous results.

We adhere to the notation of I. The function obtained by performing the two integrations is called χ; this contains the whole dependence on z of the three-particle contribution $A^{(3)}$ (cf. eq. (10) of I). The other variables on which χ depends are as follows: z_{27}, z_{35}, internal scattering angles later to be integrated over $(-1, +1)$; z'_{15}, z'_{47}, the substituted dispersion variables, integrated over some real ranges assumed outside $(-1, +1)$; λ, some function of later integration variables, restricted to $|\lambda| \leqslant 1$. We write $\cos\theta = z$, $\cos\theta_{27,35} = z_{27,35}$, $\cos\alpha = \lambda$, and use the shorthand $k(x, y, z) = x^2 + y^2 + z^2 - 1 - 2xyz$.

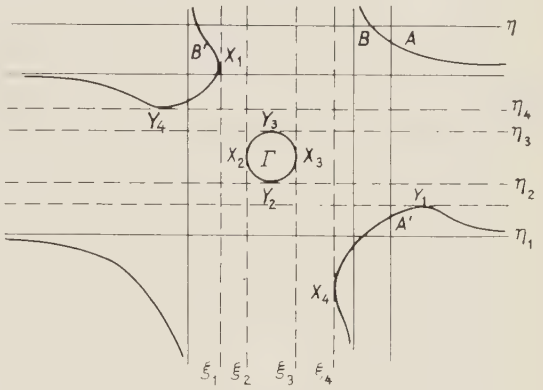

Fig. 1.

χ is given for z real and $|z| < 1$ as an integral round the closed arc (Γ) of a surface (Σ, referred to loosely as a torus) whose general real section is shown in Fig. 1. The integrand has singularities at the intersections A, A' and B, B' of Σ with

$$\xi: \quad x = \frac{z'_{15} - zz_{35}}{(1 - z^2)^{\frac{1}{2}}(1 - z_{35}^2)^{\frac{1}{2}}},$$

$$\eta: \quad y = \frac{z'_{47} - zz_{27}}{(1 - z^2)^{\frac{1}{2}}(1 - z_{27}^2)^{\frac{1}{2}}},$$

and the intersections with $x = \pm 1$, $y = \pm 1$ (*i.e.* two of the points $X_1 \ldots X_4$ and two of $Y_1 \ldots Y_4$ since these lines are pairs of the tangents to Σ).

The other pairs of tangents to Σ have equations

$$x = x_\pm \quad = \frac{-zz_{35} + \lambda z_{27} \pm (1 - \lambda^2)^{\frac{1}{2}}(1 - z_{27}^2)^{\frac{1}{2}}}{(1 - z^2)^{\frac{1}{2}}(1 - z_{35}^2)^{\frac{1}{2}}},$$

and $y = y_\pm$ similarly.

We then obtain the following coincident singularities for χ:

$a_\pm$: $z'_{15} = zz_{35} \pm (1 - z^2)^{\frac{1}{2}}(1 - z_{35}^2)^{\frac{1}{2}}$, a coincidence of A and A' at $x = \pm 1$. For z_{35}, z'_{15} in their integration ranges, this lies on an ellipse in the z-plane with foci ± 1 and semimajor axis $|z'_{15}|$.

$b_\pm$: $z'_{47} = zz_{27} \pm (1-z^2)^{\frac{1}{2}}(1-z_{27}^2)^{\frac{1}{2}}$, similarly

$c_\pm$: $z'_{15} = \lambda z_{27} \pm (1-\lambda^2)^{\frac{1}{2}}(1-z_{27}^2)^{\frac{1}{2}}$, or coincidence of A and A' at $x = x_\pm$. This is independent of z and for λ, z_{27} in their integration ranges gives two points in $|z'_{15}| < 1$.

$d_\pm$: $z'_{47} = \lambda z_{35} \pm (1-\lambda^2)^{\frac{1}{2}}(1-z_{35}^2)^{\frac{1}{2}}$, similarly

e: $(z_{35}z'_{47} + z_{27}z'_{15}) - z(z_{27}z_{35} + z'_{47}z'_{15}) = \lambda k(z, z_{35}, z'_{15})(z, z_{27}, z'_{47}) - \lambda(1-z^2) = 0$,

a coincidence of A or A' with B or B'. Solving for z we see that this lies on the real z-axis provided z'_{15}, z'_{47} lie outside the ranges $(\cos(\alpha+\theta_{27}), \cos(\alpha-\theta_{27}))$, $(\cos(\alpha+\theta_{35}), \cos(\alpha-\theta_{35}))$, respectively.

There is also a degenerate singularity when pairs of tangents $x = \pm 1$, $x = x_{\pm'}$, coincide, given by

$f_{\pm\pm'}$: $\theta \mp \theta_{35} \pm''(\theta_{27} \mp' \alpha) = 0$.
These four points lie in the physical z-region. They include coincidences of $y = \pm 1$ with $y = y_{\pm'}$. The intersection of $a_\pm$ with $c_{\pm'}$ is $f_{\pm\pm'}$.

By fixing z and moving z'_{15} (*i.e.* the line ξ) until various coincidences occurred, we obtained the following conditions on the singularities for physical z.

i) a_+ is non-singular if and only if ξ_4 is $x = +1$; a_- is non-singular, if and only if ξ_1 is $x = -1$.

ii) c_+ is non-singular if and only if ξ_4 is $x = x_+$; similarly for c_-.

iii) Similar results for b, d.

iv) e is non-singular if the intersection occurs on one of the infinite arcs of B and singular if it occurs on Γ. Since this singularity is at real z, we do not obtain more exact conditions.

Before proceeding with the continuation of χ from the physical z-region, we give a list of the possible orderings of singularities. These are connected with the possible orderings of the singularities (f) which in turn depend on the ordering and changes of ordering of the tangents to Σ. We denote by $F_{\pm\pm'}$ the coincidence of $x = \pm 1$ and $x = x_{\pm'}$. We also use the notation $(-1, x_-, x_+, +1)$, say, to denote the ordering $-1 < x_- < x_+ < +1$ and so on.

The $F_{\pm\pm'}$ give four points in the physical z-region. The main difficulty arises because F_{+-}, say, need not occur, and instead we may get two F_{++} points. When all four do occur, noting that $x_+ \geqslant x_-$ (equality occurring, independently of z, at $\lambda = \pm 1$ or $z_{27} = \pm 1$), the only possible tangent orderings are

$(-1, -1, x_-, x_+)(-1, x_-, +1, x_+)$ $(-1, x_-, x_+, -1)$ $(x_-, x_+, -1, +1)(x_-, x_+, -1, +1)$
$(x_-, -1, -1, x_+)$

and the orders of the F's are

$$(1) \qquad -1 < F_{+-} < F_{++} < F_{--} < F_{-+} < 1$$

$$(2) \qquad -1 < F_{+-} < F_{--} < F_{++} < F_{-+} < 1$$

or their inverted orderings. In our list of tangential orderings, the centre two in any ordered four give the tangents which touch Γ, *i.e.* they decide which of the $a_{\pm}c_{\pm}$ are singular (*e.g.* $(-1, +1, x_-, x_+)$ gives $+1$ and x_- touching Γ *i.e.* a_+ and c_- singular. This corresponds in (1), (2) to $-1 < z < F_{+-}$). Hence

(1)

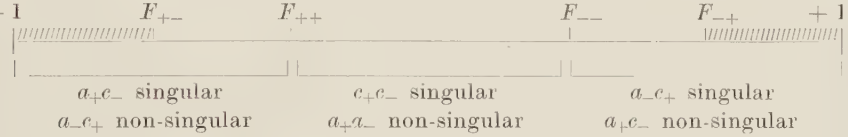

(2)

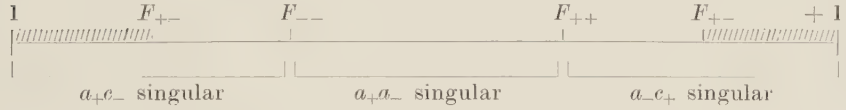

The coincidences F_{+-}, F_{-+} are different from the F_{++}, F_{--}, since they are due to the *central* two tangents coinciding, shrinking Γ to zero. They are not infinities of χ as F_{++}, F_{--} are (F_{++}, F_{--} are *always* due to the coincidence of an outside pair of tangents) and they do not influence the singularity of the a_+, c_+.

For $-1 < z < F_{+-}$ and $F_{+-} < z < +1$ in (1) and (2), Γ lies completely to one side of the x-range $(-1, 1)$. Thus our definition of the physical functions as the integral over that part or Σ lying in the square $-1 \leqslant x \leqslant 1, -1 \leqslant y \leqslant 1$ gives zero contribution in these ranges of z. This shows definitely that the defined integral at any particular z is not the continuation of the integral at all other physical z (otherwise χ would be indetically zero). We see later that the requirements i) and ii) are not consistent with the continuability of χ either.

The tangents are $x_{\pm} = A \cot\theta + B_{\pm} \operatorname{cosec}\theta$

$$A = -z_{35}/(1 - z_{35}^2)^{\frac{1}{2}}, \qquad B_{\pm} = \frac{\lambda z_{27} \pm (1 - \lambda^2)^{\frac{1}{2}}(1 - z_{27}^2)^{\frac{1}{2}}}{(1 - z_{35}^2)^{\frac{1}{2}}}.$$

As z varies over $(-1, 1)$ these tangents move steadily over the interval $(-\infty, \infty)$ provided $|A| > |B_{\pm}|$. In this case, each crosses the lines $x = \pm 1$ and all intersections $F_{\pm\pm'}$ occur, giving either case (1) or (2).

If, however $|A| \geqslant |B_\pm|$, $x_\pm$ have turning values:

$$\frac{\mathrm{d}x_\pm}{\mathrm{d}\theta} = 0 \Rightarrow \cos\theta = -A/B_\pm \qquad \text{when} \qquad x_\pm^{(m)} = \sqrt{B_\pm^2 - A^2}\,.$$

$$B_\pm^2 - A^2 - 1 = \frac{1}{1 - z_{35}^2}\left(\cos^2(\theta_{27} \mp \alpha) - 1\right) \leqslant 0\,, \qquad \text{so} \qquad |x_\pm^{(m)}| \leqslant 1\,.$$

Hence, as z varies from -1 to 1, x_+, say, moves from $-\infty$ (or $+\infty$) attains a maximum (minimum) in $(-1, +1)$ and returns to $-\infty$ $(+\infty)$. It thus crosses -1 (or $+1$) twice and $+1$ (-1) not at all, giving two F_{+-} points (F_{++}) and no F_{++} (or F_{+-}).

The possible arrangements are:

(3) x_- moves from $+\infty$ to $-\infty$, x_+ returns to $+\infty$.

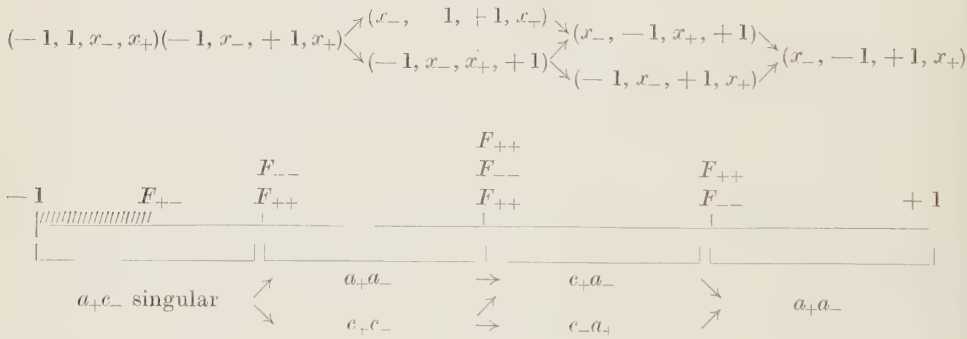

Shading indicates $\chi \equiv 0$.

(4) Both x_-, x_+ start and finish at $+\infty$.

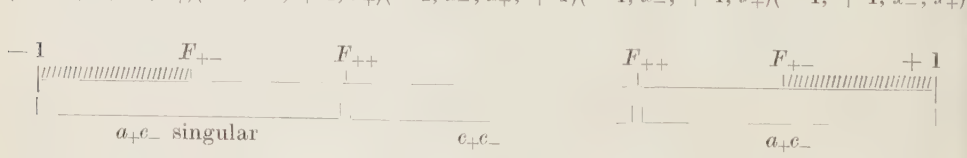

(5) x starts and finishes at $-\infty$, x_+ at $+\infty$.

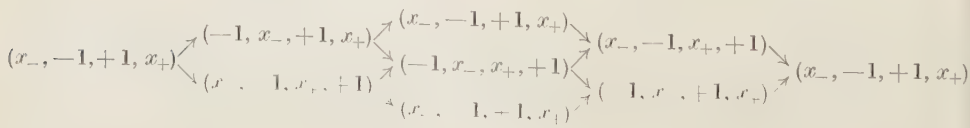

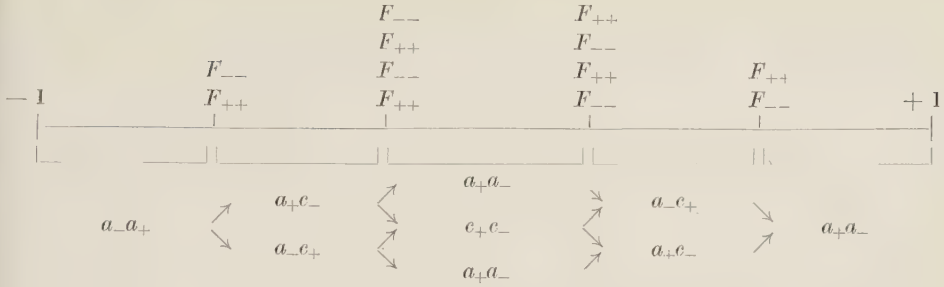

3. – Continuation of χ.

In this section we concern ourselves solely with the pair of singularities *a*) and *c*). All that we say will apply to the pair *b*) and *d*) also.

The results of Section 2 tell us when these singularities occur for physical z whether in fact they are singular or not. The problem now is to discover where they are singular when they occur for complex z. In order to do this, we take z'_{15} as a complex variable, and continue from physical z on the singular surface in $z - z'_{15}$ space. If we start from a singular point on the surface, which corresponds to two integrand singularities coinciding with the contour pinched between them, then as we move, the two singularities stay coalesced, and the contour remains pinched between them—so the surface remains singular. The only way it can stop being singular is for there to be a cut which completely divides the surface into two disjoint parts, since crossing a cut is equivalent to allowing a singularity to pass through the contour. We note that our contour has no end-points, so that a pinch cannot slide off the contour. This discussion clearly holds, *mutatis mutandis*, for a non-singular part of the surface.

The problem is then, to discover which of the other singularities can influence any one singularity, and then to discover how the cuts associated with these singularities can be drawn. We show that these cuts can be drawn in such a way that the only singularities of χ in the z-plane are arbitrarily close to the real axis. The crucial features of the singularities of χ that permit this are that the *f*) singularities are always real and that the *c*) singularities are independent of z.

We first of all dispose of the effect of the singularities at $x = \pm 1$.

Lemma 1. The cuts associated with the $x = +1$ singularity can be taken along the real axis from $-\infty$ to F_{++} or from F_{++} to ∞ or both if there are two F_{++}.

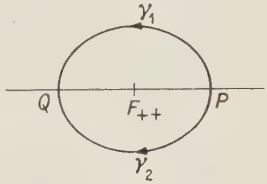

Fig. 2.

Move in z round F_{++} from a point P where ξ_4 is $x=+1$ and ξ_3 is $x=x_+$ to Q where ξ_4 is $x=x_+$ and ξ_3, $x=+1$ (Fig. 2). The point x_+ describes a circuit round $+1$, the direction of its motion depending on whether z is on γ_1 or γ_2 (Fig. 3). At the same time it takes Σ with it. The contour Γ starts at x_- at P and arrives at $+1$ at Q. During the motion, we allow it to slide round Σ; then the difference between the two limits at Q is that the contour approaches the $x=+1$ singularity from different sides. Therefore there must be a cut separating γ_1 from γ_2.

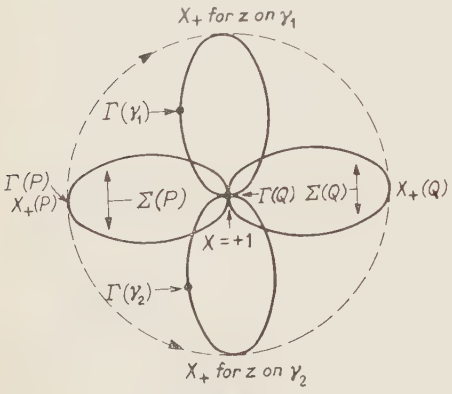

Fig. 3.

In I we artificially distorted Γ slightly round the $x=+1$ singularity in order to make the integral well-defined at Q. This means that the cut will occur slightly to one side of the real axis. If we take the limit as the deformation tends to zero, Q lies on the cut.

This holds for all Q between F_{++} and -1 (or between F_{++} and $+1$ if the Q's lie to the right of F_{++}). The extension of the cut below -1 can be defined to be along the real axis.

When the F point that we move round corresponds to the coincidence of two outside tangents, the two points of intersection of Σ with the plane $x=x_0$ move round opposite sides of the torus as x_0 moves from 1 to x_+ (Fig. 4). So that when they arrive at x_+ the points are on opposite sides of the contour (if as shown they do not pinch it at $x=1$). Hence

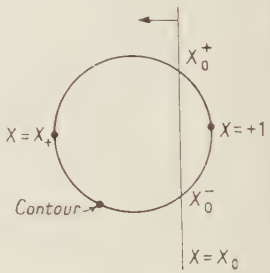

Fig. 4.

Lemma 2. The point F_{++} corresponds to the coincidence of two outside tangents. For each point z of our circuit γ round F_{++} there are values of z'_{15} at which the singularities a_+ and c_+ occur. These cannot both be non-singular.

z'_{15} at a_+ corresponds to the line ξ being at $x=+1$, and at c_+ to ξ at $x=x_+$. Changing z'_{15} from a_+ to c_+ makes the intersections ξ_+ of ξ with Σ move round Σ in opposite directions. If they did not pinch the contour at a_+, they will at c_+ if they do not pinch at c_+, they must pinch at a_+. A similar result holds for F_{--}, a_-, c_-.

Lemma 3. For fixed z, there is a cut in the z'_{15} plane attached to each singular point among the $a_\pm$, $c_\pm$ through which we are not allowed to continue any of the non-singular points: *i.e.* if we start from a non-singular point and

move round a singular point and back again, the initial point will then be singular.

Let S_1 be a non-singular point, S_2 a singular point (Fig. 5). We treat the case when the tangents for S_1 and S_2 are on the same side of the contour Γ. For z'_{15} near S_1 (at Z_1) the intersections A_1, A'_1 of ξ with Σ are close together and the contour is not between them. Moving to Z_2 near S_2 makes the A, A' move in opposite directions round Σ, so that A_2, A'_2 are close together but now *with* the contours between them. If we move completely round S_2 to Z_3, A, A' change places. In doing this they cross Γ, so that the new contour is Γ together with small circles round A_3, A'_3, in the senses shown. Moving back to Z_4 near S_1 makes A_3, A'_3 move along the paths travelled by A', A as z'_{15} was changed from Z_1 to Z_2, arriving at A_4, A'_4 still with their small circles. Clearly on letting $Z_4 \to S_1$ the singularities will pinch these circles, which do not cancel out.

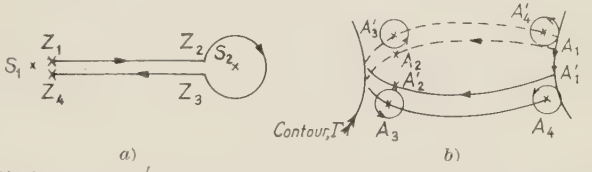

Fig. 5. – *a*) z'_{15}-plane (z-fixed). *b*) Paths of singularities on torus.

This result contrasts sharply with the result for contour integration in Euclidean space, where two coincident singularities do not interfere with one another.

Cor 3.1. F_{++} is the intersection of a_+, c_+; at any z near F_{++}, we know by Lemma 2 that one of a_+, c_+ at least is singular. We are not allowed to follow a path on the non-singular surface which encloses the singular point, which is the same as the intersection with F_{++}. For each non-singular surface, there is a cut starting at F_{++}. Similarly for the F_{--}, a_-, c_-.

Lemma 4. The conditions i) and ii) are inconsistent with the requirement that the function χ specified by the contour Γ on one side of F_{++} (and F_{--}) should be the continuation of the function specified by Γ on the other side.

Assume otherwise—*i.e.* that it is possible to continue from P to Q (Fig. 2) along some contour γ, without passing through any cuts (we know that this cannot be done both on γ_1 and γ_2 by Lemma 1 and Cor. 3.1). As we perform this continuation in z, we keep z'_{15} close to the surface a_+ which is non-singular at P. The intersections of ξ with B stay close to the tangency of $x = +1$ to Σ. In particular they cannot move round Σ (see Fig. 6).

We approach Q without passing through any cut, so we must deform Γ away from the approaching singularities A, A' (the singularity at $x = +1$ we ignore as having been disposed of in Lemma 1). Letting A, A' coincide at

$\xi \equiv x = +1$ clearly cannot pinch Γ, so a_+ remains non-singular; by Lemma 2, c_+ is singular. This contradicts i) and ii).

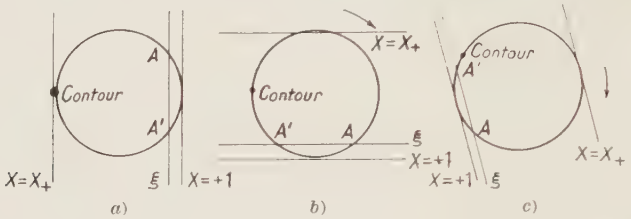

Fig. 6. – *a*) Initially at P. *b*) Half-way round γ_1. *c*) Near Q.

So χ consists of five distinct branches of an analytic function, one for each of the segments into which the four F-points divide the physical region. The problem is which branch to continue to complex z, or where to draw the cuts between different continuations. We would like to be able to draw them so as to eliminate complex singularities, *i.e.* to limit the region in which $a_\pm$ are singular to the real axis, or some neighbourhood of the real axis (since all the other singularities are either real or independent of z).

Lemma 5. It is possible to draw the cuts so as to make χ analytic except in an arbitrarily small neighbourhood of the real z axis.

Consider first case (1) in which $F_{++} < F_{--}$, so that for $F_{++} < z < F_{--}$ $c_\pm$ are singular and $a_\pm$ are non-singular. We now draw out cuts just above and below the real axis from $-\infty$ to F_{++} and from F_{--} to $+\infty$ (Fig. 7*a*). Then the singular parts of the $a_\pm$ surfaces are limited to the z-regions between the cuts *i.e.* to a neighbourhood of the real axis.

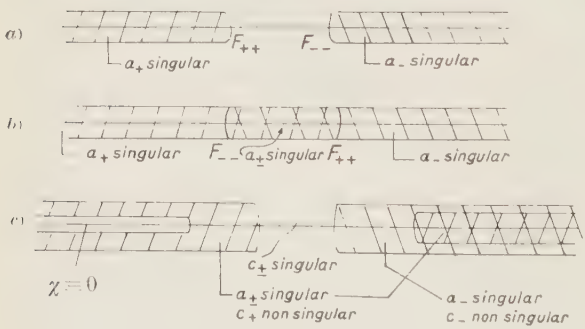

Fig. 7.

When $F_{++} > F_{--}$ (case (2)) we do precisely the same thing (Fig. 7*b*). The function we take for χ is now not the continuation of any physical value of χ. It is, however, the natural continuation in, say, the variable λ from case (1) to case (2). The relation between the values of χ in the two half-planes can be obtained by continuation in λ also, even when in case (2) the two regions have no line in common.

The cuts obtained in Lemma 1 are taken inside these cuts.

What this means can be seen as follows. In case (1) we fix z at a point where we know $a_\pm$ are not singular. By Lemma 3 we know that there are cuts attached to the points $c_\pm$ in the z'_{15} plane, through which we cannot continue the $a_\pm$. We continue in (z, z'_{15}) near to the a_+ surface, say, to that z'_{15} moves first round one side of c_+ then round the other side (Fig. 8*a*), in each case ending near the cut (at Z_1, Z_2 respectively). During this, z moves round F_{--} (Fig. 2). Along γ'_1, γ'_2 the integrand singularities A, A' stay near to the tangency of $x=+1$ with Σ, which moves round Σ, the direction in which it moves depending on which of γ_1, γ_2 we move on, as in the proof of Lemma 1.

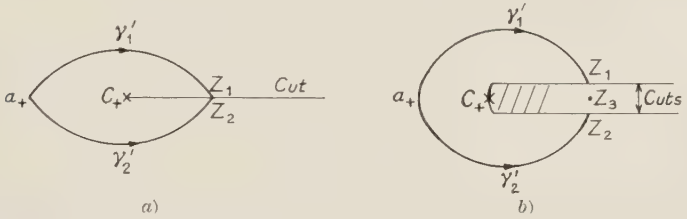

Fig. 8.

So the difference between Z_1 and Z_2 as far as a_+ is concerned is that the two singularities A, A' are together on one side or the other of the contour. The cut from c_+ is thus a double one, in the sense that passing over it corresponds to two integrand singularities passing through the contour. It is quite permissible to split this cut into two (Fig. 8*b*) corresponding to the two singularities passing one at a time through the contour. Between the cuts, say at Z_3, A and A' are on opposite sides of the contour for z at a_+, which is therefore singular, and similarly c_+ is non-singular.

We have to choose the region between the cuts to include on the a_+ surface the physical z-region between -1 and F_{++}. We choose it to be small, and to contain the real z-axis from -1 to $-\infty$.

Two loose ends remain. Firstly we must discuss F_{+-} and F_{-+}. We have seen that they are not infinities of χ and that they do not influence the presence of other singularities. So if it were not for the fact that χ as defined is zero in the physical region outside (F_{--}, F_{-+}), we could, forget about them. The simplest solution is merely to separate off the offending region by cuts starting at F_{+-}, F_{-+} and going to $-\infty$, $+\infty$ respectively, inside the cuts of Lemma 5, and to allow χ to be identically zero inside these new cuts.

Secondly, when there are two F_{++}, say, we can proceed in exactly the same way, splitting the cuts from the F's so as to limit the region in which the $a_\pm$ are singular to strips about the real axis; *e.g.* in case (3) we can have $-1<F_{+-}<F_{++}<F_{--}<F_{++}<1$, so we take cuts as in Fig. 7*c*. Again these cuts overlap if there is no real axis region with both $c_\pm$ singular.

4. – General unitarity terms.

The n-particle term in the unitarity equation is given by

$$A^{(n)}(s_{12},z) = \int \prod_{k=5}^{n+4} \delta(p_k^2 - m_k^2)\, \mathrm{d}^4 p_k \cdot \delta\Big(p_1 + p_2 - \sum_{k=5}^{n+4} p_k\Big) \cdot \\ \cdot M_1^{(n)*}(p_1, p_2, p_5 \dots p_{n+4})\, M_2^{(n)}(p_3, p_4, p_5 \dots p_{n+4}) \,.$$

We perform the p_6 integration by means of the energy-momentum conservation δ-function, then transform each of the other integrations to integrations over invariants by means of the variable changes:

$$(19) \qquad p_k \to p_k^2\,, \qquad s_k = (p_k - p_1 - p_2)^2\,, \qquad s_k^{(1)} = (p_k + p_k^{(1)})^2\,, \qquad s_k^{(2)} = (p_k + p_k^{(2)})^2\,, \\ (k = 5, 7, \dots, n+4),$$

where $p_k^{(1)}$, $p_k^{(2)}$ will be chosen later. If we take the centre of momentum frame of the ingoing particles, so that

$$p_k = (E_k, q_k)\,, \qquad p_k^{(i)} = (E_k^{(i)}, q_k^{(i)}) \qquad (i = 1, 2),$$

the transformation Jacobians become

$$\left\{\frac{\partial(p_k^2 \dots s_k^{(2)})}{\partial(p_{k,0} \dots p_{k,3})}\right\}^2 = 2^8 s_{12} \begin{vmatrix} q_k^2 & q_k \cdot q_k^{(1)} & q_k \cdot q_k^{(2)} \\ q_k \cdot q_k^{(1)} & q_k^{(1)2} & q_k^{(1)} \cdot q_k^{(2)} \\ q_k \cdot q_k^{(2)} & q_k^{(1)} \cdot q_k^{(2)} & q_k^{(2)2} \end{vmatrix} = D_k^2\,,$$

say, (cf. Appendix I of I).

We can now integrate out the δ-functions, except $\delta(p_6^2 - m_6^2)$, leaving

$$A^{(n)} = \int M_1^* M_2 \delta(p_6^2 - m_6^2) \prod_{k=5}^{n+4}{}' \frac{\mathrm{d}s_k\, \mathrm{d}s_k^{(1)}\, \mathrm{d}s_k^{(2)}}{D_k}\,, \qquad \left(\begin{array}{c}\text{where by } \prod_k{}' \text{ we mean the} \\ k = 6 \text{ term is omitted}\end{array}\right).$$

The problem is now to choose the $p_k^{(i)}$ in such a way as to make $(p_6^2 - m_6^2)$ and the D_k simple. This is solved by the following choice for $n \geqslant 4$:

$$p_5^{(1)} = -p_1\,, \quad p_5^{(2)} = -p_3\,, \quad p_7^{(1)} = -p_2\,, \quad p_7^{(2)} = -p_4 \qquad \text{as in I;}$$

$$p_8^{(1)} = p_5\,, \quad p_8^{(2)} = p_7\,; \quad \text{and} \quad p_k^{(1)} = p_5 + p_7\,, \quad p_k^{(2)} = \sum_{j=8}^{k-1} p_j\,, \qquad (k \geqslant 9).$$

This gives a complete set of invariants for M_1 and M_2 (*i.e.* there are $4(n-2)-10$ invariants for each function, and they are clearly independent since, from

definition, they allow an inductive construction of the system of momenta). In terms of these invariants we have

$$p_6^2 - m_6^2 = \left[s_{12}^{\frac{1}{2}} - \sum_5^{n+4}{}' E_k\right]^2 - \left[\sum_5^{n+4}{}' q_k\right]^2 - m_6^2 .$$

The terms of $\left[\sum' q_k\right]^2$ are

$$(q_5 + q_7)^2 = q_5^2 + q_7^2 + 2q_5 \cdot q_7 ,$$

$$2(q_5 + q_7)\cdot \sum_{k=8}^{n+4} q_k = 2m_8^2 + m_5^2 + m_7^2 + 2E_8(E_5 + E_7) - s_8^{(1)} - s_8^{(2)} + \\ + \left[\sum_{k=9}^{n+4} m_k^2 + m_5^2 + m_7^2 + 2(E_5E_k + E_7E_k + E_5E_7) - s_k^{(1)} - 2q_5 \cdot q_7\right] ,$$

$$\left[\sum_{k=8}^{n+4} q_k\right]^2 = - s_{n+4}^{(2)} + \left[\sum_{k=8}^{n+4} E_k\right]^2 .$$

Noting that $E_k = (1/2s_{12}^{\frac{1}{2}})(s_{12} + m_k^2 - s_k)$, $q_k^2 = E_k^2 - m_k^2$ depend only on the s_k, we see that we can write

$$p_6^2 - m_6^2 = A + 2(n-5)q_5 \cdot q_7 ,$$

where A depends only on the s_k, and $s_l^{(1)}$, $s_l^{(2)}$ for $l \geqslant 8$; in particular the dependence of $p_6^2 - m_6^2$ on $s_5^{(i)}$ and $s_7^{(i)}$ comes only from $q_5 \cdot q_7$. Introducing $z_{57} = \cos(q_5, q_7)$, for $n \neq 5$ we have $p_6^2 - m_6^2 = 2(n-5)q_5q_7(\lambda^{(n)} + z_{57})$.

It is easily seen that the dependence of the D_k $(k \geqslant 8)$ on the $s_5^{(i)}$, $s_7^{(i)}$ also occurs through $q_5 \cdot q_7$, and this can be substituted for directly from the δ-function. We note also that with this choice of invariants the total Jacobian is the product of the separate Jacobians. Thus, after transforming the $s_5^{(i)}$, $s_7^{(i)}$ integrations to integrations over z_{15}, z_{35} and z_{27}, z_{47} as in I we are left with

$$(20) \qquad A^{(n)} = \int M_1^{(n)*} M_2^{(n)} \prod_{k=8}^{n+4} \frac{\mathrm{d}s_k \, \mathrm{d}s_k^{(1)} \mathrm{d}s_k^{(2)}}{D_k} \, \mathrm{d}s_5 \, \mathrm{d}s_7 \cdot \\ \cdot \frac{2^{n-6}}{(n-5)s_{12}} \frac{\delta(\lambda^{(n)} + z_{57}) \, \mathrm{d}z_{15} \, \mathrm{d}z_{35} \, \mathrm{d}z_{47} \, \mathrm{d}z_{27}}{\sqrt{k(z, z_{15}, z_{35})k(z, z_{27}, z_{47})}} ,$$

where we introduce a factor 2^{n-1} since each of the transformations (19) is 2 to 1. We also write $z = z_{13} = z_{24}$.

Comparing this equation with eq. (8) of I it is seen that as far as the first four integrations are concerned $A^{(n)}$ has precisely the same form as $A^{(3)}$ for all $n \geqslant 4$ except $n = 5$. Thus any conclusions reached for the three-particle terms based only on the discussion of these four integrations are immediately valid for the higher terms provided the assumptions on which they

are founded are also made for the amplitudes $M_1^{(n)}$, $M_2^{(n)}$ appearing here. In particular if we assume $M_1^{(n)}$, $M_2^{(n)}$ to be analytic in the cut planes of the variables z_{15}, z_{47} respectively (with real cuts), the results of I tell us that $A^{(n)}$ is analytic in the cut z-plane. (To show this we only, in fact, perform two of the integrations, although we do use our knowledge of the ranges of the other integrations.)

There remains, then, the five-particle term. In this the argument of the δ-function is independent of the last four integration variables. This in itself is a simplifying fact, except that it does not allow the z_{57} dependence of the D_k ($k \geqslant 8$) to be removed. However we can readily draw one conclusion: the end-points of the z_{15} integration are the roots of $k(z, z_{35}, z_{15}) = 0$, so that if $M_1^{(5)}$ has a singularity at $z_{15} = z'_{15}$, $A^{(5)}$ will have an end-point singularity where $k(z, z_{35}, z'_{15}) = 0$. For z'_{15} real and greater than unity this singularity maps out in the z-plane an ellipse with foci ± 1 and semi-major axis $|z'_{15}|$ as z_{35} covers the interval $[-1, 1]$. This singularity is certainly present, since it is of end-point type. There will always be a fixed minimum real z'_{15} at which $M_1^{(5)}$ has a singularity, so we will always be confined within some ellipse, and no amount of iteration of the unitarity equation will allow us to extend the analyticity domain for $A^{(5)}$ beyond it.

* * *

I am indebted to Dr. J. C. Polkinghorne for continued help. I would also like to thank Dr. R. J. Eden and Professor S. B. Treiman for discussions on this work.

RIASSUNTO (*)

Si discute con maggiore completezza una analisi precedente sull'analiticità del contributo dell'unitarietà di tre particelle alla parte assorbente dello scattering. Si mostra che il termine generico si riduce alla stessa forma del termine a tre particelle.

(*) *Traduzione a cura della Redazione.*

IL NUOVO CIMENTO Vol. XX, N. 4 16 Maggio 1961

Transformations of Relativistic Two-Particle Equations.

E. Eriksen

Institute for Theoretical Physics, University of Oslo - Blindern

(ricevuto il 6 Marzo 1961)

Summary. — It is shown that relativistic two-particle equations like the Breit equation and the Hermitian part of the three-dimensional Bethe-Salpeter equation, in the c.m. system can be transformed to new canonical forms which are generalizations of the Foldy-Wouthuysen-Tani representation and the Cini-Touschek representation, respectively. The expansion of the transformed Hamiltonian is in powers of the inverse momentum. In the case of particles with equal masses also an expansion in powers of the electric charge is made.

1. – Introduction.

In the last decade there has been an increasing interest in certain new representations of relativistic wave equations. The reason is partly that computations may become simpler in the new representations, partly that the transformed equations in a more direct way exhibit the particle's properties in the non-relativistic and the ultra-relativistic limit.

In the well-known Foldy-Wouthuysen [1]-Tani [2] (FWT) representation the Hamiltonian for a free fermion is $H=\beta E_0=\beta(m^2+p^2)^{\frac{1}{2}}$. The Dirac matrix β is a constant of the motion, which represents the sign of the energy. In the non-relativistic limit this Hamiltonian and Dirac's Hamiltonian are equal. In the case of external fields, a sequence of transformations can be made, making β to be a constant of the motion to any order in the inverse mass. This expansion is obviously restricted to weak fields and to non-relativistic velocities. The dominating part of the wave equation is essentially Pauli's equation for spin $\frac{1}{2}$ particles.

(1) L. L. Foldy and S. A. Wouthuysen: *Phys. Rev.*, **78**, 29 (1950).
(2) S. Tani: *Progr. Theor. Phys.*, **6**, 267 (1951).

A similar expansion for relativistic two-particle equations has been given by CHRAPLYVY ([3]). He showed that the Hamiltonian for particles with unequal masses can be transformed to an even-even matrix to any order in the inverse masses. It was however found that the case of equal masses represented a singularity, giving an infinite expression for the transformations which remove odd-odd terms. When the less stringent requirement of an upper-upper separating transformed Hamiltonian was introduced, CHRAPLYVY was able to remove undesired terms to any order in the inverse mass.

In the Cini-Touschek (CT) representation ([4-6]) the sign of the energy of a free Dirac-particle is given by $\alpha_p \equiv \boldsymbol{\alpha p}/p = -\gamma_5\sigma_p$, where γ_5 represents the chirality and σ_p the helicity $\equiv \boldsymbol{\sigma p}/p$. The Hamiltonian is $H = \alpha_p E_0$, which is equal to Dirac's Hamiltonian in the limit of vanishing mass. This representation is—to the author's knowledge—not generalized to interacting particles. There seems to be different possibilities for generalizations, depending on whether the expansions are made in powers of $1/p$ or in powers of the coupling constant, say, and depending on whether one wants to have α_p^{I} and α_p^{II} or γ_5^{I} and γ_5^{II} as constants of the motion.

In the case of a single particle in a static field, PURSEY ([7]) has made an expansion in powers of the mass with γ_5 as a constant of the motion.

Recently ERIKSEN and KOLSRUD ([8]) have found certain transformations for a fermion in an external field, giving an even Hamiltonian as a series expansion in powers of the coupling constant.

In the present paper we shall be concerned with relativistic two-particle equations like the Breit equation and the Hermitian part of the three-dimensional Bethe-Salpeter ([9]) equation. These equations will be transformed to new canonical forms in the center of mass system. These are generalizations of respectively the FWT-equation and the CT-equation. The Hamiltonians are series expansions in powers of the inverse momentum. In the case of equal masses the expansion is also made in powers of the electric charge.

2. – Notation and classification of terms.

The transformation method which will be used is not contingent upon any special type of interaction between the two fermions. However, in order to

([3]) Z. V. CHRAPLYVY: *Phys. Rev.*, **91**, 388; **92**, 1310 (1953).
([4]) M. CINI and B. TOUSCHEK: *Nuovo Cimento*, **7**, 422 (1958).
([5]) S. K. BOSE, A. GAMBA and E. C. G. SUDARSHAN: *Phys. Rev.*, **113**, 1661 (1959).
([6]) P. Y. PAC: *Progr. Theor. Phys.*, **21**, 64; **22**, 857 (1959).
([7]) D. L. PURSEY: *Nucl. Phys.*, **8**, 595 (1958).
([8]) E. ERIKSEN and M. KOLSRUD: *Suppl. Nuovo Cimento*, to be published.
([9]) E. E. SALPETER: *Phys. Rev.*, **87**, 328 (1952).

explain notation and classification of terms, let us write down the equations which we shall have in mind. The Hermitian part of the three-dimensional Bethe-Salpeter (9) equation reads

$$(1) \qquad i\frac{\partial \Psi}{\partial t} = (H_0^{\mathrm{I}} + H_0^{\mathrm{II}} + \tfrac{1}{4}[\lambda_0^{\mathrm{I}} + \lambda_0^{\mathrm{II}}, V_B]_+)\Psi ,$$

where
$$H_0^{\mathrm{I}} = \beta^{\mathrm{I}} m^{\mathrm{I}} + \boldsymbol{\alpha}^{\mathrm{I}} \boldsymbol{p}^{\mathrm{I}} ,$$
$$H_0^{\mathrm{II}} = \beta^{\mathrm{II}} m^{\mathrm{II}} + \boldsymbol{\alpha}^{\mathrm{II}} \boldsymbol{p}^{\mathrm{II}} ,$$
$$\lambda_0^{\mathrm{I}} = H_0^{\mathrm{I}}/E_0^{\mathrm{I}} = \text{sign of } H_0^{\mathrm{I}} ,$$
$$\lambda_0^{\mathrm{II}} = H_0^{\mathrm{II}}/E_0^{\mathrm{II}} = \text{sign of } H_0^{\mathrm{II}} .$$

V_B is the Breit interaction term,

$$(2) \qquad V_B \quad \frac{e^{\mathrm{I}} e^{\mathrm{II}}}{r}\left(1 - \frac{\boldsymbol{\alpha}^{\mathrm{I}}\boldsymbol{\alpha}^{\mathrm{II}}}{2} \quad \frac{(\boldsymbol{\alpha}^{\mathrm{I}}\boldsymbol{r})(\boldsymbol{\alpha}^{\mathrm{II}}\boldsymbol{r})}{2r^2}\right).$$

If the sum $\lambda_0^{\mathrm{I}} + \lambda_0^{\mathrm{I}}$ in the anticommutator is replaced by 2, we obtain the well known Breit equation,

$$(3) \qquad i\frac{\partial \Psi}{\partial t} = (H_0^{\mathrm{I}} + H_0^{\mathrm{II}} + V_B)\Psi .$$

Units are chosen such that $\hbar = c = 1$. Quantities referring to each of the two particles are labelled by roman numbers I and II, respectively. The wave function has sixteen components Ψ_{kK} with $k, K = 1, 2, 3, 4$. The lower case subscript refers to particle I and the capital one to particle II. The Hamiltonian is composed of terms which are direct products of Dirac matrices, labelled by I and II, respectively. When a matrix is single, the direct product with the unit matrix is understood. When a matrix $\omega^{\mathrm{I}}\omega^{\mathrm{II}}$ acts on Ψ, the first matrix acts on the index k and the second matrix on the index K. Any Dirac matrix labelled by I commutes with any of those labelled by II.

Let us choose a quantity (say $1/p$ or $e^{\mathrm{I}}e^{\mathrm{II}}$) to characterize the order of magnitude and let us express the Hamiltonian as a sum of terms of increasing order:

$$(4) \qquad H = H^{\mathrm{I}} + H^{\mathrm{II}} + (\mathscr{C}\mathscr{C})_1 + (\mathscr{C}\mathscr{A})_1 + (\mathscr{A}\mathscr{C})_1 + (\mathscr{A}\mathscr{A})_1 + \\ + (\mathscr{C}\mathscr{C})_2 + (\mathscr{C}\mathscr{A})_2 + (\mathscr{A}\mathscr{C})_2 + (\mathscr{A}\mathscr{A})_2 + \dots .$$

The lowest order terms are the operators H^{I} and H^{II}, which are assumed to commute. The partition of the remaining terms is made by means of the

operators

$$\lambda^{\mathrm{I}} = H^{\mathrm{I}}/E^{\mathrm{I}}, \qquad \text{where } E^{\mathrm{I}} = |H^{\mathrm{I}}|,$$
$$\lambda^{\mathrm{II}} = H^{\mathrm{II}}/E^{\mathrm{II}}, \qquad \text{where } E^{\mathrm{II}} = |H^{\mathrm{II}}|.$$

Any operator, F, can be written as the sum of four parts,

$$F = (\mathscr{C}\mathscr{C}) + (\mathscr{C}\mathscr{A}) + (\mathscr{A}\mathscr{C}) + (\mathscr{A}\mathscr{A}),$$

where $(\mathscr{C}\mathscr{C})$ commutes with λ^{I} and λ^{II}, $(\mathscr{C}\mathscr{A})$ commutes with λ^{I} and anticommutes with λ^{II}, and so forth.

$$(\mathscr{C}\mathscr{C}\ ) = \tfrac{1}{4}\lambda^{\mathrm{I}}\lambda^{\mathrm{II}}[\lambda^{\mathrm{I}}, [\lambda^{\mathrm{II}}, F]_+]_+$$
$$(\mathscr{C}\mathscr{A}\ ) = \tfrac{1}{4}\lambda^{\mathrm{I}}\lambda^{\mathrm{II}}[\lambda^{\mathrm{I}}, [\lambda^{\mathrm{II}}, F]]_+$$
$$(\mathscr{A}\mathscr{C}\ ) = \tfrac{1}{4}\lambda^{\mathrm{I}}\lambda^{\mathrm{II}}[\lambda^{\mathrm{II}}, [\lambda^{\mathrm{I}}, F]]_+$$
$$(\mathscr{A}\mathscr{A}) = \tfrac{1}{4}\lambda^{\mathrm{I}}\lambda^{\mathrm{II}}[\lambda^{\mathrm{II}}, [\lambda^{\mathrm{I}}, F]].$$

This way of classifying terms is quite analogous to the classification in terms of even-even, even-odd, odd-even and odd-odd operators. In fact, if we let the inverse masses determine the order of magnitude, we have,

$$H^{\mathrm{I}} = \beta^{\mathrm{I}} m^{\mathrm{I}} \qquad H^{\mathrm{II}} = \beta^{\mathrm{II}} m^{\mathrm{II}}$$
$$\lambda^{\mathrm{I}} = \beta^{\mathrm{I}} \qquad \lambda^{\mathrm{II}} = \beta^{\mathrm{II}}$$

and

$$H = \beta^{\mathrm{I}} m^{\mathrm{I}} + \beta^{\mathrm{II}} m^{\mathrm{II}} + (\mathscr{E}\mathscr{E})_1 + (\mathscr{E}\mathscr{O})_1 + (\mathscr{O}\mathscr{E})_1 + (\mathscr{O}\mathscr{O})_1 + \ldots .$$

Let us write down the four types of terms in the following cases:

a) Order of magnitude defined by $e^{\mathrm{I}}e^{\mathrm{II}}$.

$$H^{\mathrm{I}} = \beta^{\mathrm{I}} m^{\mathrm{I}} + \boldsymbol{\alpha}^{\mathrm{I}}\boldsymbol{p}^{\mathrm{I}} \qquad H^{\mathrm{II}} = \beta^{\mathrm{II}} m^{\mathrm{II}} + \boldsymbol{\alpha}^{\mathrm{II}}\boldsymbol{p}^{\mathrm{II}}$$
$$\lambda^{\mathrm{I}} = H^{\mathrm{I}}/E^{\mathrm{I}} \qquad \lambda^{\mathrm{II}} = H^{\mathrm{II}}/E^{\mathrm{II}}.$$

Breit equation:

(5*a*) $$(\mathscr{C}\mathscr{C}\ )_1 = V_B^{cc} = \tfrac{1}{4}\lambda^{\mathrm{I}}\lambda^{\mathrm{II}}[\lambda^{\mathrm{I}}, [\lambda^{\mathrm{II}}, V_B]_+]_+$$

(5*b*) $$(\mathscr{C}\mathscr{A}\ )_1 = V_B^{ca} = \tfrac{1}{4}\lambda^{\mathrm{I}}\lambda^{\mathrm{II}}[\lambda^{\mathrm{I}}, [\lambda^{\mathrm{II}}, V_B]]_+$$

(5*c*) $$(\mathscr{A}\mathscr{C}\ )_1 = V_B^{ac} = \tfrac{1}{4}\lambda^{\mathrm{I}}\lambda^{\mathrm{II}}[\lambda^{\mathrm{II}}, [\lambda^{\mathrm{I}}, V_B]]_+$$

(5*d*) $$(\mathscr{A}\mathscr{A})_1 = V_B^{aa} = \tfrac{1}{4}\lambda^{\mathrm{I}}\lambda^{\mathrm{II}}[\lambda^{\mathrm{II}}, [\lambda^{\mathrm{I}}, V_B]].$$

Higher order terms are zero.

Bethe-Salpeter equation:

$$(6a) \qquad (\mathscr{C}\mathscr{C}\ )_1 = \tfrac{1}{2}(\lambda^{\mathrm{I}} + \lambda^{\mathrm{II}})\, V_B^{cc}$$

$$(6b) \qquad (\mathscr{C}\mathscr{A}\ )_1 = \tfrac{1}{2}\lambda^{\mathrm{I}} V_B^{ca}$$

$$(6c) \qquad (\mathscr{A}\mathscr{C}\ )_1 = \tfrac{1}{2}\lambda^{\mathrm{II}} V_B^{ac}$$

$$(6d) \qquad (\mathscr{A}\mathscr{A})_1 = 0\,.$$

Higher order terms are zero.

b) Order of magnitude defined by $1/p^{\mathrm{I}}$ and $1/p^{\mathrm{II}}$.

$$H^{\mathrm{I}} = \boldsymbol{\alpha}^{\mathrm{I}}\boldsymbol{p}^{\mathrm{I}}\,, \qquad H^{\mathrm{II}} = \boldsymbol{\alpha}^{\mathrm{II}}\boldsymbol{p}^{\mathrm{II}}\,,$$

$$\lambda^{\mathrm{I}} = \alpha_p^{\mathrm{I}} = \frac{\boldsymbol{\alpha}^{\mathrm{I}}\boldsymbol{p}^{\mathrm{I}}}{p^{\mathrm{I}}}\,, \qquad \lambda^{\mathrm{II}} = \alpha_p^{\mathrm{II}} = \frac{\boldsymbol{\alpha}^{\mathrm{II}}\boldsymbol{p}^{\mathrm{II}}}{p^{\mathrm{II}}}\,.$$

Breit equation:

$$(7a) \qquad (\mathscr{C}\mathscr{C}\ )_1 = V_B^{cc} = \tfrac{1}{4}\,\alpha_p^{\mathrm{I}}\alpha_p^{\mathrm{II}}[\alpha_p^{\mathrm{I}}, [\alpha_p^{\mathrm{II}}\, V_B]_+]_+$$

$$(7b) \qquad (\mathscr{C}\mathscr{A}\ )_1 = m^{\mathrm{II}}\beta^{\mathrm{II}} + V_B^{cA} = m^{\mathrm{II}}\beta^{\mathrm{II}} + \tfrac{1}{4}\alpha_p^{\mathrm{I}}\alpha_p^{\mathrm{II}}[\alpha_p^{\mathrm{I}}, [\alpha_p^{\mathrm{II}}, V_B]]_+$$

$$(7c) \qquad (\mathscr{A}\mathscr{C}\ )_1 = m^{\mathrm{I}}\beta^{\mathrm{I}} + V_B^{Ac} = m^{\mathrm{I}}\beta^{\mathrm{I}} + \tfrac{1}{4}\alpha_p^{\mathrm{I}}\alpha_p^{\mathrm{II}}[\alpha_p^{\mathrm{II}}, [\alpha_p^{\mathrm{I}}, V_B]]_+$$

$$(7d) \qquad (\mathscr{A}\mathscr{A})_1 = V_B^{AA} = \tfrac{1}{4}\alpha_p^{\mathrm{I}}\alpha_p^{\mathrm{II}}[\alpha_p^{\mathrm{I}}, [\alpha_p^{\mathrm{II}}, V_B]]\,.$$

Higher order terms are zero.

Bethe-Salpeter equation:

$$(8a) \qquad (\mathscr{C}\mathscr{C}\ )_1 = \tfrac{1}{2}(\alpha_p^{\mathrm{I}} + \alpha_p^{\mathrm{II}})\, V_B^{cc},$$

$$(8b) \qquad (\mathscr{C}\mathscr{A}\ )_1 = m^{\mathrm{II}}\beta^{\mathrm{II}} + \tfrac{1}{2}\,\alpha_p^{\mathrm{I}}\, V_B^{cA},$$

$$(8c) \qquad (\mathscr{A}\mathscr{C}\ )_1 = m^{\mathrm{I}}\beta^{\mathrm{I}} + \tfrac{1}{2}\,\alpha_p^{\mathrm{II}} V_B^{Ac}\,,$$

$$(8d) \qquad (\mathscr{A}\mathscr{A})_1 = 0\,,$$

$$(8e) \qquad (\mathscr{C}\mathscr{C}\ )_2 = \frac{1}{4}\, m^{\mathrm{I}}\left[\beta^{\mathrm{I}}\frac{1}{p^{\mathrm{I}}},\ V_B^{Ac}\right]_+ + \frac{1}{4}\, m^{\mathrm{II}}\left[\beta^{\mathrm{II}}\frac{1}{p^{\mathrm{II}}},\ V_B^{cA}\right]_+,$$

and so forth.

3. – Transformation theory.

We consider a Hamiltonian where the terms are ordered and classified as explained above,

$$H = H^{\mathrm{I}} + H^{\mathrm{II}} + (\mathscr{C}\mathscr{C})_1 + (\mathscr{C}\mathscr{A})_1 + (\mathscr{A}\mathscr{C})_1 + (\mathscr{A}\mathscr{A})_1 + \text{higher order terms}\,.$$

In addition to the assumption, $[H^{\mathrm{I}}, H^{\mathrm{II}}] = 0$, we also postulate a much stronger condition, namely

$$(H^{\mathrm{I}})^2 = (H^{\mathrm{II}})^2 , \tag{9}$$

$$i.e. \quad |H^{\mathrm{I}}| = |H^{\mathrm{II}}| = E .$$

In the center-of-mass system—which we take as our system of reference in the following—we have

$$\boldsymbol{p}^{\mathrm{I}} = -\boldsymbol{p}^{\mathrm{II}} = \boldsymbol{p} ,$$

$$(\alpha^{\mathrm{I}}\boldsymbol{p}^{\mathrm{I}})^2 = (\alpha^{\mathrm{II}}\boldsymbol{p}^{\mathrm{II}})^2 = p^2 ,$$

i.e. the condition is satisfied when the expansion is in powers of $1/p$.

If the expansion is in powers of the coupling constant $e^{\mathrm{I}}e^{\mathrm{II}}$, the condition is

$$(\beta^{\mathrm{I}}m^{\mathrm{I}} + \alpha^{\mathrm{I}}\boldsymbol{p})^2 = (\beta^{\mathrm{II}}m^{\mathrm{II}} - \boldsymbol{\alpha}^{\mathrm{II}}\boldsymbol{p})^2 ,$$

$$i.e. \quad m^{\mathrm{I}} = m^{\mathrm{II}} .$$

Let us examine whether there exists a transformation which converts the Hamiltonian

$$H = (\lambda^{\mathrm{I}} + \lambda^{\mathrm{II}})E + (\mathscr{C}\mathscr{C})_1 + (\mathscr{C}\mathscr{A})_1 + (\mathscr{A}\mathscr{C})_1 + (\mathscr{A}\mathscr{A})_1 + \ldots$$

to an operator which is of the $\mathscr{C}\mathscr{C}$-type to first order. We make a transformation generated by the first order Hermitian operator S_1.

$$H' = \exp[iS_1]H\exp[-iS_1] =$$

$$= (\lambda^{\mathrm{I}} + \lambda^{\mathrm{II}})E + i[S_1, \lambda^{\mathrm{I}}E + \lambda^{\mathrm{II}}E] + (\mathscr{C}\mathscr{C})_1 + (\mathscr{C}\mathscr{A})_1 + (\mathscr{A}\mathscr{C})_1 + (\mathscr{A}\mathscr{A})_1 +$$

$$+ \text{terms of 2nd and higher order.}$$

We get the following three equations,

$$i[S_1^{ca}, \lambda^{\mathrm{I}}E + \lambda^{\mathrm{II}}E] + (\mathscr{C}\mathscr{A})_1 = 0 , \tag{10a}$$

$$i[S_1^{ac}, \lambda^{\mathrm{I}}E + \lambda^{\mathrm{II}}E] + (\mathscr{A}\mathscr{C})_1 = 0 , \tag{10b}$$

$$i[S_1^{aa}, \lambda^{\mathrm{I}}E + \lambda^{\mathrm{II}}E] + (\mathscr{A}\mathscr{A})_1 = 0 , \tag{10c}$$

where the operators S_1^{ca}, S_1^{ac} and S_1^{aa} are respectively the $\mathscr{C}\mathscr{A}$-part, the $\mathscr{A}\mathscr{C}$-part, and the $\mathscr{A}\mathscr{A}$-part of S_1.

Eq. (10*a*) is satisfied by

$$S_1^{ca} = \frac{i}{4}\left[(\mathscr{C}\mathscr{A})_1, \frac{\lambda^{\mathrm{I}} + \lambda^{\mathrm{II}}}{E}\right] , \tag{11}$$

which can be seen as follows:

$$i[S_1^{ca}, \lambda^{\mathrm{I}}E + \lambda^{\mathrm{II}}E] = -\frac{1}{4}\left[\left[(\mathscr{C}\mathscr{A})_1, \frac{\lambda^{\mathrm{I}} + \lambda^{\mathrm{II}}}{E}\right], \lambda^{\mathrm{I}}E + \lambda^{\mathrm{II}}E\right] =$$

$$= -\frac{1}{4}(\mathscr{C}\mathscr{A})_1(\lambda^{\mathrm{I}} + \lambda^{\mathrm{II}})^2 + \frac{1}{4}\frac{\lambda^{\mathrm{I}} + \lambda^{\mathrm{II}}}{E}(\mathscr{C}\mathscr{A})_1(\lambda^{\mathrm{I}} + \lambda^{\mathrm{II}})E +$$

$$+ \frac{1}{4}(\lambda^{\mathrm{I}} + \lambda^{\mathrm{II}})E(\mathscr{C}\mathscr{A})_1\frac{\lambda^{\mathrm{I}} + \lambda^{\mathrm{II}}}{E} - \frac{1}{4}(\lambda^{\mathrm{I}} + \lambda^{\mathrm{II}})^2(\mathscr{C}\mathscr{A})_1 =$$

$$= -\frac{1}{4}(\mathscr{C}\mathscr{A})_1(\lambda^{\mathrm{I}} + \lambda^{\mathrm{II}})^2 - \frac{1}{4}(\lambda^{\mathrm{I}} + \lambda^{\mathrm{II}})^2(\mathscr{C}\mathscr{A})_1 =$$

$$= -\frac{1}{2}(\mathscr{C}\mathscr{A})_1(1 + \lambda^{\mathrm{I}}\lambda^{\mathrm{II}}) - \frac{1}{2}(1 + \lambda^{\mathrm{I}}\lambda^{\mathrm{II}})(\mathscr{C}\mathscr{A})_1 = -(\mathscr{C}\mathscr{A})_1\,, \quad \text{q.e.d.}$$

Then, eq. (10*b*) obviously has the solution,

$$S_1^{ac} = \frac{i}{4}\left[(\mathscr{A}\mathscr{C})_1, \frac{\lambda^{\mathrm{I}} + \lambda^{\mathrm{II}}}{E}\right]. \tag{12}$$

As regards eq. (10*c*), we can easily derive a necessary condition for S_1^{aa} to exist. Multiplying from the left by the operator $1 - \lambda^{\mathrm{I}}\lambda^{\mathrm{II}}$, we get

$$i[S_1^{aa}, (1 - \lambda^{\mathrm{I}}\lambda^{\mathrm{II}})(\lambda^{\mathrm{I}} + \lambda^{\mathrm{II}})E] + (1 - \lambda^{\mathrm{I}}\lambda^{\mathrm{II}})(\mathscr{A}\mathscr{A})_1 = 0\,,$$

$$i.e. \qquad (1 - \lambda^{\mathrm{I}}\lambda^{\mathrm{II}})(\mathscr{A}\mathscr{A})_1 = 0\,.$$

This equation is satisfied only when $(\mathscr{A}\mathscr{A})_1$ contains the operator $1 + \lambda^{\mathrm{I}}\lambda^{\mathrm{II}}$ to the left (or right). Thus we have to postulate a weaker condition on the transformed Hamiltonian (as was also CHRAPLYVY forced to do because of the $\mathscr{C}\mathscr{C}$-terms). We require the transformed Hamiltonian to be an operator which can be expressed as

$$H^{\mathrm{tr}} = (\mathscr{C}\mathscr{C}) + \tfrac{1}{2}(\mathscr{A}\mathscr{A})(1 - \lambda^{\mathrm{I}}\lambda^{\mathrm{II}})\,. \tag{13}$$

(This is equivalent to requiring the transformed Hamiltonian to commute with $(1+\lambda^{\mathrm{I}})(1+\lambda^{\mathrm{II}})$ and with $\lambda^{\mathrm{I}}\lambda^{\mathrm{II}}$.)

Then eq. (10*c*) is replaced by the equation,

$$i\,[S_1^{aa}, \lambda^{\mathrm{I}}E + \lambda^{\mathrm{II}}E] + \tfrac{1}{2}(1 + \lambda^{\mathrm{I}}\lambda^{\mathrm{II}})(\mathscr{A}\mathscr{A})_1 = 0\,, \tag{14}$$

a solution of which is

$$S_1^{aa} = -\frac{i}{4}(\lambda^{\mathrm{I}} + \lambda^{\mathrm{II}})\int_{-\infty}^{0}\exp[E\tau](\mathscr{A}\mathscr{A})_1\exp[E\tau]\,\mathrm{d}\tau\,. \tag{15}$$

This can be seen as follows:

$$i[S_1^{aa}, \lambda^{\mathrm{I}}E + \lambda^{\mathrm{II}}E] = \frac{1}{4}\Big[(\lambda^{\mathrm{I}} + \lambda^{\mathrm{II}})\int_{-\infty}^{0}\exp[E\tau](\mathscr{A}\mathscr{A})_1 \exp[E\tau]\,\mathrm{d}\tau,\ \lambda^{\mathrm{I}}\dot{E} + \lambda^{\mathrm{II}}E\Big] -$$

$$= -\frac{1}{4}(\lambda^{\mathrm{I}} + \lambda^{\mathrm{II}})^2\int_{-\infty}^{0}\exp[E\tau](\mathscr{A}\mathscr{A})_1 \exp[E\tau]\,\mathrm{d}\tau\, E -$$

$$-\frac{1}{4}(\lambda^{\mathrm{I}} + \lambda^{\mathrm{II}})^2 E\int_{-\infty}^{0}\exp[E\tau]\,(\mathscr{A}\mathscr{A})_1 \exp[E\tau]\,\mathrm{d}\tau =$$

$$= -\frac{1}{2}(1 - \lambda^{\mathrm{I}}\lambda^{\mathrm{II}})\int_{-\infty}^{0}\{\exp[E\tau](\mathscr{A}\mathscr{A})_1 \exp[E\tau]\,E - E\exp[E\tau](\mathscr{A}\mathscr{A})_1 \exp[E\tau]\}\,\mathrm{d}\tau =$$

$$= -\frac{1}{2}(1 + \lambda^{\mathrm{I}}\lambda^{\mathrm{II}})\int_{-\infty}^{0}\mathrm{d}\{\exp[E\tau](\mathscr{A}\mathscr{A})_1 \exp[E\tau]\} = -\frac{1}{2}(1 + \lambda^{\mathrm{I}}\lambda^{\mathrm{II}})(\mathscr{A}\mathscr{A})_1\,, \quad \text{q.e.d.}$$

To this solution we can add solutions of the homogeneous equation,

$$[X_1^{aa}, \lambda E^{\mathrm{I}} + \lambda^{\mathrm{II}}E] = 0\,,$$

$$i.e. \quad X_1^{aa} = i(\lambda^{\mathrm{I}} - \lambda^{\mathrm{II}})Y_1^{aa}\,,$$

Y_1^{aa} being an arbitrary Hermitian $\mathscr{A}\mathscr{A}$-type operator of first order. We shall not introduce any generalizations of this kind.

By means of the generating operators above, the undesired terms of first order can now be removed from the Hamiltonian. By a sequence of further canonical transformations the Hamiltonian can be brought to the desired form to any order.

At any step, the generators of the transformations are given by

$$S_n^{ca} = \frac{i}{4}\Big[(\mathscr{C}\mathscr{A})_n, \frac{\lambda^{\mathrm{I}} + \lambda^{\mathrm{II}}}{E}\Big], \tag{16}$$

$$S_n^{ac} = \frac{i}{4}\Big[(\mathscr{A}\mathscr{C})_n, \frac{\lambda^{\mathrm{I}} + \lambda^{\mathrm{II}}}{E}\Big], \tag{17}$$

$$S_n^{aa} = -\frac{i}{4}(\lambda^{\mathrm{I}} + \lambda^{\mathrm{II}})\int_{-\infty}^{0}\exp[E\tau](\mathscr{A}\mathscr{A})_n \exp[E\tau]\,\mathrm{d}\tau\,, \tag{18}$$

where $(\mathscr{C}\mathscr{A})_n$, $(\mathscr{A}\mathscr{C})_n$ and $(\mathscr{A}\mathscr{A})_n$ are the lowest order undesired terms.

To second order the result is

$$H^{\mathrm{tr}} = \lambda^{\mathrm{I}}E + \lambda^{\mathrm{II}}E + (\mathscr{C}\mathscr{C})_1 + (\mathscr{C}\mathscr{C})_2 + \tag{19a}$$

$$+ \frac{1}{8}\left[\frac{1}{E}, (\mathscr{C}\mathscr{A})_1^2 + (\mathscr{A}\mathscr{C})_1^2\right]_+ (\lambda^{\mathrm{I}} + \lambda^{\mathrm{II}})) + \tag{19b}$$

$$+ \frac{1}{8}\left[(\mathscr{A}\mathscr{A})_1, \int_{-\infty}^{0} \exp[E\tau](\mathscr{A}\mathscr{A})_1 \exp[E\tau]\,\mathrm{d}\tau\right]_+ (\lambda^{\mathrm{I}} + \lambda^{\mathrm{II}}) - \tag{19c}$$

$$- \frac{1}{4}\left\{(\mathscr{C}\mathscr{A})_1 \frac{\lambda^{\mathrm{I}}}{E}(\mathscr{C}\mathscr{A})_1 + (\mathscr{A}\mathscr{C})_1 \frac{\lambda^{\mathrm{II}}}{E}(\mathscr{A}\mathscr{C})_1\right\}(1 - \lambda^{\mathrm{I}}\lambda^{\mathrm{II}}) + \tag{19d}$$

$$+ \frac{1}{2}\{(\mathscr{A}\mathscr{A})_1 + (\mathscr{A}\mathscr{A})_2\}(1 - \lambda^{\mathrm{I}}\lambda^{\mathrm{II}})\,. \tag{19e}$$

We see that this operator is of the type given by eq. (13). The quantity $\lambda^{\mathrm{I}}\lambda^{\mathrm{II}}$ is a constant of the motion. If we put

$$(1 - \lambda^{\mathrm{I}}\lambda^{\mathrm{II}})\Psi = 0\,, \tag{20}$$

the terms containing the factor $(1 - \lambda^{\mathrm{I}}\lambda^{\mathrm{II}})$ on the right-hand side can be replaced by zero, and the Hamiltonian becomes a $\mathscr{C}\mathscr{C}$-type operator. This permits us to put

$$\lambda^{\mathrm{I}}\Psi' = \lambda^{\mathrm{II}}\Psi = \Psi \quad \text{or} \quad \lambda^{\mathrm{I}}\Psi' = \lambda^{\mathrm{II}}\Psi = -\Psi'\,. \tag{21a, b}$$

It should be noticed that for the Bethe-Salpeter equation with $e^{\mathrm{I}}e^{\mathrm{II}}$ as expansion parameter, the transformed Hamiltonian is by itself a $\mathscr{C}\mathscr{C}$-type operator to the order considered:

$$H_{BS}^{\mathrm{tr}} = \lambda^{\mathrm{I}}E + \lambda^{\mathrm{II}}E + (\mathscr{C}\mathscr{C})_1 + \tag{22a}$$

$$+ \frac{1}{8}\left[\frac{1}{E}, (\mathscr{C}\mathscr{A})_1^2 + (\mathscr{A}\mathscr{C})_1^2\right]_+ (\lambda^{\mathrm{I}} + \lambda^{\mathrm{II}}) - \tag{22b}$$

$$- \frac{1}{4}\left\{(\mathscr{C}\mathscr{A})_1 \frac{\lambda^{\mathrm{I}}}{E}(\mathscr{C}\mathscr{A})_1 + (\mathscr{A}\mathscr{C})_1 \frac{\lambda^{\mathrm{II}}}{E}(\mathscr{A}\mathscr{C})_1\right\}(1 - \lambda^{\mathrm{I}}\lambda^{\mathrm{II}})\,. \tag{22c}$$

Then, λ^{I} and λ^{II} (which are operators for the sign of the free particle energies) independent of each other can take the values $+1$ or -1.

4. – FWT- and CT-transformations for two interacting fermions.

Our starting point is a transformed Hamiltonian of the type

$$H = \lambda^{\mathrm{I}}E + \lambda^{\mathrm{II}}E + (\mathscr{C}\mathscr{C}) + \tfrac{1}{2}(\mathscr{A}\mathscr{A})(1 - \lambda^{\mathrm{I}}\lambda^{\mathrm{II}})\,, \tag{23}$$

where

$$[\lambda^{\mathrm{I}}, \lambda^{\mathrm{II}}] = 0\,, \qquad (\lambda^{\mathrm{I}})^2 = (\lambda^{\mathrm{II}})^2 = 1\,, \tag{24}$$

$$[(\mathscr{C}\mathscr{C}), \lambda^{\mathrm{I}}] = [(\mathscr{C}\mathscr{C}), \lambda^{\mathrm{II}}] = [(\mathscr{A}\mathscr{A}), \lambda^{\mathrm{I}}]_+ = [(\mathscr{A}\mathscr{A}), \lambda^{\mathrm{II}}]_+ = 0\,. \tag{25}$$

By means of an additional unitary transformation, λ^{I} and λ^{II} can be transformed into various types of new operators. Of special interest are the transformations

$$\lambda^{\mathrm{I}} \to \beta^{\mathrm{I}}\,, \qquad \lambda^{\mathrm{II}} \to \beta^{\mathrm{II}}$$

and

$$\lambda^{\mathrm{I}} \to \alpha_p^{\mathrm{I}}\,, \qquad \lambda^{\mathrm{II}} \to \alpha_p^{\mathrm{II}}\,,$$

giving a generalization of the FWT- and the CT-transformation, respectively.

a) *Expansion in powers of* $e^{\mathrm{I}}e^{\mathrm{II}}$. In this case we have

$$E = (m^2 + p^2)^{\frac{1}{2}}\,, \qquad \lambda^{\mathrm{I}} = \frac{\beta^{\mathrm{I}} m + \boldsymbol{\alpha}^{\mathrm{I}}\boldsymbol{p}}{E}\,, \qquad \lambda^{\mathrm{II}} = \frac{\beta^{\mathrm{II}} m - \boldsymbol{\alpha}^{\mathrm{II}}\boldsymbol{p}}{E}\,.$$

In order to get a representation related to the FWT-representation we choose a transformation $U = U^{\mathrm{I}}U^{\mathrm{II}}$, where U^{I} and U^{II} are free particle FWT-transformations,

$$U^{\mathrm{I}} = \frac{E + m + \beta^{\mathrm{I}}\boldsymbol{\alpha}^{\mathrm{I}}\boldsymbol{p}}{\sqrt{2E(E+m)}}\,, \qquad U^{\mathrm{II}} = \frac{E + m - \beta^{\mathrm{II}}\boldsymbol{\alpha}^{\mathrm{II}}\boldsymbol{p}}{\sqrt{2E(E+m)}}\,.$$

Then the $(\mathscr{C}\mathscr{C})$ term is transformed into an even-even term, and the $(\mathscr{A}\mathscr{A})$ term is transformed into an odd-odd term. The transformed result is,

$$H' = \beta^{\mathrm{I}}E + \beta^{\mathrm{II}}E + (\mathscr{E}\mathscr{E}) + \tfrac{1}{2}(\mathscr{O}\mathscr{O})(1 - \beta^{\mathrm{I}}\beta^{\mathrm{II}})\,,$$

where

$$(\mathscr{E}\mathscr{E}) = U(\mathscr{C}\mathscr{C})U^*\,, \qquad (\mathscr{O}\mathscr{O}) = U(\mathscr{A}\mathscr{A})U^*\,.$$

Putting $\beta^{\mathrm{I}}\beta^{\mathrm{II}} = 1$ and making use of eq. (5), (6) and (19), we get the following results to second order:

Breit equation:

$$H'_B = \beta^{\mathrm{I}}E + \beta^{\mathrm{II}}E + (\mathscr{E}\mathscr{E}) + \frac{1}{8}\left|\frac{1}{E}, (\mathscr{E}\mathscr{O})^2 + (\mathscr{O}\mathscr{E})^2\right|_+ (\beta^{\mathrm{I}} + \beta^{\mathrm{II}}) + \tag{26}$$

$$+ \frac{1}{8}\left|(\mathscr{O}\mathscr{O}), \int_{-\infty}^{0} \exp[E\tau](\mathscr{O}\mathscr{O})\exp[E\tau]\,\mathrm{d}\tau\right|_+ (\beta^{\mathrm{I}} + \beta^{\mathrm{II}})\,.$$

Bethe-Salpeter equation:

$$H'_{BS} = \beta^{\mathrm{I}}E + \beta^{\mathrm{II}}E + \frac{1}{2}(\mathscr{E}\mathscr{E})(\beta^{\mathrm{I}} + \beta^{\mathrm{II}}) + \frac{1}{32}\left[\frac{1}{E}, (\mathscr{E}\mathscr{O})^2 + (\mathscr{O}\mathscr{E})^2\right]_+ (\beta^{\mathrm{I}} + \beta^{\mathrm{II}})\,. \tag{27}$$

In these expressions,

$$(28)\qquad \begin{cases} (\mathscr{E}\mathscr{E}) \text{ is the even-even part of } UV_BU^*, \\ (\mathscr{E}\mathscr{O}) \text{ is the even-odd part of } UV_BU^*, \end{cases}$$

and so forth.

In order to obtain a representation related to the CT-representation we want to have λ^{I} and λ^{II} transformed into the operators $\alpha_p^{\mathrm{I}} \equiv (1/p)\boldsymbol{\alpha}^{\mathrm{I}}\boldsymbol{p}$ and $\alpha_p^{\mathrm{II}} \equiv -(1/p)\boldsymbol{\alpha}^{\mathrm{II}}\boldsymbol{p}$, respectively. This is done by the transformation $T = T^{\mathrm{I}}T^{\mathrm{II}}$ where T^{I} and T^{II} are free particle CT-transformations,

$$T^{\mathrm{I}} = \frac{E + p + \alpha_p^{\mathrm{I}}\beta^{\mathrm{I}}m}{\sqrt{2E(E+p)}}, \qquad T^{\mathrm{II}} = \frac{E + p + \alpha_p^{\mathrm{II}}\beta^{\mathrm{II}}m}{\sqrt{2E(E+p)}}.$$

Making this transformation on the Hamiltonian (23), we get terms which are classified by means of the operators α_p^{I} and α_p^{II}. Putting $\alpha_p^{\mathrm{I}}\alpha_p^{\mathrm{II}} = 1$, we get results which are quite analogous to (26) and (27):

Breit equation:

$$(29)\qquad H_B' = \alpha_p^{\mathrm{I}}E + \alpha_p^{\mathrm{II}}E + (\mathscr{C}\mathscr{C}) + \frac{1}{8}\left[\frac{1}{E}, (\mathscr{C}\mathscr{A})^2 + (\mathscr{A}\mathscr{C})^2\right]_+ (\alpha_p^{\mathrm{I}} + \alpha_p^{\mathrm{II}}) +$$

$$+ \frac{1}{8}\left[(\mathscr{A}\mathscr{A}), \int_{-\infty}^{0} \exp[E\tau](\mathscr{A}\mathscr{A})\exp[E\tau]\,\mathrm{d}\tau\right]_+ (\alpha_p^{\mathrm{I}} + \alpha_p^{\mathrm{II}}).$$

Bethe-Salpeter equation:

$$(30)\quad H_{BS}' = \alpha_p^{\mathrm{I}}E + \alpha_p^{\mathrm{II}}E + \frac{1}{2}(\mathscr{C}\mathscr{C})(\alpha_p^{\mathrm{I}} + \alpha_p^{\mathrm{II}}) + \frac{1}{32}\left[\frac{1}{E}, (\mathscr{C}\mathscr{A})^2 + (\mathscr{A}\mathscr{C})^2\right]_+ (\alpha_p^{\mathrm{I}} + \alpha_p^{\mathrm{II}}).$$

In eq. (29) and (30) the notation is:

$$(31)\qquad \begin{cases} (\mathscr{C}\mathscr{C}) = -\frac{1}{4}\alpha_p^{\mathrm{I}}\alpha_p^{\mathrm{II}}(\alpha_p^{\mathrm{I}}, [\alpha_p^{\mathrm{II}}, TV_BT^*]_+)_+, \\ (\mathscr{C}\mathscr{A}) = \frac{1}{4}\alpha_p^{\mathrm{I}}\alpha_p^{\mathrm{II}}(\alpha_p^{\mathrm{I}}, [\alpha_p^{\mathrm{II}}, TV_BT^*])_+, \\ (\mathscr{A}\mathscr{C}) = -\frac{1}{4}\alpha_p^{\mathrm{I}}\alpha_p^{\mathrm{II}}(\alpha_p^{\mathrm{II}}, [\alpha_p^{\mathrm{I}}, TV_BT^*])_+, \\ (\mathscr{A}\mathscr{A}) = \frac{1}{4}\alpha_p^{\mathrm{I}}\alpha_p^{\mathrm{II}}(\alpha_p^{\mathrm{I}}, [\alpha_p^{\mathrm{II}}, TV_BT^*]). \end{cases}$$

b) Expansion in powers of $1/p$. In the transformed Hamiltonian (19) the expansion is now in powers of $1/p$. Then we have

$$\lambda^{\mathrm{I}} = \alpha_p^{\mathrm{I}}, \qquad \lambda^{\mathrm{II}} = \alpha_p^{\mathrm{II}}, \qquad E = p.$$

Without further transformations, the Hamiltonian represents a generalization of the CT-Hamiltonian. Putting $\alpha_p^{\mathrm{I}}\alpha_p^{\mathrm{II}} = 1$, we get the following results from eq. (7), (8) and (19):

Breit equation:

$$(32)\qquad H_B' = \boldsymbol{\alpha}^{\mathrm{I}}\boldsymbol{p} - \boldsymbol{\alpha}^{\mathrm{II}}\boldsymbol{p} + V_B^{CC} + \frac{1}{8}\left[\frac{1}{p}, (V_B^{CA})^2 + (V_B^{AC})^2\right]_+ (\alpha_p^{\mathrm{I}} + \alpha_p^{\mathrm{II}})$$
$$+ \frac{m}{8}\left[\frac{1}{p}, [\beta^{\mathrm{II}}, V_B^{CA}]_+ + [\beta^{\mathrm{I}}, V_B^{AC}]_+\right]_+ (\alpha_p^{\mathrm{I}} + \alpha_p^{\mathrm{II}})$$
$$+ \frac{m^2}{2p}(\alpha_p^{\mathrm{I}} + \alpha_p^{\mathrm{II}}) + \frac{1}{8}\left[V_B^{AA}, \int_{\infty}^{0} \exp[p\tau]\, V_B^{AA} \exp[p\tau]\, \mathrm{d}\tau\right]_+ (\alpha_p^{\mathrm{I}} + \alpha_p^{\mathrm{II}}) .$$

Bethe-Salpeter equation:

$$(33)\qquad H_{BS}' = \boldsymbol{\alpha}^{\mathrm{I}}\boldsymbol{p} - \boldsymbol{\alpha}^{\mathrm{II}}\boldsymbol{p} + \frac{1}{2} V_B^{CC}(\alpha_p^{\mathrm{I}} + \alpha_p^{\mathrm{II}}) +$$
$$+ \frac{1}{32}\left[\frac{1}{p}, (V_B^{CA})^2 + (V_B^{AC})^2\right]_+ (\alpha_p^{\mathrm{I}} + \alpha_p^{\mathrm{II}}) + \frac{m}{4}\left[\frac{\beta^{\mathrm{I}}}{p}, V_B^{AC}\right]_+ + \frac{m}{4}\left[\frac{\beta^{\mathrm{II}}}{p}, V_B^{CA}\right]_+ +$$
$$- \frac{m}{8}\left[\frac{1}{p}, [\beta^{\mathrm{II}}, V_B^{CA}]_+ + [\beta^{\mathrm{I}}, V_B^{AC}]_+\right]_+ + \frac{m^2}{2p}(\alpha_p^{\mathrm{I}} + \alpha_p^{\mathrm{II}}) .$$

In these Hamiltonians we can put

$$\alpha_p^{\mathrm{I}} = \alpha_p^{\mathrm{II}} = 1 , \qquad i.e. \qquad \boldsymbol{\alpha}^{\mathrm{I}}\boldsymbol{p} - \boldsymbol{\alpha}^{\mathrm{II}}\boldsymbol{p} = 2p ,$$

or

$$\alpha_p^{\mathrm{I}} = \alpha_p^{\mathrm{II}} = -1 , \qquad i.e. \qquad \boldsymbol{\alpha}^{\mathrm{I}}\boldsymbol{p} - \boldsymbol{\alpha}^{\mathrm{II}}\boldsymbol{p} = -2p .$$

The meaning of the symbols V_B^{CC}, V_B^{CA}, V_B^{AC} and V_B^{AA} is evident from eq. (7).

RIASSUNTO (*)

Dimostro che le equazioni relativistiche a due particelle, come l'equazione di Breit e la parte hermitiana della equazione tridimensionale di Bethe-Salpeter, nel sistema del centro di massa possono essere trasformate in nuove forme canoniche che sono rispettivamente generalizzazioni della rappresentazione di Foldy-Wouthuysen-Tani e della rappresentazione di Cini-Touschek. Lo sviluppo dell'hamiltoniano trasformato si effettua in serie di potenze del momento inverso. Nel caso di particelle di massa uguale si effettua anche uno sviluppo in serie di potenze della carica elettrica.

(*) *Traduzione a cura della Redazione.*

IL NUOVO CIMENTO Vol. XX, N. 4 16 Maggio 1961

Correlation Theory of Stationary Electromagnetic Fields.

Part III. - The Presence of Random Sources (*).

P. Roman (**)

Department of Physics, Boston University, Boston, Mass.

(ricevuto il 10 Marzo 1961)

Summary. — The previously developed correlation theory of stationary random electromagnetic fields is extended to the case in which the fields interact with stationary random charges and currents. The basic field equations are deduced and are found to be second order partial differential equations. An analogue to the equation of continuity is derived and some illustrative examples are discussed. Wave equations, which are of the fourth order, are deduced for the electric and magnetic correlation tensors. The theory presented in this paper may have various applications for the theory of plasmas.

1. – Introduction and notation.

In recent years considerable success has been achieved in formulating rigorous laws for the propagation of the second order correlation functions related to stationary electromagnetic fields [1-3].

(*) This research has been supported in part by the Electronics Research Directorate of the U. S. Air Force Research Division, Air Research and Development Command, under Contract AF 19(604)-8022.

(**) On leave of absence from the Department of Theoretical Physics, University of Manchester, Manchester 13, England.

(1) E. Wolf: *Nuovo Cimento*, **12**, 884 (1954).

(2) E. Wolf: *Nuovo Cimento*, **13**, 1165 (1959).

(3) E. Wolf: Contribution in *Proc. Symposium on Astronom. Optics* (Amsterdam, 1956), p. 177.

In particular, in two recent papers ([4,5]), ROMAN and WOLF derived a set of basic second-order differential equations which govern the space-time behavior of the correlation tensors. They also discussed the symmetry properties of these equations and derived from them various wave equations and a number of conservation laws (*). These studies have been carried out in the framework of *free* fields, *i.e.*, the fields are considered in regions in which no charges and currents are present.

The aim of the present paper is to generalize the results of paper I to the case in which the random electromagnetic field is coupled to random, stationary sources. The consideration of this problem has considerable importance, because its results may ultimately be utilized for the study of the propagation of electromagnetic fields in plasmas and for the study of the plasma radiations themselves. We may think, in particular, of using the theory for purposes of plasma diagnostics.

The electromagnetic correlation tensors have been defined in paper I as follows:

$$
\left\{
\begin{aligned}
&\mathscr{E}_{jk}(\boldsymbol{x}_1, \boldsymbol{x}_2, \tau) = \langle E_j(\boldsymbol{x}_1, t+\tau) E_k^*(\boldsymbol{x}_2, t)\rangle ,\\
&\mathscr{H}_{jk}(\boldsymbol{x}_1, \boldsymbol{x}_2, \tau) = \langle H_j(\boldsymbol{x}_1, t+\tau) H_k^*(\boldsymbol{x}_2, t)\rangle ,\\
&\mathscr{G}_{jk}(\boldsymbol{x}_1, \boldsymbol{x}_2, \tau) = \langle E_j(\boldsymbol{x}_1, t+\tau) H_k^*(\boldsymbol{x}_2, t)\rangle ,\\
&\tilde{\mathscr{G}}_{jk}(\boldsymbol{x}_1, \boldsymbol{x}_2, \tau) = \langle H_j(\boldsymbol{x}_1, t+\tau) E_k^*(\boldsymbol{x}_2, t)\rangle .
\end{aligned}
\right. \tag{1.1}
$$

Here $\langle \ldots \rangle$ denotes time averaging, and E_j and H_k are the *analytic signals* associated with the electric and magnetic field components, respectively. The tensors (1.1) satisfy the following symmetry relations:

$$
\left\{
\begin{aligned}
&\mathscr{E}_{jk}^*(\boldsymbol{x}_1, \boldsymbol{x}_2, \tau) = \mathscr{E}_{kj}(\boldsymbol{x}_2, \boldsymbol{x}_1, -\tau) ,\\
&\mathscr{H}_{jk}^*(\boldsymbol{x}_1, \boldsymbol{x}_2, \tau) = \mathscr{H}_{kj}(\boldsymbol{x}_2, \boldsymbol{x}_1, -\tau) ,\\
&\tilde{\mathscr{G}}_{jk}^*(\boldsymbol{x}_1, \boldsymbol{x}_2, \tau) = \mathscr{G}_{kj}(\boldsymbol{x}_2, \boldsymbol{x}_1, -\tau) .
\end{aligned}
\right. \tag{1.2}
$$

In addition we now define a *charge correlation scalar* and a *current correlation tensor* in the following way. Let the real charge density be $\varrho^{(r)}(\boldsymbol{x}, t)$ and define the associated analytic signal by writing the complex charge density

$$\varrho = \varrho^{(r)} + i\varrho^{(i)} ,$$

([4]) P. ROMAN and E. WOLF: *Nuovo Cimento*, **17**, 462 (1960).
([5]) P. ROMAN and E. WOLF: *Nuovo Cimento*, **17**, 477 (1960).
(*) In the following we shall refer to ref. ([4]) as Paper I. Formulae from this paper will be denoted as (I.3.11*a*) etc.

where $\varrho^{(r)}$ is the Hilbert transform of $\varrho^{(r)}$. Then define the charge correlation by

$$\mathscr{P}(\boldsymbol{x}_1, \boldsymbol{x}_2, \tau) = \langle \varrho(\boldsymbol{x}_1, t+\tau)\, \varrho^*(\boldsymbol{x}_2, t) \rangle \,. \tag{1.3}$$

In an analogous manner, with $\boldsymbol{i}^{(r)}(\boldsymbol{x}, t)$ the real current vector and $\boldsymbol{i}$ the associated analytic signal, the current correlation tensor $\mathscr{I}_{jk}$ is defined by

$$\mathscr{I}_{jk}(\boldsymbol{x}_1, \boldsymbol{x}_2, \tau) = \langle i_j(\boldsymbol{x}_1, t+\tau)\, i_k^*(\boldsymbol{x}_2, t) \rangle \,. \tag{1.4}$$

By using formula (I.A.VI) it is obvious that

$$\mathscr{P}(\boldsymbol{x}, \boldsymbol{x}, 0) = 2\langle \big(\varrho^{(r)}(\boldsymbol{x}, t)\big)^2 \rangle \,, \qquad \operatorname{Sp} \mathscr{I}(\boldsymbol{x}, \boldsymbol{x}, 0) = 2\langle \big(\boldsymbol{i}^{(r)}(\boldsymbol{x}, t)\big)^2 \rangle \,, \tag{1.5}$$

i.e., in the limiting case $\mathscr{P}$ and $\mathscr{I}$ are simply related to the mean square value of the charge- and current-density respectively.

Because of the assumed stationary nature of the problem we immediately obtain the symmetry relations

$$\mathscr{P}^*(\boldsymbol{x}_1, \boldsymbol{x}_2, \tau) = \mathscr{P}(\boldsymbol{x}_2, \boldsymbol{x}_1, -\tau) \,, \qquad \mathscr{I}_{jk}^*(\boldsymbol{x}_1, \boldsymbol{x}_2, \tau) = \mathscr{I}_{kj}(\boldsymbol{x}_2, \boldsymbol{x}_1, -\tau) \,. \tag{1.6}$$

For notational convenience, we further introduce the *auxiliary* correlations

$$\left\{ \begin{aligned} \alpha_j\ (\boldsymbol{x}_1, \boldsymbol{x}_2, \tau) &= \langle E_j(\boldsymbol{x}_1, t+\tau)\, \varrho^*(\boldsymbol{x}_2, t) \rangle \,, \\ \gamma_{jk}(\boldsymbol{x}_1, \boldsymbol{x}_2, \tau) &= \langle E_j(\boldsymbol{x}_1, t+\tau)\, i_k^*(\boldsymbol{x}_2, t) \rangle \,, \\ \eta_{jk}(\boldsymbol{x}_1, \boldsymbol{x}_2, \tau) &= \langle H_j(\boldsymbol{x}_1, t+\tau)\, i_k^*(\boldsymbol{x}_2, t) \rangle \,. \end{aligned} \right. \tag{1.7}$$

2. – Derivation of the basic field equations.

The Maxwell equations in the presence of sources read, if we adopt the convenient notation of Paper I,

$$\varepsilon_{jkl}\, \partial_k^1 E_l(\boldsymbol{x}_1, t_1) + \frac{1}{c} \frac{\partial}{\partial t_1} H_j(\boldsymbol{x}_1, t_1) = 0 \,, \tag{2.1}$$

$$\varepsilon_{jkl}\, \partial_k^1 H_l(\boldsymbol{x}_1, t_1) - \frac{1}{c} \frac{\partial}{\partial t_1} E_j(\boldsymbol{x}_1, t_1) = \frac{4\pi}{c}\, i_j(\boldsymbol{x}_1, t_1) \,, \tag{2.2}$$

$$\partial_j^1 E_j(\boldsymbol{x}_1, t_1) = 4\pi\, \varrho(\boldsymbol{x}_1, t_1) \,, \tag{2.3}$$

$$\partial_j^1 H_j(\boldsymbol{x}_1, t_1) = 0 \,. \tag{2.4}$$

Here all quantities denote the appropriate analytic signals.

First, because it is easier and it also demonstrates the method, we shall derive the correlation equations corresponding to the divergence eq. (2.3) and (2.4).

If we multiply (2.3) by $\varrho^*(\boldsymbol{x}_2, t_2)$, set $t_1 = t_2 + \tau$, and $t_2 = t$, and then average over t, we obtain

$$\partial_j^1 \alpha_j(\boldsymbol{x}_1, \boldsymbol{x}_2, \tau) = 4\pi \mathscr{P}(\boldsymbol{x}_1, \boldsymbol{x}_2, \tau) . \tag{2.5}$$

We must now eliminate the quantity α_j which has no direct physical significance. To this end, let us take the complex conjugate of (2.3). Change the notation $\boldsymbol{x}_1 \to \boldsymbol{x}_2$, $t_1 \to t_2$, $\partial^1 \to \partial^2$; multiply then by $E_j(\boldsymbol{x}_1, t_1)$; setting $t_1 = t_2 + \tau$, $t_2 = t$ and averaging over t, we obtain

$$\partial^2 \mathscr{E}_{jk}(\boldsymbol{x}_1, \boldsymbol{x}_2, \tau) = 4\pi \alpha_j(\boldsymbol{x}_1, \boldsymbol{x}_2, \tau) . \tag{2.6}$$

Substituting this into (2.5) we arrive at the second order « divergence equation »

$$\partial_j^1 \partial_k^2 \mathscr{E}_{jk}(\boldsymbol{x}_1, \boldsymbol{x}_2, \tau) = 16\pi^2 \mathscr{P}(\boldsymbol{x}_1, \boldsymbol{x}_2, \tau) . \tag{2.7}$$

If charges are present, eq. (2.7) replaces the simple divergence eq. (I.3.13*a*). All other divergence equations of I remain, however, unchanged. This is so, because (I.3.15*a*) and (I.3.16*a*) follow from (2.4) which is the same as for sourceless fields. Further, by multiplying (2.3) with H_k^* and then eliminating $\varrho(\boldsymbol{x}_1, t_1 + \tau) H_k^*(\boldsymbol{x}_2, t)$ by using the complex conjugate of (2.4) and multiplying this with ϱ we obtain

$$\partial_j^1 \partial_k^2 \mathscr{G}_{jk} = 0 .$$

However, this equation is not a new result. It is merely a consequence of $\partial_k^2 \mathscr{G}_{jk} = 0$ which, as was the case in I, follows directly from (2.4) and is, in fact, the complex conjugate of (2.8*a*) below. Hence, in addition to (2.7) we have only the divergence equations

$$\partial_j^1 \tilde{\mathscr{G}}_{jk} = 0 , \tag{2.8a}$$

$$\partial_j^1 \mathscr{H}_{jk} = 0 . \tag{2.8b}$$

Note that eq. (I.3.14*a*) has no analogue.

Now we turn to the more difficult task of deriving the correlation equations from (2.2). Multiplying eq. (2.2) by $i_n^*(\boldsymbol{x}_2, t_2)$ and using the same procedure of averaging as before we get

$$\varepsilon_{jkl} \partial_k^1 \eta_{ln} - \frac{1}{c} \frac{\partial}{\partial \tau} \gamma_{jn} = \frac{4\pi}{c} \mathscr{J}_{jn} . \tag{2.9}$$

We must now eliminate the non-physical η_{ln} and γ_{jn}. We proceed as follows. Taking the complex conjugate of (2.2), changing $\boldsymbol{x}_1 \to \boldsymbol{x}_2$, $t_1 \to t_2$, and changing the indices, we get

$$\varepsilon_{nab}\,\partial_a^2\,H_b^*(\boldsymbol{x}_2, t_2) - \frac{1}{c}\frac{\partial}{\partial t_2}\,E_n^*(\boldsymbol{x}_2, t_2) = \frac{4\pi}{c}\,i_n^*(\boldsymbol{x}_2, t_2)\,. \tag{2.10}$$

We multiply this by $H_l(\boldsymbol{x}_1, t_1)$, set, in the present case, $t_2 = t_1 - \tau$ with $t_1 = t$, and average over t. Utilizing the fact that for stationary random functions

$$\langle A(\boldsymbol{x}_1, t)\,B^*(\boldsymbol{x}_2, t-\tau)\rangle = \langle A(\boldsymbol{x}_1, t+\tau)\,B^*(\boldsymbol{x}_2, t)\rangle\,,$$

we thus get

$$\varepsilon_{nab}\,\partial_a^2\,\mathscr{H}_{lb} + \frac{1}{c}\frac{\partial}{\partial\tau}\,\tilde{\mathscr{G}}_{ln} = \frac{4\pi}{c}\,\eta_{ln}\,. \tag{2.11}$$

We now again write out (2.10) but change the dummy indices $a \to k$, $b \to l$. Then we multiply by $E_j(\boldsymbol{x}_1, t_1)$ and use exactly the same procedure as in the previous step. This yields the equation

$$\varepsilon_{nkl}\,\partial_k^2\,\mathscr{G}_{jl} - \frac{1}{c}\frac{\partial}{\partial\tau}\,\mathscr{E}_{jn} = \frac{4\pi}{c}\,\gamma_{jn}\,. \tag{2.12}$$

Eq. (2.11) and (2.12) are interesting in themselves: they relate the non-physical correlations η_{ln} and γ_{jn} to the correlations in the electromagnetic fields. We now use these equations to eliminate η and γ from (2.9) and immediately get

$$\varepsilon_{jkl}\varepsilon_{nab}\,\partial_k^1\partial_a^2\,\mathscr{H}_{lb} + \frac{1}{c}\,\varepsilon_{jkl}\,\partial_k^1\frac{\partial}{\partial\tau}\,\tilde{\mathscr{G}}_{ln} - \frac{1}{c}\,\varepsilon_{nkl}\,\partial_k^2\frac{\partial}{\partial\tau}\,\mathscr{G}_{jl} - \frac{1}{c^2}\frac{\partial^2}{\partial\tau^2}\,\mathscr{E}_{jn} = \frac{16\pi^2}{c^2}\,\mathscr{J}_{jn}\,. \tag{2.13}$$

This symmetric second order equation replaces the simpler eq. (I.3.11a) which is valid only for free fields.

Since the remaining Maxwell eq. (2.1) is the same as for the free field case, we obtain from it, as was the case in I, the simple first order eq. (I.3.9a) and (I.3.10a), *viz*,

$$\varepsilon_{jkl}\,\partial_k^1\mathscr{E}_{ln} + \frac{1}{c}\frac{\partial}{\partial\tau}\,\tilde{\mathscr{G}}_{jn} = 0\,, \tag{2.14a}$$

$$\varepsilon_{jkl}\,\partial_k^1\mathscr{G}_{ln} + \frac{1}{c}\frac{\partial}{\partial\tau}\,\mathscr{H}_{jn} = 0\,. \tag{2.14b}$$

Following the same procedure as in I, *p.* 472-473, it can easily be seen that the divergence eq. (2.7), (2.8a, b) merely play the role of initial conditions for

the remaining eq. (2.13), (2.14*a*), (2.14*b*). However, we must now face the following unpleasant situation. These remaining equations are 27 in number, whereas we have 36 unknown functions, *i.e.* the components of $\mathscr{E}$, $\mathscr{H}$, $\mathscr{G}$ and $\tilde{\mathscr{G}}$. This difficulty can, however, be avoided by completely eliminating $\mathscr{G}$ and $\tilde{\mathscr{G}}$, which, in any case, have a less significant physical meaning than $\mathscr{E}$ and $\mathscr{H}$. Indeed, if we take the complex conjugate of (2.14*a*), then utilizing the symmetry properties (1.2), we obtain, as has been shown in I,

$$\varepsilon_{nab}\,\hat{c}_a^2\mathscr{E}_{lb} - \frac{1}{c}\frac{\hat{c}}{\partial\tau}\,\mathscr{G}_{ln} = 0\,. \tag{2.15}$$

Next we apply $(1/c)\hat{c}/\hat{c}\tau$ onto eq. (2.14*b*) and then eliminate, in the first term, the resulting factor $(1/c)(\partial/\partial\tau)\,\mathscr{G}_{ln}$ by using (2.15). Thus we obtain

$$\varepsilon_{jkl}\varepsilon_{nab}\,\hat{c}_k^1\hat{c}_a^2\mathscr{E}_{lb} + \frac{1}{c^2}\frac{\hat{c}^2}{\hat{c}\tau^2}\,\mathscr{H}_{jn} = 0\,. \tag{2.16}$$

This equation contains only $\mathscr{E}$ and $\mathscr{H}$.

The elimination of $\mathscr{G}$ and $\tilde{\mathscr{G}}$ from (2.13) is carried out as follows. We first change the indices in (2.14*a*) according to $j\to l$, $k\to a$, $l\to b$, and then apply $\varepsilon_{jkl}\hat{c}_k^1$. We obtain, using the identity

$$\varepsilon_{jkl}\varepsilon_{lab} = \delta_{ja}\delta_{kb} - \delta_{jb}\delta_{ka}\,,$$

the equation

$$\hat{c}_j^1\hat{c}_k^1\mathscr{E}_{kn} - \hat{c}_k^1\hat{c}_k^1\mathscr{E}_{jn} + \frac{1}{c}\varepsilon_{jkl}\,\hat{c}_k^1\frac{\hat{c}}{\partial\tau}\,\tilde{\mathscr{G}}_{ln} = 0\,. \tag{2.17}$$

Treating (2.15) similarly, we get

$$\hat{c}_n^2\hat{c}_k^2\mathscr{E}_{jk} - \hat{c}_k^2\hat{c}_k^2\mathscr{E}_{jn} - \frac{1}{c}\varepsilon_{nkl}\,\hat{c}_k^2\frac{\hat{c}}{\partial\tau}\,\mathscr{G}_{jl} = 0\,. \tag{2.18}$$

Using (2.17) and (2.18), the unwanted second and third term in (2.13) can now be eliminated and we are led to

$$\varepsilon_{jkl}\varepsilon_{nab}\,\hat{c}_k^1\hat{c}_a^2\mathscr{H}_{lb} - \hat{c}_j^1\hat{c}_k^1\mathscr{E}_{kn} + \hat{c}_k^1\hat{c}_k^1\mathscr{E}_{jn} - \hat{c}_n^2\hat{c}_k^2\mathscr{E}_{jk} + \hat{c}_k^2\hat{c}_k^2\mathscr{E}_{jn} - \frac{1}{c^2}\frac{\partial^2}{\partial\tau^2}\,\mathscr{E}_{jn} = \frac{16\pi^2}{c^2}\,\mathscr{J}_{jn}\,. \tag{2.19}$$

Thus our field equations are now reduced to eq. (2.16) and (2.19), *i.e.*, we now have 18 equations for the components of $\mathscr{E}$ and $\mathscr{H}$.

Incidentally, if one desires to get some partial information about $\mathscr{G}$ and $\tilde{\mathscr{G}}$, one can feed back the solution $\mathscr{E}$, $\mathscr{H}$ of (2.16) and (2.19) into (2.14*a*, *b*).

If we had started with the complex conjugates of (2.1)–(2.4), we would have arrived at a second set of correlation-equations, just as was the case in I. However, as has been pointed out in I, this second set is, because of the symmetry relations (1.2) (and now also (1.6)) equivalent to the original set; *i.e.*, they are just the respective complex conjugate equations. Moreover, in the present case, (2.16), (2.19) and (2.7) are now *identical* to the corresponding equations of the second set. This can be easily verified by taking their complex conjugates and using the symmetry relations (1.2), (1.6).

It will be convenient at this point to gather together the final set of equations. They are

$$\varepsilon_{jkl}\varepsilon_{nab}\,\partial_k^1\partial_a^2\mathscr{E}_{lb}+\frac{1}{c^2}\frac{\partial^2}{\partial\tau^2}\mathscr{H}_{jn}=0\,, \tag{2.20}$$

$$\varepsilon_{jkl}\varepsilon_{nab}\,\partial_k^1\partial_a^2\mathscr{H}_{lb}-\partial_j^1\partial_k^1\mathscr{E}_{kn}+\Delta^1\mathscr{E}_{jn}- \\ -\partial_n^2\partial_k^2\mathscr{E}_{jk}+\Delta^2\mathscr{E}_{jn}-\frac{1}{c^2}\frac{\partial^2}{\partial\tau^2}\mathscr{E}_{jn}=\frac{16\pi^2}{c^2}\mathscr{J}_{jn}\,, \tag{2.21}$$

$$\partial_j^1\partial_k^2\mathscr{E}_{jk}=16\pi^2\mathscr{P}\,, \tag{2.22}$$

$$\partial_j^1\mathscr{H}_{jk}=0\,. \tag{2.23}$$

Here Δ^1 and Δ^2 are the Laplacians with respect to $\boldsymbol{x}_1$ and $\boldsymbol{x}_2$, respectively.

3. – The equation of continuity and illustrative examples.

Let us apply the differential operator $\partial_j^1\partial_n^2$ onto eq. (2.21). Then, by symmetry, the first term on the left-hand side vanishes. In evaluating the remaining terms, we make use of (2.22), and find that the second term cancels the third and the fourth term cancels the fifth. Thus we eventually obtain

$$\frac{\partial^2}{\partial\tau^2}\mathscr{P}+\partial_j^1\partial_n^2\mathscr{J}_{jn}=0\,. \tag{3.1}$$

This is the obvious analogue of the conventional equation of continuity. It should be noted that it is a second order differential equation which imposes a restriction on the charge- and current correlation tensors if they are coupled to electromagnetic field correlations.

To illustrate the usefulness of this relation, we consider a plasma. In this case, under fairly broad assumptions, the generalized « Ohm's law » reads as

$$\boldsymbol{i}=\sigma\boldsymbol{E}+\sigma\frac{1}{c}\boldsymbol{v}\times\boldsymbol{H}\,;$$

or, in component notation,

$$i_j = \sigma E_j + \sigma \frac{1}{c} \varepsilon_{jlm} v_l H_m \,, \tag{3.2}$$

where σ is the (real) conductivity and $\boldsymbol{v}$ the plasma velocity. We now want to construct the current correlation tensor corresponding to (3.2). Multiplying (3.2) by i_n^* and using the standard averaging procedure, we get

$$\mathscr{I}_{jn} = \sigma \gamma_{jn} + \frac{1}{c} \sigma \varepsilon_{jlm} \langle v_l(\boldsymbol{x}_1, t+\tau) H_m(\boldsymbol{x}_1, t+\tau) i_n^*(\boldsymbol{x}_2, t) \quad . \tag{3.3}$$

If we now take the complex conjugate of (3.2), change the index $j \to n$, and replace $\boldsymbol{x}_1 \to \boldsymbol{x}_2$, $t_1 \to t_2$, we obtain, on multiplying by $E_j(\boldsymbol{x}_1, t_1)$ and averaging,

$$\gamma_{jn} = \sigma \mathscr{E}_{jn} + \frac{1}{c} \sigma \varepsilon_{nlm} \langle E_j(\boldsymbol{x}_1, t+\tau) v_l^*(\boldsymbol{x}_2, t) H_m^*(\boldsymbol{x}_2, t) \quad . \tag{3.4a}$$

In a similar manner, multiplying the complex conjugate of (3.2) by $v_l(\boldsymbol{x}_1, t_1) \cdot H_m(\boldsymbol{x}_1, t_1)$ we get

$$\begin{aligned} \langle v_l(\boldsymbol{x}_1, t+\tau) H_m(\boldsymbol{x}_1, t+\tau) i_n^*(\boldsymbol{x}_2, t) \rangle = \\ = \sigma \langle v_l(\boldsymbol{x}_1, t+\tau) H_m(\boldsymbol{x}_1, t+\tau) E_n^*(\boldsymbol{x}_2, t) \rangle + \\ + \frac{1}{c} \sigma \varepsilon_{nab} \langle v_l(\boldsymbol{x}_1, t+\tau) H_m(\boldsymbol{x}_1, t+\tau) v_a^*(\boldsymbol{x}_2, t) H_b^*(\boldsymbol{x}_2, t) \rangle \,. \end{aligned} \tag{3.4b}$$

Putting (3.4*a*, *b*) back into (3.3) we eventually obtain

$$\begin{aligned} \mathscr{I}_{jn} = \sigma^2 \mathscr{E}_{jn} + \frac{1}{c} \sigma^2 \varepsilon_{nlm} \langle E_j(\boldsymbol{x}_1, t+\tau) v_l^*(\boldsymbol{x}_2, t) H_m^*(\boldsymbol{x}_2, t) \rangle + \\ + \frac{1}{c} \sigma^2 \varepsilon_{jlm} \langle v_l(\boldsymbol{x}_1, t+\tau) H_m(\boldsymbol{x}_1, t+\tau) E_n^*(\boldsymbol{x}_2, t) \rangle + \\ + \frac{1}{c^2} \sigma^2 \varepsilon_{jlm} \varepsilon_{nab} \langle v_l(\boldsymbol{x}_1, t+\tau) H_m(\boldsymbol{x}_1, t+\tau) v_a^*(\boldsymbol{x}_2, t) H_b^*(\boldsymbol{x}_2, t) \rangle \,. \end{aligned} \tag{3.5}$$

The three- and fourfold correlations may be reduced by applying the general formula

$$\langle V_1 V_2 V_3 V_4 \rangle = \langle V_1 V_2 \rangle \langle V_3 V \rangle - \langle \Delta(V_1 V_2) \Delta(V_3 V_4) \rangle \,,$$

where Δ denotes the deviation from the mean. (When applying this formula to the 2-nd and 3-rd term in (3.5), we must set one of the V's equal to unity.) Yet, the resulting expression is too complicated in the general case

and its application would require the knowledge of further correlations involving the velocity. If we, however, restrict ourselves to the important case for which $v/c \ll 1$ or $H \approx 0$, then (3.5) simplifies to

$$\mathscr{I}_{jn} = \sigma^2 \mathscr{E}_{jn} . \tag{3.6}$$

Applying the equation of continuity (3.1) to this case, we obtain

$$\frac{\partial^2}{\partial \tau^2} \mathscr{P} + \sigma \hat{\partial}_j^1 \hat{\partial}_n^2 \mathscr{E}_{jn} = 0 ,$$

which, because of (2.22), gives

$$\frac{\partial^2}{\partial \tau^2} \mathscr{P} + 16\pi^2 \sigma^2 \mathscr{P} = 0 . \tag{3.7}$$

The solution of (3.7) is

$$\mathscr{P} = \mathscr{A}(\boldsymbol{x}_1, \boldsymbol{x}_2) \exp [i\omega\tau] , \tag{3.8}$$

where ω, the frequency of oscillation, is given by

$$\omega = 4\pi\sigma . \tag{3.8a}$$

Another interesting case presents itself if the second term in (3.1) vanishes. This may often happen even if $\mathscr{I}_{jn} \neq 0$. For example, it occurs if

$$\mathscr{I}_{jn}(\boldsymbol{x}_1, \boldsymbol{x}_2, \tau) = - \mathscr{I}_{nj}(\boldsymbol{x}_2, \boldsymbol{x}_1, \tau) , \tag{3.9}$$

because this symmetry property is sufficient to cause the double-divergence to vanish. Incidentally, because of the inherent symmetry property (1.6), the condition (3.9) merely demands that

$$\mathscr{I}_{jn}(\boldsymbol{x}_1, \boldsymbol{x}_2, \tau) = - \mathscr{I}_{jn}^*(\boldsymbol{x}_1, \boldsymbol{x}_2, -\tau) , \tag{3.10}$$

which, in turns, implies

$$\mathscr{I}_{jn}^{(r)}(\boldsymbol{x}_1, \boldsymbol{x}_2, \tau) = - \mathscr{I}_{jn}^{(r)}(\boldsymbol{x}_1, \boldsymbol{x}_2, -\tau) , \tag{3.11}$$

i.e., the real current correlation is an odd function of the time-shift τ.

If this happens (or, if for any other reason, the term in question vanishes)

then (3.1) immediately gives

$$\mathscr{P} = \mathscr{B}(\boldsymbol{x}_1, \boldsymbol{x}_2)\tau + \mathscr{C}(\boldsymbol{x}_1, \boldsymbol{x}_2)\,, \tag{3.12}$$

i.e., the charge correlation is a linear function of the time-shift.

4. – Wave equations.

If we apply $(1/c^2)(\partial^2/\partial^2\tau^2)$ onto the field eq. (2.20) and then express $(1/c^2)(\partial^2/\partial\tau^2)\mathscr{E}_{lb}$ by using (2.21), we obtain, noting that $\varepsilon_{abc}\partial_b\partial_c X = 0$,

$$\varepsilon_{jkl}\varepsilon_{nab}\varepsilon_{lfs}\varepsilon_{brv}\partial_k^1\partial_f^1\partial_a^2\partial_r^2\mathscr{H}_{sv} + \varepsilon_{jkl}\varepsilon_{nab}\partial_k^1\partial_a^2(\Delta^1+\Delta^2)\mathscr{E}_{lb} + \\ + \frac{1}{c^4}\frac{\partial^4}{\partial\tau^4}\mathscr{H}_{jn} - \frac{16\pi^2}{c^2}\varepsilon_{jkl}\varepsilon_{nab}\partial_k^1\partial_a^2\mathscr{J}_{lb} = 0\,.$$

In the second term we use (2.20) to rewrite it as

$$-\frac{1}{c^2}(\Delta^1+\Delta^2)\frac{\partial^2}{\partial\tau^2}\mathscr{H}_{jn}\,.$$

In the first term we join the ε's pairwise and transform them, identically, into products of δ's. Then, applying (2.23) and its complex conjugate, only one term remains, *viz.*, $\Delta^1\Delta^2\mathscr{H}_{jn}$. Hence, we obtain the 4-th order wave equation

$$\Delta^1\Delta^2\mathscr{H}_{jn} - \frac{1}{c^2}(\Delta^1+\Delta^2)\frac{\partial^2}{\partial\tau^2}\mathscr{H}_{jn} + \frac{1}{c^4}\frac{\partial^4}{\partial\tau^4}\mathscr{H}_{jn} - \frac{16\pi^2}{c^2}\varepsilon_{jkl}\varepsilon_{nab}\partial_k^1\partial_a^2\mathscr{J}_{lb} = 0\,. \tag{4.1}$$

To derive the wave equation for $\mathscr{E}$ is a more involved task. We start as in the previous case: apply $(1/c^2)(\partial^2/\partial\tau^2)$ onto (2.21) and express $(1/c^2)(\partial^2/\partial\tau^2)\mathscr{H}_{lb}$ by eq. (2.20), obtaining

$$-\varepsilon_{jkl}\varepsilon_{nab}\varepsilon_{lfs}\varepsilon_{brv}\partial_k^1\partial_f^1\partial_a^2\partial_r^2\mathscr{E}_{sv} - \frac{1}{c^2}\partial_j^1\partial_k^1\frac{\partial^2}{\partial\tau^2}\mathscr{E}_{kn} - \\ - \frac{1}{c^2}\partial_n^2\partial_k^2\frac{\partial^2}{\partial\tau^2}\mathscr{E}_{jk} + \frac{1}{c^2}(\Delta^1+\Delta^2)\frac{\partial^2}{\partial\tau^2}\mathscr{E}_{jn} - \frac{1}{c^4}\frac{\partial^4}{\partial\tau^4}\mathscr{E}_{jn} - \frac{16\pi^2}{c^4}\frac{\partial^2}{\partial\tau^2}\mathscr{J}_{jn} = 0\,. \tag{4.2}$$

In the first term we again reduce identically the ε-product to fourfold δ-products, and we get

$$-\Delta^1\Delta^2\mathscr{E}_{jn} + \partial_k^1\partial_j^1\Delta^1\mathscr{E}_{kn} + \partial_a^2\partial_n^2\Delta^2\mathscr{E}_{ka} - \partial_k^1\partial_j^1\partial_a^2\partial_n^2\mathscr{E}_{ka}\,.$$

Here, in the last term, we use (2.22), so that eq. (4.2) becomes

$$(4.3)\qquad -\Delta^1\Delta^2\mathscr{E}_{jn}+\frac{1}{c^2}(\Delta^1+\Delta^2)\frac{\partial^2}{\partial\tau^2}\mathscr{E}_{jn}-\frac{1}{c^4}\frac{\partial^4}{\partial\tau^4}\mathscr{E}_{jn}+\hat{\partial}_k^2\hat{\partial}_n^2\left(\Delta^1\mathscr{E}_{jk}-\frac{1}{c^2}\frac{\partial^2}{\partial\tau^2}\mathscr{E}_{jk}\right)+$$

$$+\hat{\partial}_k^1\hat{\partial}_j^1\left(\Delta^2\mathscr{E}_{kn}-\frac{1}{c^2}\frac{\partial^2}{\partial\tau^2}\mathscr{E}_{kn}\right)-16\pi^2\hat{\partial}_j^1\hat{\partial}_n^2\mathscr{P}-\frac{16\pi^2}{c^4}\frac{\partial^2}{\partial\tau^2}\mathscr{I}_{jn}=0\,.$$

The 4-th and 5-th terms are disturbing. We eliminate them by using (2.21) twice to express the terms in the parentheses. Then, utilizing symmetries and noting cancellations, the unwanted 4-th and 5-th terms give simply

$$2\,\partial_j^1\partial_r^1\partial_k^2\partial_n^2\mathscr{E}_{rs}+\frac{16\pi^2}{c^2}(\partial_j^1\partial_k^1\mathscr{I}_{km}+\partial_k^2\partial_n^2\mathscr{I}_{jk})\,.$$

Applying here in the first term (2.22), and putting back all this into (4.3), we finally obtain the wave equation for $\mathscr{E}$,

$$(4.4)\qquad \Delta^1\Delta^2\mathscr{E}_{jn}-\frac{1}{c^2}(\Delta^1+\Delta^2)\frac{\partial^2}{\partial\tau^2}\mathscr{E}_{jn}+\frac{1}{c^4}\frac{\partial^4}{\partial\tau^4}\mathscr{E}_{jn}-$$

$$-16\pi^2\partial_j^1\partial_n^2\mathscr{P}-\frac{16\pi^2}{c^2}\left(\partial_j^1\partial_k^1\mathscr{I}_{kn}+\partial_k^2\partial_n^2\mathscr{I}_{jk}-\frac{1}{c^2}\frac{\partial^2}{\partial\tau^2}\mathscr{I}_{jn}\right)=0\,.$$

This is as far as we can go without specifying an « Ohm's law ». If, however, this is given, the last terms in (4.1) and (4.4) can be expressed by the fields. If, in particular, (3.6) applies, the last term in (4.1) gives

$$-\frac{16\pi^2\sigma^2}{c^2}\varepsilon_{jkl}\varepsilon_{nab}\hat{\partial}_k^1\hat{\partial}_a^2\mathscr{E}_{lb}\,.$$

Using the field eq. (2.20), this reduces to

$$\frac{16\pi^2\sigma^2}{c^4}\frac{\partial^2}{\partial\tau^2}\mathscr{H}_{jn}\,,$$

so that (4.1) becomes, in this case,

$$(4.5)\qquad \Delta^1\Delta^2\mathscr{H}_{jn}-\frac{1}{c^2}(\Delta^1+\Delta^2)\frac{\partial^2}{\partial\tau^2}\mathscr{H}_{jn}+\frac{1}{c^4}\frac{\partial^4}{\partial\tau^4}\mathscr{H}_{jn}+\frac{16\pi^2\sigma^2}{c^4}\frac{\partial^2}{\partial\tau^2}\mathscr{H}_{jn}=0\,.$$

The last term plays the part of a damping term.

Similarly, when the simple connection (3.6) is valid, the last term in (4.4) becomes the not so simple damping term

$$\frac{16\pi\sigma}{c^2}\left(\hat{\partial}_j^1\hat{\partial}_k^1\mathscr{E}_{kn}+\hat{\partial}_k^2\hat{\partial}_n^2\mathscr{E}_{jk}-\frac{1}{c^2}\frac{\hat{\partial}^2}{\hat{\partial}\tau^2}\mathscr{E}_{jn}\right).$$

5. – The limiting case of vanishing sources.

One would expect that for $\varrho\equiv 0$, $\boldsymbol{i}\equiv 0$ our field equations go identically over into the free field equations of paper I. But, just looking at the basic set (2.20)–(2.23), this does not seem to be immediately evident. Of course, if there are no sources, the solutions of the free field eq. (I.3.9*a*)–(I.3.16*a*) satisfy eq. (2.20)–(2.23) as well, because, in this case, as can be easily checked (and as should be clear from the way of deriving the present set of equations), our present equations are merely *consequences* or the first order equations of I. However, one might think that we might get additional solutions as well since the second order homogeneous equations are only consequences of the first order equations. This, however, is not the case. The boundary conditions do not allow further solutions. In fact, our eq. (2.20)–(2.23) become homogeneous even if $\varrho\not\equiv 0$, $\boldsymbol{i}\not\equiv 0$, but for, some reason, $\mathscr{P}=0$, $\mathscr{I}_{jn}=0$ for all points (except, of course, for $\boldsymbol{x}_1=\boldsymbol{x}_2$, which would imply $\varrho\equiv 0$, $\boldsymbol{i}\equiv 0$). Now, the solutions of our equations are unique once the boundary conditions are given. But the boundary conditions for $\mathscr{P}=0$, $\mathscr{I}=0$ (but $\varrho\not\equiv 0$, $\boldsymbol{i}\not\equiv 0$) are always different from these which apply for the same homogeneous equations in the $\varrho\equiv 0$, $\boldsymbol{i}\equiv 0$ case. Hence the solutions in the latter case must be different from any «extra» solutions that the homogeneous second order equations permit. But then, they can be only solutions that occur within the set of solutions of the first order equations of I. Of course, using the second order homogeneous equations for the source-free case, we will not get as much information about them as we would if we had used the original first order equations of I. This is already evident from the fact that $\mathscr{G}$ and $\tilde{\mathscr{G}}$ do not appear in the second order equations.

To illustrate the situation, let us consider the «electrostatic» case. Here, in the customary theory, the field equation is

$$\varepsilon_{jkl}\hat{\partial}_k^1 E_l(\boldsymbol{x}_1, t_1)=0\,, \tag{5.1}$$

which must be solved under the boundary condition

$$\int E_j(\boldsymbol{x}_1, t_1)\,\mathrm{d}f_j(\boldsymbol{x}_1)=\int\varrho(\boldsymbol{x}_1, t_1)\,\mathrm{d}V(\boldsymbol{x}_1)\,. \tag{5.2}$$

(We assume that all charges are contained within the boundary surface.) Multiplying (5.2) by $E_k^*(\boldsymbol{x}_2, t_2)$ we obtain

$$\int \mathscr{E}_{jk}(\boldsymbol{x}_1, \boldsymbol{x}_2, \tau)\, \mathrm{d}f_j(\boldsymbol{x}_1) = \int \langle \varrho(\boldsymbol{x}_1, t+\tau) E_k^*(\boldsymbol{x}_2, t)\rangle\, \mathrm{d}V(\boldsymbol{x}_1), \tag{5.3}$$

and multiplying the complex conjugate of (5.2), taken at $\boldsymbol{x}_2$, by $\varrho(\boldsymbol{x}_1, t_1)$, we have

$$\int \langle \varrho(\boldsymbol{x}_1, t+\tau) E_k^*(\boldsymbol{x}_2, t)\rangle\, \mathrm{d}f_k(\boldsymbol{x}_2) = \int \mathscr{P}(\boldsymbol{x}_1, \boldsymbol{x}_2, \tau)\, \mathrm{d}V(\boldsymbol{x}_2)\,. \tag{5.4}$$

If we integrate (5.3) over $\mathrm{d}f_k(\boldsymbol{x}_2)$ and then use (5.4), we obtain

$$\int \mathscr{E}_{jk}(\boldsymbol{x}_1, \boldsymbol{x}_2, \tau)\, \mathrm{d}f_{jk}(\boldsymbol{x}_1, \boldsymbol{x}_2) = \int \mathscr{P}(\boldsymbol{x}_1, \boldsymbol{x}_2, \tau)\, \mathrm{d}^6 V(\boldsymbol{x}_1, \boldsymbol{x}_2)\,, \tag{5.5}$$

where we have put

$$\int \ldots \mathrm{d}f_{jk}(\boldsymbol{x}_1, \boldsymbol{x}_2) \equiv \int\int \ldots \mathrm{d}f_j(\boldsymbol{x}_1)\, \mathrm{d}f_k(\boldsymbol{x}_2)\,.$$

Now suppose that $\varrho \not\equiv 0$, but $\mathscr{P} = 0$ $(\boldsymbol{x}_1 \neq \boldsymbol{x}_2)$. In this case we cannot conclude from (5.5) that

$$\int \mathscr{E}_{jk}\, \mathrm{d}f_j(\boldsymbol{x}_1) = 0\,, \tag{5.6}$$

not even if for some special, additional reason $\int \mathscr{P}\, \mathrm{d}^6 V = 0$. For, if (5.6) were true, then (5.3) would give

$$\int \langle \varrho(\boldsymbol{x}_1, t+\tau) E_k^*(\boldsymbol{x}_2, t)\rangle\, \mathrm{d}V(\boldsymbol{x}_1) = \langle e(t+\tau) E_k^*(\boldsymbol{x}_2, t)\rangle = e\langle E_k^*(\boldsymbol{x}_2, t)\rangle = 0\,,$$

since the total charge in the whole space is independent of time. But this is impossible, because, by assumption, the mean value of the random but *static* electric field is not zero. Hence, (5.6), does not hold, so that $\partial_j^1 \mathscr{E}_{jk} \neq 0$. Thus is $\varrho \not\equiv 0$, we can only have the more restricted relation

$$\int \mathscr{E}_{jk}\, \mathrm{d}f_{jk} = 0\,,$$

which implies that

$$\partial_j^1 \partial_k^2 \mathscr{E}_{jk} = 0\,.$$

On the other hand, suppose that $\varrho = 0$. Then $\mathscr{E}_{jk}$ certainly satisfies $\hat{c}^1_j \hat{c}^2_k \mathscr{E}_{jk} = 0$. But solutions that do not already satisfy $\hat{c}^1_j \mathscr{E}_{jk} = 0$ can not be solutions in congruence with the pertinent boundary conditions. Because if only the second order equation were fulfilled but not the first order equation, then, working backwards, this would mean that the boundary condition of the $\varrho \neq 0$, $\mathscr{P} = 0$ case is satisfied. But such solutions pertain to the non-free fields.

* * *

In the course of writing up this paper I have learned that Drs. G. B. Parrent and M. Beran are working on similar lines. I also acknowledge a conversation on this topic with them.

RIASSUNTO (*)

Estendo la teoria dei campi elettromagnetici casuali stazionari, sviluppata in precedenza, al caso in cui i campi interagiscono con cariche e correnti casuali stazionarie. Deduco le equazioni di campo fondamentali e trovo che sono equazioni differenziali parziali del secondo ordine. Derivo un'analoga della equazione di continuità e discuto alcuni esempi illustrativi. Deduco equazioni d'onda, che sono del quarto ordine, per i tensori di correlazione elettrici e magnetici. La teoria presentata in questo scritto può avere varie applicazioni nella teoria del plasma.

(*) *Traduzione a cura della Redazione.*

Solution of the Equations for the Green's Functions of a two Dimensional Relativistic Field Theory (*).

K. Johnson

Department of Physics and Laboratory of Nuclear Science, Massachusetts Institute of Technology - Cambridge, Mass.

(ricevuto l'11 Marzo 1961)

Summary. — The explicit solution of the coupled set of equations for the Green's functions for the self-coupled field theory model of Thirring is given. It is found that the infra-red problem causes no special difficulty. The question of how to define products of singular field operators at coincident space-time points arises and it is shown that the commutation relations for such products are not consistently given by making use of the formal expressions and the canonical commutation relations. The problem of gauge invariance in an external field is studied and it is shown that: *a*) the current and charge density do not commute at equal times, and *b*) this is necessary for and consistent with the gauge invariance of the field equations.

1. – Introduction.

Thirring (1) has proposed a two dimensional (one space, one time) self-coupled field theory model which is of some interest because its exact solubility enables one to study some of the general conjectures which have been proposed in regard to the behavior of local relativistic fields. In spite of the model, no general solutions have been proposed which are free from possible criticism because of the rather formal manner in which they have been ob-

(*) This work is supported in part through AEC Contract AT(30-1)-2098, by funds provided by the U. S. Atomic Energy Commission, the Office of Naval Research and the Air Force Office of Scientific Research.

(1) W. Thirring: *Ann. of Phys.*, **3**, 91 (1958).

tained (²). The model is exactly soluble only when the mass parameter of the field vanishes, and in this case no dimensional parameter remains (the coupling constant is dimensionless). Thus, the use of a formal construct such as an asymptotic field which presumably has meaning in a theory where there are dimensional quantities is in this case a rather dubious procedure since no parameter exists in the theory to characterize the « asymptotic » domain. Even worse, since the theory describes a field with no mass, presumably all real processes involve infinite numbers of infra-red pairs and thus even the concept of particle scattering states with finite occupation number is meaningless.

In this note we shall show how the vacuum expectation values of all time-ordered products of the fields, (*i.e.*, Green's functions) may be calculated. With the aid of these, all properly put questions about transitions can presumably be answered. The definition of these Green's functions however does not require the existence of an asymptotic field operator, rather the latter construct would follow if the Green's functions exhibit a structure consistent with the existence of multiple particle scattering states. However, the absence of this type of state does not preclude the existence of Green's functions. We shall calculate the solutions of the model by making use of the invariance of the theory under two continuous gauge groups. The solutions will enable us to study such groups and the operators which generate them in sufficient detail that we can also apply the results to the study of more realistic field theories which are invariant under such groups. In particular, we shall settle the questions associated with the lack of commutation of the charge and current density operators at equal times.

2. – Solution of the model.

The field equation of the model is

$$\gamma^\mu \frac{1}{i} \partial_\mu \psi(x) = \lambda j^\mu(x) \gamma_\mu \psi(x) , \tag{1}$$

where the current $j^\mu(x)$ is the « defined » by the formal expression

$$j^\mu(x) = \tfrac{1}{2} [\overline{\psi}(x) \gamma^\mu, \psi(x)] . \tag{2}$$

λ is the dimensionless coupling constant. The Dirac matrices γ^μ can be taken as the 2×2 set, $(\gamma^0, \gamma^1) = (\sigma^2, i\sigma^1)$ which is completed by $\gamma^5 = \gamma^0 \gamma^1 = \sigma^3$. We

(²) V. GLASER: *Nuovo Cimento*, **9**, 990 (1958). F. SCARF: *Phys. Rev.*, **117**, 868 (1960). T. PRADHAN: *Nucl. Phys.*, **9**, 124 (1958-59).

shall solve for the Green's functions of the theory by way of the so-called « generalized » Ward identity ([3]). Thus, since the field equations are invariant under the group

$$\delta\psi(x) = i\alpha\psi(x) \,, \tag{3}$$

the current is conserved

$$\partial^\mu j_\mu(x) = 0 \,. \tag{4}$$

Further, because the mass of the particle has been taken as zero, (1) is also invariant under the group

$$\delta\psi(x) = i\alpha\gamma_5\psi(x) \tag{5}$$

and thus, the pseudovector current which is (again formally) defined by

$$\boldsymbol{j}^\mu = \tfrac{1}{2}[\overline{\psi}(x)\gamma^\mu\gamma^5, \psi(x)] = \varepsilon^{\mu\nu} j_\nu(x) \,, \tag{6}$$

where $\varepsilon^{\mu\nu}$ is the antisymmetric symbol, is also conserved,

$$\partial^\mu \boldsymbol{j}_\mu = \partial^\mu \varepsilon_{\mu\nu} j^\nu = 0 \,. \tag{7}$$

Thus, both curl and divergence of the vector field $j^\mu(x)$ vanish. (4) and (7) lead to a set of two « Ward identities » for an arbitrary vertex which can be integrated to give the vertex in terms of the corresponding Green's function. This is the reason which accounts for the solubility of the model in closed form. For clarity, we shall confine the discussion to the lowest order Green's functions, defined by

$$G_+(xy) = \quad i\langle 0 \,|\, T\big(\psi(x)\,\overline{\psi}(y)\big) \,|\, 0\rangle \,, \tag{8}$$

$$G_+(xx'yy') = -\langle 0 \,|\, T\big(\psi(x)\,\psi(x')\,\overline{\psi}(y')\,\overline{\psi}(y)\big) \,|\, 0\rangle \,. \tag{9}$$

The equation for (8) implied by the field equations and canonical commutation relations is

$$\gamma^\mu \frac{1}{i}\,\partial_\mu G_+(xy) = \delta(xy) + \lambda\gamma^\mu i\langle 0 \,|\, T\big(j_\mu(x)\,\psi(x)\,\overline{\psi}(y)\big) \,|\, 0\rangle \,. \tag{10}$$

The vertex which enters this equation is connected to the next higher order Green's function (9) by the formal expression for the current (2). However,

([3]) Y. Takahashi: *Nuovo Cimento*, **6**, 371 (1957).

because of the conservation eq. (4) and (7) satisfied by the current there are two identities satisfied by the general form of the vertex

$$i\langle 0 \,|\, T\big(j^{\mu}(\xi)\,\psi(x)\,\overline{\psi}(y)\big) \,|\, 0\rangle \tag{11}$$

which are sufficient to calculate the form of (11) without making use of (2). To derive these identities we must know the equal time commutators

$$[\psi(x),\, j^{0}(y)]\,, \qquad [\psi(x),\, j^{1}(x)]\,. \tag{12}$$

It is at this point where it is necessary to explicitly take note that the formal expressions (2) and (6) are meaningless because of the singular nature of the Green's functions on the light cone. Thus the operator

$$\overline{\psi}(x+\varepsilon)\gamma^{\mu}\,\psi(x) \tag{13}$$

has singular matrix elements in the limit $\varepsilon \to 0$, and in order to give a proper definition of the current a well-defined limiting prescription must be given in terms of the non-local operator (13). We shall discover what that definition is below. It should and will be such that the operator $j^{\mu}(x)$ is covariant and is conserved. The same remarks hold for $\varepsilon^{\mu\nu} j_{\nu}(x) = \boldsymbol{j}^{\mu}(x)$. Once it is explicitly recognized that j^{μ} must be defined as a limit applied to a non-local operator it is also evident that the commutators (12) need not be correctly given by making use of the formal expressions (2) and (6) and the canonical commutation relations. In fact only if $j^{\mu}(x)$ can be defined in terms of (13) when only spacelike displacements ε^{μ} are involved will (12) follow with the use of the canonical commutation relations alone. However, it is clear that if $j^{\mu}(x)$ can be consistently defined as a conserved operator, then the equal time commutation relation must have the form

$$[\psi(x),\, j^{0}(y)] = a\,\delta(x-y)\,\psi(x) \tag{14}$$

since when j^{μ} is conserved, j^{0} generates the local form of the gauge group (3). The constant a however, is not specified by such a group argument. Of course, a must turn out to be 1 if j^{μ} is definable in terms of (13) when ε is always spacelike, since then the canonical commutation rules yield (14) with $a = 1$. Likewise, if $\varepsilon^{\mu\nu} j_{\nu}(x) = \boldsymbol{j}^{\mu}(x)$ is conserved we must have

$$[\psi(x), \boldsymbol{j}^{0}(y)] = \bar{a}\,\delta(x-y)\gamma_{5}\,\psi(x)\,. \tag{15}$$

With these expressions for the equal time commutators we obtain the iden-

tities

$$\partial_\mu[i\langle 0|T(j^\mu(\xi)\psi(x)\overline{\psi}(y))|0\rangle] = a[\delta(\xi-x)-\delta(\xi-y)]\, i\langle 0|T(\psi(x)\overline{\psi}(y))|0\rangle, \tag{16}$$

$$\partial_\mu[i\langle 0|T(\boldsymbol{j}^\mu(\xi)\psi(x)\overline{\psi}(y))|0\rangle = \overline{a}[\delta(\xi-x)\gamma_{5x}+\delta(\xi-y)\gamma_{5y}]\, i\langle 0|T(\psi(x)\overline{\psi}(y))|0\rangle, \tag{17}$$

where γ_{5x} acts on $\psi(x)$, γ_{5y} on $\overline{\psi}(y)$. Because of the invariance (5),

$$\gamma_5 G(x-y) = -G(x-y)\gamma_5,$$

so (17) can also be written in the form

$$\partial_\mu[i\langle 0|T(\boldsymbol{j}^\mu(\xi)\psi(x)\overline{\psi}(y))|0\rangle = \overline{a}(\delta(\xi-x)-\delta(\xi-y))\gamma_5\, i\langle 0|T(\psi(x)\overline{\psi}(y))|0\rangle. \tag{18}$$

Eq. (16) and (17) specify completely the divergence and curl of a vector field. Further, the vacuum matrix elements impose boundary conditions. Thus, we can integrate (16) and (17) to find

$$i\langle 0|T(j^\mu(\xi)\psi(x)\overline{\psi}(y)|0\rangle = (g^{\mu\nu}a+\varepsilon^{\mu\nu}\overline{a}\,\gamma_5)\partial_\nu[D_+(\xi-x)-D_+(\xi-y)]G_+(xy), \tag{19}$$

where

$$-\Box^2 D_+(x) = \delta(x)$$

and is the function with positive frequencies for $x^0>0$, negative frequencies for $x^0<0$ [4].

The constants a and $\overline{a}$ are so far undetermined, but the important thing is that the form of the vertex function is given by the conservation laws alone. In order to find the equation for the Green's function $G_+(xy)$ we must allow the space-time point ξ coincide with x. That is, we must define the product of the singular operators $j^\mu(x)$ and $\psi(x)$. We shall define the product by the limit

$$f(x)\equiv\gamma_\mu j^\mu(x)\psi(x)\equiv\lim_{\varepsilon\to 0}\tfrac{1}{2}[j^\mu(x+\varepsilon)\gamma_\mu\psi(w)+\gamma_\mu\psi(x)j^\mu(x-\varepsilon)]. \tag{20}$$

We shall find that our general definition of the products of singular operators to be given below is in this case equivalent to (20). Thus, we obtain [5]

$$i\gamma^\mu\langle 0|T(j_\mu(x)\psi(x)\overline{\psi}(y))|0\rangle = -(a-\overline{a})\gamma^\mu\partial_\mu D_+(x-y)\,G_+(x-y). \tag{21}$$

---

[4] See appendix.

[5] We note the difficulty which would occur if $a=\overline{a}$, namely, the vertex would vanish. This would imply that the operator $f(x)=\gamma^\mu(1/i)\partial_\mu\psi(x)$ vanishes if the theory is local and the metric in Hilbert space positive [6]. However, the vanishing of f would be in contradiction to (25) with $a=\overline{a}$.

[6] P. Federbush and K. Johnson: *Phys. Rev.*, **120**, 1926 (196.).

The equation for $G_+(xy)$, (10), may then be integrated and yields

$$G_+(xy) = \exp\left[-i\lambda(a-\bar{a})[D_+(x-y)-D_+(0)]\right] G_+^{(0)}(xy)\,, \tag{22}$$

where $G_+^{(0)}(xy)$ is the free field function,

$$\gamma^\mu \frac{1}{i}\,\partial_\mu G_+^{(0)}(xy) = \delta(xy)\,. \tag{23}$$

We shall discuss (22) in Section 3.

Let us now consider the equation for the Green's function $G_+(xx'yy')$,

$$\gamma_x^\mu \frac{1}{i}\,\hat{c}_\mu^x G_+(xx'yy') = \delta(xy)G_+(x'y') - \delta(xy')G_+(x'y) - \\ - \lambda\gamma_x^\mu \langle 0\,|\,T[j_\mu(x)\psi(x)\psi(x')\,\overline{\psi}(y')\,\overline{\psi}(y)]\,|\,0\rangle\,. \tag{24}$$

With the use of the same method that was applied to the vertex to give a closed equation for $G_-(xy)$ we can also calculate the form of the Green's function $G_+(xx'yy')$ uniquely in terms of the two constants $a, \bar{a}$. If we then require that $G_+(xx'yy')$ yield the vertex (19) as $x'-y'\to 0$, we will enforce the coupling between the various Green's functions implied by the field equations. This requirement yields two equations for the constants a and $\bar{a}$. The general form of the vertex which enters (24) is obtained as

$$-\langle 0\,|\,T[j^\mu(\xi)\psi(x)\psi(x')\,\overline{\psi}(y')\,\overline{\psi}(y)]\,|\,0\rangle = \tag{25}$$

$$= [a\partial^\mu\big(D_+(\xi-x)+D_+(\xi-x')-D_+(\xi-y)-D_+(\xi-y')\big)+$$

$$+\bar{a}\varepsilon^{\mu\nu}\partial_\nu\big(D_+(\xi-x)\gamma_{5x}+D_+(\xi-x')\gamma_{5x'}+D_+(\xi-y)\gamma_{5y}+D_+(\xi-y')\big)\gamma_{5y'}]G_+(xx'yy')\,,$$

by making use of the conservation equations and equal time commutation rules. With the use of (25), (24) can be integrated and gives

$$G_+(xx'yy') = \tag{26}$$

$$= \exp\left[i\lambda(a-\bar{a}\,\gamma_{5x}\gamma_{5x'})[D_+(x-x')-D_+(x-y')+D_+(y-y')-D_+(y-x')]\right]\cdot$$

$$\cdot G_+(xy)\,G_+(x'y') -$$

$$-\exp\left[i\lambda(a-\bar{a}\,\gamma_{5x}\gamma_{5x'})[D_+(x-x')-D(x-y)+D_+(y-y')-D_+(y'-x')]\right]\cdot$$

$$\cdot G_+(xy)'\,G_+(x'y)\,.$$

In order to calculate the vertex (19), we allow $x'-y'=\varepsilon\to 0$. In this limit the Green's function $G(x'y')=G(\varepsilon)$ becomes singular,

$$G(\varepsilon)\to\frac{\gamma\varepsilon}{\varepsilon^2}\cdot\frac{1}{2\pi}\,. \tag{27}$$

We also note that the exponential factor in the first term of (26) approaches

$$\exp\left[i\lambda(a-\bar{a}\,\gamma_{5x}\gamma_{5x'})\varepsilon^{\alpha}\partial_{\alpha}[D_{+}(x-x')-D_{+}(y-x')]\right].$$

Thus, if we average the limiting forms for ε and $-\varepsilon$ we find a contribution from the first term of (26) multiplying the quantity

$$\frac{\varepsilon^{\alpha}\varepsilon^{\beta}}{\varepsilon^{2}},$$

for small ε. It is thus clear that if the current is defined in terms of the operator

$$j^{\mu}(x;\varepsilon)=\tfrac{1}{2}[\overline{\psi}(x+\varepsilon)\gamma^{\mu}\psi(x)-\psi(x)\,\overline{\psi}(x-\varepsilon)\gamma^{\mu}] \tag{28}$$

as $\varepsilon\to 0$, the limiting operator will be finite but not covariant, since $\varepsilon^{\alpha}\varepsilon^{\mu}/\varepsilon^{2}$ approaches a finite limit as in any frame, but « remembers » the frame in which the components of ε vanish. It is not possible to make a covariant limit by averaging over all directions ε^{μ} in a hyperbolic space because the volume of the surface $\varepsilon^{2}=\text{const}$ is divergent. We shall do the next best thing. Thus, take ε^{μ} to be timelike and define a reciprocal spacelike vector by

$$\varepsilon^{\mu}\tilde{\varepsilon}_{\mu}=0\,.$$

We shall then let

$$j^{\mu}(x)\equiv\tfrac{1}{2}[j^{\mu}(x;\varepsilon)+j^{\mu}(x;\tilde{\varepsilon})]_{\substack{\varepsilon\to 0\\ \tilde{\varepsilon}\to 0}}. \tag{29}$$

In this case, since

$$\frac{\varepsilon^{\alpha}\varepsilon^{\beta}}{\varepsilon^{2}}+\frac{\tilde{\varepsilon}^{\alpha}\tilde{\varepsilon}^{\beta}}{\tilde{\varepsilon}^{2}}=g^{\alpha\beta},$$

we obtain a covariant limiting operator. Consequently, the first term of (26) as well as the second gives a contribution to the vertex and we obtain

$$\begin{aligned} i\langle 0\,|\,T[j^{\mu}(\xi)\psi(x)\,\overline{\psi}(y)]\,|\,0\rangle &= \\ &=\left[\left(1+\frac{\lambda}{2\pi}\,a\right)g^{\mu\nu}+\left(1-\frac{\lambda}{2\pi}\,\bar{a}\right)\gamma_{5}\varepsilon^{\mu\nu}\right]\partial_{\nu}[D_{+}(\xi-x)-D_{+}(\xi-y)]\,G_{+}(xy)\,. \end{aligned} \tag{30}$$

If we compare with (19) we find

$$a=\frac{1}{1-\lambda/2\pi}\,,\qquad \bar{a}=\frac{1}{1+\lambda/2\pi}\,. \tag{31}$$

In summary, we find that the definition (29) of the current operator leads to a conserved, covariant operator whose commutation relations with the field are given by (14) and (15) with constants a, $\bar{a}$ which differ from unity. This conclusion is not in contradiction with the canonical commutation rules since, the definition (29) involves infinitesimal displacements in both timelike and spacelike directions. Finally, it may be remarked that the above procedure has been applied to the general Green's functions with the result that (31) emerges consistently in the general case. Hence, we have a complete and consistent solution of the model.

3. – Renormalization.

If we replace a and $\bar{a}$ by (31) in the expression for $G_+(xy)$ we have

$$G_+(xy) = \exp\left[-i\frac{\lambda^2/\pi}{1-(\lambda/2\pi)^2}[D_+(x-y)-D_+(0)]\right]G_+^{(0)}(x-y)\,. \tag{32}$$

The Green's function $D_+(x)$ is singular at $x^2=0$. In fact, the solution is

$$D_+(x) = \frac{i\pi}{(2\pi)^2}\log\left\{\frac{x_0^2}{x^2}\right\}, \tag{33}$$

where $(1/x_0^2)^{\frac{1}{2}}$ is an arbitrary constant with the dimensions of a mass. Thus, the positive-negative frequency boundary condition does not specify the constant, zero frequency term in $D_+(x)$. Naturally, since only differences of D_+ enter the equations, the constant term is arbitrary. However, since $D_+(0)$ diverges, the solution (32) is only formal, that is, the Green's functions require a renormalization since the coupled fields do not admit a true canonical commutator. We may renormalize by making the matrix element of the operator $\psi[\langle 0|\psi|p''\rangle,\ p^2=-m^2]$ take on a chosen value at an arbitrary state. Naturally, no physical question will depend upon either the normalization chosen, or the mass of the state. In this way we define the « renormalization » constant

$$Z_2 = \exp\left|i\frac{\lambda^2/\pi}{1-(\lambda/2\pi)^2}D_+(0)\right| = \exp\left[-\frac{(\lambda/2\pi)^2}{1-(\lambda/2\pi)^2}\log\frac{x_0^2}{x^2}\right|_{x^2=0}, \tag{34}$$

$$= 0\,,$$

so the « renormalized » Green's function is

$$G_+(xy) = \exp\left[\frac{(\lambda/2\pi)^2}{1-(\lambda/2\pi)^2}\log\frac{x_0^2}{(x-y)^2}\right]G_+^{(0)}(xy) - \frac{G(xy)}{Z_2}\,, \tag{35}$$

$G(xy)$ admits the spectral representation in momentum space

$$G(p) = \frac{\sin \pi\alpha}{\pi} \int_0^\infty \frac{dk}{k} \left(\frac{k}{m}\right)^{2\alpha} \frac{-2\gamma p}{p^2 + k^2} = \frac{1}{\gamma p} (p^2/m^2)^\alpha, \tag{36}$$

where

$$\alpha = \frac{(\lambda/2\pi)^2}{1 - (\lambda/2\pi)^2} \qquad \text{and} \qquad m^2 = \frac{4}{x_0^2} \left(\frac{\alpha!}{-\alpha!}\right)^{1/\alpha},$$

(we assume $\alpha < 1$). We notice that an attempt to expand the spectral function in powers of α (or λ) would lead to a sequence of infra-red divergent integrals. The cause is the zero mass of the field and the confluence of an infinite sequence of thresholds at $k = 0$. Because G has no pole, a single particle state does not exist in the theory, and hence also, no asymptotic field. The theory provides a perfect model of the infra-red structure of massless fields. Thus, the particle Green's function in quantum electrodynamics has precisely the singularity described by (36) when $p^2 \to p^2 + m_e^2 \sim 0$ (7).

4. – Coupling to an external field.

It is interesting to discuss the coupling of the current to an external field because such a coupling presents problems quite analogous to those regarding the questions of gauge invariance in quantum electrodynamics.

Suppose the equation in an external field is

$$\gamma^\mu \frac{1}{i} \partial_\mu \psi(x) = a\gamma^\mu \varphi_\mu(x)\, \psi(x) + \lambda j^\mu(x) \cdot \gamma_\mu \psi(x)\,. \tag{37}$$

The renormalizing factor a is included for convenience since we have already discovered that the local group generated by j^0 includes such a factor. Thus, (32) is invariant under the group

$$\begin{cases} \delta\psi(x) &= ia\alpha(x)\,\psi(x)\,, \\ \delta\varphi_\mu(x) &= \partial_\mu \alpha(x)\,, \end{cases} \tag{38}$$

if we assume that the current operator is invariant under this group. Again, $j^\mu(x)$ is a conserved vector field with this assumption. To insure the invariance of the local current under (38), we shall define it as the local limit of the gauge

(7) K. JOHNSON and B. ZUMINO: *Phys. Rev. Lett.*, **3**, 351 (1959).

invariant ([8]) non-local operator

$$(39)\qquad j^{\mu}(x,\varepsilon) = \\ = \frac{1}{2}\left|\overline{\psi}(x+\varepsilon)\gamma^{\mu}\psi(x)\exp\left[ia\int_{x}^{x+\varepsilon}\mathrm{d}\xi^{\mu}q_{\mu}\right] - \psi(x)\,\overline{\psi}(x-\varepsilon)\gamma^{\mu}\exp\left[-ia\int_{x-\varepsilon}^{x}\mathrm{d}\xi^{\mu}q_{\mu}\right]\right| .$$

in the sense of the limiting procedure (29). It might be supposed that (37) is also invariant under the group

$$(40)\qquad \begin{cases} \delta\psi(x) = i\bar{a}\,\alpha(x)\gamma_5\psi(x)\,, \\ \delta q_{\mu}(x) = \varepsilon_{\mu\nu}\partial^{\nu}\alpha(x)\,. \end{cases}$$

If this is to be true, we should also be able to write (37) in the form

$$(41)\qquad \gamma^{\mu}\frac{1}{i}\,\partial_{\mu}\psi(x) = \bar{a}\gamma^{\mu}\gamma_5\varepsilon_{\mu\nu}\varphi^{\nu}(x)\,\psi(x) + \lambda\gamma^{\mu}\gamma_5\boldsymbol{j}_{\mu}(x)\,\psi(x)\,.$$

In this case $\boldsymbol{j}^{\mu}$ must be defined in terms of the non-local operator invariant under (40), namely

$$(42)\qquad \boldsymbol{j}^{\mu}(x;\varepsilon) = \frac{1}{2}\left|\overline{\psi}(x+\varepsilon)\gamma^{\mu}\gamma_5\exp\left[i\bar{a}\gamma_5\int_{x}^{x+\varepsilon}\mathrm{d}\xi^{\mu}\varepsilon_{\mu\nu}\varphi^{\nu}\right]\psi(x) - \right. \\ \left. - \psi(x)\,\overline{\psi}(x-\varepsilon)\gamma^{\mu}\gamma_5\exp\left[-i\bar{a}\gamma_5\int_{x-\varepsilon}^{x}\mathrm{d}\xi^{\mu}\,\varepsilon_{\mu\nu}\varphi^{\nu}\right]\right| .$$

in the sense of (29). It would not be possible for (37) and (41) to be mutually consistent if the relation $\boldsymbol{j}^{\mu} = \varepsilon^{\mu\nu}j_{\nu}$ held for the current operators in the presence of an external field. We see that the operators j^{μ} and $\boldsymbol{j}^{\mu}$ are no longer necessarily connected in this way since they are defined by a limiting procedure applied to non-local operators no longer related by $\varepsilon^{\mu\nu}$. In fact, if eq. (37) and (41) are consistent, the connection between the operators j^{μ} and $\boldsymbol{j}^{\mu}$ must be

$$(43)\qquad \boldsymbol{j}^{\mu} = \varepsilon^{\mu\nu}j_{\nu} + (a-\bar{a})\frac{1}{\lambda}\,\varepsilon^{\mu\nu}\varphi_{\nu} = \varepsilon^{\mu\nu}j_{\nu} + \frac{1}{\pi}\frac{1}{1-(\lambda/2\pi)^2}\,\varepsilon^{\mu\nu}\varphi_{\nu}\,.$$

We shall find that this is indeed the relation between the operators implied by the definitions (39) and (42).

([8]) J. Schwinger: *Phys. Rev.*, **82**, 664 (1951).

To show this, let us accept the consistency of (37) and (41), or, equivalently, (43). We may then calculate the vacuum current induced by the external field by making use of the conservation laws for j^μ and $\boldsymbol{j}^\mu$. We compare this with the current calculated by first determining the Green's function in the external field and then making use of the definition of the current operator in terms of (39). A similar comparison can likewise be made working with the general Green's function in which case it shows that the definitions (39) and (42) lead to *operators* related by (43).

Let $\langle \text{out}| = \langle 0,\ t \to +\infty|$, $|\text{in}\rangle = |0,\ t \to -\infty\rangle$, where the external perturbation is turned off in the distant future and past. In virtue of the conservation of current

$$\partial_\mu \langle \text{out}|\, j^\mu(\xi)\,|\text{in}\rangle = 0 \tag{44}$$

and because of the conservation of $\boldsymbol{j}^\mu$ and (43)

$$\partial_\mu \langle \text{out}|\, j^\mu(\xi)\,|\text{in}\rangle = -\frac{1}{\pi}\frac{1}{1-(\lambda/2\pi)^2}\,\partial_\mu \varepsilon^{\mu\nu}\varphi_\nu(\xi)\langle \text{out}|\text{in}\rangle \quad . \tag{45}$$

Hence

$$\frac{\langle \text{out}|\, j^\mu(\xi)\,|\text{in}\rangle}{\langle \text{out}|\text{in}\rangle} = -\frac{1}{\pi}\frac{1}{1-(\lambda/2\pi)^2}\,\varepsilon^{\mu\alpha}\partial_\alpha\,\varepsilon^{\nu\beta}\partial_\beta \int D_-(\xi-\xi')\varphi_\nu(\xi')(\mathrm{d}\xi') \,. \tag{46}$$

Next, we calculate $G_+(xy;\varphi)$ and then show with (39) that (46) results. Thus

$$G_+(xy;\varphi) \equiv \frac{i\langle \text{out}|\, T(\psi(x)\,\overline{\psi}(y))\,|\text{in}\rangle}{\langle \text{out}|\text{in}\rangle} \,, \tag{47}$$

and

$$\gamma^\mu \frac{1}{i}\partial_\mu G_+(xy;\varphi) = \delta(xy) + a\gamma^\mu \varphi_\mu(x) G_+(xy;\varphi) + \\ + \lambda\gamma^\mu \frac{i\langle \text{out}|\, T(j_\mu(x)\psi(x)\,\overline{\psi}(y))\,|\text{in}\rangle}{\langle \text{out}|\text{in}\rangle} \,. \tag{48}$$

If we again use (43) and the conservation equations for j^μ and $\boldsymbol{j}^\mu$ the, vertex function is

$$\frac{i\langle \text{out}|\, T(j^\mu\psi\overline{\psi})\,|\text{in}\rangle}{\langle \text{out}|\text{in}\rangle} = [a g^{\mu\alpha} + \bar{a}\,\varepsilon^{\mu\alpha}\gamma_5]\,\partial_\alpha[D_+(\xi-x) - D_+(\xi-y)]\cdot \\ \cdot G_+(xy;\varphi) - \frac{1}{\pi}\frac{1}{1-(\lambda/2\pi)^2}\,\varphi^\mu(\xi) G(xy;\varphi) + \\ + \frac{1}{\pi}\frac{1}{1-(\lambda/2\pi)^2}\int \partial^\mu \partial^\nu D_+(\xi-\xi')\varphi_\nu(\xi')(\mathrm{d}\xi')\cdot G_+(xy;\varphi) \,. \tag{49}$$

If we let $\xi \to x$ and use this expression in (48) we can integrate the resulting equation to find

$$(50) \qquad G(xy;\varphi) = \exp\left[-i\lambda(a-\bar{a})[D_+(x-y)-D_+(0)]\right]\cdot$$
$$\cdot\exp\left[-ia\int[D_+(x-\xi)-D_+(y-\xi)]\partial^\mu\varphi_\mu(\xi)(\mathrm{d}\xi)\right]\cdot$$
$$\cdot\exp\left[-i\bar{a}\gamma_5\int[D_+(x-\xi)-D_+(y-\xi)]\partial^\mu\varepsilon_{\mu\nu}\varphi^\nu(\xi)(\mathrm{d}\xi)\right]G^{(0)}(xy)\,.$$

We then let $x-y\to 0$ and calculate the current. With the important factors which make the operator $j^\mu(x;\varepsilon)$ gauge invariant, the result agrees exactly with (46). By making use of the techniques used in this section explicit formulas for the general Green's function in an external field may be given.

5. – The current-charge density commutator.

The gauge problem similar to one in quantum electrodynamics may now be raised. The question arises from the lack of commutation at equal times of the current and charge density operators ([2,9]). In quantum electrodynamics the commutator is proportional to a positive divergent integral also identified as a « photon mass ». It hence has been argued that « since in a gauge invariant theory the photon mass must be zero, this commutator must vanish ». We wish to point out that the commutator in fact cannot vanish, and secondly, that this entails no contradiction to gauge invariance, but indeed is required by gauge invariance. We shall investigate the question of this commutator in the context of the model studied in this paper but exactly the same general remarks apply also in quantum electrodynamics ([10]).

The current operator $j^\mu(x)$ has been defined so that it is invariant under the group (38). The generator of (38) on the field operators ψ is the operator $j^0(y)$. Yet, it *cannot* be true that ([10,11])

$$(51) \qquad [j^1(x), j^0(y)]_{x^0=y^0} = 0$$

for this would raise a contradiction to the conservation of charge. Let us review briefly that contradiction. If (51) is assumed, then from $\partial_\mu j^\mu = 0$ it follows that

$$0 = [\partial_1 j^1(x), j^0(y)] = -[\partial_0 j^0(x), j^0(x)]$$

or

$$0 = [[j^0(x), H], j^0(y)]\,,$$

([9]) F. L. Scarf: *Nucl. Phys.*, **11**, 475 (1959).
([10]) K. Johnson: to be published.
([11]) J. Schwinger: *Phys. Rev. Lett.*, **3**, 296 (1959).

where H is the Hamiltonian operator. But since $\langle 0|$ is the lowest energy eigenstate $(H|0\rangle = 0)$

$$\sum_{\gamma,E} \langle 0|j^0(x)|E,\gamma\rangle E\langle E,\gamma|j^0(y)|0\rangle = 0 \tag{52}$$

which implies

$$\langle 0|j^0(x) = 0 \qquad \text{or} \qquad \langle 0|j^\mu(x) = 0\,. \tag{53}$$

This, in a local, relativistic field theory, means that $j^\mu(x) = 0$ ([6]). Hence (51) contradicts the conservation of charge, and the non-vanishing of $j^\mu(x)$. Yet, if (51) does not hold, how is it that the current operator is invariant under the local gauge group which is necessary for the law of charge conservation? This dilemma can also be sharply put by observing that the usual formula for the current induced in the vacuum by an external perturbation (for simplicity, to lowest order in the external field) is

$$\langle \text{out}|j^\mu(x)|\text{in}\rangle = i\int \langle 0|T(j^\mu(x)j^\nu(y))|0\rangle \varphi_\nu(y)(\mathrm{d}y)\,, \tag{54}$$

and from (54) it would appear that the induced current is *not* conserved unless $[j^0(x), j^1(y)] = 0$, *i.e.*, unless j^1 is invariant under the group generated by j^0.

The operator which generates the gauge group (38) is

$$G = -\int (\mathrm{d}y)\alpha(y)j^0(y)\,, \tag{55}$$

thus

$$\delta\psi(x) = \frac{1}{i}[\psi(x), G] = ia\alpha(x)\psi(x)\,. \tag{56}$$

But the *full invariance* for the theory means we must also perform the compensating change in the external potential

$$\delta\varphi^\mu(x) \simeq \partial^\mu\alpha(x)\,. \tag{57}$$

Thus, the change in the current operator produced by the generator (55) is

$$\delta j^\mu(x) = i\int \mathrm{d}y\,\alpha(y)[j^\mu(x), j^0(y)]\,,$$

and because $j^\mu(x)$ is invariant if we *also* perform (57), the change in the current produced by (57) alone must be

$$\tilde{\delta} j^\mu(x) = -i\int \mathrm{d}y\,\alpha(y)[j^\mu(x), j^0(y)]\,. \tag{58}$$

The invariance of $j^\mu(x)$ under the combined transformation is guaranteed since the non-local form of the current is invariant under this full group at every stage, hence the limiting operator will also be characterized by this invariance. Accordingly, if $[j^\mu(x), j^0(y)]$ does not vanish, there is no contradiction to the conservation law, because (54) is not a correct equation for the induced vacuum current. This is because (54) is derived with the (implicitly made) assumption that the current operator does not *explicitly* depend upon the external perturbation q^μ, and this assumption is not consistent with (58). In fact, if we take into account the explicit dependence of $j^\mu(\xi)$ on $q^\mu(\xi)$ denoting it by

$$\tilde{\delta} j^\mu(\xi) = S^{\mu\nu}\,\delta q_\nu(\xi) \tag{59}$$

then the correct version of (54) is

$$\langle \text{out}\,|\,j^\mu(\xi)\,|\,\text{in}\rangle = \int \left(i\langle 0\,|\,T\big(j^\mu(\xi) j^\nu(\xi')\big)\,|\,0\rangle + S^{\mu\nu}\,\delta(\xi-\xi')\right) \varphi_\nu(\xi')(\mathrm{d}\xi') \,, \tag{60}$$

(in this model, $S^{\mu\nu}$ turns out not to be an operator).

Since

$$0 = \partial_\mu \langle \text{out}\,|\,j^\mu(\xi)\,|\,\text{in}\rangle \,,$$

we find

$$\delta(\xi^0-\xi'^0)\, i\langle 0\,|\,[j^0(\xi),\, j^\mu(\xi')]\,|\,0\rangle + S^{\mu\nu}\partial_\nu \delta(\xi-\xi') = 0$$

or $S^{01} = S^{10} = S^{00} = 0$ and

$$\langle 0\,|\,[j^0(\xi),\, j^1(\xi')]\,|\,0\rangle = i S^{11} \partial_1 \delta(\xi-\xi') \,. \tag{61}$$

Now, this structure for $S^{\mu\nu}$ indicates that $i\langle 0\,|\,T\big(j^\mu(\xi)\, j^\nu(\xi')\,|\,0\rangle$ is not a covariant function. Indeed this is the case as we can now show by an explicit calculation of $\langle 0\,|\,j^\mu(\xi) j^\nu(\xi')\,|\,0\rangle$. This matrix element may be calculated from (18), and the definition of the current operator in terms of (28) and (29). Thus we find

$$\langle 0\,|\,j^\mu(\xi) j^\nu(\xi')\,|\,0\rangle = -\frac{1}{\pi}\,\frac{1}{1-(\lambda/2\pi)^2}\,\partial^\mu \partial^\nu D^{(+)}(\xi-\xi') \,, \tag{62}$$

where $-\square^2 D^{(+)}(x) = 0$, and $D^{(+)}$ contains only positive frequencies. The time-ordered function is defined by

$$\langle 0\,|\,T\big(j^\mu(\xi) j^\nu(\xi')\big)\,|\,0\rangle \equiv \theta(\xi^0-\xi'^0)\langle 0\,|\,j^\mu(\xi) j^\nu(\xi')\,|\,0\rangle + \\ + \theta(\xi'^0-\xi^0)\langle 0\,|\,j^\nu(\xi') j^\mu(\xi)\,|\,0\rangle \,. \tag{63}$$

We see immediately that

$$\langle 0 \,|\, [j^0(\xi),\, j^1(\xi')] \,|\, 0 \rangle = i\,\partial'\,\delta(\xi - \xi')\left\{-\frac{1}{\pi}\frac{1}{1-(\lambda/2\pi)^2}\right\}, \tag{64}$$

o $S^{11} = -(1/\pi)(1/(1-(\lambda/2\pi)^2))$. Further, with

$$D^{(+)}(\xi - \xi')\,\theta(\xi^0 - \xi'^0) + D^{(-)}(\xi - \xi')\,\theta(\xi'^0 - \xi^0) \equiv D_+(\xi - \xi')$$

we find by combination of (62) and (63)

$$\langle 0 \,|\, T(j^\mu(\xi)\, j^\nu(\xi')) \,|\, 0 \rangle = -\frac{1}{\pi}\frac{1}{1-(\lambda/2\pi)^2}\,\partial^\mu\partial^\nu D_+(\xi - \xi') + \tag{65}$$

$$+\,\delta^{\mu 0}\delta^{\nu 0}\frac{1}{\pi}\delta(\xi - \xi')\,\frac{1}{1-(\lambda/2\pi)^2},$$

which explicitly shows the lack of covariance of this function. Nevertheless, we find that the correct Green's function for the induced current

$$i\langle 0 \,|\, T(j^\mu(\xi)\, j^\nu(\xi')) \,|\, 0 \rangle + S^{\mu\nu}\,\delta(\xi - \xi') = \tag{66}$$

$$= +\frac{1}{\pi}\frac{1}{1-(\lambda/2\pi)^2}\,(g^{\mu\nu}\,\Box^2 - \partial^\mu\partial^\nu)\,D_+(\xi - \xi'),$$

is covariant and conserved. We also see the consistency with our previous result (46). Naturally, the remarks made here apply as well to the pseudovector current $\boldsymbol{j}^\mu$. Thus, the analogue of (59) is

$$\delta\boldsymbol{j}^\mu = S^{\mu\varkappa}\varepsilon_{\varkappa\nu}\delta\varphi^\nu \tag{67}$$

or

$$\begin{cases} \delta\boldsymbol{j}^1 = -\dfrac{1}{\pi}\dfrac{1}{1-(\lambda/2\pi)^2}\,\varepsilon_{10}\delta\varphi^0, \\ \delta\boldsymbol{j}^0 = 0, \end{cases} \tag{68}$$

but in fact, (59) and (43), which give the connection between j^μ and $\boldsymbol{j}^\mu$, are equivalent to (68), again illustrating the internal consistency of the model. (This remark also establishes the fact that $S^{\mu\nu}$ is not a field operator.)

In summary, if the current is defined in terms of the gauge invariant expression (39), no difficulty arises from the fact that the charge and current operators do not commute at equal times.

6. – Conclusions.

We have shown how it is possible to solve the two dimensional model of Thirring by making use of the existence of the two vector density conservation laws. In this solution the infra-red problem caused no special difficulty, although the physical consequences of the coupling are somewhat complicated because of the impossibility of a classification of the states by means of particle quantum numbers. However, in this connection the model is interesting because it provides a soluble theory in terms of which the infra-red structure of a relativistic field may be investigated. It was shown how it is possible to define the products of the singular operators $\psi(x)$, in order to determine other covariant operators but that these singular field products do not satisfy the equal time commutation relations with the field operators $\psi(x)$, that one would obtain by means of the canonical commutation relations, together with the use of the formal expressions for the singular field products.

In fact, it was found that in general it is necessary to make use of the gauge invariance principle to determine the correct expression for the current operator. In this connection it should be noted that other finite operators, which are vector densities, « formally » identical but in fact different, could be obtained. It is thus quite interesting that an invariance principle was needed to provide a guide to find the proper current operator.

Finally, it was shown how the lack of commutation of the charge and current densities at equal times is not something which contradicts gauge invariance but, on the contrary, is required by gauge invariance. Further, if this commutation relation is consistently treated one is led to solutions for the Green's functions and amplitudes in the presence of external fields which are invariably consistent with the gauge invariance of the original field equations.

In this note we did not discuss the question of the construction of the energy momentum operators as functions of the local field operators. This problem is complicated by the lack of finiteness of the renormalization constant.

We also did not discuss the meaning of the singularity of our solutions for $\lambda/2\pi = \pm 1$. Presumably, this is the limit on the magnitude of $\lambda/2\pi$ for which there is a ground state, (*i.e.*, a spectrum for the field Hamiltonian bounded from below), but this problem is naturally better examined in the context of a discussion of the field Hamiltonian.

* * *

The author wishes to acknowledge useful discussions with Professor P. Federbush and Dr. C. Sommerfeld about two dimensional field theories.

APPENDIX

We should like to prove that, if $a^\mu(x)$ is an arbitrary vector field in two dimensional space-time and if $\partial^\mu a_\mu$ and $\partial^\mu \varepsilon_{\mu\nu} a^\nu$ are given together with the boundary condition that a^μ has positive frequencies in the « distant » future (*i.e.*, for $x^0 > \tau$, a^μ can be given a Fourier representation with only positive frequency components) and negative frequencies in the « distant » past (*i.e.*, for $x^0 < \tau'$, a^μ etc.) then a^μ is given uniquely by

$$a^\mu(x) = -\partial^\mu \int D_+(x - x')\, \partial^\nu a_\nu(x')(\mathrm{d}x') - \varepsilon^{\mu\alpha}\partial_\alpha \int D_+(x - x')\, \partial^\nu \varepsilon_{\nu\beta} a^\beta(\mathrm{d}x') \,, \tag{A.1}$$

where

$$-\Box^2 D_+(x) = \delta(x) \,, \tag{A.2}$$

and has positive frequencies for $x^0 > 0$, negative frequencies for $x^0 < 0$.

First, it is clear that the expression (A.1) for a^μ gives the divergence and curl correctly and satisfies the mentioned boundary condition. To show the uniqueness we must ask for a function with vanishing curl and divergence which satisfies the boundary conditions. Suppose b^μ is such a function. It is clear that we can always determine a φ and $\bar{\varphi}$ such that

$$b^\mu(x) = \partial^\mu \varphi(x) + \varepsilon^{\mu\nu}\partial_\nu \bar{\varphi}(x) \,. \tag{A.3}$$

The vanishing curl and divergence are equivalent to

$$\Box^2 \varphi = 0 = \Box^2 \bar{\varphi} \,. \tag{A.4}$$

So the problem can be restated as showing that no non-constant solution of $\Box^2 \varphi = 0$ exists which satisfies the negative-positive frequency boundary condition. It is clear from the differential equation that

$$\varphi(x) = \int_{-\infty}^{+\infty} \mathrm{d}q \, \exp\,[i(qx - |q|x^0)]\varphi_+(q) + \int_{-\infty}^{+\infty} \mathrm{d}q \, \exp\,[i(qx + |q|x^0)]\varphi_-(q) \,,$$

where we can remove any zero frequency term as excluded (*i.e.*, $\varphi_\pm(0) = 0$). Further, for $x^0 > \tau$ the second term must vanish, *i.e.*,

$$\int_{-\infty}^{+\infty} \mathrm{d}q \, \exp\,[i(qx + |q|x^0)]\varphi_-(q) = 0 \,, \qquad x^0 > \tau,$$

and for $x^0 < \tau'$ the first term must vanish, *i.e.*,

$$\int_{-\infty}^{+\infty} \mathrm{d}q \, \exp\,[i(qx + |q|x^0)]\,\varphi_+(q) = 0, \qquad x^0 < \tau'.$$

If we integrate either expression $x \exp[-iq'x]$ over all x, we find

$$\exp[i|q'|x^0]\varphi_-(q') = 0\,, \qquad x^0 > \tau,$$

$$\exp[-i|q'|x^0]\varphi_+(q') = 0\,. \qquad x^0 < \tau'.$$

Hence $\varphi_+ = \varphi_- = 0$, which proves the uniqueness of (A.1).

Let us next consider the function D_+. D_+ obeys the equation

$$-\Box^2 D_+(x) = \delta(x)\,, \tag{A.5}$$

and has positive frequencies in the future, negative in the past. The function

$$D_+(x;y) = \int \frac{(\mathrm{d}q)}{(2\pi)^2} \frac{\exp[iqx] - \exp[iqy]}{q^2 - i\varepsilon}\,, \qquad \varepsilon \to +0, \tag{A.6}$$

satisfies these boundary conditions, and the differential equation. The constant, zero frequency term which involves an arbitrary vector y cannot be removed since the zero frequency part of the first term gives a divergent contribution. This, of course, plays no role in (A.1) since only

$$\partial^\mu D_+ = \int \frac{(\mathrm{d}q)}{(2\pi)^2}\, iq^\mu \frac{\exp[iqx]}{q^2 - i\varepsilon} \tag{A.7}$$

enters. If the integral (A.6) is calculated we find

$$D_+(x;y) = \frac{i\pi}{(2\pi)^2} \log\left\{\frac{x^2}{y^2}\right\}. \tag{A.8}$$

RIASSUNTO (*)

Si dà la soluzione esplicita del gruppo accoppiato di equazioni per le funzioni di Green per il modello auto-accoppiato della teoria del campo di Thirring. Si trova che il problema infrarosso non genera particolare difficoltà. Sorge la questione sul modo di definire i prodotti degli operatori di campo singolari in punti coincidenti dello spazio-tempo e si mostra che le relazioni di commutazione per questi prodotti non vengono espresse coerentemente facendo uso delle espressioni formali e delle relazioni di commutazione canonica. Si studia il problema della invarianza di gauge in un campo esterno e si mostra *a*) che la corrente e la densità di carica non commutano in tempi uguali, e *b*) che questo è necessario per l'invarianza di gauge delle equazioni del campo, e coerente con essa.

(*) *Traduzione a cura della Redazione.*

IL NUOVO CIMENTO Vol. XX, N. 4 16 Maggio 1961

Note on the $\Delta I = \frac{1}{2}$ Selection Rule in the Composite Model of Elementary Particles.

S. Okubo (*) and R. E. Marshak (**)

CERN - Geneva

(ricevuto il 21 Marzo 1961)

Summary. — The Salam-Ward hypothesis concerning the $\Delta I = \frac{1}{2}$ selection rule in weak interactions is examined from the viewpoint of the composite model of elementary particles. In this theory, the non-leptonic weak decays have a different origin than the leptonic decays and are attributed to a small perturbation on the strong interactions.

One is on the horns of a dilemma [1] in attempting to explain the well-established [2] $\Delta I = \frac{1}{2}$ selection rule in non-leptonic weak decays. On the one hand, if one accepts a current-current interaction as the origin of both the non-leptonic and leptonic weak decays, one is led to introduce neutral baryon currents (with [3] or without [4] intermediate bosons) without the analogous neutral lepton currents. On the other hand, if one wishes to maintain the symmetry between the baryon and lepton currents (which is attractive from several points of view [5]), one must seek the explanation of the $\Delta I = \frac{1}{2}$ se-

(*) Supported by the National Science Foundation, U.S.A.

(**) Guest Professor under the Ford Foundation and Guggenheim Fellow, on leave from the University of Rochester for the academic year 1960-61.

(1) Cf. L. B. Okun: *Proc. of the 1960 Ann. Inter. Conf. on High Energy Physics at Rochester* (New York), p. 743. Also R. E. Marshak: *Proc. of the 1959 Ann. Inter. Conf. on High Energy Physics at Kiev*, Session VIII, p. 269.

(2) Cf. M. Schwarz: *Proc. of the 1960 Ann. Inter. Conf. on High Energy Physics at Rochester* (New York), p. 726.

(3) T. D. Lee and C. N. Yang: *Phys. Rev.*, **119**, 1410 (1960). See however, B. D'Espagnat: *Proc. of the 1960 Ann. Inter. Conf. on High Energy Physics at Rochester* (New York), p. 589.

(4) A. Pais: *Nuovo Cimento*, **18**, 1003 (1960); *Phys. Rev.* **122**, 317 (1961).

(5) Cf. R. E. Marshak and S. Okubo: *Nuovo Cimento* **19**, 1226 (1961).

lection rule in the special status of the non-leptonic weak decays compared to the leptonic decays (6). This second approach has been adopted by SALAM and WARD (7) who deduce the $\Delta I = \frac{1}{2}$ selection rule in weak interactions from a special hypothesis concerning the strong interactions, namely they assume that the K-meson field operator K possesses a very small non-vanishing vacuum expectation value in the Yukawa-type strong interaction, say $\Lambda N K^*$. The purpose of this note is to indicate in what fashion a composite model of elementary particles (of the type proposed by SAKATA (8) or the present authors (5)) provides a natural basis for the hypothesis of SALAM and WARD.

The strong interaction Hamiltonian containing both Λ and $\mathcal{N}$ (nucleon) may be written

$$H_1 = \sum_\lambda g_\lambda (\bar{\Lambda} Q_\lambda \Lambda)(\bar{\mathcal{N}} Q_\lambda \mathcal{N}) , \tag{1}$$

where Q_λ denotes the usual five covariant expressions (S, V, T, A, P), formed from the Dirac γ-matrices. Note that

$$\bar{\mathcal{N}} Q_\lambda \mathcal{N} = (\bar{p} Q_\lambda p) + (\bar{n} Q_\lambda n) , \tag{2}$$

where p and n represent the proton and neutron respectively. Then, the part containing the neutron can be transformed by means of the Fierz identity as follows:

$$\begin{cases} H_n = \sum_\lambda g_\lambda (\bar{\Lambda} Q_\lambda \Lambda)(\bar{n} Q_\lambda n) , \\ \quad = \sum_\lambda f_\lambda (\bar{\Lambda} Q_\lambda n)(\bar{n} Q_\lambda \Lambda) . \end{cases} \tag{3}$$

Now, in the usual theory, the vacuum expectation value $\langle \bar{n} Q_\lambda \Lambda \rangle_0$ must be zero, because of strangeness conservation. However, we suppose for the moment that somehow

$$c_\lambda = \langle \bar{n} Q_\lambda \Lambda \rangle_0 \neq 0 \qquad \text{for } \lambda = S \text{ or } P. \tag{4}$$

For $\lambda = V$, A or T, $c_\lambda = 0$ follows from Lorentz covariance. Then, eq. (3) would contain an interaction (9) of the form:

$$(f_s c_s)(\bar{\Lambda} n) + (f_p c_p)(\bar{\Lambda} \gamma_5 n). \tag{5}$$

(6) The consequences of the $\Delta I = \frac{1}{2}$ selection rule in strangeness-violating leptonic decays are identical with the $I = \frac{1}{2}$ current hypothesis (see R. E. MARSHAK, ref. (1)).

(7) A. SALAM and J. C. WARD: *Phys. Rev. Lett.*, **5**, 390 (1960). *Note added in proof.* It has come to our notice that a similar idea has already been expressed by T. H. R. SKYRME; *Proc. Roy. Soc.*, A **252**, 236 (1959), eq. (44).

(8) S. SAKATA: *Progr. Theor. Phys.*, **16**, 686 (1956).

(9) Such interactions have been already considered by several authors: R. F. SAWYER: *Phys. Rev.*, **112**, 2135 (1958); H. OBAYASHI: *Progr. Theor. Phys.*, **22**, 835 (1959); S. OKUBO: *Nuovo Cimento*, **16**, 963 (1960); S. ONEDA, J. C. PATI and B. SAKITA: *Phys. Rev.*, **119**, 482 (1960).

Thus, if eq. (4) happened to be true, with small constants c_s and c_p (or f_s and f_p), then the desired $\Delta I = \frac{1}{2}$ selection rule in weak interactions would follow from the strong interaction eq. (3). Note that if $f_s \cdot f_p \cdot c_s \cdot c_p \neq 0$, then eq. (5) would automatically lead to parity non-conservation. This is somewhat more natural than the original proposal of SALAM and WARD [7], who postulate the existence of a scalar particle K′ with unit strangeness in addition to the pseudoscalar K-meson, in order to explain parity violation in non-leptonic weak decays.

We must try to give an argument justifying eq. (4). To do this, let us consider the theory of Nambu and Jona-Lasinio [10]. We recall their argument for deriving a finite mass for the fermion, starting with a chirality-invariant Lagrangian. In the usual perturbational treatment, the vacuum expectation value $\langle \bar{\psi}(x)\, \psi(x) \rangle_0$ must be zero in a chirality-invariant theory. However, Nambu and Jona-Lasinio postulate from the beginning that

$$c = \langle \bar{\psi}(x)\, \psi(x) \rangle_0 \neq 0 \tag{6}$$

and, in a self-consistent fashion, they determine the value of the non-zero c. We now apply the same type of argument to eq. (4), and in the same way, we may obtain a non-zero value for c_λ. The desired $\Delta I = \frac{1}{2}$ weak interaction eq. (5) would then follow.

Let us illustrate our point of view in greater detail. For definiteness, we have recourse to the Tamm-Dancoff procedure previously used by DÜRR *et al.* [11] and by the present authors [5]. Furthermore, for simplicity, we assume $f_p = 0$. The equation of motion for the neutron is then

$$\left(\gamma \frac{\partial}{\partial x} + m_n \right) n = - f_s (\bar{\Lambda} n) \Lambda \,, \tag{7}$$

and we define the Green's function $K(x-y)$ by

$$K(x-y) = \langle (n(x)\, \bar{\Lambda}(y))_+ \rangle_0 \,. \tag{8}$$

Using eq. (7), we obtain

$$\left(\gamma \frac{\partial}{\partial x} + m_n \right) K(x-y) = - f_s \langle (\bar{\Lambda}(x)\, n(x)\, \Lambda(x)\, \bar{\Lambda}(y))_+ \rangle_0 \,, \tag{9}$$

where we have assumed

$$[n(x), \bar{\Lambda}(y)]_+ = 0 \qquad \text{for } x_0 = y_0 \,. \tag{10}$$

[10] Y. NAMBU and G. JONA-LASINIO: *Phys. Rev.* **122**, 345 (1961).

[11] H. P. DÜRR, W. HEISENBERG, H. MITTER, S. SCHLIEDER and K. YAMAZAKI: *Zeits. f. Naturfor.*, **14***a*, 441 (1959).

As a first-order approximation of the Tamm-Dancoff method [11], we may replace

$$\langle(\bar{\Lambda}_\lambda(x)n_\varkappa(x)\Lambda_\mu(x)\bar{\Lambda}_\nu(y))_+\rangle_0 \simeq \langle(\bar{\Lambda}_\varkappa(x)n_\varkappa(x))_+\rangle_0\langle(\Lambda_\mu(x)\bar{\Lambda}_\nu(y))_+\rangle_0 - \tag{11}$$
$$-\langle(\bar{\Lambda}_\lambda(x)\Lambda_\mu(x))_-\rangle_0\langle(n_\varkappa(x)\bar{\Lambda}_\nu(y))_+\rangle_0 .$$

The second term of the r.h.s. of eq. (11) can be incorporated into the m_n of eq. (9), *i.e.*, it only yields a mass renormalization and hence we omit this term.

Thus, eq. (11) becomes

$$\langle(\bar{\Lambda}_\lambda(x)n_\varkappa(x)\Lambda_\mu(x)\bar{\Lambda}_\nu(y)_+)\rangle_0 \simeq -(\mathrm{Tr}\,K(0))\cdot S_{F\mu\nu}^{(\Lambda)}(x-y)\,, \tag{12}$$

where, of course, $S_F^{(\Lambda)}(x-y) = \langle(\Lambda(x)\bar{\Lambda}(y))_-\rangle_0$ is the Λ propagator. Inserting eq. (12) into eq. (9), we obtain:

$$\left(\gamma\frac{\partial}{\partial x}+m_n\right)K(x-y) = f_s(\mathrm{Tr}\,K(0))\,S_F^{(\Lambda)}(x-y)\,.$$

Integrating this equation under the assumption that $K(x-y)$ does not contain any free field part, we find

$$K(x-y) = f_s(\mathrm{Tr}\,K(0))\int \mathrm{d}^4x'\,G^{(n)}(x-x')\,S_F^{(\Lambda)}(x'-y)\,, \tag{13}$$

where $G^{(n)}$ is the Green's function satisfying the equation:

$$\left(\gamma\frac{\partial}{\partial x}+m_n\right)G^{(n)}(x-x') = \delta(x-x')\,.$$

Equating $x=y$ in eq. (13) and taking the trace, we get

$$c_s = f_s c_s\int \mathrm{d}^4x'\,\mathrm{Tr}\,[G^{(n)}(x-x')\,S_F^{(\Lambda)}(x'-x)]\,, \tag{14}$$

where we have put

$$c_s = -\,\mathrm{Tr}\,K(0)$$

in accordance with eq. (14).

Writing out eq. (12), we have

$$c_s = c_s\cdot f_s\cdot\frac{-4i}{(2\pi)^4}\int \mathrm{d}^4p\,\frac{1}{p^2+m_n^2}\cdot\frac{1}{p^2+m_\Lambda^2}\,(m_n m_\Lambda - p^2)\,, \tag{15}$$

where the integral is divergent and actually, we should introduce a cut-off factor. Eq. (15) gives $c_s = 0$ in general, unless:

$$1 = f_s \cdot \frac{-4i}{(2\pi)^4} \int \mathrm{d}^4 p \, \frac{1}{p^2 + m_n^2} \, \frac{1}{p^2 + m_\Lambda^2} \, (m_n m_\Lambda - p^2) \, . \tag{16}$$

The quantity c_s is then completely arbitrary, which is obviously ridiculous.

The above implies that our approximation eq. (11) is insufficient and we must go on to the next approximation. This is exactly similar to the situation which DÜRR *et al.* ([11,5]) encountered. The approximation eq. (11) corresponds to the fact that we are calculating the bubble diagram, Fig. 1. We must calculate higher order diagrams, see Fig. 2.

Fig. 1.

In Fig. 1 and 2 the broken line represents the new propagator $K(x - y)$ given by eq. (8) and the solid line represents the usual propagator $S_F^{(A)}$ or $S_F^{(n)}$. In principle these contributions can be calculated by means of the method of DÜRR *et al.* ([11]), but we do not give the explicit results because they are not particularly interesting. The important point is that eq. (13) will then be transformed into a more complicated expression and that, roughly speaking, we shall have an equation of the form:

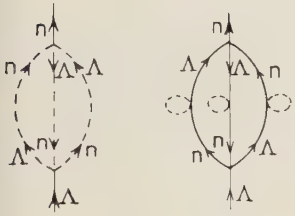
Fig. 2.

$$c_s = a_0 c_s + a_1 c_s^3 + a_2 c_s^5 + \ldots \tag{17}$$

instead of eq. (15), where a_0 is given by the r.h.s. of eq. (16) in the lowest order in f_s. Note that in general there is no guarantee that c_s will be extremely small. A sufficient condition would be $1 \doteqdot a_0$, *i.e.* eq. (14) should be satisfied to a good approximation. This means that a small non-zero c_s can arise when there is a suitable restriction in the coupling constant f_s in connection with the non-perturbative solution of the non-linear equation with which one starts. There is no *a priori* reason why this possibility should not occur but it must also be admitted that a demonstration has not been given.

In this connection, we should remark that the idea of deriving a weak interaction as a small correction to a strong interaction is neither new, nor difficult. In a simple model, VAN HOVE ([12]) has shown how such a programme can be carried out.

Finally, it should be emphasized that the proposed explanation for the $\Delta I = \frac{1}{2}$ selection rule in non-leptonic weak decays does not work for the leptonic decays, since there are no strong interactions involving leptons. Within

([12]) L. VAN HOVE: *Physica*, **25**, 365 (1959).

this framework, the origin of the leptonic weak interactions must be entirely different from that of the non-leptonic weak interactions and the universal V-A weak interaction should then apply only to the leptonic interactions. This differentiation between the non-leptonic and leptonic weak interactions has one attractive feature: the parity violation of the leptonic interaction can be ascribed to the two-component character of the neutrino. Furthermore, this distinction is in line with the idea of the present authors ([5]) that the occurrence of β-decay may be attributed to the breakdown of the orthogonality of the baryon and lepton Hilbert spaces resulting from the switching-on of the electromagnetic interaction since the same argument cannot be used for the non-leptonic weak interactions.

RIASSUNTO (*)

Esaminiamo dal punto di vista del modello composito delle particelle elementari l'ipotesi di Salam-Ward sulla regola di selezione $\Delta I = \frac{1}{2}$ nelle interazioni deboli. In quella teoria, i decadimenti deboli non leptonici hanno una origine differente da quella de. decadimenti leptonici e sono attribuiti a piccole perturbazioni delle interazioni fortii

(*) *Traduzione a cura della Redazione.*

IL NUOVO CIMENTO Vol. XX, N. 4 16 Maggio 1961

On Weak Pion Interaction in Non-Leptonic Hyperon Decays.

W. Królikowski (*)

Institute for Advanced Study - Princeton, N. J.

(ricevuto il 25 Marzo 1961)

Summary. — It is shown that isotopic and parity properties of non-leptonic hyperon decays can be explained qualitatively by a weak pion-baryon interaction, in which: (i) pions are coupled to matrices describing fundamental (or doublet) and strange isospins of baryons; (ii) all isospin matrices are multiplied by a strangeness-changing neutral matrix; (iii) the fundamental isospin matrices are multiplied by γ_5, whereas the strange ones are not. It follows form (i) and (ii) that this interaction satisfies automatically the rule $|\Delta \boldsymbol{T}| = \frac{1}{2}$ and also the Pais' rule $|\Delta \boldsymbol{I}| = 0$ or 1. The hypothetic connection (iii) between $\boldsymbol{\tau}$ matrices and γ_5 may be significant for understanding the mutual relations of strong and weak pion interactions. It gives the « parity clash » discussed by Pais.

1. – Introduction.

It is well known that the rule $|\Delta \boldsymbol{T}| = \frac{1}{2}$ established experimentally for non-leptonic weak processes implies the corresponding interaction to be a neutral component of an isospinor.

From the formal point of view the rule $|\Delta \boldsymbol{T}| = \frac{1}{2}$ leads to the rule $|\Delta S| = 1$ or $|\Delta T_3| = \frac{1}{2}$ but not vice versa. This is a reason, why non-leptonic weak processes are so hard to explain by the current × current interaction, when the rule $\Delta S = \Delta Q$ or even $|\Delta S| = |\Delta Q|$ applies to the strangeness-changing part of the weak current. Another reason is given by parity properties of non-leptonic Σ-decays that disagree with the overall maximal parity violation, while the weak current has this property.

(*) On leave from Institute for Nuclear Research, Polish Academy of Sciences, Warsaw, and Institute of Theoretical Physics, University of Warsaw.

Both reasons have led some physicists to search for a non-leptonic weak interaction independent of the current / current hypothesis. Recently PAIS starting from former attempts by D'ESPAGNAT and PRENTKI [1] and by TREIMAN [2] has formulated some conditions, which imposed on the interaction bring it to agreement with the isotopic and parity properties of non-leptonic hyperon decays [3].

In the present note a special interaction satisfying Pais' requirements is proposed, but it is not obtained by further specification of those requirements. This interaction is based instead on some assumptions of a rather dynamical character. Especially the rule $|\Delta \boldsymbol{T}| = \frac{1}{2}$ and also Pais' rule $\Delta \boldsymbol{I} = 0$ or 1 are not assumed, but they follow from the structure of the interaction, proposed not *ad hoc* to incorporate those rules.

2. – Weak pion-baryon interaction.

As it was previously shown [4] the isospin of baryons is given by

$$\boldsymbol{T}^B = \int \mathrm{d}_3 x \, B^*(x)(\tfrac{1}{2}\boldsymbol{\tau} + \tfrac{1}{2}\xi^*_\alpha \boldsymbol{\tau}_{\alpha\beta}\xi_\beta) B(x) \,. \tag{1}$$

Here $B(x)$ is a many-component baryon field,

$$B(x) = \begin{pmatrix} B_A(x) \\ B_{A\alpha_1}(x) \\ B_{A\alpha_1\alpha_2}(x) \end{pmatrix}, \tag{2}$$

where

$$\begin{cases} \left.\begin{matrix} p \\ n \end{matrix}\right\} = B_A \,, \quad \Lambda = \dfrac{B_{12} - B_{21}}{\sqrt{2}} \,, \quad \Sigma^+ = B_{11} \,, \\ \Sigma^0 = \dfrac{B_{12} + B_{21}}{\sqrt{2}} \,, \quad \Sigma^- = B_{22} \,, \quad \left.\begin{matrix} \Xi^0 \\ \Xi^- \end{matrix}\right\} = \dfrac{B_{A12} - B_{A21}}{\sqrt{2}} \,; \end{cases} \tag{3}$$

$\boldsymbol{\tau} = (\boldsymbol{\tau}_{AB})$ are $\frac{1}{2}$-isospin matrices acting on $B(x)$; and finally ξ_α or ξ^*_α are matrices acting on $B(x)$ and then annihilating or creating the strange degree of freedom

(1) B. D'ESPAGNAT and J. PRENTKI: *Phys. Rev.*, **144**, 1366 (1959).
(2) S. TREIMAN: *Nuovo Cimento*, **15**, 916 (1960).
(3) A. PAIS: *Nuovo Cimento*, **18**, 1003 (1960); preprint UCRL-9460 (1960).
(4) W. KRÓLIKOWSKI: *Nucl. Phys.*, **8**, 461 (1958); **17**, 421 (1960); **23**, 53 (1961); preprint IAS (1961) (submitted for publication in *Nucl. Phys.*).

of baryons, α. Anticommutation relations imposed on ξ_α and ξ^*_α imply an exclusion principle for strange degrees of freedom of baryons, called intrinsic Pauli principle (4). The isospin index $A = 1, 2$ corresponds to charges $+e$, 0, whereas the isospin index $\alpha = 1, 2$, corresponds to charges 0, $-e$. For detailed explanation of all used symbols compare (4).

Remark that bilinear forms $\bar{B}\xi_\alpha B$ and $\bar{B}\tau_i B$ or $\bar{B}\xi^*_\alpha \tau_{i\alpha\beta}\xi_\beta B$ are isospinors and isovectors respectively. We can see that isospinor transformation properties are intimately connected with the change of strangeness and just this fact will enable us to relate the rule $|\Delta \boldsymbol{T}| = \frac{1}{2}$ to the rule $|\Delta S| = 1$, if some dynamical assumptions are made on the interaction. Note that the neutral component of a bilinear isospinor is labelled by $\alpha = 1$.

The parts of $\boldsymbol{T}^B$ corresponding to $\frac{1}{2}\boldsymbol{\tau}$ and $\frac{1}{2}\xi^*_\alpha \boldsymbol{\tau}_{\alpha\beta}\xi_\beta$ have been called the fundamental and strange isospin respectively (4). Denote them by $\boldsymbol{T}^B_F$ and $\boldsymbol{T}^B_S$. The doublet symmetry (DS) or restricted global symmetry (RGS) of strong or weak pion-baryon interactions can be defined as an invariance under transformations generated by the $\boldsymbol{T}_F = \boldsymbol{T}^B_F +$ pion isospin. Isospins $\boldsymbol{T}_F$ and $\boldsymbol{T}_S = \boldsymbol{T}^B_S$ are identical with $\boldsymbol{I}$ and $\boldsymbol{K}$ isospins discussed by PAIS (3), as far as baryons and pions are concerned.

It is well known that the strong pion-baryon interaction was suggested to have the DS and to be of the form

$$\bar{B}g_\pi(\xi^*_\alpha\xi_\alpha)\gamma_5\boldsymbol{\tau}B\cdot\boldsymbol{\pi} = \tag{4}$$
$$= \left[g_\pi(0)\bar{N}\gamma_5\boldsymbol{\tau}N + g_\pi(1)(\bar{Y}\gamma_5\boldsymbol{\tau}Y + \bar{Z}\gamma_5\boldsymbol{\tau}Z) + g_\pi(2)\bar{\Xi}\gamma_5\boldsymbol{\tau}\Xi\right]\cdot\boldsymbol{\pi}\,,$$

where

$$\left|\begin{array}{l} N_A = B_A = \begin{cases} p \\ n \end{cases}, \qquad Y_A = B_{A1} = \begin{cases} \Sigma^+ \\ \dfrac{\Sigma^0 - \Lambda}{\sqrt{2}} \end{cases}, \\ \\ Z_A = B_{A2} = \begin{cases} \dfrac{\Sigma^0 + \Lambda}{\sqrt{2}} \\ \Sigma^- \end{cases}, \qquad \Xi_A = \dfrac{B_{A12} - B_{A21}}{\sqrt{2}} = \begin{cases} \Xi_1 \\ \Xi^- \end{cases}. \end{array}\right. \tag{5}$$

Here $g_\pi(\lambda)$ stands for an unknown function. If $g_\pi(\lambda) = \text{const}$, we have the global symmetry.

If (4) is true, one can ask a somewhat philosophical question, why pions are coupled only to $\boldsymbol{\tau}$ and not to $\xi^*_\alpha\boldsymbol{\tau}_{\alpha\beta}\xi_\beta$. In interaction (4) $\boldsymbol{\tau}$ is multiplied by γ_5. Suppose for a moment that $\boldsymbol{\tau}$ must appear in couplings always together with γ_5, whereas $\xi^*_\alpha\boldsymbol{\tau}_{\alpha\beta}\xi_\beta$ without γ_5. Then, pions cannot be coupled to $\xi^*_\alpha\boldsymbol{\tau}_{\alpha\beta}\xi_\alpha$,

since they cannot be coupled by the form

$$\bar{B}\, g_\pi(\xi^*_\gamma \xi_\gamma)\, \xi^*_\alpha \boldsymbol{\tau}_{\alpha\beta} \xi_\beta B\cdot\boldsymbol{\pi}\,, \tag{6}$$

if the PC-invariance is to hold.

Remark, however, that in the case of vector coupling $\gamma_\mu \partial_\mu \boldsymbol{\pi}$, pions can be coupled both to $\gamma_5\boldsymbol{\tau}$ and $\xi^*_\alpha \boldsymbol{\tau}_{\alpha\beta}\xi_\beta$ without violating the PC-invariance. We assume it is just the case for the non-leptonic weak interaction. We get then the « parity clash » discusseed by PAIS.

Now, let us formulate explicitly our assumptions about the weak pion-baryon interaction:

i) pions are coupled to isospins: $\boldsymbol{\tau}\cdot\boldsymbol{\pi}$ and $\xi_\alpha \boldsymbol{\tau}_{\alpha\beta}\xi_\beta\cdot\boldsymbol{\pi}$,

ii) the rule $|\Delta S| = 1$ is valid *i.e.* $\boldsymbol{\tau}$ and $\xi_\alpha \boldsymbol{\tau}_{\alpha\beta}\xi_\beta$ must be multiplied by ξ_1,

iii) $\boldsymbol{\tau}$ is multiplied by γ_5, whereas $\xi^*_\alpha \boldsymbol{\tau}_{\alpha\beta}\xi_\beta$ is not,

iv) vector coupling should be used: $\gamma_\mu \partial_\mu \boldsymbol{\pi}$,

v) the matrix $\boldsymbol{\tau}\cdot\xi^*_\alpha \boldsymbol{\tau}_{\alpha\beta}\xi_\beta$ spoiling the DS does not appear.

We can see that the rule $|\Delta \boldsymbol{T}| = \frac{1}{2}$ follows from i) and ii). Also the Pais' rule, $|\Delta \boldsymbol{T}_F| = 0$ or 1 and $|\Delta \boldsymbol{T}_S| = \frac{1}{2}$, follows from i), ii) and v), namely couplings $\xi_1 \boldsymbol{\tau}\cdot\boldsymbol{\pi}$ and $\xi_1 \xi^*_\alpha \boldsymbol{\tau}_{\alpha\beta}\xi_\beta\cdot\boldsymbol{\pi}$ give $\Delta \boldsymbol{T}_F| = 0$ and 1 respectively, and both give $|\Delta \boldsymbol{T}_S| = \frac{1}{2}$. For $\xi_1 \boldsymbol{\tau}\cdot\boldsymbol{\pi}$ our statement is evident, for $\xi_1 \xi^*_\alpha \boldsymbol{\tau}_{\alpha\beta}\xi_\beta\cdot\boldsymbol{\pi}$ it follows from (9) and (5). Note that coupling $\xi_1 \boldsymbol{\tau}\cdot\boldsymbol{\pi}$ preserves the DS as defined above, whereas coupling $\xi_1 \xi^*_\alpha \boldsymbol{\tau}_{\alpha\beta}\xi_\beta\cdot\boldsymbol{\pi}$ violates it.

There are three independent interactions satisfying conditions i)–v):

$$\bar{B}\, C_A(\xi^*_\gamma \xi_\gamma)\gamma_\mu\gamma_5 \boldsymbol{\tau}\xi_1 B\cdot\partial_\mu\boldsymbol{\pi} = \sqrt{2}\,[C_A(0)\,\bar{N}\gamma_\mu\gamma_5\boldsymbol{\tau}_- Y - C_A(1)\,\bar{Z}\gamma_\mu\gamma_5\boldsymbol{\tau}_-\Xi]\,\partial_\mu\pi^+ + \tag{7}$$

$$+\sqrt{2}\,[C_A(0)\,\bar{N}\gamma_\mu\gamma_5\boldsymbol{\tau}_+ Y - C_A(1)\bar{Z}\gamma_\mu\gamma_5\boldsymbol{\tau}_+\Xi]\,\partial_\mu\pi^- + [C_A(0)\,\bar{N}\gamma_\mu\gamma_5\boldsymbol{\tau}_3 Y - C_A(1)\,\bar{Z}\gamma_\mu\gamma_5\boldsymbol{\tau}_3\Xi]\,\partial_\mu\pi^0$$

and

$$\bar{B}\, C_V(\xi^*_\gamma \xi_\gamma)\gamma_\mu \xi^*_\alpha \boldsymbol{\tau}_{\alpha\beta}\xi_\beta\xi_1 B\cdot\partial_\mu\boldsymbol{\pi} = C_V(1)\big(-\sqrt{2}\,\bar{Y}\gamma_\mu\Xi\,\partial_\mu\pi^+ + \bar{Z}\gamma_\mu\Xi\,\partial_\mu\pi^0\big) \tag{8}$$

and

$$\bar{B}\, C_V(\xi^*_\gamma \xi_\gamma)\gamma_\mu\xi_1\xi^*_\alpha \boldsymbol{\tau}_{\alpha\beta}\xi_\beta B\cdot\partial_\mu\boldsymbol{\pi} = C_V(0)\big(\sqrt{2}\,\bar{N}\gamma_\mu Z\partial_\mu\pi^+ + \bar{N}\gamma_\mu\, Y\,\partial_\mu\pi^0\big)\,, \tag{9}$$

where $C_A(\lambda)$ and $C_V(\lambda)$ are unknown functions.

Since $C_A(0)$, $C_A(1)$ and $C_V(0)$, $C_V(1)$ are arbitrary constants the whole inter-

action can be written *e.g.* in the form (7) + (8)–(9):

$$(10)\qquad \bar{B}\gamma\{C_A(\xi^*_\gamma\xi_\gamma)\gamma_5\boldsymbol{\tau}\xi_1 + C_V(\xi^*_\gamma\xi_\gamma)[\xi^*_\alpha\boldsymbol{\tau}_{\alpha\beta}\xi_\beta,\ \xi_1]\}B\cdot\partial_\mu + \text{h.c.} =$$

$$= -\bar{p}\gamma_\mu(C^0_V + C^0_A\gamma_5)\Lambda\,\partial_\mu\pi^+ + \frac{1}{\sqrt{2}}\,\bar{n}\gamma_\mu(C^0_V + C^0_A\gamma_5)\Lambda\,\partial_\mu\pi^0 - \bar{p}\gamma_\mu(C^0_V - C^0_A\gamma_5)\Sigma^0\,\partial_\mu\pi^+ -$$

$$- \frac{1}{\sqrt{2}}\,\bar{n}\gamma_\mu(C^0_V + C^0_A\gamma_5)\Sigma^0\,\partial_\mu\pi^0 + \sqrt{2}\,\bar{n}\gamma_\mu C^0_A\gamma_5\Sigma^+\partial_\mu\pi^- - p\gamma_\mu(C^0_V - C^0_A\gamma_5)\Sigma^+\partial_\mu\pi^0 -$$

$$- \sqrt{2}\,\bar{n}\gamma_\mu C^0_V\Sigma^-\partial_\mu\pi^+ + \text{h.c.} + \bar{\Lambda}\gamma_\mu(C'_V - C'_V\gamma_5)\Xi^-\partial_\mu\pi^+ +$$

$$+ \frac{1}{\sqrt{2}}\,\bar{\Lambda}\gamma_\mu(C'_V - C'_A\gamma_5)\Xi^0\,\partial_\mu\pi^0 - \bar{\Sigma}^0\gamma_\mu(C'_V + C'_A\gamma_5)\Xi^-\partial_\mu\pi^+ +$$

$$+ \frac{1}{\sqrt{2}}\,\bar{\Sigma}^0\gamma_\mu(C'_V - C'_A\gamma_5)\Xi^0\,\partial_\mu\pi^0 - \sqrt{2}\,\bar{\Sigma}^-\gamma_\mu C'_A\gamma_5\Xi^0\,\partial_\mu\pi^- +$$

$$+ \bar{\Sigma}^-\gamma_\mu(C'_A + C'_A\gamma_5)\Xi^-\partial_\mu\pi^0 - \sqrt{2}\,\bar{\Sigma}^+\gamma_\mu C'_V\Xi^0\,\partial_\mu\pi^+ + \text{h.c.}$$

where $C^0_A = C_A(0)$, $C^0_V = C_V(0)$ and $C'_A = C_A(1)$, $C'_V = C_V(1)$.

If $C_A(\lambda) = \text{const}$ and $C_V(\lambda) = \text{const}$, then

$$(11)\qquad C^0_A = C'_A\,, \qquad C^0_V = C'_V\,,$$

and we have here an analogy of the global symmetry of the strong pion-baryon interaction. Remember, however, that the DS as defined above does not hold here. In the case of (11) interaction (1) fulfills all Pais' conditions.

We can recognize from (10) that asymmetry parameters in hyperon decays have the properties

$$(12)\qquad \alpha(\Sigma^+ \to \text{p} + \pi^0) = -\alpha(\Lambda \to \text{p} + \pi^-)$$

and

$$(13)\qquad \alpha(\Sigma^+ \to \text{n} + \pi^+) = 0\,, \qquad \alpha(\Sigma^- \to \text{n} + \pi^-) = 0\,,$$

if contributing strong interactions are DS-invariant and if one puts $M_\Lambda = M_\Sigma$. Formulae (12) and (13) are known consequences of Pais' conditions. Amplitudes for decays $\Sigma^+ \to \text{n} + \pi^+$ and $\Sigma^- \to \text{n} + \pi^-$ are in the case of (10) pure P- and S-waves respectively. Further we get

$$(14)\qquad \alpha(\Xi^- \to \Lambda + \pi^-) \approx -\alpha(\Lambda \to \text{p} + \pi^-)\,,$$

when assuming the global symmetry for contributing strong interactions and additionally

$$(15)\qquad \frac{C^0_A}{C'_A} = \frac{C^0_V}{C'_V}\,,$$

for the interaction (10). Relation (15) is satisfied in particular in the case of symmetry (11). When the absolute values of both sides of (14) are taken, this equality is a result of Pais' conditions. Including the minus sign it follows from (10) and (15).

It is known that relations (13) and (14) are in qualitative agreement with the experiment. We know also that the mode $\Sigma^+ \to p + \pi^0$ shows, like the mode $\Lambda \to p + \pi^-$, nearly maximal parity violation. The relative sign of $\alpha(\Sigma^+ \to p + \pi^0)$ and $\alpha(\Lambda \to p + \pi^-)$ has not yet been determined. This nearly maximal parity violation suggests that

$$C_A^0 = \pm C_V^0 \tag{16}$$

and by (15) also

$$C_A' = \pm C_V' . \tag{17}$$

if the helicity of the proton in $\Lambda \to p + \pi^-$ is left or right respectively. When (16) and (17) hold, the interaction (10) contains two different constants C^0 and C'. If in addition symmetry (11) is valid, the interaction (10) takes the form

$$C \bar{B} \gamma_\mu \{ \gamma_5 \boldsymbol{\tau} \xi_1 \pm [\xi_\alpha^* \boldsymbol{\tau}_{\alpha\beta} \xi_\beta, \xi_1] \} B \partial_\mu \boldsymbol{\pi} + \text{h. c.} , \tag{18}$$

where only one constant C appears.

* * *

I take the opportunity to express my gratitude to Professor J. R. Oppenheimer for his kind hospitality extended to me at the Institute for Advanced Study in Princeton.

RIASSUNTO (*)

Dimostriamo che le proprietà isotopiche e di parità dei decadimenti non leptonici degli iperoni possono essere spiegate qualitaticamente da una interazione debole pione-barione, in cui: 1) i pioni sono accoppiati a matrici che descrivono gli isospin fondamentali (o di doppietto) e strani dei barioni; 2) tutte le matrici di isospin sono moltiplicate per una matrice neutra, che cambia la stranezza; 3) le matrici fondamentali di isospin vengono moltiplicate per γ_5, mentre non lo sono quelle strane. Segue da 1) e 2) che questa interazione soddisfa automaticamente alla legge $|\Delta \boldsymbol{T}| = \frac{1}{2}$ ed anche alla legge di Pais $|\Delta \boldsymbol{I}| = 0$ ed 1. La connessione ipotetica 3) fra matrici $\boldsymbol{\tau}$ e γ_5 può essere significativa per comprendere le relazioni mutue delle interazioni pioniche deboli e forti. Essa dà il « conflitto di parità » discusso da Pais.

(*) *Traduzione a cura della Redazione.*

LETTERE ALLA REDAZIONE

(La responsabilità scientifica degli scritti inseriti in questa rubrica è completamente lasciata dalla Direzione del periodico ai singoli autori)

Photoproduction of Neutral Vector Mesons.

M. Bassetti

Laboratori Nazionali del CNEN - Frascati

(ricevuto il 27 Febbraio 1961)

The striking [1] success of the $\Delta T = \frac{1}{2}$ rule in explaining the experimental branching ratios in Λ^0-decay and in K^0-decay and in giving a consistent explanation of the data for Σ-decay and for τ-decay has led to the general belief that this rule may correspond to a fundamental symmetry property of weak interactions. It is well-known [2] that the $\Delta T = \frac{1}{2}$ rule can be embodied in the theory of weak interactions if one introduces weak neutral currents besides charged currents — provided there is no coupling of the strangeness non-conserving neutral current to the leptons. In the intermediary meson theory of weak interactions such currents are coupled to hypothetical spin-one bosons. Lee and Yang [3] assume a minimal set of such bosons, leading to four particles W^+W^0, $\bar{W}^0W^-$, of isospin $\frac{1}{2}$ coupled in a charge-independent way to the strangeness non-conserving currents. The set W^+, $-(1/\sqrt{2})(W^0+\bar{W}^0)$, W^- of isospin 1 is similarly coupled in a charge-independent way to the strangeness-conserving currents.

We shall calculate here the cross-section for the process

$$\gamma + p \to p + X ,$$

where X is a neutral vector meson.

If one adopts the Lee-Yang suggestion, X is to be identified with $-(1/\sqrt{2})\cdot(W^0+\bar{W}^0)$, and is coupled in a charge-independent way to pairs of nucleons. This allows one to determine the strength of its coupling from the strength of the coupling of the charged W's.

Since there is no coupling of W^0 to leptons (or at most a very weak coupling) W^0 will only decay through its coupling to the neutral strangeness-conserving current (pion decay modes) or to the neutral strangeness non-conserving current

(1) See for instance the report by M. Schwartz at the Rochester Conference 1960 (*Proceedings of the 1960 Annual International Conference on High Energy Physics of Rochester*, p. 727).

(2) See, for instance, R. Gatto: Lectures at the International School of Physics, Varenna 1958, in *Supplemento al Nuovo Cimento*, **14**, 340, 1959.

(3) Lee and Yang: *Phys. Rev.*, **119**, 1410 (1960).

(K-decay modes). Among the pion decay modes, $W^0 \to \pi^+ + \pi^-$, can serve to the identification of the intermediate W^0. For energies lower than that required for $\gamma + p \to \Lambda + K$, any K-decay mode of W^0 would simulate a process with strangeness change. If W^0 decays according to $W^0 \to K^- + \pi^+$ the corresponding threshold for direct production of the secondaries would be that of the reaction $\gamma + p \to K^- + K^+ + p$ of much higher threshold. However indirect K^- production can be obtained through K^0 production together with a $K^0 \to \bar{K}^0$ transition [4] and $\bar{K}^0 \to K^-$ by charge exchange.

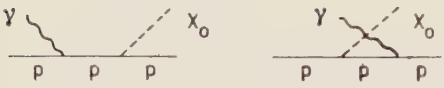

Fig. 1.

In the first perturbation approximations the diagrams for $\gamma + p \to X + p$ are (fig. 1).

We have assumed the Lagrangians $-ie\bar{\psi}\gamma'_\mu \psi A_\mu$ for the electromagnetic vertex, and $ig\bar{\psi}\gamma_\lambda(1 + a\gamma_5)\psi\gamma_\lambda$ for the other vertex with $(g^2/M_X^2) = 10^{-5}$.

Assuming charge independence, from the rate of axial and vector coupling of β-decay, « a » is about 1.21.

The result, averaged on the polarization of the initial particles and summed on the polarization of the final one is, in the c.m.

$$\frac{d\sigma}{d\Omega} = \left(\frac{e^2}{4\pi}\right)\left(\frac{g^2}{M_X^2}\right)\left(\frac{1}{16\pi}\right)\frac{M_X^2 K_{p'}}{\omega_p \omega_K(\omega_p + \omega_K)} \cdot$$

$$\cdot\left\{\left\{(2M^4 + M^2 M_X^2)\left|\frac{1}{(pK)} - \frac{1}{(p'K)}\right|^2 + \frac{2M^2 M_X^2 + M_X^4}{(pK)(p'K)} + 2\left[\frac{(pK)}{(p'K)} + \frac{(p'K)}{(pK)}\right] - \right.\right.$$

$$\left. - (4M^2 + 2M_X^2)\left[\frac{1}{(pK)} - \frac{1}{(p'K)}\right]\right\} - a^2\left\{(4M^4 - M^2 M_X^2)\left[\frac{1}{(pK)} - \frac{1}{(p'K)}\right]^2 + \right.$$

$$\left. + \frac{4M^2 M_X^2 - M_X^4}{(pK)(p'K)} - 2\left[\frac{(pK)}{(p'K)} + \frac{(p'K)}{(pK)}\right] - (8M^2 - 2M_X^2)\left[\frac{1}{(pK)} - \frac{1}{(p'K)}\right] - \right.$$

$$\left.\left. - \frac{4M^2}{M_X^2}\frac{[(pK) - (p'K)]^2}{(pK)(p'K)}\right\}\right\}.$$

The meaning of the symbols in the (2) is:

M_X mass of the vector meson;

M nucleon mass;

ω_p initial nucleon's energy;

ω_K photon's energy;

p initial nucleon's four-momentum;

p' final nucleon's four-momentum;

K photon's four-momentum;

K_p space-momentum of the vector meson.

[4] A. Pais and O. Piccioni: *Phys. Rev.*, **100**, 1488 (1955).

Integrating in $d\Omega$ we have obtained the total cross section in the c.m.

$$\sigma = \left(\frac{e^2}{4\pi}\right)\left(\frac{g^2}{M_X^2}\right)\frac{M_X^2 K_{p'}}{4\omega_p \omega_K(\omega_p + \omega_K)} \cdot$$

$$\cdot\left\{\left\{[(2M^4 + M^2M_X^2) - a^2(4M^4 - M^2M_X^2)]\frac{1}{(pK)^2}\right\} + \left\{[4M^4 - M_X^4 - 2(pK)^2 - 4M^2(pK) + 2M_X^2(pK)] - a^2\left[8M^4 - 6M^2M_X^2 + M_X^4 + 2(pK)^2 - 8M^2(pK) + 2M_X^2(pK) + \frac{4M^2}{M_X^2}(pK)^2\right]\right\}\left\{\frac{\ln(\omega_{p'} + K_{p'})/M}{(pK)\omega_K K_{p'}} + \left\{\frac{2M^4 + M^2M_X^2 - a^2(4M^4 - M^2M_X^2)}{M^2\omega_K^2}\right\} + \left\{\frac{2\omega_{p'}\omega_K + 4M^2 + 2M_X^2 + a^2(2\omega_{p'}\omega_K - 8M^2 + 2M_X^2)}{(pK)}\right\} - \left\{\frac{a^2[4M^2(pK) + 4M^2\omega_{p'}\omega_K]}{(pK)M_X^2}\right\}\right\}\right\} .$$

The following formulae give the relations between the quantities in the c.m. frame and the photon's energy « E » in the laboratory.

$$\omega_K = \frac{ME}{\sqrt{M^2 + 2ME}}, \qquad \omega_p = \frac{M(M+E)}{\sqrt{M^2 + 2ME}}, \qquad \omega_p + \omega_K = \sqrt{M^2 + 2ME},$$

$$K_{p'} = \frac{[(2ME - M_X^2)^2 - 4M^2M_X^2]^{\frac{1}{2}}}{2\sqrt{M^2 + 2ME}}, \qquad \omega_{p'} = \sqrt{M^2 + K_{p'}^2}, \qquad (pK) = -ME .$$

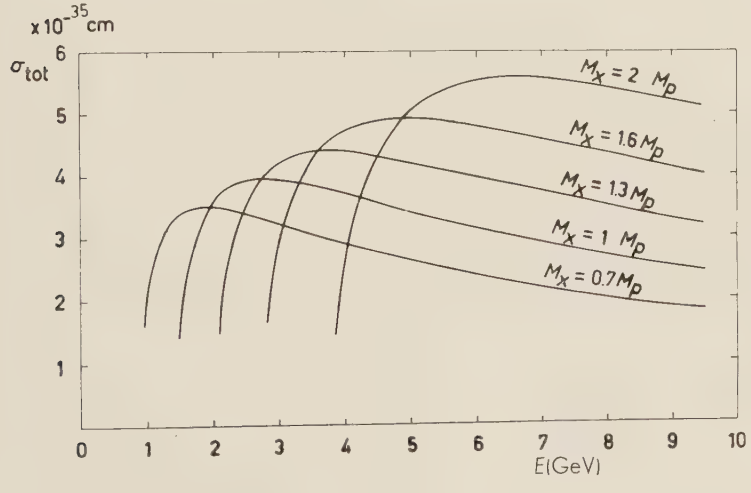

Fig. 2.

In Fig. 2 we give the plot of the total cross-section *vs.* « E », for different values of the schizon's mass using a H_2 target.

X-Ray Induced Conversion in the Absorption Bands of Additively Colored KCl (*).

G. Baldini, (**) L. Dalla Croce and R. Fieschi

Istituto di Scienze Fisiche dell'Università - Milano
Istituto Nazionale di Fisica Nucleare - Sezione di Milano

(ricevuto il 6 Marzo 1961)

1. – The effect of X-ray irradiation on the optical properties of alkali halides has been studied, so far, by measuring the color center production, in particular the F center growth curves under irradiation. Different mechanisms have been proposed, for the F center production. In 1946 [1] F. Seitz suggested that the electrons and holes generated by the primary photo-electron could free single vacancies from small clusters and from surface of cracks present in a virgin specimen: the fluctuations in electrostatic charge which occur when a wandering electron or a hole is captured by the complex imperfections should be responsible of the loosening and of the repulsion of vacancies. Later, in his review of 1954 [2], Seitz thought that vacancies « evaporate » as a result of thermal spikes due to thermal decay of excitons captured at jogs on dislocations or at vacancy clusters. Different mechanisms of formation of single vacancies and color centers have been proposed and discussed later [3].

The direct optical effect of vacancy clusters and dislocations should be detectable in the spectral region of the tail of the edge absorption, as a perturbation to the exciton absorption due either to change of the lattice potential or to the breaking of the momentum selection rule. Quantitative studies however, are uncertain, because the tail of the edge absorption is very sensitive to the structure and to the purity of the sample; clear results have been obtained only for the negative vacancies and for the F center (α and β bands). It is hence difficult to know directly the effect of X-rays on vacancy clusters by means of measurements on the change of the absorption spectra.

We thought it worth-while to consider the analogous effect of X-rays on vacancy clusters which bind one (or more) electrons, namely the changes induced by the ionizing radiation on

(*) This research was supported by the Consiglio Nazionale delle Ricerche.

(**) On leave at the Institute of Optics, University of Rochester, Rochester, N.Y.

(1) F. Seitz: *Rev. Mod. Phys.*, **18**, 384 (1946).

(2) F. Seitz: *Rev. Mod. Phys.*, **26**, 7 (1954).

(3) For a review see S. Amelinx: *Radiation effects in ionic crystals* (*Rendiconti S.I.F.*, 1960), to be published.

the complex absorption centers (M, R and N); we have looked also for the effect on the Z centers, *i.e.* on the absorption centers which are present in alkali-halides containing small additions of alkali earth halides [4].

Recently UETA and coworkers [5] studied the effect of excitons on F and U centers, and on the complex centers (M, R and N); they found that the $F \rightarrow U$ conversion is due to a local thermal effect, because each exciton destroys more than one F center. They worked with additively coloured crystals, in

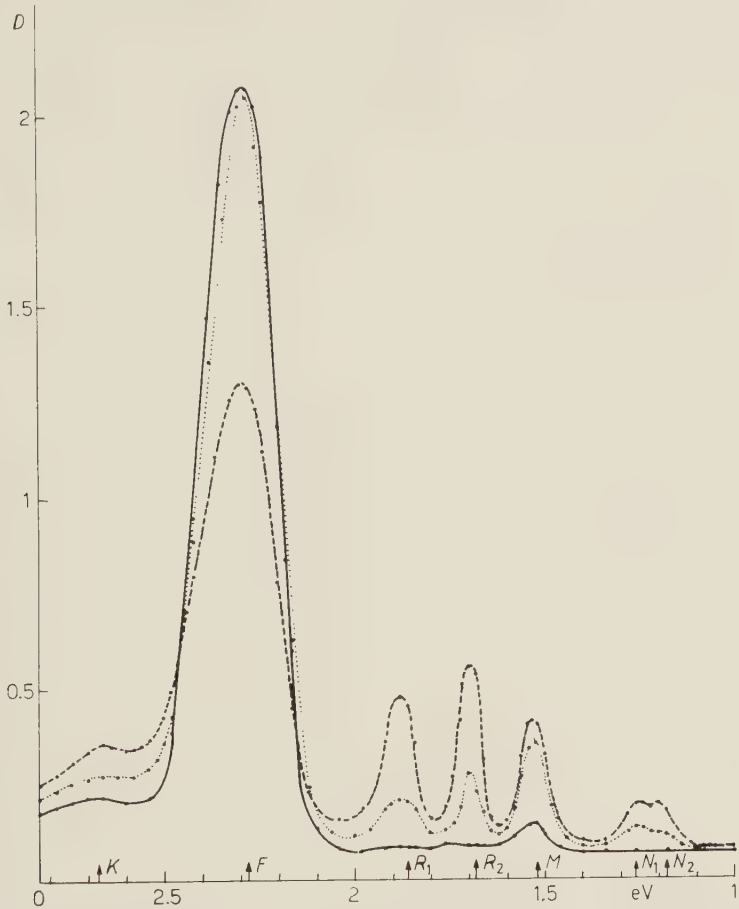

Fig. 1. – Absorption spectra of additively coloured KCl at —180 °C: —— after quenching; – – – irradiated with F light at room temperature: for 1 h; . . . successively exposed to the X-ray beam for 1 h, 30'.

[4] Preliminary results were presented at the XLVI Conference of the Italian Physical Society (Naples, October 1960). Some results on the X-ray induced conversion in colour centers are mentioned by R. CASLER, P. PRINGSHEIM and P. YUSTER: *Journ. Chem. Phys.*, **18**, 1564 (1950).

[5] M. UETA, M. HIRAI and H. WATANABE: *Journ. Phys. Soc. Japan*, **14**, 253 (1959); M. UETA and M. HIRAI: *Journ. Phys. Soc. Japan*, **14**, 546 (1959).

order to avoid the recombination bleaching characteristic of crystals coloured by ionizing radiation. We also used additively coloured crystals; the work on pure salts was done with KCl obtained from the Harshaw Chemical Company, while contaminated crystals were grown in our laboratory by means of Bridgmann and Kyropoulos methods, by adding a fraction of 10^{-4} about of $SrCl_2$ or $CaCl_2$ to the potassium cloride. The crystals were additively coloured with K vapour at approximately 550 °C for 2 h 30 min; quenches were performed with an air jet. The absorption measurements were taken with a Beckmann *DU* spectrophotometer; the cleaned samples, ~ 0.4 mm thick, were put in a metal vacuum cryostat for observation at liquid nitrogen temperature. The irradiation was made with X-rays obtained from a tube having 1 mm aluminium windows and a tungsten target operated at 50 kV and 50 mA; the distance of the crystal from the target was approximately 17 cm.

2. – The spectrum of the additively coloured samples showed a strong F band and, seldom, very weak M and R bands. Successive illumination with F-light at room temperature caused the well known conversion of F centers into M, R and N centers; the illumination was continued until saturation was obtained (Fig. 1). Crystals pre-treated in the above indicated way were X-rayed at various temperatures, and the absorption spectra were recorded, after increasing X-ray exposure, at liquid nitrogen temperature.

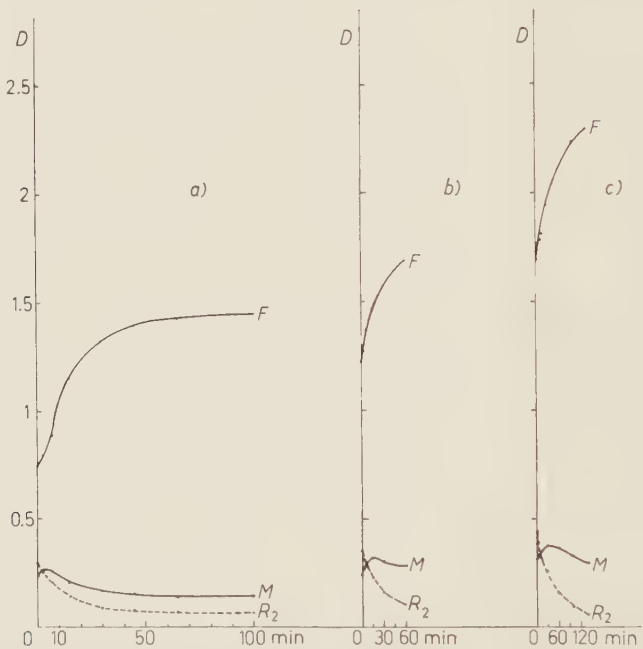

Fig. 2. – Maximum absorption coefficients of F, M and R bands, at — 180 °C as a function of the X-ray exposure time (note the different unit in the abscissae): *A*) irradiation temperature 20 °C; *B*) 0 °C; *C*) — 75 °C. (The base line and the contribution of the other bands has been subtracted).

Fig. 2 shows the maximum absorption coefficients of the various bands, as a function of X-ray exposure time. One can see that the shape of the curves for a given band is similar at the dif-

ferent temperatures: the conversion processes among the absorption centers are simply slowed down when the X-ray irradiation is performed at lower temperatures. The F band grows monotonically; the growth lasts even when the conversion process has ended and no further change is observed in the other bands, because of the usual F-center production, characteristic of the second (or slow) stage ([6]). After long X-ray exposures the absorption bands due to the complex centers tend to different saturation values. The M band increases during the first stages of the irradiation, than decreases; the R bands decrease quickly, approximately in an exponential way; the ratio between the intensities of R_1 and R_2 remaining constant; the K, N_1 and N_2 bands (which are not shown in Fig. 2) decrease at a lower rate, showing a more complicated behaviour.

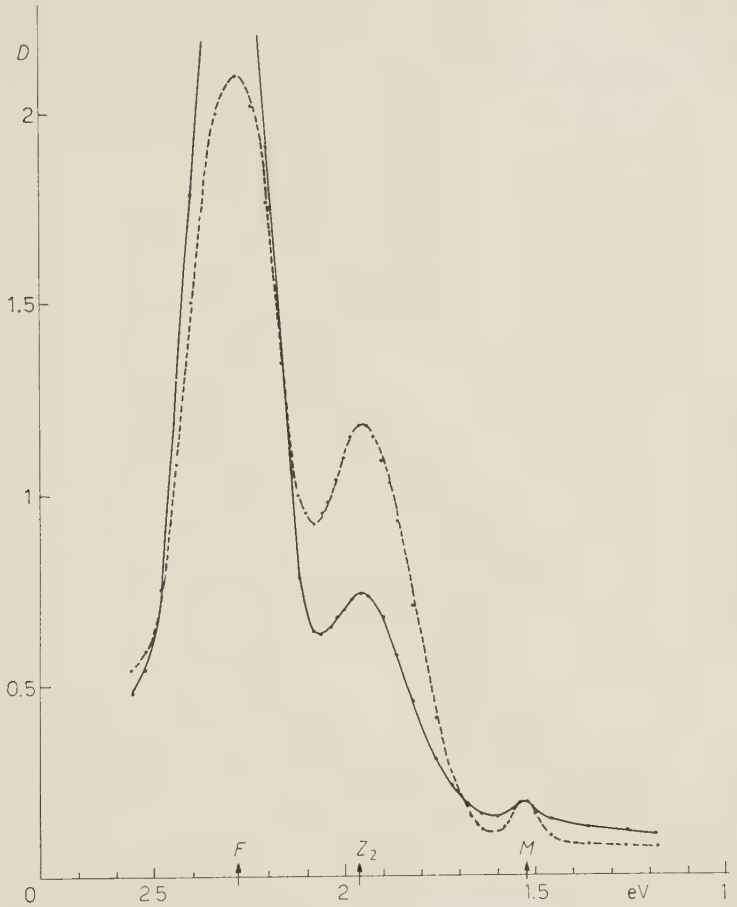

Fig. 3. – Absorption spectra at — 180 °C, of additively coloured KCl: $SrCl_2$: – – – kept 4 h at 100 °C; —— X-ray irradiated for 1 h, at 20 °C.

The observed behaviour of the complex centers could be explained as due

([6]) P. W. MITCHELL, D. A. WIEGAND and R. SMOLUCHOWSKI: *Phys. Rev.*, **117**, 442 (1960).

to thermal spikes caused by radiationless recombination of electrons and holes or excitons, or as a consequence of hole trapping by the electronic center, followed by dissociation of the vacancy aggregate, caused by the repulsive electrostatic forces between the positive and negative ion vacancies. A comparison with the effect of a purely thermal bleaching above 200 °C followed by quenching seems to show that the first mechanism does not play the major role, because one obtained, in this case, nearly pure F band, while X-rayed crystals show a considerable amount of M, R and N bands even after very long exposures. Moreover, the behaviour of the N_1 and N_2 bands during a thermal bleaching is different from the behaviour during the conversion induced by X-ray irradiation.

As to the behaviour of the various bands, the following remarks can be made. The K band diminishes while the F band rises, ruling out any possible interpretation of an excited state of the F center. The stability of the ratio of the intensities of R_1 and R_2 bands confirms the model which attributes the two bands to transitions of the same center [7]. The behaviour of the M band can be qualitatively explained on the basis of Pick's models [8], which attributes an F_3 structure to the R center, and an F_2 structure to the M center: the conversion $R \rightarrow M + F$ could explain the initial increase of the M band. On the contrary, it seems hard to explain the results by means of the M model of Seitz or of Knox [9].

3. – Analogous experiences were carried out with crystals containing F, Z_1 and Z_2 centers [10]. At liquid nitrogen temperature the X-ray exposure does not affect the Z bands. Fig. 3 shows the absorption spectra of a sample containing the F and Z_2 bands (obtained by means of the usual thermal treatments) before and after the X-ray

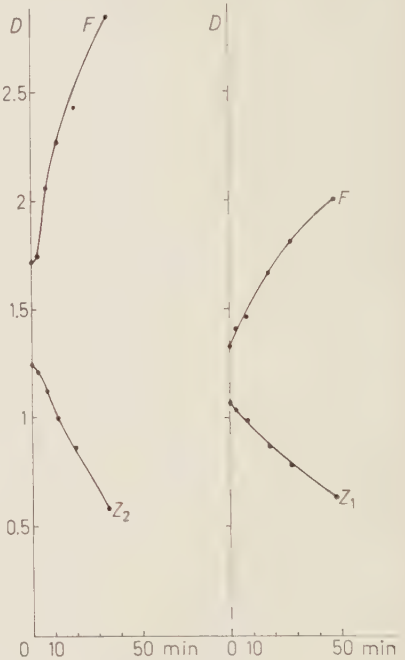

Fig. 4. – Maximum absorption coefficients of F and Z bands at — 180 °C as a function of the X-ray exposure time; temperature of irradiation 20°C.

irradiation at room temperature. A similar behaviour is shown by the Z_1 band; the rate of $Z_1 \rightarrow F$ conversion is lower than for the $Z_2 \rightarrow F$ conversion (Fig. 4), while on the basis of a purely thermal mechanism for the destruction of the Z centers, one would expect a

(7) R. Hermann, M. C. Wallis and R. F. Wallis: *Phys. Rev.*, **103**, 87 (1956); G. R. Cole and R. Y. Friauf: *Phys. Rev.*, **105**, 1464 (1957).
(8) H. Pick: *Zeits. Phys.*, **159**, 69 (1960).
(9) M. S. Knox: *Phys. Rev. Lett.*, **2**, 87 (1959).
(10) See, for instance, P. Camagni, S. Cerasara and G. Chiarotti: *Phys. Rev.*, **118**, 1226 (1960); M. Ishigura, E. Sigioka and N. Takeuchi: *Journ. Phys. Soc. Japan*, **15**, 1302 (1960).

faster destruction of the Z_1, which is thermally less stable than the Z_2 center.

In order to gain further insight in the process of electron and hole capture by the centers, we are now studying the change in the absorption spectra of additively coloured crystals, containing either F, M, R and N centers, or F and Z centers, when the sample is previously X-rayed, at liquid nitrogen temperature, subsequently heated, in order to have bursts of free electrons and holes.

* * *

We would like to thank Dr. Fumio Okamoto for communicating his unpublished results on analogous experiences; Dr. P. Camagni and Prof. G. Chiarotti for many useful advices and discussions.

Some Remarks on High-Energy Inelastic Collisions with Small Momentum Transfer.

P. Beckmann

Institut für Theoretische Physik - Heidelberg

(ricevuto l'8 Marzo 1961)

Inelastic processes with small momentum transfer are often considered to receive their dominant contribution from graphs corresponding to the exchange of a low mass state between the target and the beam particle. For reactions of the type A+B→A+B+C one might expect the graph of Fig. 1 to be especially important for small values of the momentum transfer $\Delta^2 = -(p-p')^2$ if C is the particle with the lowest mass that can be exchanged. We use the notation:

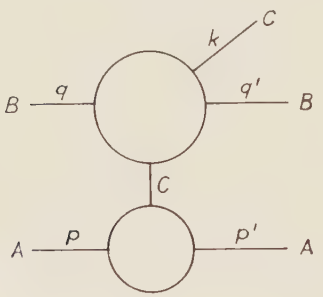

Fig. 1.

$$W^2 = (p+q)^2\,, \qquad W'^2 = (q'+k)^2\,,$$

$$\Delta'^2 = (q'-q)^2\,.$$

Then the contribution from this graph could be written as

$$(1) \qquad T_1 = \frac{\Gamma_{\mathrm{ACA}}(p,p')}{\Delta^2 + m_C^2}\, T_{\mathrm{BC}}(W'^2, \Delta'^2)\,.$$

Here $\Gamma_{\mathrm{ACA}}(p, p')$ is the AC vertex function and $T_{\mathrm{BC}}(W'^2, \Delta'^2)$ the elastic scattering amplitude for particles B and C at c.m.s. energy W' and momentum transfer Δ'.

We want to compare the contribution of graph 1 with the contribution of graph 2 (Fig. 2) where particle B is

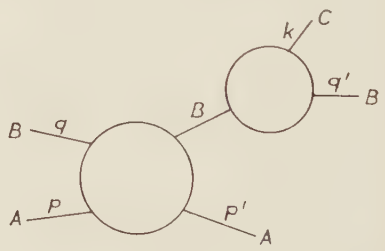

Fig. 2.

first elastically scattered and then dissociates into B and C. Its contribution would be written as

$$(2) \qquad T_2 = T_{\mathrm{AB}}(W^2, \Delta^2)\, \frac{\Gamma_{\mathrm{BCB}}(k, q')}{W'^2 - m_{\mathrm{B}}^2}\,.$$

It seems plausible that for fixed W' and Δ the contribution from graph 2 becomes larger than the one from graph 1 if the energy W is only taken high enough. This is simply due to the fact, that $|T_{AB}(W^2, \Delta^2)|$, which at high energies mostly containes diffraction scattering, increases with W while T_1 is independent of W. For instance, in inelastic proton-proton scattering ($p+p \to p+p+\pi^0$ combined with $p+p \to p+n+\pi^+$) where A is the observed recoil proton, setting W' at the (3.3) resonance and $\Delta^2=(m_\pi/3)^2$ one finds that for incident proton energies above (2÷3) GeV in the lab. system graph 2 would give a larger contribution to $\partial^2\sigma/\partial\Delta^2\partial W'^2$ than would graph 1. For this estimate a simple optical model for high energy p-p scattering has been used where

$$\frac{d\sigma}{d\Omega} = \frac{\sigma_{elast}}{\pi}\left|\frac{F_1(\Delta R)}{\Delta R}\right|^2,$$

with $\sigma_{elast} \approx 15$ mb $R \approx 1 \cdot 10^{-13}$ cm .

If one only keeps Δ^2 fixed and integrates over W' too, at very high energies W graph 1 would give a larger contribution to $d\sigma/d\Delta^2$ than would graph 2. This is due to the different W' dependence: while $|T_1|^2$ integrated over the angle variables increases with W', $|T_2|^2$ decreases. Since the upper limit of the W' integration for small Δ and W large is approximately given by $W'=m_B^2+(\Delta/m_A)W^2$, the W' integration can make up for the W dependence of graph 2. But for sufficiently small values of $(\Delta/m_A)W^2$ graph 2 again would contribute more.

* * *

Finally we remark that for p-p scattering both graphs have the property that their contributions to $\partial^2\sigma/\partial\Delta^2\partial W'^2$ have a maximum at $\Delta^2 \approx m_\pi^2$, in graph 1 this is due to the denominator $(\Delta^2+m_\pi^2)$, for graph 2 this is brought about by the diffraction-like dependence of $T_{AB}(W^2, \Delta^2)$.

LIBRI RICEVUTI E RECENSIONI

J. Irving and N. Mullineux – *Mathematics in Physics and Engineering*. Academic Press, New York e London, 1959; pp. 883.

In questo grosso volume sono esposti numerosi algoritmi matematici, scelti fra quelli che si sono rivelati più utili nello studio di problemi di fisica o di ingegneria. Avendo di mira esclusivamente le applicazioni a tali problemi, l'esposizione si svolge su un piano puramente formale. La parte matematica risulta perciò assai mediocre; di maggior valore è invece la raccolta di esempi destinati ad illustrare l'uso dei vari metodi esposti.

La materia è divisa in 12 capitoli seguiti da un'Appendice nella quale sono richiamate varie nozioni di carattere elementare usate nei capitoli precedenti. Alla fine di ogni capitolo e dell'Appendice vi è una raccolta di 20 problemi proposti al lettore; di tutti questi problemi son date le soluzioni alla fine del volume.

Un po' strano può esser giudicato l'ordine con cui si susseguono i vari capitoli; si può notare, ad esempio, che si comincia con le equazioni a derivate parziali (cap. I) e poi si passa alle equazioni differenziali ordinarie (cap. II); che si parla della trasformazione di Laplace nel cap. IV senza far uso del concetto di funzione analitica, riprendendone poi lo studio nel cap. X, ecc. Ogni capitolo appare come una cosa a sè e non si scorge un filo conduttore che colleghi i vari capitoli e giustifichi la loro successione. Lo stesso disordine si nota in seno ad ogni capitolo ove i vari argomenti sono collocati un po' a caso e spesso slegati fra di loro.

A ciascun capitolo sono aggiunte delle notizie bibliografiche; esse sono però assai incomplete e limitate quasi esclusivamente a testi di lingua inglese.

Le precedenti critiche non debbono tuttavia far credere che il nostro giudizio sul volume sia del tutto negativo. In complesso riteniamo che il libro possa riuscire utile ed istruttivo ai giovani studiosi di fisica od ingegneria; pensiamo però che un migliore ordinamento della materia ed un approfondimento concettuale di certi punti avrebbe reso l'opera assai più idonea agli scopi che gli Autori si erano prefissi.

Esaminiamo ora rapidamente il contenuto dei 12 capitoli. Il cap. I, sulle equazioni a derivate parziali, è essenzialmente dedicato alle classiche equazioni di 2° ordine delle onde, di Laplace e del calore ed al metodo di separazione delle variabili per ricavarne soluzioni particolari; lo stesso metodo viene poi usato per l'equazione di 4° ordine delle piastre; il capitolo termina con qualche generalità sulle equazioni quasi lineari del 2° ordine, con particolare riguardo a quelle di tipo iperbolico. Il cap. II tratta del metodo di Frobenius per le equazioni lineari del 2° ordine con applicazioni alle equazioni di Bessel, di Legendre, ipergeometrica, ecc.; sono introdotti i polinomi di Tschebyscheff, di Jacobi, di Laguerre, di Hermite e vien data qualche

nozione sulle serie semiconvergenti; si passa poi ad un certo tipo di equazioni non lineari, descrivendo per esso il metodo delle perturbazioni. Nel cap. III si studiano le funzioni di Bessel, di Legendre e si danno brevi cenni sulle funzioni sferiche. Nel cap. IV è esposta la teoria elementare della trasformazione di Laplace con varie applicazioni (calcolo simbolico). Il cap. V è dedicato alle matrici; oltre alla parte elementare, sono esposti vari teoremi sugli autovalori e descritti metodi di calcolo numerico. Il cap. VI è rivolto alla meccanica analitica, sia classica che ondulatoria (equazioni di Lagrange, Hamilton, Schrödinger). Il cap. VII è dedicato al calcolo delle variazioni nell'indirizzo classico, in una o più variabili; son fatte applicazioni ai problemi di Sturm-Liouville, all'equazione delle piastre e son esposti sommariamente i metodi di Ritz e di Trefftz per il calcolo degli autovalori Il cap. VIII contiene le prime nozioni sulle funzioni analitiche di una variabile complessa e la rappresentazione conforme; notevoli le applicazioni idro ed aero-dinamiche. Nel cap. IX si prosegue lo studio delle funzioni analitiche, servendosi del concetto di integrale e son date molte applicazioni del calcolo dei residui; si tratta anche del criterio di stabilità di Nyquist e degli sviluppi asintotici, esponendo il metodo del punto di sella. Il cap. X contiene nozioni sulle trasformazioni di Fourier, di Laplace, di Hilbert (con un cenno su quella di Hankel) e sulle loro formule d'inversione; varie ed interessanti le applicazioni. Nel cap. XI sono esposti metodi di calcolo numerico; poche ed assai elementari le cose esposte; a nostro parere, questo capitolo avrebbe meritato un ben maggiore sviluppo. Infine il cap. XII è dedicato alle equazioni integrali; anche questo capitolo ci sembra redatto molto sommariamente perchè in esso si tratta quasi esclusivamente della traduzione in equazioni integrali di problemi sulle equazioni differenziali.

È chiaro da questo sommario che, come già si è detto, il libro è in sostanza una specie di dizionario di nozioni matematiche disposte alla rinfusa; ripetiamo però che queste nozioni sono tutte illustrate da numerosi ed efficaci esempi e che questi costituiscono la parte migliore e più convincente del volume.

A. Ghizzetti

S. Yiftah, D. Okrent and P. A. Moldaver – *Fast Reactor Cross-Sections. A Study Leading to a 16 Group Set.* Pergamon Press, London, 1960; pp. 130; s 35.

L'interesse per i reattori veloci, dovuto alla possibilità di breeding che tali reattori offrono, è testimoniato dall'intensa attività di ricerca svolta in tale campo.

Accanto a misure di dati microscopici su materiali fissili, fertili, refrigeranti o strutturali, sono state eseguite misure integrali su insiemi veloci, critici o sottocritici. I parametri microscopici sinora misurati sono tuttavia insufficienti al calcolo di tali reattori, generalmente svolto con teorie a molti gruppi e macchine calcolatrici. I gruppi di costanti da impostare in queste teorie sono largamente frutto di interpolazioni sia per quanto riguarda gli intervalli di energia, che per quanto riguarda l'intero andamento dei parametri nucleari di un nuclide, con riferimento a quelli vicini. La procedura seguita nel fissare le costanti per ogni gruppo di energia, consiste generalmente nell'aggiustare « a posteriori » ed empiricamente alcuni parametri microscopici al fine di ottenere l'accordo tra i calcoli eseguiti ed un certo numero, limitato, di risultati di esperienze integrali. Come gli Autori rilevano, questo metodo non dà la possibilità di stimare la validità delle costanti impiegate e rende difficile l'inserimento

di nuovi o più precisi dati microscopici nel complesso dei dati utilizzati.

Pertanto gli Autori hanno preferito stabilire, indipendentemente dai dati integrali, un insieme di dati microscopici per 16 gruppi di energia, avvalendosi di quanto noto fino al Marzo 1960.

Merito principale del libro è quello di spiegare sempre i motivi delle scelte fatte sia quando si avevano a disposizione diverse misure non concordanti, sia quando era necessario, in mancanza di dati sperimentali, interpolare tra dati noti. Naturalmente la spiegazione effettiva della scelta fatta è data solo per sommi capi e consiste essenzialmente nel rimandare il lettore alla bibliografia sull'argomento che è ricca ed aggiornata. Questo è però da considerarsi inevitabile in un lavoro che riassume una situazione sperimentale ancora fluida.

Il paragone tra le previsioni teoriche ed i risultati di esperimenti critici mostra che l'insieme delle costanti microscopiche scelte porta a prevedere rapporti tra sezioni d'urto medie generalmente in buon accordo con i dati sperimentali. Malgrado alcune deviazioni, ciò è indice di un ragionevole successo nella precisione dello spettro neutronico.

Non altrettanto buona è la precisione delle masse critiche che risultano sempre minori di quelle sperimentali.

In generale si può quindi dire che il libro in oggetto rappresenta una guida aggiornata sulla situazione attuale nel campo della misura dei parametri nucleari per neutroni veloci. L'aggiunta di un capitolo che, sia pure sotto forma di tabella, riassume per 25 nuclidi gli intervalli di energia entro i quali mancano dati sperimentali, e le contraddizioni tra i risultati di vari sperimentatori è un altro pregio del volume.

M. Marseguerra

Direttore responsabile: G. POLVANI

Tipografia Compositori - Bologna

Questo fascicolo è stato licenziato dai torchi il 24-V-1961